A PARAMETRIC APPROACH TO OPTIMIZE SOLAR ACCESS FOR ENERGY EFFICIENCY IN HIGH-RISE RESIDENTIAL BUILDINGS IN DENSE URBAN TROPICS

Nadeeka Jayaweera

178001H

Thesis submitted in partial fulfilment of the requirements for the degree

Doctor of Philosophy in Architecture

Department of Architecture

University of Moratuwa

Sri Lanka

April 2022

Declaration page

"I declare that this is my own work and this thesis does not incorporate without acknowledgement any material previously submitted for a Degree or Diploma in any other University or institute of higher learning and to the best of my knowledge and belief it does not contain any material previously published or written by another person except where the acknowledgement is made in the text. Also, I hereby grant to University of Moratuwa the nonexclusive right to reproduce and distribute my thesis, in whole or in part in print, electronic or other medium. I retain the right to use this content in whole or part in future works (such as articles or books)."

Signature: *UOM Verified Signature*

Date: 03.04.2022

The above candidate has carried out research for the PhD thesis under my supervision.

Name of the supervisor: Dr. R.M.K.U. Rajapaksha

Signature of the supervisor: *UOM Verified Signature*

Date: April 06 2022

Name of the supervisor: Dr. M.M.I.D. Manthilake

Signature of the supervisor: *UOM Verified Signature*

Date: 07/04/2022

Abstract

Solar access in buildings is a topic predominantly investigated in the urban contexts at higher latitudes and to a much lesser extent in the tropics. Existing research focuses on ensuring unobstructed solar access, whereas, in the tropics, unobstructed solar access is avoided in buildings due to external heat gain. In addition, most regulations for high-rise residential buildings in the tropics are inadequate to ensure sunlight exposure for residents. Four research objectives were formulated in this study to investigate the definition, typology, planning and architectural issues of solar access in high-rise residential buildings in dense urban tropics.

This study investigated the shading effect of the urban context on solar access in terms of energy savings and daylight in high-rise residential buildings in the tropical city of Colombo, Sri Lanka. The methodology consisted of three phases. In Phase I, three simulation models of 11, 21 and 31 floors (SM1, SM2, and SM3) were developed based on the archetypal high-rise residential building characteristics in Sri Lanka.

In Phase II, the study demonstrated a parametric urban context for the simulation models utilizing simulation software *Rhino3D* and the *Grasshopper* interface. *Archsim* and *DIVA4* plugins were used to simulate the effects of the urban context on spatial daylight autonomy (sDA), annual energy use for cooling, and annual day-time lighting energy use. A multi-objective optimization process applying the Pareto-front identified the thresholds for optimum solar access.

Phase III of the study investigated the daylight and energy performance of external shading scenarios of a high-rise residential building in a dense urban context.

This study defined the optimum solar access for a perimeter zone in a high-rise residential building that achieves 75 sDA $_{(300lx|50)}$ with corresponding annual energy savings of 28%-36% in the east-west and 8%-12% in the north-south directions. The prescribed building setback curves for ensuring optimum solar access were validated with three calibrated case studies located in Colombo, Sri Lanka. All case studies demonstrated 50% of interior spaces (living rooms and bedrooms) with 55 sDA $_{(300lx/50)}$ and annual energy savings of 26-31% in east-west and 8%-15% in the north-south direction. The Floor area ratios (FAR) calculated for optimum building density for SM1, SM2, and SM3 were 4.2, 6.5, and 8.4, respectively.

The best performance external shading scenario in the vertical façade of the 11-floor Simulation model 2 (vertical and horizontal shading on the nineteenth floor, horizontal shading only for the eleventh floor, and no shading for the second floor) satisfied 75 sDA $_{(300lx|50)}$ at all floors with corresponding energy savings of 16%-20%. The best performance scenario was applied to a 17-floor case study building located in Colombo, Sri Lanka. The simulation results indicated that 58% of the spaces had over 75 sDA for both Baseline and Best performance scenarios, while an increase in energy savings of 1%-3% was found in the Best performance scenario compared to the Baseline scenario of the case study.

This research study redefined solar access for the tropics, prescribed building setbacks for optimum solar access and informed optimum building density for the high-rise residential building typology. The study also identified the best performance external shading scenario for a high-rise residential building façade in the urban context. The research outcomes established in this study provide a much-needed platform to initiate the dialogue on solar rights in dense urban tropics.

Keywords: tropics, urban context, high-rise residential; energy savings, daylight, parametric

Dedication

I would like to dedicate this thesis to my parents.

Acknowledgement

I would like to express my sincere gratitude towards my supervisors, Dr. R.M.K.U Rajapaksha and Dr. M.M.I.D. Manthilake for their guidance for my research from the inception.

This research study was conducted under the purview of a MoU, which was signed between the University of Moratuwa and the Condominium Management Authority of Sri Lanka to promote sustainable development of high-rise residential buildings in Sri Lanka. I would like to thank Prof. A. Jayawardane, former Vice-Chancellor of the Moratuwa University and Mr. C. Wijeweere, former Chairman of the CMA, signatories to the MoU. In addition, I would also like to acknowledge Mr. J D N C Dissanayake, Deputy General Manager (Regulatory), and other staff members of the CMA for their assistance given during the survey of high-rise residential buildings. I am also grateful to the Senate Research Council of the University of Morautwa for the National Development Grant (SRC/2017/ND/01), which provided the financial assistance to enable the objectives of the MoU. My special thanks go to Prof. Stephen Lau of the University of Hong Kong for arranging my visit to the National University of Singapore to broaden my exposure. I am also very grateful to Prof. R. Halwathura, chairman of the progress review committee for his guidance during the progress reviews. I would also like to thank Dr. S. Cooray, Director of the Higher Degrees Committee of the Architecture Faculty and Dr. W. Gamage, Research Coordinator for the Department for their support. I would like to thank Mr. S. Mendis, Mr. J. Senavirathne, Mr. P. Obadage, Ms. A. Mahanama, Ms. J. Nadaraja and Mr. S. Rodrigo for their assistance in collecting field data for this research study. I am also grateful to Mr. C. Masakorala, technical officer at the Department, and the Supplies Division of the University of Morautwa for their assistance to purchase equipment for this study. I would also like to thank the staff members of the Periodicals Section of the Library of the University of Moratuwa for their assistance in obtaining much-needed reference materials. Finally, I would like to thank my family and friends for their patience and support during the research study.

Table of Contents

List of Figures

List of Tables

List of Abbreviations

Abbreviation	Description
ASE	Annual sunlight exposure
ASHRAE	American society of heating, refrigerating and air-conditioning engineers
CBDM	Climate based daylight modelling
CMA	Condominium management authority of Sri Lanka
CV (RMSE)	Coefficient of variation of root mean square error
FAR	Floor area ratio
LEED	Leadership in energy and environmental design
NMBE	Normalized mean bias error
sDA	Spatial daylight autonomy
UDA	Urban development authority of Sri Lanka
UDI	Useful daylight illuminance
URA	Urban redevelopment authority of Singapore
UVA	Unobstructed vision area
VDF	Vertical daylight factor

1 Introduction

Chapter one explores the current situation of urban housing and energy use in the tropical city of Colombo in Sri Lanka. The background of the research problem, the limitations of the research scope and the formulation of the research objectives are discussed in this Chapter.

1.1 The changing paradigm of house form in urban tropics

At present, the house has evolved from being a climate-responsive regional form to a generic unit across the world. House forms are converging as socio-cultural values of people around the world converge due to globalization and technology. The determinants of house form are argued in depth by Rapport (1969). His hypothesis is as follows:

"House form is not simply the result of physical forces or any single causal factor but is the consequence of a whole range of socio-cultural factors seen in their broadest terms. The form is in turn modified by climatic conditions and methods of construction, materials available, and the technology. I will call the socio-cultural forces primary and the others secondary or modifying."

Rapport (1969)

Rapport's hypothesis still holds to the same rigour as it did in the past in terms of socio-cultural forces. In the past, the connection with nature was essential for survival. People depended on their gardens and estates for food and other necessities. Their neighbours offered a strong support system in case of emergency. The house was the only sheltered place for all functions from weddings to funerals. At present, people are relying less and less on their immediate surroundings, with the availability of services and products at their fingertips from the internet. The city has become the source of all life, and the house is becoming merely a resting place. The modern house is increasingly reliant on air-conditioning and artificial lighting, instead of climate responsive design to maintain indoor thermal and visual comfort.

The compact residential units that populate multi-family residential developments support modern cultural conventions such as cohabitation of a nuclear family (Urban, 2011). The need for compact living drives the high-rise residential markets. From Toronto to Singapore, millions of city dwellers call the high-rise residential building their home.

1.2 High-rise residential developments in Sri Lanka

It was not until the end of a thirty-year war in 2008, that private high-rise residential developments for the middle- and upper-income groups became popular in Sri Lanka. Until then, most high-rise residential living was reserved for low-income groups, except for a small number of flats constructed during the 1960s for public servants. Market-driven high-rise residential developments are concentrated in Colombo, the commercial capital of Sri Lanka. Over 90% of high-rise residential developments take place in Colombo district (Rajapaksha and Jayaweera, 2018). A decrease in family size, household income growth, rapid urbanisation, scarcity of land, high land price, security, convenience, and location contribute to the increasing high-rise developments in Colombo (Ariyawansa and Udayanthika, 2012). At present, house value in the Sri Lankan real-estate market is decided by the proximity to the Colombo city centre. Slogans used by developers such as “living among elites” and “the right address” prove the importance of location above all other characteristics of a home. The social status previously associated with a spacious house in the country is now replaced by proximity to the city centre.

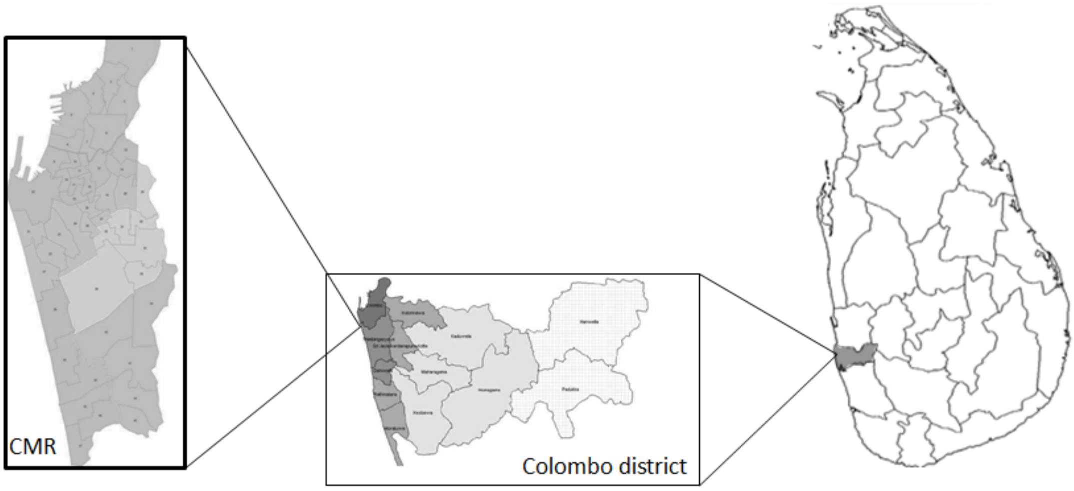

Figure 1.1: The Colombo Metropolitan Region (CMR)

Colombo city has a gross land area of 31.7 km^2 and a population density of 13,364 people per square kilometre (DCS, 2015). The city is bounded by the Colombo Metropolitan Region (Figure 1.1). Colombo is characterized by its slow immigration rate in comparison to other south Asian cities. Gunarathne (2006), attributed the slow urban migration rates to political leadership in the 1930s that mainly focused on domestic food production, dry zone colonisation, and rural development, which discouraged rapid urban-rural migration. The 30-year war on terrorism from 1983-2008, had also kept people at bay from the city, which was a target for repetitive terrorist attacks. At present, the local dynamics in urbanization are changing, and an increase in urban migration is leading to a housing deficit in the city. The Western Region Master Plan- 2030 by the Ministry of Megapolis and Western Development, states that due to migration, the demand for housing in Colombo city and its suburbs are expected to increase. Unless swift action is taken, the housing deficit could amount to 1 million (with a 1% rate of obsolescence) by 2030.

In Sri Lanka, the ownership of high-rise residential units is regulated by the 1973 Apartment Ownership Law and the Amendments by Act No. 45 of 1982, 4 of 1999 and 39 of 2003. The Apartment Ownership Act discusses ownership issues in great detail. In 2003 the Common Amenities Board was re-established as the Condominium Management Authority (CMA). The CMA regulates the ownership and management cooperations (MCs) of condominiums; however, they do not have any bearing on planning or building. The Urban Development Authority of Sri Lanka (UDA) and the relevant Municipal Councils regulate all the planning and building of residential developments in Sri Lanka. Therefore, many disparities in the regulations for high-rise residential buildings exist, due to the lack of a holistic planning, building and operational framework.

The term condominium refers to a form of tenure, a system of ownership; in which owners have full title to the individual unit and a shared interest in the common areas of the property (Dredge and Coiacetto, 2011; Rosen and Walks, 2013) as opposed to an apartment which is defined as short-term ownership or rented space. However, colloquially in Sri Lanka, the term apartment is interchangeably used for condominiums regardless of the form of ownership. The term "Condominium" is used in Sri Lanka, U.S., and Canada, while in Australia such form of ownership is known as Strata title. Elsewhere it is known by several other names including "unit titles" in New Zealand, "coproprie´te´" in France, and "commonhold" in Britain (Dredge and Coiacetto, 2011). The MCs which are the legal structure established to manage the common interests by the Act no.39 of 2003 is registered under the CMA. Such cooperations are known as 'homeowners associations' in North American systems and by the more generic term 'body corporate' in various Australian states (Dredge and Coiacetto, 2011).

According to the building regulations in Sri Lanka, any building with ground plus 4 floors is considered a high-rise building (except in the Colombo Metropolitan area where high-rise building is 13 floors or above) (Urban Development Authority, 2005). Therefore, in this study, a residential building with over ground plus 4 floors is considered a high-rise residential building. It is likely that condominiums with less than 15 units will not have over ground plus 4 floors. Out of the total number of condominiums with CMA certificates, only 31% have more than 15 units (Figure 1.2). This means that 69% of the condominium developments in Sri Lanka have less than 15 units. Therefore, most of the condominiums in Sri Lanka could be considered as low-rise residential buildings.

However, the number of high-rise residential buildings in Sri Lanka has been steadily increasing from 2015 onwards. At the end of 2017, 291 private high-rise residential buildings with over 15 units obtained the CMA certificate in the Colombo district.

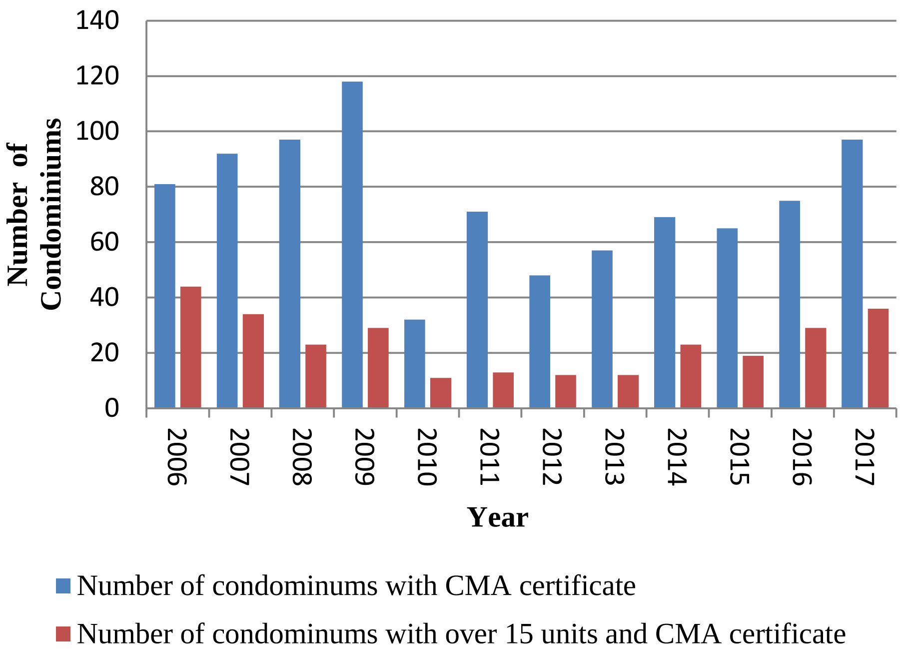

Figure 1.2: Number of condominiums with CMA certificate

Data source: Condominium Management Authority

High-rise residential buildings catering to the higher income groups are categorized as semi-luxury, luxury, and super luxury (Senarathne et al. 2006). According to Jonas La Salle (2011) from the total high-rise residential building construction in 2011, 32% have been in the luxury category. The annual household income should be above LKR 2.86 million to afford a luxury housing unit costing LKR 10 million or more (Jonas La Salle, 2011). However, the mean monthly household income in Sri Lanka was LKR 45,878.00 in 2012/13, while the mean household income in Colombo district was LKR 77,723.00 during the same time (DCS, 2015). Therefore, most buyers are high net worth individuals, non-residential Sri Lankans, and expatriates living in Colombo (Ariyawansa and Udayanthika, 2012; Jonas La Salle, 2011). Over 70% of the 4,100 condominium units sold during 2007–2011 in Colombo were for investment. This figure could be as high as 85% in some projects under the premium and luxury apartment segments (Jonass La Salle, 2011). Therefore, high-rise residential units are considered good investments.

In Sri Lanka, the high-rise residential market is still in the early stages of development. In Singapore and Hong Kong, high-rise residential developments are key partners of their economic success. The social, environmental, and economic sustainability of high-rise residential developments depend on their ability to integrate into the cityscape carefully. The planning and building regulations in Singapore have achieved a seamless integration of high-rise buildings into the cityscape. As a result, Singapore was ranked first in sustainability in the Asia-Pacific, by ARCADIS (2018), even though more than 80% of its population lived in high-rise residential buildings. Therefore, there is a need to investigate the current contribution of high-rise residential buildings in heading Colombo city towards sustainability.

1.3 Integration of high-rise residential developments into the cityscape of Colombo

The United Nations has established "Sustainable cities and communities" as Goal 11 of its Sustainability Agenda to transform the world. Sustainability goals of Sri Lanka are indicated in the National Land Use Policy, National Housing policy, and in the Western Region Master Plan (WRMP) 2030 as stated below.

"The state on behalf of the people will function as the trustee of land to enable the present and the future generations to use the land on a sustainable basis."

-Land use policy

"A sustainable and resilient region that protects the natural environment and creates a balanced approach to the use of land and its natural resources."

-Western Region-Master Plan 2030

“The goal of a housing policy is a well-functioning housing sector that takes care of the housing needs of all its citizens. That is a housing sector that best serves the interests of all its constituents and which helps to achieve broad social, economic, and sustainable development goals.”

-National housing policy

The above policy goals in urban and housing development should be enacted in the regulations for urban planning in Sri Lanka. The Urban Development Authority (UDA) is the authorized body, which develops and enforces the relevant planning and building regulations in the country. There are two main documents published by the UDA of Sri Lanka for regulating planning and building.

1. Planning and building regulations (General) published in 2015.
2. Planning and building regulations 2008-2020

In concurrence with the planning and building regulations, the development plans for the city of Colombo and five suburbs have also been approved by the parliament.

It is worth comparing the current planning and building regulations for high-rise residential buildings in Sri Lanka, with similar regulations in other tropical cities to understand the direction and targets for improving local regulations. Singapore has achieved a level of success in high-rise residential development surpassing many other developed countries. Therefore, even though there are underlying differences in land ownership and governance between Sri Lanka and Singapore, a comparison of urban planning regulations between the two countries will provide valuable information on the current path of high-rise residential development.

1.3.1 Scattering of high-rise residential developments in the Colombo Metropolitan Region

Figure 1.3 depicts the location of high-rise residential buildings in the Colombo Metropolitan Region and its suburbs.

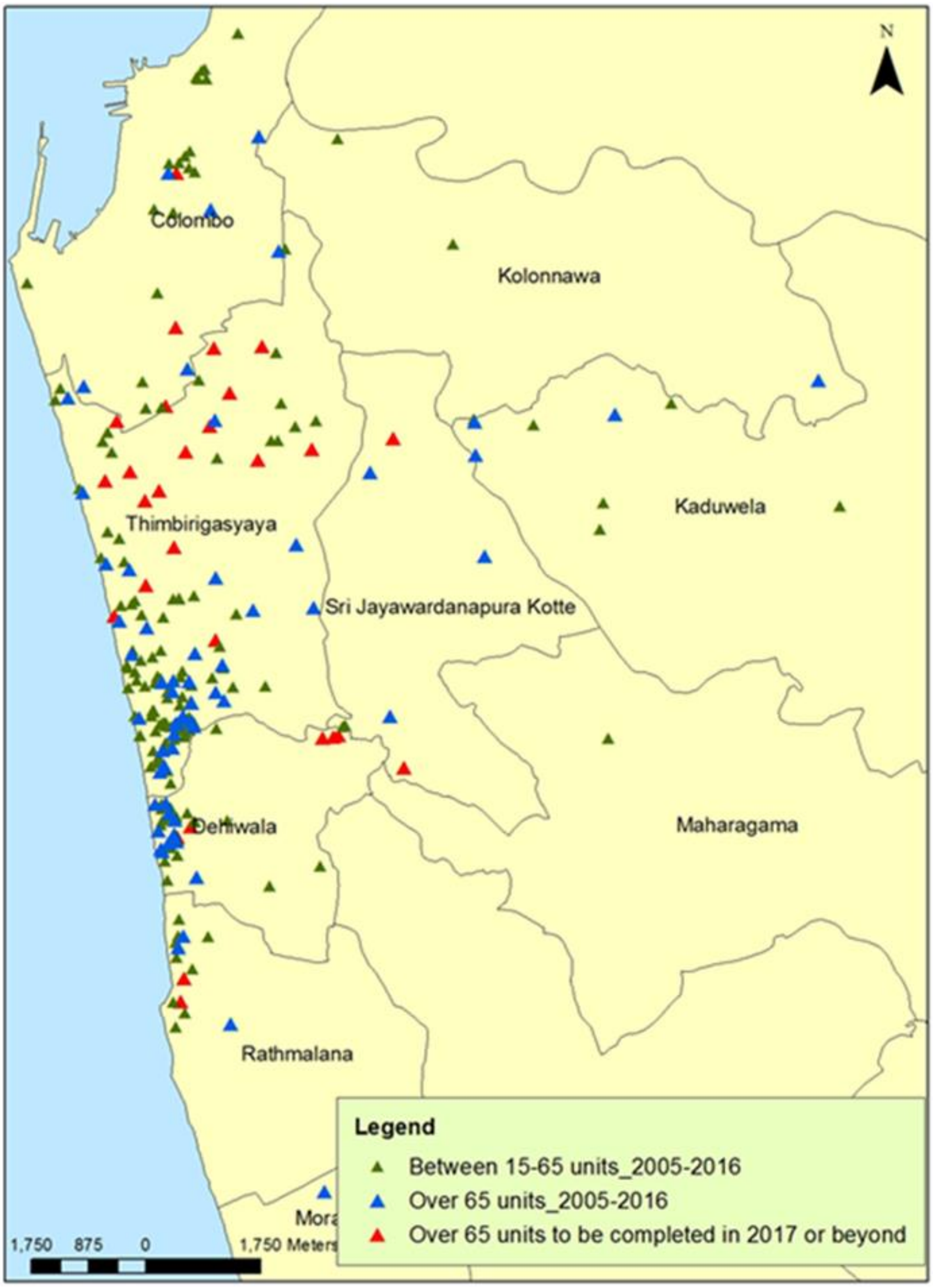

Figure 1.3: Location of high-rise residential buildings in CMR and suburbs

Source: (Rajapaksha & Jayaweera, 2018)

According to Figure 1.3, high-rise residential buildings are scattered in Colombo and suburbs in any available land plot, leading to urban sprawl (Ewing, 2008). This is mainly due to the failure in current planning regulations to identify high-rise residential buildings as a separate building typology in zoning. The zoning plan for the Colombo Metropolitan Region is given in Appendix A. Currently, high-rise residential buildings are categorized under residential buildings, which include low-rise residential development as well. Lack of differentiation between low-rise and high-rise residential developments have led to the construction of high-rise residential buildings in low-rise neighbourhood zones, as depicted in Figure 1.4.

Figure 1.4: High-rise residential building construction in -low-rise neighbourhood

When a high-rise residential building is constructed in a small land plot, the neighbouring land plot owners are forced to sell their land, due to loss of solar access, increasing road traffic, inadequate infrastructure, poor neighbourhood character etc. At present, almost all low-rise neighbourhoods in Sri Lanka are at risk of losing their neighbourhood character due to scattered high-rise residential building developments. This detrimental trend in building on alienated small land plots defines the high-rise residential building character in Sri Lanka.

The scattered development of high-rise residential buildings in Sri Lanka, is in stark contrast to Singapore. In Singapore, planning and building regulations for the residential sector differentiates between landed housing, strata landed housing, flats, and condominiums. Therefore, zoning regulations consider scale and massing of the residential building typology, protecting the neighbourhood character and providing adequate infrastructure for the development as depicted in Figure 1.5. Inadequate zoning regulations in Sri Lanka indicate the need to recognize the high-rise residential building as a separate residential building typology.

Figure 1.5: Low-rise and high-rise neighbourhoods with clear boundaries in Singapore

Source: (Google Inc., n.d.)

1.3.2 Issues in high-rise residential developments in small land plots

The issues faced due to scattered development are further complicated by the poor regulation of land size, floor area ratio, and plot ratio. Current regulations allow high-rise residential buildings which are large-scale buildings in small sites. The minimum site extent for a condominium development in Singapore is 4000 m^2 and 1000 m^2 for flats (Urban Redevelopment Authority, 2019). In Colombo and its suburbs, it was noted in the preliminary survey of high-rise residential buildings conducted by Rajapaksha and Jayaweera (2018), that over 70% of the high-rise residential developments had site extents less than 1000 m^2. A closer investigation of building plans confirmed that condominiums of seven floors had been constructed in plots less than 500 m^2.

Due to the small size of the site, it is impossible to meet many of the building regulations that ensure adequate light and ventilation for most of the units. This small-scale development model in alienated land plots is evident in Colombo city, and in the suburbs, where sprawling high-rise residential buildings dominate the skyline. In narrow lanes in the suburbs high-rise residential buildings could be seen constructed up to the street line with extended balconies (Figure 1.6). Another common practice is donating land to increase road width in front of the building as depicted in Figure 1.7. In the current planning regulations, the number of floors in a high-rise residential building depends on road width (UDA, 2008). Therefore, by increasing the road width, the number of floors allowed could also be increased. While the majority of the lane remains narrow, the above practice only contributes to unsustainably high neighbourhood densities.

Figure 1.6: High-rise residential buildings constructed up to the street line

Figure 1.7: The practice of donating land to the road to increase the number of floor levels of the high-rise-residential building in narrow roads

Lately, there has been a rise in large scale high-rise residential buildings in Colombo, albeit on tight land plots compared to similar sized developments in other countries. Only a few high-rise residential complexes in the Colombo Metropolitan Region and its suburbs could be identified as part of a fully integrated and spacious housing estate. The Havelock City Complex is the largest private high-rise residential estate, located in an extensive area of 66,000 m^2 (Figure 1.8).

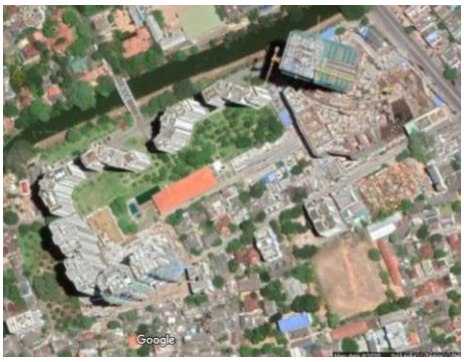

Figure 1.8: An aerial view of Havelock City Complex in Colombo 05

Source: (Google Inc., n.d.)

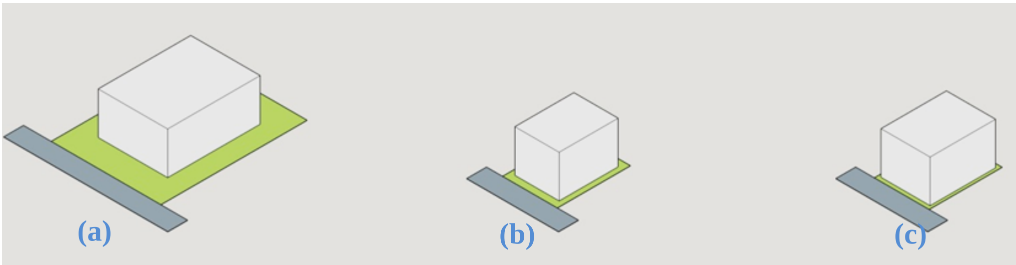

a) Maximum plot coverage for condominiums in Singapore is 40% on a minimum site area of 4000 m^2 for a condominium development.
b) Maximum plot coverage for an 8-storey residential building in the suburbs of Colombo is 65% on a 1000 m^2 according to planning and building regulations 2008-2020.
c) Plot coverage based on the data is over 80% for sites around 1000 m^2.

Figure 1.9: Comparison of plot coverage

Source: (Rajapaksha & Jayaweera, 2018)

The floor area ratio (FAR) is unique in Sri Lanka as unlimited FAR is allowed for plots of over 3500 m^2 in the Colombo Metropolitan Region. In Singapore, the guiding FAR (termed Gross Plot Ratio) for "high density" residential development is

2.8. Figure 1.10 compares FAR regulations in Sri Lanka and Singapore. Singapore is considered as a city-state with high building density. However, the density in Singapore pales in comparison to Sri Lanka. Densification in urban areas due to high-rise residential developments in Sri Lanka could be expected to at-least double compared to Singapore at the current development rate.

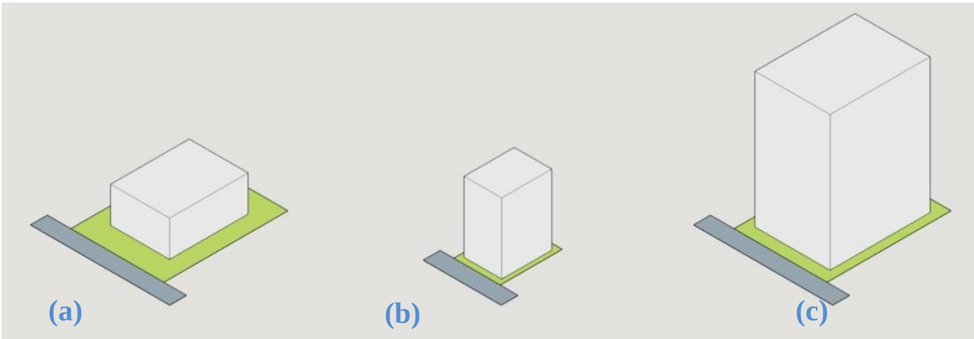

a) The general guide for FAR for high-density residential development of condominiums in Singapore is 2.8 on a site extent of 4000 m^2. The FAR is otherwise controlled by the Master Plan.
b) The FAR for buildings in 900-1000 m^2 is 1:7 in the City of Colombo Development Plan (Amendment) 2008.
c) FAR for buildings in sites over 3500 m^2 is unlimited in Sri Lanka.

Figure STYLEREF 1 \s 1. SEQ Figure
Source: (Rajapaksha & Jayaweera, 2018)

1.3.3 Restrictions to solar access due to lack of building setback

The building setback is a widely used planning tool to ensure solar access and daylight into the building. In the current planning regulations in Sri Lanka, it is enforced as the space around the building. In high-rise residential buildings, where windows of living rooms and bedrooms are always maximized to obtain a good view, the building setback regulation will decide the amount of solar access into the building.

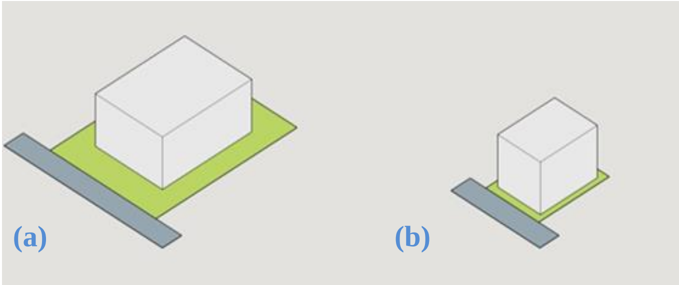

a) Setbacks for a condominium on a site extent of 4000 m^2 in Singapore.
b) Setbacks according to the schedule 6-form C of the Planning and Building regulations - 2008-2020 for site extent of 1000 m^2.

Figure 1.11: Comparison of side setbacks for an 8-storey building

Source: (Rajapaksha & Jayaweera, 2018)

A comparison of setback regulations in Sri Lanka and Singapore is illustrated in Figure 1.11. The current front, rear and side spaces for buildings of different heights in the current planning regulations in Sri Lanka are provided in Appendix B. The building setback from the boundary for condominiums in Singapore is given in Appendix C. In addition to the building setback, a 2 m wide planting strip is also to be provided in developments in Singapore further extending the setback between buildings. Having adequate building setbacks has contributed to creating a green city in Singapore. The lack of building setbacks could lead to buildings creating a continuous wall in neighbourhoods blocking solar access and ventilation into the building.

The current side setback regulation in Colombo suburbs for eight floors is 2 m on one side. This regulation had led to the restriction of solar access to residents in the high-rise residential building depicted in Figure 1.12. Construction up to 1 m from the site boundary and extending the balcony of 1 m depth towards the boundary is common in Sri Lanka, resulting in loss of solar access for many residents.

Figure 1.12: Lack of solar access in an 8-floor residential building in Dehiwela suburb

High-rise residential buildings continue to be built very close to the site boundary at the cost of solar access to themselves and their neighbours due to lack of adequate building setback requirements. For a 20-floor residential building, where at least three sides of the buildings have large openings for light and ventilation, the side setback requirement of 6 m on each side is deemed inadequate, especially compared to Singapore where side setback requirement is 11.3 m. Figure 1.13 below depicts the construction of a high-rise residential building of over 40 floors close to an existing high-rise residential building. The owners of the residential units facing the new construction experience loss of view and solar access.

Figure 1.13: A new high-rise residential building of 40-floors being constructed close to an existing high-rise residential building affecting the view and solar access of the latter

The restriction to solar access due to inadequate building setbacks is a serious issue in high-rise residential developments in Sri Lanka. Therefore, there is a need to explore how solar access could be reintroduced as a key focus in urban planning regulations in Sri Lanka. Ensuring solar access is a complex task in the tropics as increasing solar exposure results in increasing external heat gain into the building. In tropics, the highest energy consumer in residential buildings is indoor air-conditioning for cooling (Hyde,2000; IPCC,2014). Therefore, solar access cannot be studied without considering its impact on energy use in high-rise residential buildings. In the following section, the current energy situation in Sri Lanka and the need for energy efficiency in the residential sector is discussed.

1.4 The challenges in energy efficiency in the residential sector in Sri Lanka

Parallel to the transformation of the house form, the energy supply in Sri Lanka has also transformed in the past few decades. The need to decrease energy use represents a new challenge in Sri Lanka, due to the changing dynamics in its electricity supply. Before the 2000s Sri Lanka prided itself in its ability to meet the bulk of its electricity demand through hydropower, an accepted clean electricity source. However, in the past years, the increasing energy demand is being met by thermal generation while the hydro-generation capacity has stayed the same (Figure 1.14). Therefore, there is a clear shift in energy supply in Sri Lanka from clean to thermal in the past 20 years.

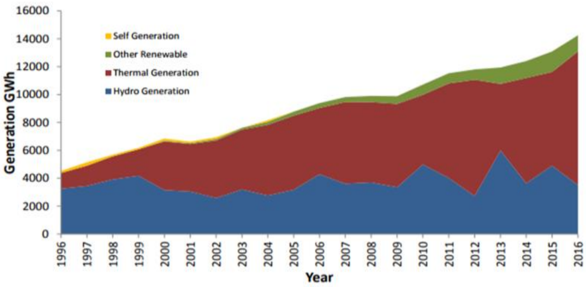

Figure 1.14: Total electricity generation by source in Sri Lanka

Source: Ceylon Electricity Board, 2017

The costs of diesel and coal have also increased significantly from 2013 to 2017 (CEB, 2014, 2017). In the absence of a viable renewable energy source, the need for reducing electricity demand should be a paramount concern for sustainable development in Sri Lanka.

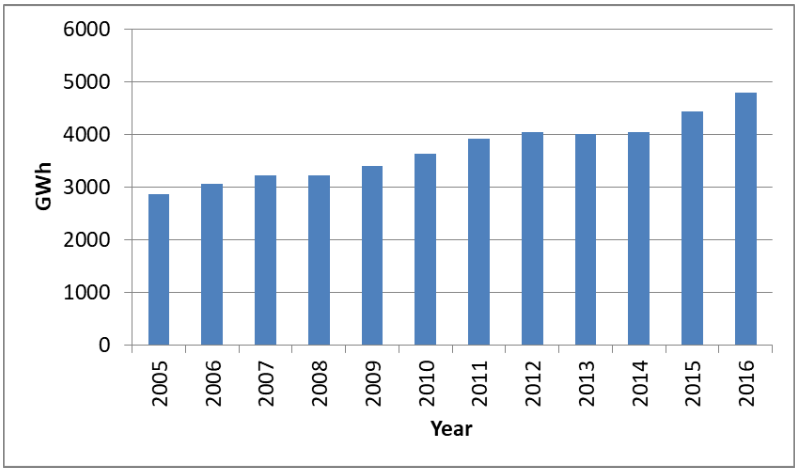

Figure 1.15: Domestic sector electricity use 2005-2016 in Sri Lanka

Data source: CEB, 2017

The electricity consumer sector in Sri Lanka is divided into domestic, religious, general-purpose, hotel, industrial, government, and street lighting. Out of the six sectors, the domestic sector accounted for the highest consumption percentage of 31.8% while the industrial sector is close behind at 31.6% (CEB, 2015). In addition, since 2005, a steady increase in energy use was observed in the domestic sector (Figure 1.15). Therefore, the domestic sector presents a higher potential for reduction in energy demand than the other sectors.

At present, there are no mandatory energy efficiency compliance regulations in Sri Lanka. The UDA is planning to introduce a Green Building Energy Code for public buildings in the immediate future. The current Energy Efficiency Building Code for Sri Lanka, released in 2008 by the Sustainable Energy Authority does not have special provision for high-rise residential building energy efficiency. Therefore, there is a need to investigate energy-efficient design strategies specific to the high-rise residential building in Sri Lanka.

1.5 Research problem, scope, objectives, and questions

Research Problem

Two main problems lie ahead for high-rise residential buildings, to become sustainable developments in Colombo. The first one is the lack of focus on achieving the sustainability goals stated in global, state, and regional policies in urban planning and building regulations. Notably, the lack of focus on ensuring solar access in high-rise residential buildings is a critical problem identified in this study. Second is the need for energy efficiency in high-rise residential buildings. In the tropics, increasing solar access will invariably increase energy use for cooling due to external heat gain. Therefore, the research problem in this study, is resolving the conflicting interests of solar access and energy efficiency in high-rise residential buildings in the urban tropics.

Research scope

The scope of research in this study is limited by the building typology and the urban context. The building typology focused here is high-rise residential buildings. The urban tropics are a relatively new context of the study to investigate the implications of increasing densities on solar access. Therefore, the scope of the study is limited to high-rise residential buildings in the urban tropical climate.

The four research objectives developed for this study are discussed below.

Research objective 1

Though tropical regions had enjoyed adequate solar access in the past, many tropical cities struggle to provide adequate solar access to building occupants due to increasing building densities. This problem is evident in high-rise residential buildings in Colombo as discussed in the Introduction. Therefore, there is a need to ensure solar access for high-rise residential buildings to ensure healthy indoor living environments. However, increasing solar access in the tropics results in an increase in energy use for cooling. Therefore, the first objective is to redefine solar access for high-density urban tropics as an optimization process of daylight and energy use.

Formulated research question 1:

What is the definition of optimum solar access for high-rise residential buildings in dense urban tropics?

Research Objective 2

Solar access is difficult to calculate at the preliminary design stages even though it is critical in creating healthy indoor environments. Therefore, the second objective of this study is to modify the building setback tool to estimate the optimum solar access for high-rise residential buildings at the early design stage.

Formulated research question 2:

2. What are the modifications to the building setback tool to ensure optimum solar access at the early design stage?

Research Objective 3

Misguided notions of densification at all costs have led to unsustainable densities in high-rise residential developments in Colombo, Sri Lanka. In addition, the lack of identification of the high-rise residential building typology is a key contributor to the current scattered development in the city. Therefore, the third objective of this study is exploring the limitations of building density in the high-rise residential building typology.

Formulated research question 3:

3. What is the optimum building density for solar access in the high-rise residential building typology in dense urban tropics?

Research Objective 4

Solar access has two main building design components. One is the urban context, which is investigated under research objectives 1 to 3. The other building design component is the vertical façade of the building. Solar access differs along with the height of the vertical facade due to contextual shading. Therefore, even though the urban context (distance between the buildings) is optimized for solar access, each floor level in the building will not enjoy the same solar exposure level. The fourth objective of this research is to explore modifications to the vertical façade of a high-rise residential building for enhancing solar access at each floor level.

Formulated research question 4:

4. What are the external shading scenarios to enhance the daylight and energy performance of a high-rise residential building façade in dense urban tropics?

1.6 Thesis structure

This thesis consists of 5 chapters. Chapter 1-Introduction described the motivation for this research study. This chapter identified the current issues of housing and energy in Sri Lanka. The research problem, the research scope, four research objectives, and the research questions are established in the first Chapter.

In Chapter 2 the focus is on the literature review. The literature review is divided into 8 sections. Section One explores the high-rise residential building typology, which was identified in the Introduction as a misguided housing form in Sri Lanka. In Section 2 and 3, solar access and energy efficiency in the urban context are discussed. Parameters of study in the urban context, solar access, daylight, and energy use are summarized in Section 4. Section 5 reviews methods in computer simulations of the urban context. Section 6 discusses the optimization methods related to building performance. In Section 7 the effects of the urban context on the daylight and energy performance of the building envelope are discussed, focusing on static external shading devices. Section 8 summarizes Chapter 2 by identifying the research gaps in Literature.

Chapter 3 discusses the methodology utilized to achieve the research objectives in the study. The research methodology is conducted in three phases. Phase I of the study, described in Section 1 and 2, focused on the characterization of the archetypal high-rise residential buildings in Sri Lanka. Phase II is discussed from Section 3 to 8. The selection of the parameters of investigation and a suitable parametric simulation software for the study, the design of the thermal and daylight model for the simulation models, and the optimization method for energy use and daylight are discussed from Sections 3 to 7 respectively. In Section 8, the calibration methods, thermal and daylight models for the case studies are discussed. Phase III of the study is discussed in Section 9 and 10. Section 9 describes the methodology for assessing the impact of the urban context on the daylight and energy performance of the external shading devices in the high-rise residential façade. Section 10 discusses the modelling of the Case study for the application of the best external shading scenario.

Chapter 4 consists of the analysis and discussion of the simulation results of the archetypal models and the calibrated case studies. The Chapter is divided into 16 sections. Sections 1 to 6 analysed the Phase II results of simulation models. In section 7, the optimization results for solar access are discussed. In Section 8, the building setback curves for optimum solar access are developed. Section 9 validated the research findings with three calibrated case studies. Section 10 calculated the building density for optimum solar access for the high-rise residential building typology. Sections 11 to 16 analysed the Phase III results of this study. Section 11 to 13 analysed the daylight and energy performance of external shading scenarios in SM2. Section 14 identified the best external shading scenario for the simulation model. The best shading scenarios are validated utilizing the Case study in Section 15, and further design options for the façade are discussed in Section 16.

The final chapter consists of the Conclusion of the study, which revisits the research questions. The conclusion is organized into 4 sections. The first 3 sections summarize the findings at each Phase of the study. The first section discusses the characteristics of the archetypal high-rise residential building in Sri Lanka. The second section discusses the development of building setbacks and density based on optimum solar access summarizing the results obtained in Phase II of the study. The third section summarizes the daylight and energy performance of different external shading scenarios of Phase III in the study. At the conclusion of the Chapter, Section 4, discusses the broader implications of the research study and future research avenues.

1.7 Summary

This chapter identified the parallel challenges in housing and energy use in Colombo, Sri Lanka. The research problem, the research scope, four research objectives, and the research questions were developed focused on current planning and design issues in high-rise residential developments in the country. The chapter is concluded with a concise description of the structure of the thesis.

2 Literature review

Solar access is a topic predominantly investigated in the urban contexts at higher latitudes and to a much lesser extent in the tropics. In this Chapter, the definitions of the key terms in this study (high-rise residential building, energy efficiency and solar access) are discussed. In addition, this Chapter summarizes the outcomes and methods of study on the effects of external shading on solar access in terms of energy efficiency and daylight in high-rise residential buildings. The Chapter is concluded by identifying the research gaps in literature.

2.1 The high-rise residential building typology

With the increasing popularity of high-rise residential developments, various questions arise about its impact on sustainable urban form, environment, social interactions, and its implications on planning cities in the future. Current research on high-rise residential buildings concentrate mostly on the issues regarding ownership. Planning and construction phases of development were the least researched in studies of multi-owner developments (Johnston and Reid, 2013; Anthonisz and Perry, 2015). In terms of architecture, the high-rise residential building does not get the same level of attention as any other building form, often becoming background buildings (Kaplan, 2007). The negative impacts due to the lack of attention to the planning and design of high-rise residential buildings in Colombo city were discussed in the Introduction. Therefore, there is a need to examine the high-rise residential building typology and its role in the sustainable city.

The concept of type in architecture is defined as:

“Something permanent and complex, a logical principle that is prior to form and that constitutes it”

(Rossi, 1931)

Rossi, 1931 further elaborated that architectural theories are also theories of typology, and it is impossible to talk about problems of form without the assumptions in type. The value of typology as opposed to the singular type in the production of the new design is that it constitutes a store of alternatives from which the starting point for the development of a promising solution might be drawn (Hawkes et al. ,2002). Hawkes et al. (2002), further acknowledged that the generalities of typology do not inhibit the realization of an appropriate response to the circumstance and situation. Residential buildings could be categorized into many typologies under the physical form, density, neighbourhood character, economic group, ownership, year of construction, household composition, etc. A high-rise residential building, therefore, could be described as a multitude of many typologies.

While on the surface, the high-rise building typology appears universal; it is diverse in different cultural contexts. High-rise residential living has mixed achievement around the world. The end of the Modern era was famously signified by the demolition of the Pruitt–Igoe mass housing project in St. Louis, Missouri, in the mid-1970s. While in the United States decades-long criticism brought about the demolition of most mass housing projects for the poor, in the booming metropolises of Shanghai and Mumbai remarkably similar developments are being built for the wealthy middle class (Urban, 2011). Many studies have been conducted on the physical and mental wellbeing of living so far above the ground (Evans et al., 2003; Fanning, 1967; Gifford, 2007; Yuen et al., 2006). Gifford (2007) in his review of existing research on the subject concluded that high-rise residential buildings are less satisfactory than other housing forms for most people, that they are not suitable for raising children, that social relations are more impersonal, and helping behaviour is less than in other housing forms, that crime and fear of crime are greater. In contrast, high-rise residential buildings in Hong Kong and Singapore have scored high in residential satisfaction (Yuen and Yeh, 2011). According to Urban (2011), the triumph or disaster of the modern high-rise residential building depends not only on design but also on social composition, location within a city, effective maintenance, and various cultural, social, and political factors.

2.1.1 Physical characteristics of the high-rise residential building typology

The high-rise residential building is a subset of mass housing. The term mass housing is defined by Kwofie et al. (2014) as:

"The design and construction of standardised multiple domestic house-units usually in the same or several geographical locations, executed within the same project scheme and under the same management and contract."

Kwofie et al. (2014)

According to the above definition, mass housing is defined by its central management and a high number of residential units. Mass housing was introduced in the mid-nineteenth century as a solution to the living conditions of the poor in industrial cities (Urban, 2011). Parallel to the development of mass housing, the house form evolved from a region-specific form to a universal one in the early twentieth century fuelled by the ideals of Modern Architecture.

In terms of a building form, the high-rise residential building typology was initially conceived within the principles of Modern Architecture. Le Corbusier's Modern Movement called for a mass-produced house (Urban, 2011). His notion of a house is in stark contrast to Rapport's views. Even though both stem from socio-cultural needs, Rapport believed indoor comfort conditions could be achieved by climate responsive design, whereas Le Corbusier depended on mechanical interventions from the onset of the design. For example, the quotes by Le Corbusier himself below show his intentions to create a universal house form sealed to maintain an interior air temperature of 18^0C.

“At this moment of general diffusion, of international scientific techniques, I propose only one house for all countries, the house of exact beating.”

“The Russian house, the Parisian, at Suez or in Buenos Aires, the luxury liner crossing the Equator will be hermetically sealed. In winter it is warm inside, in summer cool, which means that all times there is clean air inside at exactly 18 degrees.”

“The house is sealed fast! No dust can enter it. Neither flies nor mosquitos, no noise.”

Le Corbusier, 1929 during his Buenos Aires Lectures, cited in Hawkes (2008)

In defence of Le Corbusier, the current global challenges in energy use have not yet come to light during his time. Hence, burning fossil fuels was erroneously considered an unlimited and environmentally friendly source of energy.

The current high-rise residential building typology in Asian cities is deeply rooted in Le Corbusier's Radiant city concept (Yang, 2016). Le Corbusier’s goal was to create a city that could “breathe” by freeing large spaces by way of a compacted built environment.

Figure 2.1: Voisin plan for Paris (1922-1925) by Le Corbusier

Source: Curtis, 1986

Le Corbusier depicts the concept of the Radiant city in his voisin plan for Paris (1922-1925) in Figure 2.1. In the Radiant city only 5% of the area is built upon, while 95% is surrounding open space (the city becomes a park). A super-density of 3200 inhabitants per hectare was achieved by densification in the city centre. The cruciform of the skyscrapers allow solar exposure for all units. The high-rise residential buildings would free large areas of land for use as a park for the public.

Le Corbusier's goal was to create a city that could "breathe" by freeing large spaces from cluttered buildings. Proponents of the Modern movement imagined mass housing as a tall building in an extensive park in the Radiant city concept. The Modern movement governed the design of the first high-rise residential buildings in the 1930s. Precast (Industrialized) construction became the fundamental technology for mass housing in most countries, which is the main character as opposed to a traditional building (Urban, 2011) with exceptions in developing nations such as India and Sri Lanka where traditional building dominates high -rise residential building construction even today.

Figure 2.2: Unite de Habitation, Marseille by Le Corbusier

Source: (Wüstenrot Foundation, n.d.)

Stemming from the Radiant City, The Unite the Habitation, Marseille, France, was one of the first high-rise residential buildings constructed from 1947 to 1952 by Le Corbusier. It was "a slab on slits with terraces in a park" which was the most quintessential analogy for the high-rise residential buildings of the modern movement (Figure 2.2). Corbusier's vision for Unite was a bottle rack into which standardized bottles are inserted (Curtis, 1982). The Unite at Marseille (334 units) is entirely a precast construction.

Years after, Le Corbusier, principles of the Radiant City, was re-introduced as a key feature of sustainable cities (Williams et al, 2000). Densification of the city centre with high-rise residential development was the simplest way to form a compact city (Gauzin-Muller, 2002). Therefore, at present, high-rise residential developments are considered an integral part of the Sustainable city concept. However, only a few high-rise residential developments demonstrate the aptitude to extend Le Corbusier's ideas of the Radiant city without devaluing the core ideals. The Habitat 67(148 units in 5 acres), Montreal designed by Moshe Shafdie, has successfully manipulated the prefabricated system to maximize open spaces (Figure 2.3). Though it was built for the expo exhibition of '67, it was intended for a mass housing project and currently is functioning in that capacity. The increase in exposed surfaces allows more solar access to the residents.

Figure 2.3: Habitat '67, Montreal, Canada

Source: (archdaily, n.d.)

Large-scale constructions have been utilized by the Urban Redevelopment Authority (URA) in Singapore as an integral part of expanding the "city in a garden concept". One such award-winning high-rise residential development is the InterLace complex, where the objective was to maximize the green area (Figure 2.4). Having a green area that is more than the site's size is one measure of a successful construction project in Singapore. Completed in 2013, InterLace consists of 1000 units in 31 blocks, in 8 hectares. The building represents stacking blocks that maximize daylight and ventilation and open the units to the green spaces on the ground and upper levels.

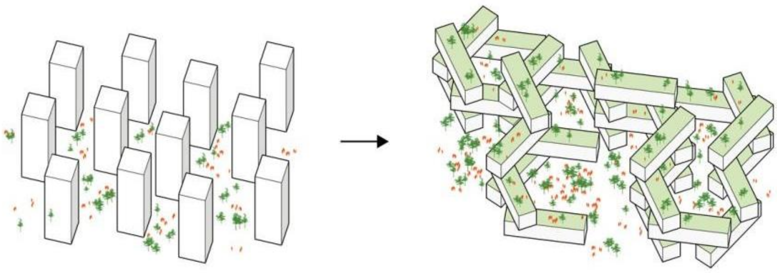

Figure 2.4: Maximizing the green space – Comparison of Interlace, Singapore and typical development of equal density

Source: (archdaily, n.d.)

The dominant characteristic in the high-rise residential building typology is the height of the building. At present, there is little definition of what height constitutes a high-rise building. The number of floors in high-rise residential buildings differs around the world. According to the Council on Tall Buildings and Urban Habitat (CTBUH), there is no absolute definition of what constitutes a "tall building". The definition is subjective, considered against one or more of the following categories. (i) Height relevant to context, (ii) Proportion and (iii) Embracing technologies relevant to tall buildings. "Super tall" is a tall building over 300 meters (984 feet) in height, and a "Mega tall" is a tall building over 600 meters (1,968 feet) in height (CTBUH, n.d.).

High-rise residential buildings in Singapore, China, and Hong Kong far exceed 10 storeys. The decision as to how tall a residential building can go depends on the needs, culture, and social acceptability and economics (Yuen and Yeh, 2011). For example, the average preferred height for residence is 29.3 in Hong Kong and 20.9 for Singapore (Yuen and Yeh, 2011). In Sri Lanka, according to the building regulations, any building with ground plus 4 floors is considered a high-rise building (except in the Colombo Metropolitan area where high-rise building is 13 floors or above) without further classification into its function; commercial, public, or residential use (Urban Development Authority, 2005). Therefore, the height of a high-rise building though critical information to the building typology is subjective to the social, cultural, and environmental needs of the site.

The high-rise residential building typology, according to the above discussion, is required to increase building density, while maintaining surrounding greening and solar access. However, the more common interpretations of high-rise residential typology fail to fall in line with the Radiant city and the Sustainable city concepts. Most high-rise residential buildings boast densification at the cost of greenery and solar access. They are devoid of communal areas, greenery, terraces, and architecture (Curtis, 1986). Most high-rise residential buildings in Colombo are constructed to free space for more buildings and not greenery and better solar access.

The cause of such unsustainable construction is the lack of understanding of the high-rise residential building typology. Therefore, there is a need to investigate the impact of high building density on solar access and greenery in the high-rise-residential building typology.

2.2 Solar access in buildings

The benefits of exposure to sunlight for human wellbeing and productivity have been well documented (Durvasula et al., 2010; Ratcliffe & Day, 2004; Razzaque, 2018; Sakamoto, 2019). Many studies provide evidence of vitamin D deficiency, due to the lack of sun exposure (Durvasula et al., 2012; Lau et al., 2011; Sakamoto, 2019). Eighty percent of the required vitamin D in humans is obtained by UVB sunlight (Razzaque, 2018). Therefore, limited sun exposure increases risks for vitamin D deficiency (Sakamoto, 2019). Many resolve to take vitamin D supplements to cover for inadequate solar exposure. However, the drawbacks of vitamin D supplements are also noted in research (Razzaque, 2018). In addition to vitamin D deficiency, regular exposure to sunlight contributes to preventing many other diseases, such as colon-, breast-, prostate cancer, non-Hodgkin lymphoma, multiple sclerosis, hypertension, and diabetes (Van der Rhee et al., 2016).

Recent attention to the benefits of sunlight in reducing COVID-19 infections and recovery rate has reinstated the need to ensure sunlight exposure (Asyary & Veruswati, 2020; Lansiaux et al., 2020). Most activities are now conducted indoors and therefore, buildings should ensure residents with adequate solar exposure to keep healthy while at home. The increased time spent at home due to the COVID-19 situation has also further emphasized the need for solar access in residential buildings.

The spectrum of solar radiation extends from 290 to 2300 nm. The two main benefits of solar radiation, come from visible light (380 nm-700 nm) and short infra-red radiation (700 nm-2300 nm). Ultra-violet radiation (290 to 380 nm) is avoided due to harmful effects on the skin (Koenigsberger et al., 1973). The spectral energy distribution varies with altitude due to the atmosphere's filtering effect, latitude, and the tilt of the earth's axis.

Solar radiation is measured in solar irradiance in watts per square metre (W/m^2). The distribution of incoming solar irradiance close to the earth surface is a collection of reflected, diffused, and direct solar radiation (Givoni, 1998). The quantity of horizontal solar radiation on the site depends on the transparency of the atmosphere, slope and orientation of the site and nearby obstructions. Solar radiation incident on the vertical surface is impacted by the orientation and surface material.

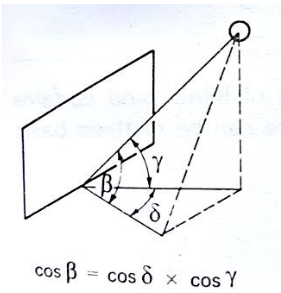

Figure 2.5: Angle of incidence

Source: (Koenigsberger et al., 1973)

The sun's position in relation to the building elevation must be established for the given point of time to find the angle of incidence of solar radiation as depicted in Figure 2.5. The solar azimuth angle (δ) and the solar altitude angle (γ) could be read off the sun path diagrams for any hour and date of the year. From the above two angles, the sun's position in relation to the wall surface of any orientation can be established as in Figure 2.5. The angle of incidence (β) is utilized for calculating the incident solar radiation on an external wall surface of the building.

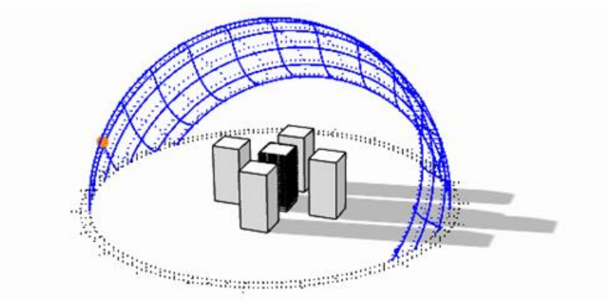

Figure 2.6: The sun path and shadows simulated in *DIVA4* software

At present numerous computer software exists which could develop a 3D sun path diagram and quantify the solar radiation incident on the vertical surface of the building (Figure 2.6).

2.2.1 Solar access in dense urban contexts

The high-rise residential buildings are a part of a high-density urban context. The most challenging passive design strategy in a dense urban context is ensuring adequate solar access (Han et al., 2017; Seong et al., 2006). The term "solar access" is defined as the ability of a unit to continuously receive sunlight without obstruction from any other properties or structures (Knowles, 2003; Lau et al., 2011; Shaviv & Yezioro, 1997). Due to the reduction in solar access as a result of dense urban contexts (D. H.W. Li et al., 2006; Lima et al., 2019; O'Brien et al., 2010; Ratti et al., 2015; Steemers, 2003), solar access is considered a legal right in parts of the world where solar insolation is limited (De Luca & Dogan, 2019; Hraška, 2020). In South Korea, where there are a large number of high-rise residential buildings, solar rights are generally associated with ensuring human health, work productivity, thermal comfort, and visual comfort in apartment buildings (Seong et al., 2006). In the U.S., solar rights law protects a homeowner’s right to solar access to produce renewable energy (Grout, 1980).

The solar envelope method enables the protection of the solar rights of the building occupants (Capeluto and Shaviv, 2001). Introduced by R.L Knowles, the buildings within the solar envelope will not overshadow their surroundings during the critical periods of solar access (Knowles, 2003). Capeluto and Shaviv (2001) have introduced the “solar rights envelope” and “solar collector envelope” which extend the application of the solar envelope. Further developments have been made to the solar envelope by including the neighbouring buildings in the overshadowing calculation (De Luca and Dogan, 2019).

One of the first regulations to ensure adequate solar access is the obstruction angle, the angle between the distance between buildings and the height difference of the floor level and the obstruction. A 45° obstruction was considered as a suitable standard in the medium latitudes of Europe (Hraška, 2020). More recent regulations focus on specific direct sunlight hours or a particular time during the day (the cities of Boulder and Ashland in the US), the quantity of direct sunlight hours during the day (Czech Republic, Slovenia, Poland, Slovakia, Germany and China) or a ratio or percentage of the actual quantity of direct solar access during the day (UK and Estonia) (De Luca and Dogan, 2019). The European standard EN 17037 also requires at least 1.5 hours of direct sunlight exposure per day.

From the above discussion, it was observed, that current research and regulations focus on unobstructed solar access for regions of higher latitudes, where solar insolation is low. In the tropics, where solar insolation is high unobstructed solar access is avoided due to heat gain in buildings (Emmanuel, 2005; Givoni, 1998; Hyde, 2000). At present many tropical cities struggle to provide adequate solar access despite the high levels of solar insolation due to increasing building heights and densities. Therefore, solar access and solar rights are emerging topics for discussion on the sustainability of the tropical city.

2.2.2 Indoor daylight in dense urban contexts

Daylight is the visual spectrum of solar radiation, indicated by a narrow bandwidth of 380 to 780 nm. Daylight could enter the building through openings and glazed surfaces; in the form of direct light, skylight reflected light, and internally reflected light (Figure 2.7).

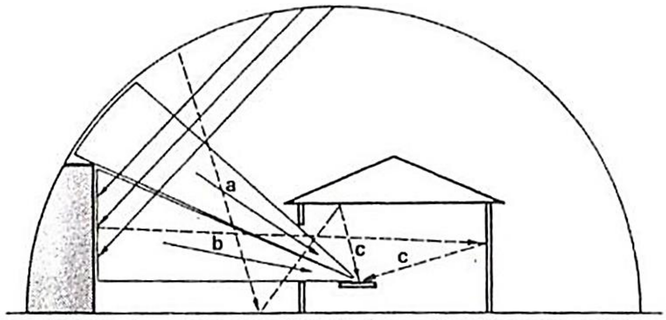

a= Diffused or skylight through window or opening

b = Externally reflected light (by the ground or other building), through windows

c= Internally reflected light form walls, ceiling, or other internal surfaces

d= Direct sunlight, along a straight path from the sun, through a window to the given point

Figure 2.7: Daylight in an indoor environment

Source: (Koenigsberger et al., 1973)

Daylight is the desirable source of lighting in interior spaces for many. However, in the tropics, the abundance of daylight is often sacrificed to minimize heat gain. Daylight is measured in illuminance (Lux). When in bright sunshine, the illuminance is around 100,000 lux, and the corresponding intensity of thermal radiation is likely to be about 1 kW/m^2 (Koenigsberger et al., 1973).

In the past, residents in the tropics did not experience any discomfort due to lack of indoor daylight and solar access, as many activities were carried out outside and most interior spaces were used for short term stay or sleeping at night. This dynamic has now changed, as many living in cities conduct their daily activities indoors, increasing the need for indoor daylight. Dense urban contexts further compound the issue by reducing daylight into buildings by shading. Especially in high-density residential contexts, such as in Hong Kong, certain studies find indoor daylight levels to be severely reduced in the lower floors due to neighbouring buildings, and residents relying on artificial lighting during daytime (Hamzah & Lau, 2016; D. H.W. Li et al., 2006; Xie et al., 2017; Xue et al., 2014). Hamzah and Lau (2016) found the required daylight level is difficult to achieve in Hong Kong due to high densities. Therefore, even though the tropics experience ample daylight, high building densities, and current lifestyles increase the need for indoor daylighting levels.

The main factors that affect indoor daylight levels are the distance between buildings, the height of the facing buildings, the orientation of the building, the reflectance for the facing buildings, the size of the openings and the size of shading devices (Santamouris, 2001). Standards ensure adequate daylight in buildings by dictating the above factors. One of the basic standards for daylight requirement in building design is dictating the window opening size. In Sri Lanka daylight standards for residential rooms are met by providing 15% of the floor space area of the room as the size for the window opening. At least 70% of the window should be openable (UDA, 2008).

2.2.2.1 Daylight metrics

Daylight calculations take into account the visible sky area. The Vertical daylight factor (VDF) is defined as the ratio of the total amount of daylight illuminance falling onto a building's vertical surface compared to the amount of unobstructed daylight available outside under overcast sky conditions. In Hong Kong, the VDF taken in the centre of the window pane should be 8% for habitable rooms and 4% for kitchens (Hamzah & Lau, 2016). The Unobstructed vision area (UVA) method is practised to calculate the Vertical daylight factor (VDF) of the highly obstructed urban contexts (Ng, 2003). The VDF is calculated as a ratio, limiting its ability to express the actual indoor daylight levels.

The first European standard for daylight in buildings-EN 17037 was published in 2018. EN 17037, has four standards for the assessment of daylight in interior spaces: daylight provision, view out, exposure to sunlight and protection from glare. For the daylight provision, 95% of the space of at least 100 lux is required for at least 50% of the daylight hours in the year, and 50% of the space of at least 300 lux is required for at 50% of the daylight hours. EN 17037 proposes to use the daylight factor to assess the daylight in a space (EN 17037, 2018).

This study focuses on the dual characteristics of heat gain and daylight from solar access into the building. Therefore, measuring indoor daylight levels would allow for the comparison of heat gain due to solar access.

At present, new daylight metrics based on Climate Based Daylight Modelling (CBDM) such as Useful daylight illuminance (UDI), Spatial daylight autonomy (sDA), and Annual sunlight exposure (ASE) are available. Spatial daylight autonomy (sDA) is calculated as the percentage of floor area that receives at least 300 lux for at least 50% of the annual occupied hours. The sky conditions for simulation of the sDA are obtained from the weather file of the location. ASE is calculated as a percentage of the floor area that receives 1000lx for 250 hours annually. LEED (Leadership in Energy and Environmental Design) requires to demonstrate through annual computer simulations that $sDA_{(300lx/50)}$ is achieved by at least 55% (2pts) or 75% (3pts) of the occupied spaces for new construction, core and shell, schools, retail, data centres, warehouses & distribution centres and hospitality (*LEED BD+C: Healthcare | v4 - LEED v4 Daylight*, n.d.). The standard also requires $ASE_{(1000\ lx,\ 250)}$ of no more than 10% to be achieved.

Noting a lack of standards for residential buildings, Dogan and Park (2017) developed a Residential daylight scoreboard based on 60% Residential daylight autonomy ($RDA_{(300lx,50)}$) for diurnal and seasonal analysis timeframes and direct solar access. The authors note the limitations in application to hot-humid climates. Therefore, there is a shortcoming of indoor daylighting standards for the residential sector in the tropics.

It is becoming more challenging to regulate indoor daylight levels without considering the effects of the urban context.

2.3 Energy efficiency in buildings

Three global events brought the energy crisis to the forefront. Firstly, the oil crisis of the 1970s, secondly, the Kyoto protocol in 1997, and thirdly, the publication of the Inter-governmental Panel for Climate Change (IPCC) reports in 2007. The oil crisis of the early 1970s highlighted the risks of the energy dependence of buildings. In the 1980s and 1990s, interest in energy efficiency waned considerably due to the narrow predictability of the deterministic climate-conscious architecture (Emmanuel, 2005). Almost 30 decades later, the impact of the burning of fossil fuels on Climate Change was first bought to the global platform. The Kyoto Protocol identified industrialized countries as the cause of Climate Change and bound them to operate the United Nations Framework for Climate Change (UNFCC). However, many governments failed to take substantive action to mitigate climate change due to a lack of information. Understanding the gaps in the literature, the IPCC produced their first report on Climate Change in 2007. The three working groups in the IPCC cover physical science, impacts, adaptation and vulnerability, and mitigation of climate change, hence becoming the most reliable source of information on the topic (IPCC, 2014). Since then, there has been a steady growth in publications, standards, guidelines, competitions, and incentives that focus on reducing CO_2 emissions through energy efficiency.

"Energy efficiency" is a generic term, and there is no single quantitative measure of energy efficiency. In general, energy efficiency refers to using less energy to produce the same number of services or useful output (Patterson, 1996). According to Patterson (1996), the generally used measure for building energy efficiency is energy input per square meter. Recently, most research utilizes energy use intensity (EUI) and energy performance indicators (EPI) as the measure of energy efficiency with slightly varying definitions (Pérez-Lombard et al., 2009). Energy use per floor area

(Chung et al., 2006; Quan et al., 2016; Samuelson et al., 2016), energy use per person per year (Shabunko et al., 2014) and energy use per square meter per year (Toutou et al., 2018; J. Zhang et al., 2019) are expressions of EUI commonly used in literature.

Benchmarking the energy efficiency of buildings allows identifying the best practices in the sector. The two main benchmarking methods are the empirical methods that allow the rating of a building and the simulation model-based method that further improves the building's energy performance (Cohen & Bordass, 2006). Simulation models have many applications in benchmarking, as they can manipulate a wide range of parameters that contribute to variations in energy use (Attia et al., 2012; Fumo et al., 2010; Pérez-Lombard et al., 2009). They are also used to generate targets and compare design alternatives (Nikolaou et al., 2011; Tereci et al., 2013). A disadvantage of benchmarks based on simulation models is that they may not be well calibrated to the actual buildings stock data(Pérez-Lombard et al., 2009). Therefore, simulation models of the building stock for benchmarking should be calibrated independently to verify simulation results.

In building energy benchmarking, specific indices are used to compare and rate building energy efficiency. The Energy Star Program which is the flagship energy standard for buildings by the Department of Energy in the United States uses Energy Efficiency Ratio (EER), which is calculated as actual EUI (EUI_{act}) divided by predicted EUI (EUI_{pred}). It is shown in Eq. (1)(Gao & Malkawi, 2014).

$$EER = \frac{EUI_{act}}{EUI_{pred}}$$

Equation 1: Energy Efficiency Ratio

Energy efficiency in buildings can be divided into demand-side and supply-side energy efficiency. Supply-side energy comes from the building components that power the building, whilst demand-side energy is related to components that use power (Hyde, 2000). Buildings utilize energy during construction as well as in operation. The term "Embodied energy" is used to assess energy use in the production of building materials. "Operational energy" is the energy used during the operation of a building for lighting, equipment, air conditioning, etc. Many factors contribute to the operational energy efficiency of a residential unit. According to Steemers and Baker (2000) demand-side energy depends on five factors: climate, urban geometry, building design, systems efficiency, and user behaviour. Therefore, improving demand-side energy efficiency is a complex task that includes many input and output variables.

In an age where Climate Change is arguably the greatest challenge to the modern world and bodies such as the IPCC predict a temperature increase of between 1.8ºC and 4ºC by the end of the century, energy efficiency measures need to be promptly adopted by the construction sector. In 2010, buildings accounted for 32% of total global energy use, 19% of energy-related GHG emissions (including electricity-related), and approximately one-third of black carbon emissions (IPCC, 2014). The IPCC further reassures the growing trend in electricity use in buildings in the future. Due to climate change, improving demand-side energy efficiency in buildings has become a key concern in global architectural practice and research.

2.3.1 Energy efficiency in the residential sector

In 2010, out of the 32% of global energy use for buildings, 27% was consumed by the residential sector. Apart from being the largest energy consumer by sector, residential energy use quintupled from 1970 to 2010 (IPCC, 2014). Most of this increase has occurred in developing countries, driven by population, urbanization, and economic growth (Nejat et al., 2015).

The residential sector energy use could further be divided by residential building types and by household type. Table 2.1 depicts the household energy use in the United States in 2009 by house type, household member, and square area.

Table 2.1: Household energy use in the United States of America -2009

Housing Unit Characteristics and Energy Usage Indicators	**Per Household** (million Btu)	**Per Household Member** (million Btu)	**Per Square Foot** (thousand Btu)
Housing Unit Type			
Single-Family total	103.6	37.7	42.8
Single-Family Detached	105.7	38.0	42.6
Single-Family Attached	81.3	33.0	46.0
Multi-Family total	55.8	27.2	60.0
Apartments in 2-4 Unit Buildings	76.1	32.8	69.2
Apartments in 5 or More Unit Buildings	**46.3**	**24.0**	**54.5**
Mobile Homes	67.9	25.8	62.5

Source: (Ko, 2013)

From the above Table, it is clear that multifamily units use less energy per household but more energy per square foot than single-family housing. Lower per household energy consumption in apartments can be explained by the number of people in the household. More than 75% of the apartments are occupied by less than two people (RECS, 2009). Table 2.1 shows no distinction between apartments with more than 5 units in the study as high-rise or low-rise residential buildings. In the residential sector, energy use measurement by floor area, housing type, and household member differs significantly; hence, selecting the correct energy efficiency measure is critical to compare data. Table 2.1 indicates that in the U.S. energy use is lower in apartments of more than 5 units in terms of household energy use; however, there is room for improvement in building design as per square foot consumption is higher in multi-family apartments.

2.3.2 Energy efficiency in the residential sector in the tropics

Buildings consume energy primarily in environmental control processes in mediating between the external climate and the internal environment (Hawkes, 1996).

The hot-humid climate of the tropics is described as follows.

“The warm humid climate which prevails in cities like Jakarta, Singapore and Colombo are near the equator expanding 15 degrees of N and S. In these climates there is very little seasonal variation, the only punctuation being the periods with more or less rain and the occurrence of gusty wind and electric storms. In the shade air temperature reaches a mean maximum during the day of between 27-32^{0}C, but occasionally it may exceed the later value. At night the mean minimum varies between 21^{0}C and 27^{0}C. Both the diurnal and annual range of temperature are quite low. Humidity remains high at above 75%."

(Koenigsberger et al., 1973)

The urban areas in the tropics create a micro-climate of their own, deviating significantly from the microclimate of the region (Givoni, 1998). This phenomenon is referred to as the Urban heat island (UHI) effect. Several studies find that the increase in ambient air temperature due to UHI effect increases the building energy demand for indoor thermal comfort (C. Li et al., 2018; Santamouris et al., 2015). Nocturnal UHI intensity is low relative to daytime UHI; however, it affects night time thermal stress (Giridharan et al., 2005). Therefore, the urban climate presents additional challenges for achieving day and night-time thermal comfort in buildings than the macroclimate of the tropics.

The tropics' primary sensory thermal responses are the sensations of heat and the discomfort from sensible perspiration (Emmanuel, 2005; Hyde, 2000; Koenigsberger et al., 1973). Due to high humidity year-round in the tropics, heat dissipation from the body does not happen to a desirable level to achieve thermal comfort. High humidity levels in the airflow of naturally ventilated buildings aid heat dissipation from the body. Therefore, maximizing air movement and minimizing heat gain are the key strategies to achieve thermal comfort in buildings in the tropics.

Primarily, heat is gained into a building by conduction through walls and other exposed surfaces, convection through openings, and radiation through direct sunlight exposure as depicted in Figure 2.8. In the tropics, the direct heat gains through the glazed and opaque surfaces contribute to increased indoor air temperature.

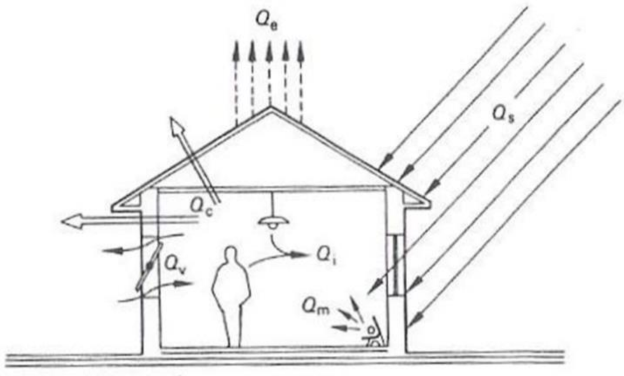

The Thermal balance, i.e. the existing thermal condition, is maintained if:

$Q_{i\ (internal\ heat\ gain)} + Q_{s\ (solar\ heat\ gain)} + Q_{c(conduction)} + Q_{v(convection)} + Q_{m(mechanical\ controls)} + Q_{e\ (evaporation)} = 0$

Figure 2.8: Heat gain in a building

Source: (Koenigsberger et al., 1973)

If the sum of the equation in Figure 2.8: is less than zero (negative), the building will be cooling, and it is more than zero, the temperature in the building will increase. In the tropics, the sum of the above equation is almost always considerably over zero. Therefore, the highest percentage of energy in the tropics is used to maintain indoor thermal comfort due to external heat gains in buildings (Givoni, 1998; Hyde, 2000). Figure 2.9 illustrates the residential energy use pattern in Singapore, which has a tropical climate.

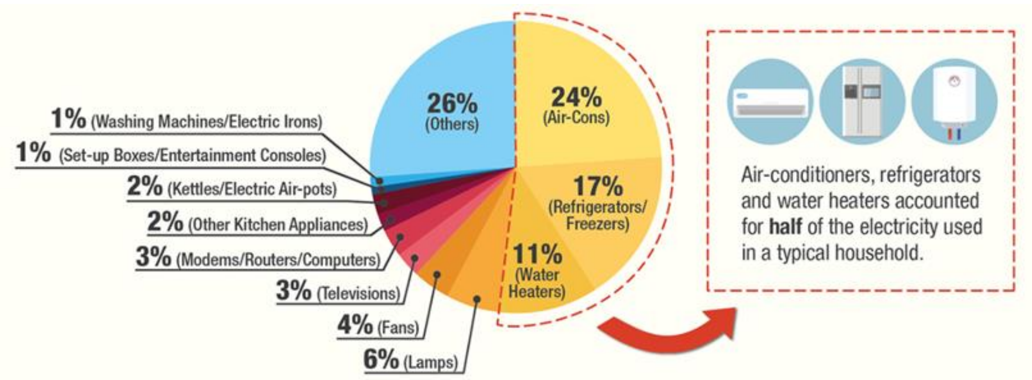

Figure 2.9: Breakdown of household energy consumption in Singapore-2017

Source: (National Energy Agency, 2017)

It is clear from Figure 2.9 that the bulk of the energy in a typical household is used for air-conditioning in Singapore. Therefore, a key determinant of demand-side energy efficiency of a residential unit is energy use for cooling. A field study on thermal comfort in buildings in tropical climates by Mallick (1996) indicated a high tolerance level to higher temperature and humidity levels in tropics. However, the study also noted the lack of experience in air-conditioned environments contributes to a high level of tolerance. Current trends in increasing air-conditioning in the tropics (Cheshmehzangi & Butters, 2015) indicate that the tolerance level of residents for high temperature and humidity is becoming less in the tropics. Considering the above trends cooling energy use in residential and commercial buildings is expected to grow by 84%, respectively, over 2010–2050 in a business-as-usual scenario (IPCC, 2014).

Nevertheless, the IPCC noted that many future urban GHG emissions reduction opportunities exist in small to medium-sized cities in developing countries located in the tropics (IPCC, 2014). The main reason cited in the report is that urbanization is still early in these countries. Therefore, it could be directed to a sustainable path from early on in the urbanization process. Due to buildings' long-life span, if energy efficiency is not dealt with at the urban planning stage, rectifying them when consequences become evident is nearly impossible. Countries like Singapore have urbanized with sustainability intentions in the last half-century and are now reaping the benefits. Therefore, attention must be given to energy efficiency at the early stages of urbanization in small to medium tropical cities in developing countries.

2.3.3 Energy efficiency in dense urban contexts

Many cities now focus on increasing residential density within city limits to align with the compact city concept (Williams et al, 2000; Gauzin-Muller, 2002). High-density built environments are associated with higher energy efficiency levels (Newman & Kenworthy, 2006; Rode et al., 2014). In the residential sector, high-density residential development/multifamily housing reports better energy savings compared to low-density development/ single-family housing (C. K. Cheung et al., 2005; Ewing, 2010; Givoni, 1998; Ko, 2013; C. Li et al., 2018; Norman et al., 2006; O'Brien et al., 2010; Rode et al., 2014). Therefore, high-density, high-rise housing is preferred over low-density, low-rise housing in terms of energy sustainability.

One of the first studies on quantification of energy savings from the urban context, by Ratti et al. (2003) attributed 10% variation in building energy performance to the urban context. Since then, several studies (Han et al., 2017; Lima et al., 2019; Pisello et al., 2014; Samuelson et al., 2016) quantified the effect of urban context on operational energy use indicate substantial energy savings. A study on the impact of the urban context on energy use in an office building in a hot-humid climate found average reductions in the thermal load of 16–18% due to the context (Lima et al., 2019). A survey of commercial buildings in subtropical Hong Kong found that the cooling load was over-estimated by 2% due to neglecting contextual shading benefits (Lam, 2000). In contrast, in cold climates, solar obstruction of 30^0 to the south facade of a passive solar house can increase heating energy by 22%, compared to an unobstructed façade (Steemers, 2003). Therefore, in warm climates, significant energy savings could be accounted due to contextual shading (Han et al., 2017; Lima et al., 2019; Pisello et al., 2012) while in cooler climates an increase in energy use could be expected (Steemers, 2003).

However, the relationship between building density (excluding transport energy) and energy efficiency, is observed to be non-linear mainly due to the reduced solar access at high building densities in several studies (Ko, 2013; Quan et al., 2014; Resch et al., 2016; Steemers, 2003) Therefore, the upper limits of density in terms of energy efficiency and solar access merit further investigation.

The above literature review ascertains that the high-density urban context obstructs solar access (Han et al., 2017; Seong et al., 2006), reduces indoor luminous comfort (Xue et al., 2014), increase daytime lighting use (Pisello et al., 2014; N. H. Wong & Li, 2007), and increases heating energy use (Steemers, 2003) but significantly decreases cooling energy use (Han et al., 2017; Lima et al., 2019; Samuelson et al., 2016). Therefore, the dual characteristics of solar access-daylight and energy use, both need to be optimized to ensure solar access in the dense urban tropics.

2.4 Parameters of investigation in the urban context

The objectives of this study focus on investigating the impact of the urban context on solar access in dense urban tropics. Therefore, the selection and application of parameters of investigation in the urban context and solar access in current literature is discussed in this section.

2.4.1 Measures of residential density

The urban context is described in most research studies by measures of density. At its simplest, density is a number of units in a given area (Forsyth, 2003). Depending on the type of unit and the size of the given area, the meaning of the density measure will be very different. For example, Net density refers to the number of dwellings per area on land for residential development, and Gross density means the density of a given area, including infrastructures such as public roads, public open space, and in some instances non-residential development such as schools and shops (Forsyth, 2003).

Philosophically density can be measured as physical and perceived density (Bâldea and Dumitrescu, 2013). Physical Density measures include a number of people, a number of dwelling units per acre, and related land-use intensity measures such as coverage and floor area ratios (Alexander et al, 1988). It is the measurement that discriminates between urban and rural areas. Perceived density represents the individual perception of an estimated number of people present in a given area or that of the vacant space and its organization. Perceived density refers to the relative relations between individuals and space and the relations between individuals located in the same space (Bâldea and Dumitrescu, 2013).

Numerous physical urban density measures, such as population density, residential density, and building density, describe the urban context. The calculation of each measure will depend on the purpose and scale of the study or application. The limitations of the current measures of density in describing residential building typologies have been discussed by Alexander et al. (1988); Berghauser Pont and Haput (2007) and Forsyth (2003). The relationship between housing type and density is explored by Alexander et al. (1988) using four housing typologies- single-family detached housing, row housing, low-rise garden apartments, and high-rise multiple-family housing. The study confirmed that a relationship between density range for single-family housing and high-rise housing exists; while row housing and apartments have a broad range of intermediate densities. A study of residential typologies and density by Berghauser Pont and Haput (2007) found that different building density measures such as FAR, building height, Plot coverage and Ground Space index generate very different house typologies. Another aspect of confusion in density is physical measures of land-use intensity, including building bulk and coverage. Often people confuse density with residential building type and assume, for example, that detached houses are lower density than attached housing types. While this is generally true, it is not always the case. A high-rise residential building with large units set on a park-like site may be lower density than a set of detached houses on small lots (Forsyth, 2003).

Floor Area Ratio (FAR)	Building height	Plot Coverage	Building setback
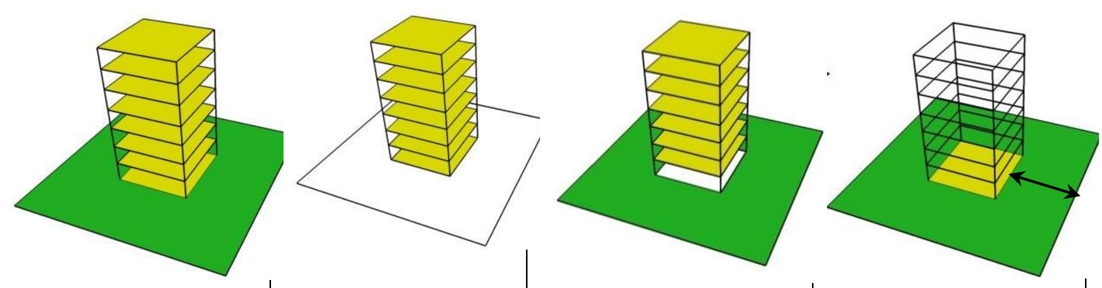			
Total floor area of the building divided by site area	Total number of floors of the building	Built space at ground level divided by site area	Distance to the boundary from the building

Figure 2.10: Building density measurements

In Figure 2.10, four-building density measures are illustrated. Each measure gives a robust understanding of the density within the plot, and in terms of the urban density of the neighbourhood. Berghauser Pont and Haput (2007, 2010) concluded that only when density is seen as a composite of aspects, such as intensity, compactness, height, and spaciousness, can it be satisfactorily used to differentiate between urban fabrics, understand their characteristics, and design guidelines for future developments. Therefore, more than one density measure is needed to represent the physical characteristics of the residential building typology.

2.4.2 Parameters of investigation in the urban context on solar access

In this section, parameters of investigation in studies on the effects of the urban context on solar access are discussed. Urban density measures, solar access indicators, the climate of study and the building type are compared in Appendix D.

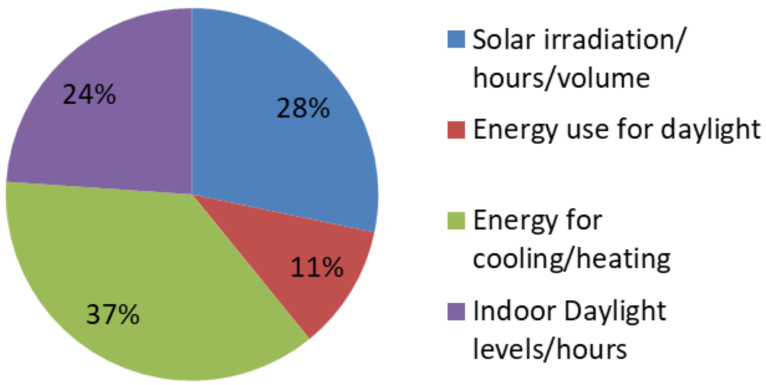

Figure 2.11: Solar access indicators in studies

Figure 2.11 summarized four solar access indicators identified in the literature review. The four solar access indicators were solar radiation, daylight levels, energy use for daylight and energy use for heating/cooling. In 28% of the studies, the measure of solar access was solar radiation on exposed building surfaces. However, it was noted that in a few studies, the research objective was to measure photovoltaic energy generation potential in an urban context and not the impact of solar access. The term "solar potential" often refers to the ability of a surface to receive solar radiation for the generation of energy (Lobaccaro et al., 2017; J. Zhang et al., 2019), which is beyond the scope of this study. However, it was included in the analysis as similar parameters for solar access are utilized.

The most favoured solar access indicator is the building energy use, which was utilized in 37% of the studies. Only 11% of the studies account for artificial lighting when estimating the energy savings/increase due to contextual shading. Neglecting artificial day-time lighting requirements could lead to over-estimated energy savings in the urban tropics. 24% of the studies focused on indoor daylight levels. An increase in daylight availability studies in urban contexts was noted in recent years (Kosir & Sprah, 2019; Santos et al., 2017), which could be attributed to new software such as *Radiance* interfaces (*DIVA4)*.

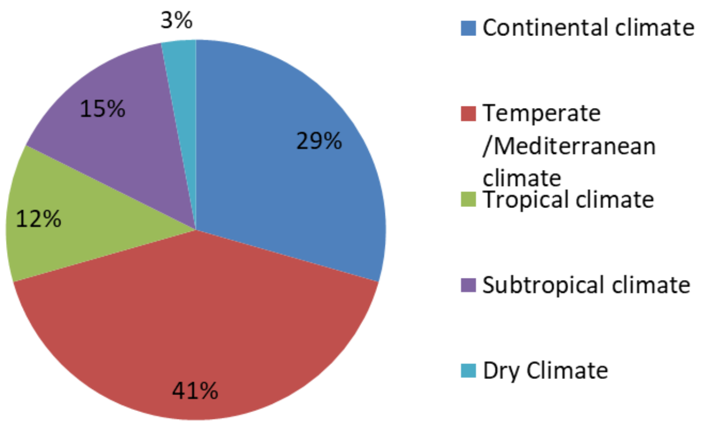

Figure 2.12: Climate of study

Most studies on solar access are conducted in the Continental, Temperate/ Mediterranean climates (27% and 47% respectively) as depicted in Figure 2.12, where solar insolation needs to be maximized during most of the year. 15% of the studies focus on the subtropical region of Hong Kong. Twelve percent of the studies on solar access/potential were conducted in the tropics of Singapore, Brazil, and Miami city in the United States. A few studies compared the analysis across different climates (De Luca & Dogan, 2019; Han et al., 2017; Pisello et al., 2012; Samuelson et al., 2016). A lack of studies in dense tropical cities in South Asia such as Chennai, Colombo, Dhaka was noted. Due to rapid urban migration and poor urban planning in South Asia (World Bank, 2016), the impact of high densities on solar access merits investigation. It was also observed that due to the lack of studies in this region, the assumptions for the thermal and daylight simulation models were not well established.

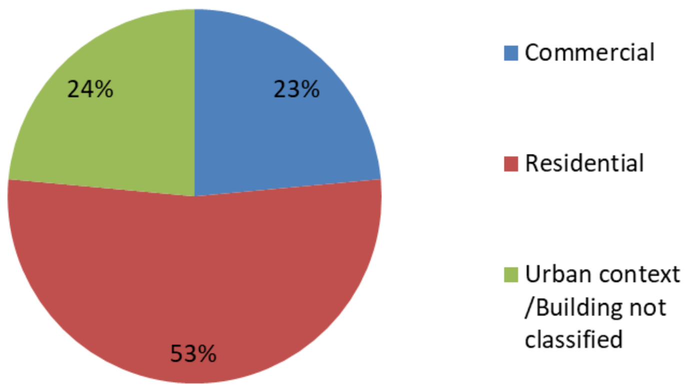

Figure 2.13: Building typology of study

Figure 2.13 compares the building typologies (commercial, residential, and urban). Most of the studies on solar access are conducted in a residential context (53%), as the need for solar access for human well-being is most pronounced in residential spaces. Due to the complexity of the urban context, most building typologies were simplified or generalized before being simulated.

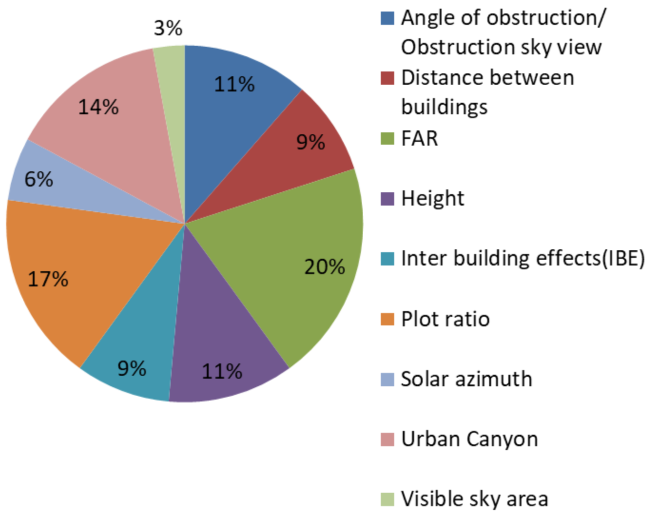

Figure 2.14: Urban density measures in studies

Several parameters of the urban context were utilized to assess the impact on solar access as tabulated in Appendix D. Several studies use block typologies to indicate urban densities (Lima et al., 2019; Samuelson et al., 2016; J. Zhang et al., 2019). Block typologies are not density measures, and therefore, are not considered to populate Figure 2.14, which compares the density measures utilized in studies of solar access.

Ten density parameters were utilized in the studies. The most common density parameter investigated in determining solar access is FAR at 20%, followed by plot coverage at 17%, urban canyon at 14%, building height at 11%, and distance between buildings at 9%. Except for the urban canyon parameter, the other parameters are urban planning regulations. Though the FAR was the most popular density parameter of investigation, due to the many forms that could be taken under a given FAR, the question arises to what extent could the FAR determine solar access into the building. As discussed in the previous section 2.4.1, a single density tool could not accurately depict all urban density characteristics. Out of the commonly utilized urban planning tools, the distance between buildings (building setback) was the least investigated. Nevertheless, the building setback could give a more accurate indication of solar access as it has a fixed distance to the site boundary from the building.

The urban canyon is the most effective predictor of solar access in the urban context as it takes into account building height and distance between buildings. However, as it involves measuring the buildings outside the site boundary, making it difficult to utilize it as a planning regulation. Using existing urban planning tools to explore the effects of urban density on solar access could incorporate the research output into the current urban planning regulations more effectively.

2.5 Approaches in the simulation of the urban context

Since the late 1990's, several tools were developed to simulate shading from the urban context. (Shaviv & Yezioro, 1997) developed a *CAD* (Computer-aided design) tool that can analyse the mutual shading between buildings and surrounding objects, such as trees. However, it does not consider the indoor air temperature, daylight, and energy use of the building. One of the first studies that quantified the effects of the urban context on energy use at the city scale was conducted by Ratti et al. (Ratti et al., 2015) using the LT (Lighting and Thermal) model coupled with the analysis of the Digital Elevated Model (DEM). New developments such as *Umi* -Urban Modelling Software (Reinhart et al., 2013) conducts fast calculations on the effects of the urban context on building operational energy, walkability and building embodied energy.

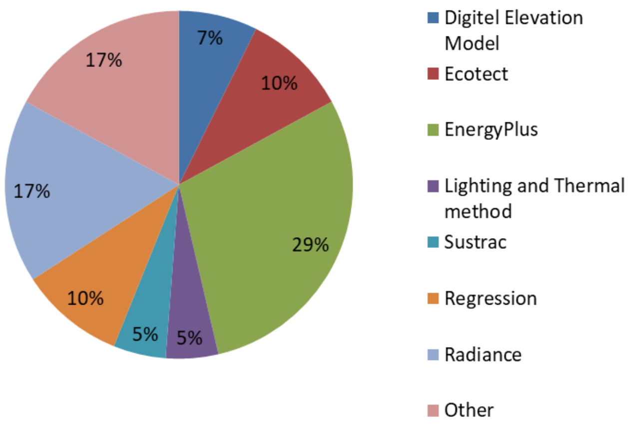

Figure 2.15: Simulation tools and statistical methods for quantifying the effects of the urban context on solar access

Figure 2.15 illustrates the simulation tools and statistical methods employed to quantify the effects of the urban context on solar access, energy use, and daylight. *EnergyPlus* remains the most popular platform for investigating shading effects on building energy performance (Han et al., 2017; Li et al., 2006; Lima et al., 2019; Pisello et al., 2012, 2014) according to Figure 2.15. *EnergyPlus* accounts for solar gains from diffused and direct solar radiation, however, does not account for reflected radiation. Ideally, modelling effects of solar radiation in the urban context should consider shading due to surrounding buildings, building reflections, and the Urban heat island effect (UHI). Several studies find that shading from the urban context has a significantly higher effect over, building reflections, and UHI effect on building energy use (Han et al., 2017; Lima et al., 2019). Shading was found to reduce energy consumption by 14-16% while solar reflections only accounted for 3-4% while changing the weather file to simulate UHI did not result in a notable change in a study of energy use of an office building in a tropical climate (Lima et al., 2019). Therefore, utilizing *EnergyPlus* would be adequate for most studies focusing only on shading effects of the urban context on building energy performance.

Radiance remains the most popular simulation engine for daylight studies (Compagnon, 2004; De Luca & Dogan, 2019; Hamzah & Lau, 2016; Kosir & Sprah, 2019; M. Lu & Du, 2013a; Natanian et al., 2019). *Radiance* has the capacity to model direct, diffused, and reflected radiation from nearby buildings and shading effects. *EnergyPlus* approaches daylight simulations with the split-flux method (DOE, n.d.) while Radiance employs the ray-tracing technique (Jakubiec & Reinhart, 2011). Studies find that the split flux method overestimates luminance values (Ramos & Ghisi, 2010; Versage et al., 2010; Yoon et al., 2014). Therefore, many studies support the *Radiance* method of estimating daylighting levels and lighting energy use than the *EnergyPlus* method (Chi et al., 2017).

2.5.1 Parametric models for simulating the urban context.

The term “parametric” refers to the assumption of values in a parameter. If several values need to be assumed for the analysis, the method utilized is termed a parametric analysis. However, if there is only one value assumed, then such methods are known as non-parametric analysis. Parametric methods allow the generation of several options for selecting the optimum solution or a set of solutions.

An early study of parametric computer modelling was conducted by Capeluto & Shaviv (2001) with the computer software *Sustrac* to ensure adequate solar access to an urban block in Tel Aviv, Israel. The parameters of the investigation were the distances between the buildings.

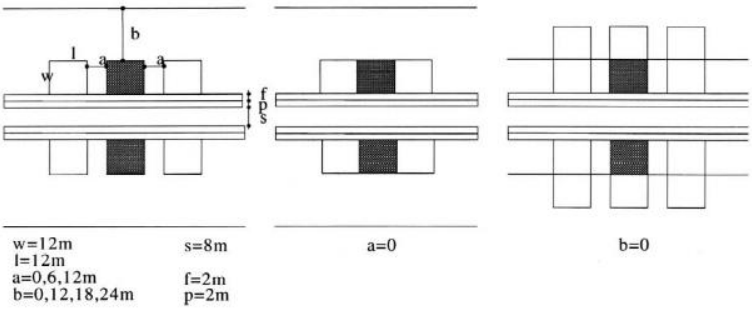

Figure 2.16: -Different configuration for the urban fabric

Source:(Capeluto & Shaviv, 2001)

Various layouts for the urban fabric are created by assigning distinct values to the distance from the building to the street (b) and the distance between buildings (a). Values of 0, 6, and 12 m, to *a* and values 0, 12, 18, 24 m to *b* are assigned by the authors (see Figure 2.16). The distance between the building and the sidewalk assumes 12 combinations to detect an optimum scenario. For each of the 12 combinations, the model calculates the maximum allowed 'solar volume' to be built without violating the solar rights from each building and open space during a predefined period of the year. The study found that high urban densities could be achieved while protecting the solar rights of the building in the neighbourhood.

At present, by using computer algorithms for parametric modelling, a large number of design options could be simulated with minimum manual interventions. Samuelsson et al. (2018) simulated 12,096 different design combinations for a high-rise residential building for generalized urban contexts in Beijing, New York City, and Shenzhen. The parameters of investigation were WWR, building rotation, building shape, glass type, window shading, plug-in loads and wall insulation. The authors explore the impact of the selected parameters on energy use intensity (EUI), peak loads, and passive design of the building. A lower floor (15 m above ground) of a high-rise building, which would be affected by the shading from neighbouring buildings, was simulated in the study. Finally, the authors compared the no context scenario with the high, medium and low-density urban designs in the climates of Beijing, New York City, and Shenzhen. The thermal zone was modelled utilizing the perimeter/core thermal zoning method. The authors used *Rhino3D* modelling software including *Grasshopper*-based plug-in *Archsim* to translate the building model information into input files for *EnergyPlus*.

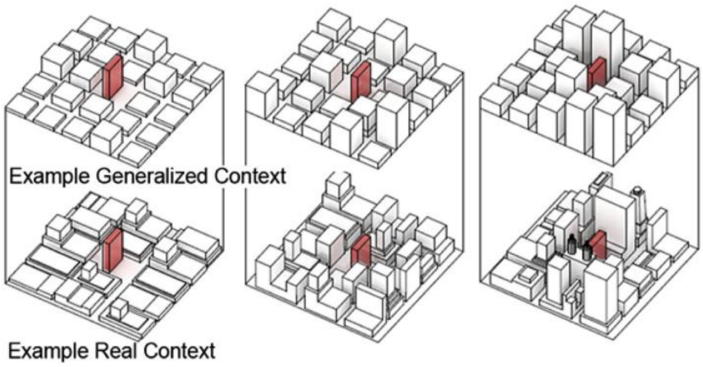

Figure 2.17: Example generalized context

Source:(Samuelsson et al. ,2018)

The authors developed a script in *Grasshopper* for generalizing the urban context. The algorithm used a fixed lot, and street size then randomized neighbouring building heights while maintaining a district's maximum Floor Area Ratio (FAR) and height limits (see Figure 2.17). The study found the effect of urban context to have a substantial impact on the design optimization. Therefore, disregarding the urban context in energy simulation, a common practice in the research of building energy performance would misinform designers resulting in sub-optimal design decisions.

Natanian et al. (2019) investigated the impact of the urban context on the dual characteristics of solar access, energy use and daylight of a parametric urban context developed for Tel Aviv, Israel. The parameters of investigation are building typologies, WWR, Glazing properties (Tv/SHGC), the distance between buildings, urban grid rotation and floor to Area Ratio (FAR). The quantified environmental variables are average energy Load Match (Av.LM) and spatial daylight autonomy (sDA) for each urban block.

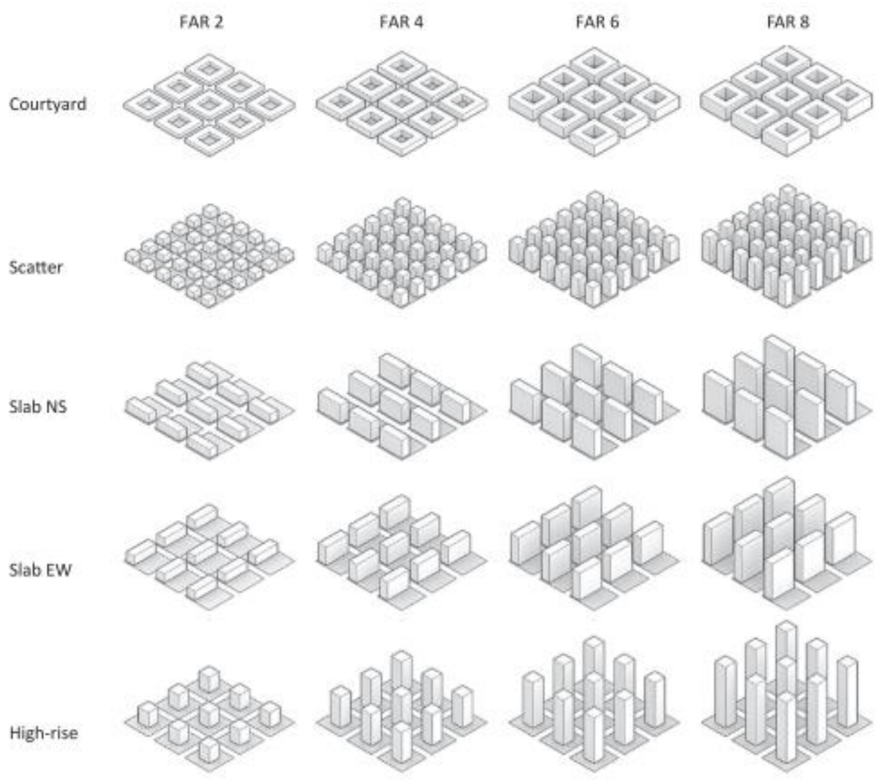

Figure 2.18: Floor area ratio (FAR) variations. FAR was modified in each iteration by increasing the number of floors

Source: (Natanian et al.,2019)

The urban blocks investigated are developed for combinations of FAR, the distance between building and heights for five building typologies, as illustrated in Figure 2.18. The authors automated the simulation process through *Grasshopper* in *Rhino 3D*, including a total of 1920 iterations. The daylight and energy simulations were conducted by *Ladybug* and *Honeybee* plug-ins. The above study results indicated significant differences in daylight and energy performance between typologies under various design scenarios.

Lobaccaro et al. (2017) investigated the solar potential in a residential building, a simplified urban district scenario and a Case study. The plugin *-DIVA4* in *Rhino3D* was used at the urban scale to conduct solar radiation analysis and to generate radiation maps to (i) calculate the solar potential of buildings' surfaces, (ii) identify the most irradiated surfaces, and (iii) identify the most shaded surfaces due to the overshadowing effect created by the urban surroundings. Next, the energy analysis was conducted using the Urban modelling interface (*Umi*) tool. The study quantified the solar potential on two residential building typologies row houses and high-rise apartment blocks. The buildings' dimensions are based on a survey of residential buildings in Trondheim, Norway.

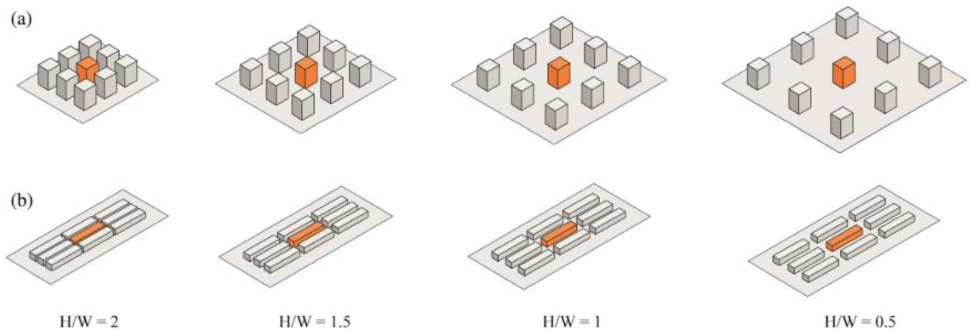

Figure 2.19: Variation of the aspect ratio H/W of the single urban districts for the high-rise apartment blocks (a) and the row house (b)

Source: (Lobaccaro et al.,2017)

The urban context was developed with varying the aspect ratio (height to the distance between buildings) as seen in Figure 2.19. The authors also applied the design principles to a Case study of the master plan area of Øvre Rotvoll, in Trondheim.

Parametric methods were also utilized to assess the effectiveness of planning and building regulations. Kosir & Sprah (2019) investigated the effects of urban planning parameters (floor area ratio, site coverage, development layout, and building typology) on compliance with European Standard EN 17037. The standard was established in 2018 to ensure appropriately daylit spaces in buildings. The urban context developed in the study was a 9 x 9 grid similar to Lobaccaro et al. (2017). One hundred eighty variations of the urban context (varied by FAR, plot ratio and building placement) were studied. The environmental parameters simulated in this study are the Average vertical daylight factor on the building façade (VDF_{ave}) and Daylight factor of the typical room (DF).

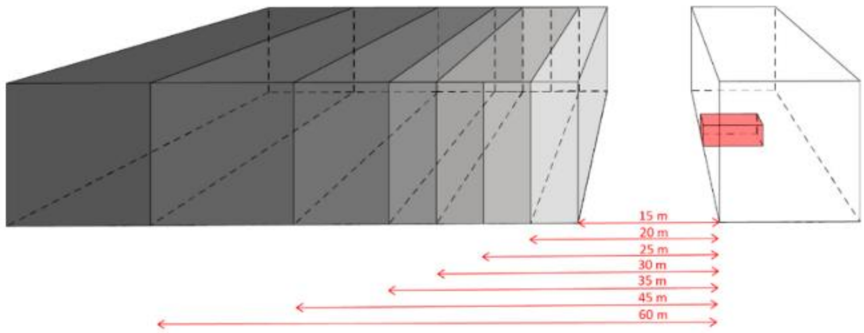

Figure 2.20: Addition of an opposing building at various distances to reduce the VDF_{ave} and the amount of daylight in the modelled room

Source:(Kosir & Sprah, 2019)

Subsequently, simulations with the addition of an opposing building with the dimensions of 45 × 15 × 15 m (w × d × h) at a distance of 60, 45, 30, 25, 20 and 15 m, were carried out, to reduce the amount of daylight on the facade due to overshadowing (Figure 2.20). Different room depths of 4, 5, 6, 7 and 7.5 m for the typical room were also investigated. The impact of 180 variations of the urban context was simulated in the *Grasshopper* parametric interface *in Rhino 3D* software. The VDF_{ave} and DF levels were simulated by the DIVA4 plugin.

The above studies in the literature review have used parametric computer simulation methods to achieve research objectives similar to that of this research study. Several important observations were noted in the current use of parametric simulation for the urban context. First, except for the initial study, all the other studies utilize *Rhion3D,* including the *Grasshopper* interface, to model the parametric urban context. For simulating energy performance *Honeybee* and *Archsim* plug-ins are utilized. For the simulation of daylight, *DIVA4* is used in the studies. Only one study considers the effects of daylight levels and energy use in the same urban context (Natanian et al., 2019).

It was also noted that in the above studies, the urban context is limited by a set number of combinations. For example, the distance between buildings is limited to

10, 20, 30 m and FAR to 2,4,6,8 (Natanian et al., 2019). H/W ratio in the study by Lobaccaro et al. (2017) is limited to 0.5, 1.0, 1.5 and 2.0. In Kosir & Sprah (2019) an urban block was modelled at a distance of 60, 45, 30, 25, 20 and 15 m, to simulate the effects of shading on daylight. Therefore, the solution space in the urban context is not exhaustively explored as the parameters for the urban context utilize a very limited number of values. Another aspect observed in the above analysis is the lack of studies using parametric software in the urban tropics.

2.6 Optimization methods for building energy and daylight performance

The workflow for optimization modelling in urban design consists of three steps – data collection, urban form generation and optimization (Shi et al., 2017). The data collection step provides the information needed to identify the parameters of the urban form. Based on the selected parameters, the urban form is generated by simulation software. In the final step, the optimum urban form is selected from the performance of each parameter in the optimization process. In any optimization process, three components have to be satisfied. First is identifying the parameters that need to be optimized, second is the optimization criteria and third, is the constraints of the solution space (Brownlee & Wright, 2012; Roy et al., 2008).

Optimization processes also differentiate between *a-priori*-optimization and *a-posteriori* optimization methods (David et al., 2015). In *a-priori* optimization method, the decision-maker has considerable knowledge of the outcome and therefore, could limit the solution space by imposing constraints on the parameters of the investigation. In the case of *a-posteriori* optimization, the entire solution space is searched for an answer without constraints to the parameters due to the lack of prior knowledge of the outcomes of the optimization process.

The dual characteristics of solar access, daylight and energy savings are conflicting objectives and therefore, needs to be resolved under multi-objective optimization. The Pareto optimization is the most common method utilized in multi-objective optimization, where one objective cannot be increased without decreasing the other

(Gossard et al., 2013; Machairas et al., 2014; X. Shi, 2011). Most multi-objective optimization engines automatically visualize the Pareto-front to identify the trade-offs between Pareto-optimal (non-dominated) sets. A Pareto-front of two objectives is depicted in Figure 2.21.

Multi-objective optimization in building performance consists of coupling building simulation modelling with computational algorithms for optimization (Méndez Echenagucia et al., 2015; Nguyen et al., 2014; Z. Shi et al., 2017; Vermeulen et al., 2015). Most building performance optimization engines are based on Genetic Algorithms (Ascione et al., 2015; Toutou et al., 2018; Yi & Kim, 2015; A. Zhang et al., 2017) and Particle swarm optimization (Futrell et al., 2015; Z. Shi et al., 2017) and non-dominated Sorting Genetic Algorithm II (NSGA-II) (Brownlee & Wright, 2012; Méndez Echenagucia et al., 2015). These optimization engines can simulate a large number of solutions for a large number of parameters. However, they require computers with high processing power. In addition, extensive calculation time, inadequate advertisement, and lack of a standard method or procedure are identified as the top three hindrances for applying building optimization tools in the building sector (Tian et al., 2018).

The final step in multi-criteria decision-making consists of selecting a single optimal solution or a smaller set of solutions from the Pareto-optimal sets providing the best trade-offs between objectives (Lu et al., 2011). There are two methods which could help identify the Pareto-optimal set on the Pareto-front. The Utopia point method selects the “best” set of design variables closest to the Utopia point, minimizing both objective functions (Ascione et al., 2015).

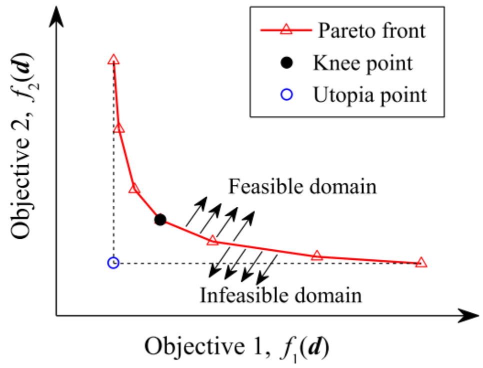

Figure 2.21: Conceptual sketch of Pareto-front, Utopia point and Knee point.

Source: (Khoshnevisan et al., 2014)

The Utopia point is illustrated in figure 2.21. Another method to select the Pareto-optimal sets is called identification of the Knee. At the Knee region, a small improvement in one objective would lead to a considerable deterioration in at least one other objective (Branke et al., 2004; Khoshnevisan et al., 2014). Existence of the Knee region is easily identified on the Pareto-front visualization (Figure 2.21). However, it should be noted that the point closest to the Utopia point may not always be the Knee point, as indicated in Figure 2.21.

2.7 The daylight and energy performance of the high-rise residential building envelope in the tropics

The relationships between the microclimate, the form and the envelope are not mutually exclusive and have a combined effect on indoor comfort, as depicted in Figure 2.22.

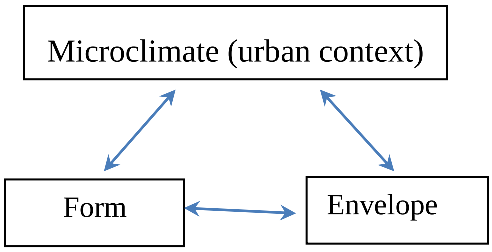

Figure 2.22: The relationship of the microclimate (urban context), form, and envelope of a building

The microclimate of a high-rise residential building is usually a part of a high-density, high-rise neighbourhood or estate. Therefore, the microclimate of a high-rise residential building inevitably becomes a dense urban context. Thus, the effects of the urban context on the form and envelope design of the archetypal high-rise residential building merit investigation. Modelling the impact of the urban context on the varying building forms of a high-rise residential building is a complicated task. It was, therefore, considered beyond the scope of the time-frame for this research study. However, the effects of the urban context on variations in the building envelope design were investigated within the limited time-frame.

The building façade (envelope) acts as a filter between the indoor and outdoor environment. Therefore, it must be designed to allow the desirable environmental aspects such as daylight in but keeping heat out. Envelope elements such as physical properties of the walls, glazed areas, vertical landscaping and shading devices play an important role in mitigating external heat gain in the tropics and are discussed below.

Physical properties of walls - The external walls and glazing construction are the foremost important consideration for minimizing solar heat gains in the tropics (Al-tamimi et al., 2011; Lai & Wang, 2011). An increase in wall thickness makes a significant difference in the comfort performance of urban houses (Mallick, 1996). Rajasekar & Ramachandraiah (2011) found that in general buildings constructed of solid blocks perform thermally better than those constructed of aerated concrete blocks.

Nguyen and Reiter (2014) found that the reflectance of a building envelope also impacts indoor thermal comfort. In addition, the indoor temperature is much stabilized particularly when night ventilation is adopted due to relatively high thermal mass (Alfataao et al., 2015). Farid and Wonorahardjo (2018) applied thermal mass theory with a balance of heavyweight and lightweight material for the building envelope in their simulation. The authors found that the east-west wall collects the heat from direct sunlight and releases the heat to the air, while the north-south wall may indirectly collect the heat from the air. Therefore, lightweight materials should be used on the east-west side building envelope.

Glazing material - Yildiz et al. (2011) found that the total window area, the heat transfer coefficient, and the solar heat gain coefficient (SHGC) of the glazing based on the orientation have the most considerable influence on the energy performance of apartment buildings in hot-humid climates. Studies find that an energy-efficient building envelope design can be achieved primarily by selecting low heat transfer materials for windows, while reducing the window size can be given a lower priority (C. T. Cheung et al., 2015; Nguyen et al., 2014).

Vertical Landscaping - The built environment is increasingly covering the earth surface with impervious surfaces. Therefore, incorporating green facades could mitigate heat gain and increase the green cover in the urban context (Yeang, 1994). Lin et al. (2018) conducted a field study on the impact of shading and heat reflection performance of green façade in a high-rise residential project in Guangzhou, China. The study provides evidence for the shading effect and the decrease of the heat reflection of green facades. The study found that the air average temperature shaded by the green façade (GF) s on sunny days is reduced by 0.6℃(East) and 0.7℃(South), and the maximum reduction is up to 3.2℃(East) and 3.8℃(South) at noon. The surface average temperature of the GFs is reduced by 4.7℃ in comparison to the bare wall, and the whole façade was decreased about 3-4℃ with the GFs, where the foliage coverage ratio (FCR) s are 37.5-54.4%.

External shading devices - After optimizing the wall properties and glazing further savings can be expected by optimizing external shading for glazed surfaces. Shading devices have played an essential role in passive climate responsive design and aesthetics in tropical architecture (Givoni, 1998; Hyde, 2000; Koenigsberger et al., 1973). Traditional shading devices in low-rise residential buildings such as extended eaves, verandas, and window shades, block direct solar radiation and prevent rain from entering indoors in the tropics.

In high-rise residential buildings, the main purpose of a shading device is to minimize solar heat gains by reducing solar radiation incident on the glazed area. In addition to being more effective than internal shading devices, external shading devices minimize obstructing the view, are economical and low maintenance (Cho et al., 2014; J. Kim, 2013; Kim & Kim, 2010; Offiong & Ukpoho, 2004; Valladares-Rendón et al., 2017). A well-designed shading device could provide a right balance between shading, daylighting, and visibility (Valladares-Rendón et al., 2017). The following section expands the literature review on external shading devices.

2.7.1 Energy and daylight performance of external shading devices

The performance of a shading device is assessed by the Horizontal shadow angle (HSA) and the Vertical shadow angle (VSA). The Horizontal shadow angle (δ) is the difference between the solar azimuth and the wall azimuth as indicated in Figure 2.23, which is the same as the horizontal component of the Angle of incident. The Vertical shadow angle (ε) of a horizontal shading device is the measure on a vertical angle to the normal to the elevation considered (Figure 2.24).

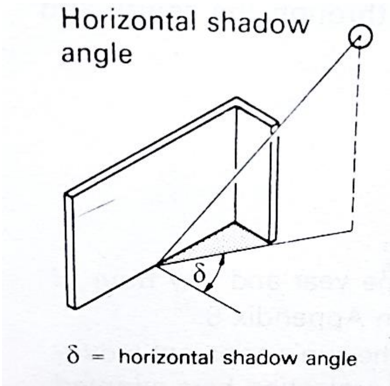

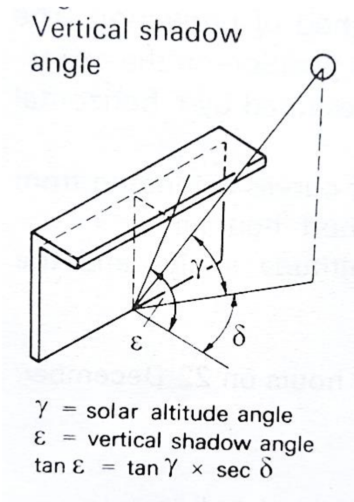

Figure 2.23: Horizontal shadow angle

Figure 2.24: Vertical shadow angle

Source: (Koenigsberger et al., 1973)

A large number of open-source computer software now aids in calculating the shadow angles and informs the optimum length and width of shading devices for different climate and building characteristics. Also, the software incorporates energy savings from shading performance as well. Presently, the effectiveness of shading devices in most studies is measured in energy savings (Al-tamimi et al., 2012; Cho et al., 2014; Chua & Chou, 2010; Khin et al., 2016; Wu et al., 2017). A few studies utilize indoor temperature (Al-tamimi et al., 2011; Arifin & Denan, 2015; Freewan, 2014; Offiong & Ukpoho, 2004) as the dependent environmental variable.

An effective design of exterior shading devices could replace expensive, high-performance glass (Cho et al., 2014). The application of external shading, on clear glazing, is more effective than double glazing (Khin et al., 2016). In developing countries in the tropics, such as Sri Lanka, double glazing has the drawbacks of being too expensive and creating condensation on the exterior of the glazed surface (Laukkarinen et al., 2018). In hot-humid tropics, clear single pane glass with optimized external shading would be the most suitable option.

Studies found that complex external shading could be more effective in reducing solar gains, especially in seasonal climates (Valladares-Rendón et al., 2017). For example, a louvred dynamic shading device reduced the total amount of energy consumption by 48% compared to no shading while maintaining a comparatively uniform indoor illuminance during the entire operating period (Choi et al., 2017). In tropics where the climate has little seasonal variations, simple static shading could improve energy savings year-round and provide an unobstructed view.

External shading devices such as overhangs, vertical panels, and egg-crate were the most common strategies investigated in residential buildings (Al-tamimi et al., 2012; Cho et al., 2014; Chua & Chou, 2010; Lai & Wang, 2011; N. H. Wong & Li, 2007) while perforated solar screens were common in office buildings (Chi et al., 2017; Huang & Zhao, 2017; Lavin & Fiorito, 2017; Sherif et al., 2012). Preference in the application of overhangs, vertical panels, and egg-crates over perforated solar screens in residential buildings could be due to simple construction, low maintenance, and least obstruction to view.

Studies found the egg-crate perform better in mitigating heat gain followed by overhangs and vertical panels (Al-tamimi et al., 2011; Chua & Chou, 2010; Khin et al., 2016; Lai & Wang, 2011; Shahdan et al., 2018). Table 2.2 summarizes the impact of the orientation and size of the external shade on the energy-saving performance of shading devices. Table 2.2 also demonstrates that prioritizing shading devices in the east and west directions could result in higher cooling energy savings.

Table 2.2: Comparison of energy savings of egg-crate, overhang and fins in residential buildings

Article	Energy savings /indoor thermal comfort			Location
	Egg-crate	Horizontal shading	Vertical panel	
(N. H. Wong & Li, 2007)		By adopting a 0.3–0.9 m horizontal shading device, 2.62–10.13% cooling load could be saved in the East-West directions.		Singapore
(Al-tamimi et al., 2012)	The annual cooling load reduction by using a practical shading length of 0.6 m is about 2.34% in the south-west direction			Malaysia
(Khin et al., 2016)	Annual cooling energy savings of 3.4% was estimated in the west facade; 3.3% savings on the east facade; and 2.6% savings on the north and south facades.	Annual cooling energy savings of 1.4% on east and west facades, and 1.0% on north and south facades.	Annual cooling energy savings between 1.7% and 2.4% at different façade orientations.	Malaysia
(Lai & Wang, 2011)	Annual electricity savings was approximately 550 kWh.	Annual electricity savings were between 100 and 330 kWh	Annual electricity savings were between 80 and 220 kWh	Taiwan
(Chua & Chou, 2010)	Half egg-crate louver was found to be the most suitable shading device for residential buildings facing the north and south orientations.	Horizontal projection with 30° downward tilt was appropriate for facade facing the east and west orientations to reduce the cooling load		Singapore
(Cho et al., 2014)		Maximum annual cooling load reduction of 19.7% for the horizontal overhang,	Maximum annual cooling load reduction of 17.3% for the vertical panel.	Seoul Korea

In addition to the benefits of shading devices on minimizing heat gain, the negative effects on daylight also need to be considered. However, only a few studies address the daylight and energy performance of egg-crate, overhangs, and fins, which are the most common shading devices in the tropics(Lai & Wang, 2011; Lim et al., 2020; Xie et al., 2017). A study of daylight and cooling energy use in a high-rise residential building in Hong Kong formulated a new index- Energy daylight rate (EDR) for selecting the best scenario of envelope design for both daylighting and shading purposes (Xie et al, 2017). Lim et al., 2020 finds that egg-crate shading was the most proper shading device to block sunlight and reduce the cooling energy consumption effectively. The effects of several shading devices on heat gains and daylighting in an office building was investigated in Jordan (Freewan, 2014). The study found the egg-crate improved daylight level all day, whereas diagonal fins reduce the illuminance level in the morning, while vertical fins allow for large areas of sun patch to cover the office area in the afternoon. Though multiple horizontal overhangs have better-daylighting performance, since they are installed in the vision area of the window, they are expected to have limited applicability due to obstructed view (Cho et al., 2014). The horizontal single overhang and vertical panel, which satisfy both conditions of applicability and sun-shading/daylighting performance, could serve as rational alternatives. Another study conducted in Singapore found that shading devices with a shading coefficient of 0.55 and above allow daylight to be admitted with an illuminance exceeding the recommended level (Nyuk Hien Wong & Istiadji, 2004).

The effects of the shading effects of the urban context on the performance of external shading devices were scarcely investigated in current research studies. As the effects of contextual shading on building energy use (Han et al., 2017; Lima et al., 2019; Ratti et al., 2005) and daylight (Li et al., 2006; Xue et al., 2014) is already well established, a need arises to investigate the effects of contextual shading on the energy and daylight performance of external shading devices. One of the main effects of contextual shading is decreasing solar radiation levels on the vertical surface of the building from the top to the ground floor. The floor level of a high-rise building is an essential factor in calculating operational energy use (Dawodu &

Cheshmehzangi, 2017; D. H.W. Li et al., 2006; Nebia & Aoul, 2017; Xue et al., 2014). Higher the building, the more energy losses incurred (Dawodu & Cheshmehzangi, 2017). Therefore, the top floor is risked of overheating and better daylighting performance, which results in a conflict between overheating and daylighting design (Nebia & Aoul, 2017). Studies also find substantial differences between mean air temperature within units in the lower and upper floors due to air velocity (Aflaki et al., 2014). In Hong Kong, where very high residential densities exist, low daylighting levels were observed at the lower floors due to neighbouring obstructions resulting in artificial daytime lighting (Xue et al., 2014). Most studies on external shading devices did not consider the dual characteristics (daylight and heat gain) of solar access. Studies either focused on energy use or daylight. The opposing characteristics of solar access -heat gain and daylight, have created a dilemma regarding solar access in dense urban tropics. Therefore, shading devices in residential buildings in urban tropics should be designed to optimize solar access into building interiors considering both heat gain and daylight.

In addition, studies rarely consider the effects of contextual shading on the effectiveness of external shading devices, even though the evidence of the effects of the urban context on daylight and energy performance of buildings at different floor levels are well noted in the literature.

2.7.2 Static external shading as architectural features

External shading devices add to the architectural character in high-rise residential buildings in tropical countries such as Singapore, Malaysia and Sri Lanka while minimizing heat gain (Figure 2.25).

Figure 2.25: Overhangs, reveals, and balconies in a high-rise residential building in Singapore

In Sri Lankan urban planning regulations, “a balcony” means any stage, platform, oriel window, or other similar structure projecting outwards from the outer face of an external wall of the building, which is supported by brackets or cantilevered (UDA, 2008). In the case where such a balcony is faced to an adjacent property, a minimum of 0.8 m clearance should be maintained from the outer edge of the balcony. The regulations also state that any overhang or sun-shading device of a building shall be permitted to project up to 1 m, beyond the building line, provided that the construction material used is of non-combustible type. There is no specific mention of maximum projection length for balconies. Generally, a balcony extends 1m from the external wall in high-rise residential buildings in Sri Lanka.

The planning and building regulations for balconies in Singapore require balconies to have a continuous perimeter opening of at least 40%. The total balcony size for each dwelling unit is capped at 15% of the internal unit size. Balconies should have a minimum width of 1.5 m as measured from the external building wall. Exceptions to the width requirement may be considered arising from the design merit of the proposal, such as a curved or odd-shaped balcony, but the balcony shall be reasonably sized (Urban Redevelopment Authority, 2019).

Recently external shading devices have become an architectural statement of high-rise residential buildings. This could be due to the relative ease at which the building façade could be manipulated in comparison to the building form without disturbing the structure of the building. With attention to architectural principles such as proportion, scale, and balance between space and form, an innovative and attractive external shading system could be devised. Several examples of such designs in high-rise residential buildings are discussed below.

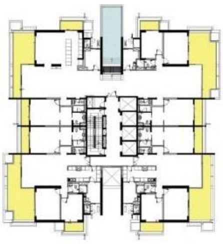

Figure 2.26: The 10th-floor plan of Clearpoint   Figure 2.27: An ariel view of the extended balconies

Source: (CTBUH, n.d.)

The Clearpoint residences, a 45-floor, high-rise residential building in Sri Lanka, utilize extended balconies of 5 m to create a hanging garden for each residential unit, as depicted in Figure 2.26 and 2.27. The high-rise residential building consisted of 121 units and was completed in 2017. The extended balcony shades the full height glazed surface below while providing the garden on the upper-level units. The building is also the only high-rise residential building partially powered by renewable energy in Sri Lanka. The convex solar panel powers the common spaces in the building on the building's roof-top. The hanging gardens from the balcony have made the building a landmark in the suburban area of Rajagiriya in Sri Lanka.

Figure 2.28: The B.S.R. Tower, Tel Aviv

Source: (CTBUH, 2015)

Another example of extended balconies is the B.S.R. twin towers located in Tel Aviv, Israel. There are two residential towers, with 30 floors and 29 floors, housing 301 units. The building was completed in 2015. Each floor consists of 4 balconies which are the dominant feature of the building. Each balcony is a double-height volume located on alternating floors at the corners of the building, as depicted in Figure 2.28.

The Acrueil ZAC de Couteau is a high-rise residential building of 14 floors located in a suburb outside Paris, France. The building was constructed in 2014. The key feature in this building is the extended balconies that take an organic shape depicted in Figure 2.29 and Figure 2.30. The apartment floor extends into the balconies accounting for an additional 50% of the total living area. The cantilevers are up to a maximum of 3 m in depth.

Figure 2.29: The 10th floor plan of Acrueil ZAC

Figure 2.30: Acrueil ZAC

Source: (archdaily, n.d.)

Static external shading devices are a key passive design feature in high-rise residential buildings that contribute immensely to cost-effectively minimizing heat gain through glazed surfaces into the building. It is also a versatile building element that can be extended into an architectural expression of the building.

2.8 Identification of gaps in the literature review and summary

Chapter two explored the literature relevant to attaining the four objectives of this study. The first section explored the high-rise residential building typology identified in the Introduction as a misguided housing form in Sri Lanka. The literature review examined the initial concepts of the high-rise residential building typology and their current interpretation. In Section 2.2, the current definition of solar access and its limitations in the application in the tropics were discussed. In Section 2.3, residential sector energy efficiency in the urban context was explored. A non-linear relationship between building density and energy efficiency in buildings was observed in the literature review. The parameters of investigation of the urban context and solar access in the current research were discussed in Section 2.4. In Section 2.5, the simulation methods in the quantification of shading of the urban context to assess solar access are explored. Section 2.5.1 detailed the current practices in parametric simulation of the urban context. The study of solar access in the tropics was identified as an optimization challenge in the literature review. Therefore, methods of multi-objective optimization were discussed in Section 2.6. In Section 2.7, the performance of the building façade in terms of energy use and daylight was described with a focus on static external shading devices.

The following gaps were noted in the literature review.

- Section 2.1 discussed the high-rise residential building typology. A key characteristic of the high-rise residential building typology as perceived in the Radiant city concept and later in the Sustainable city is the ability to ensure solar access. At present solar access is ignored in many high-rise residential developments in Colombo, as discussed in the Introduction. Therefore, there is a need to investigate the high-rise residential building typology in terms of solar access for dense urban tropics.

- In Section 2.2, it was noted that solar access studies are mostly concentrated in colder climates where maximizing solar gains is the focus of study. The term "solar access" is defined as the ability of a unit to continuously receive sunlight without obstruction from any other properties or structures. In the tropics, unobstructed solar access is avoided due to excessive heat gains into buildings. However, as cities get denser in the tropics, lack of solar access is becoming a health hazard. Therefore, the need to redefine solar access as an optimization process between daylight and energy use is the first objective of this study.

- Section 2.4 discussed the parameters of investigation, metrics, climate and building type in the literature review. Many studies focused on energy savings for cooling due to the urban context. Focusing only on cooling energy could overestimate energy savings due to the non-consideration of day-time lighting energy. Therefore, there is a need to assess the energy savings due to shading accounting for day-lighting. The building setback is one of the least investigated building density parameters in current research, even though it could effectively ensure solar access than other planning tools such as the Floor area ratio. The second objective of this study is to modify the building setback tool for optimum solar access.

- The need for energy efficiency in the residential sector is discussed in section 2.3. According to the literature review, a positive relationship between energy efficiency and higher densities in the tropics is established in research. However, some authors note that due to issues in daylight and solar access, this relationship is non-linear. The benefits of energy efficiency due to higher densities have led to the justification of high-residential buildings with no solar access in Sri Lanka. Therefore, the need to investigate the optimum building density for high-rise residential buildings in urban tropics is the third objective in this study.

- Computer modelling of the urban context was mostly conducted in cold and subtropical climates, as discussed in Section 2.4. Therefore, the assumptions for the thermal and daylight simulation models in tropical climates were not adequately validated. There is a need to conduct more studies on urban context modelling in the tropics to refine the assumption for the daylight and thermal models.

- The parametric methods currently used in the studies could only generate a limited number of urban contexts for analysis, as discussed in Section 2.5. This limits the number of solutions for multi-objective optimization. Therefore, there is a need to explore parametric methods to generate multiple solutions to facilitate the optimization process.

- As discussed in Section 2.6, current optimization processes are coupled with the building performance simulation model. As this study focused on the optimization of dual characteristics of solar access-daylight and energy use, a multi-objective optimization method was utilized in this study. However, due to the requirement of the high processing power of the computer and time-consuming optimization engines, simplified methods for optimization of the building performance need to be explored.

- The impact of the urban context on the building vertical façade is discussed in Section 2.7. It was noted in the literature review that most studies do not consider energy and daylight performance of external shading devices in high-rise residential buildings. Studies also did not account for the effects of the urban context on the performance of external shading devices in buildings. Therefore, considering the daylight and energy performance of external shading devices in high-rise residential buildings in an urban context is the fourth objective of this study.

3 Methodology

The research study is conducted in three phases. The input, analytical and output components in the three phases and their relationship to each other are illustrated in Figure 3.1.

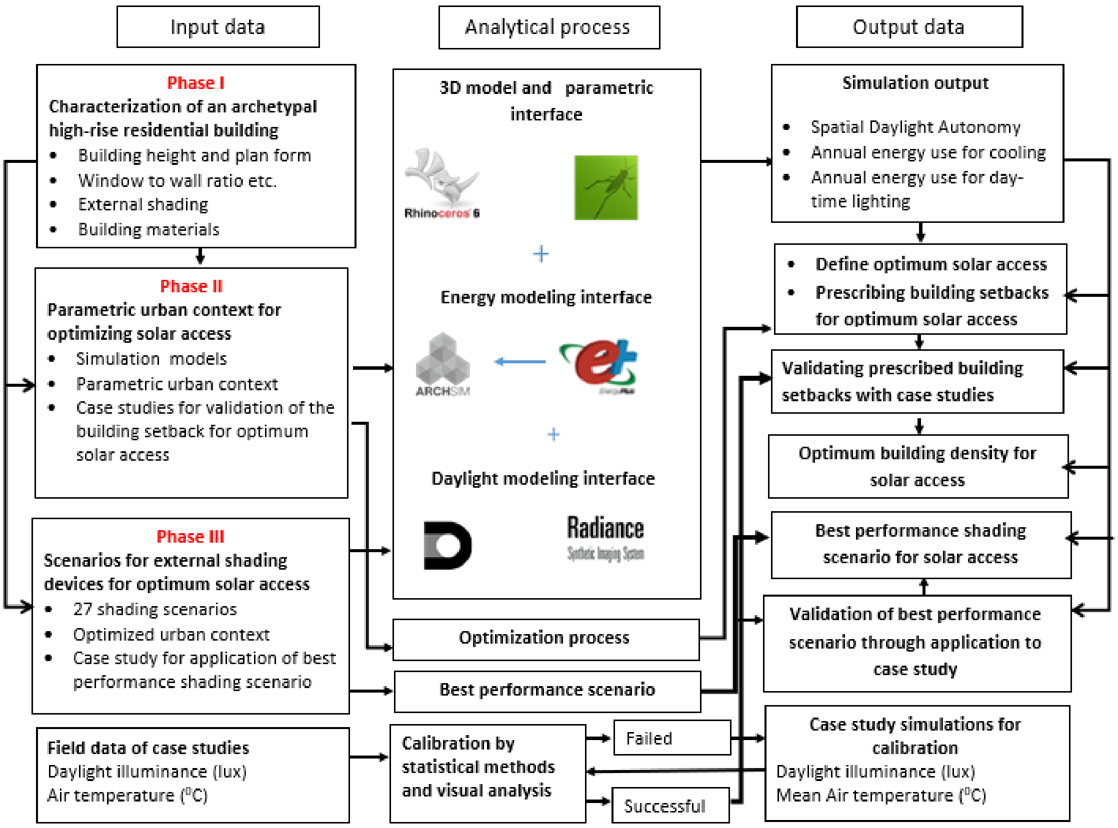

Figure 3.1: Research methodology

In Phase I of the study, the archetypal characteristics of high-rise residential buildings in a tropical climate were developed using data obtained from a field survey in Colombo, Sri Lanka.

In Phase II, three simulation models (SM1, SM2 and SM3) based on the archetypal high-rise residential building characteristics identified in Phase I are incorporated into a parametric urban context. Computer simulation software indicated in Figure 3.1 quantify the impact of contextual shading on solar access in the simulation models. The simulation results are utilized to resolve the conflicting objectives of daylight and energy use through an optimization process. The optimum solar access thresholds are further utilized to prescribe building setback curves. The building setback curves inform the optimum building density for solar access as well. The building setback curves are validated with calibrated case studies, as indicated in Figure 3.1.

In Phase III, the shading effects of the urban context on 27 external shading scenarios are simulated for an archetypal high-rise residential building (Figure 3.1). The best performance scenario is validated with a Case study.

Phase I

3.1 Survey of high-rise residential developments in the Colombo metropolitan region and its suburbs

Ninety per cent of high-rise residential buildings are constructed in the Colombo metropolitan region and its suburbs, as discussed in the Introduction in this study. To identify the archetypal high-rise residential building characteristics, a sample of high-rise residential buildings was selected from the list of buildings that have received the Condominium Management Authority (CMA) certificate. The CMA certificate is given to residential buildings, which have completed construction, meeting the regulations of the Condominium Management Authority of Sri Lanka. Between 2005 and 2017, 914 residential buildings received CMA certificates. Out of the total number of residential buildings with the certification, only 31% had over 15 units. It is unlikely that high-rise residential buildings (considered as having ground plus four floors according to the general planning and building regulations in Sri Lanka) have fewer than 15 units. Therefore, only residential buildings with 15 units or more were considered for selecting the sample for the survey.

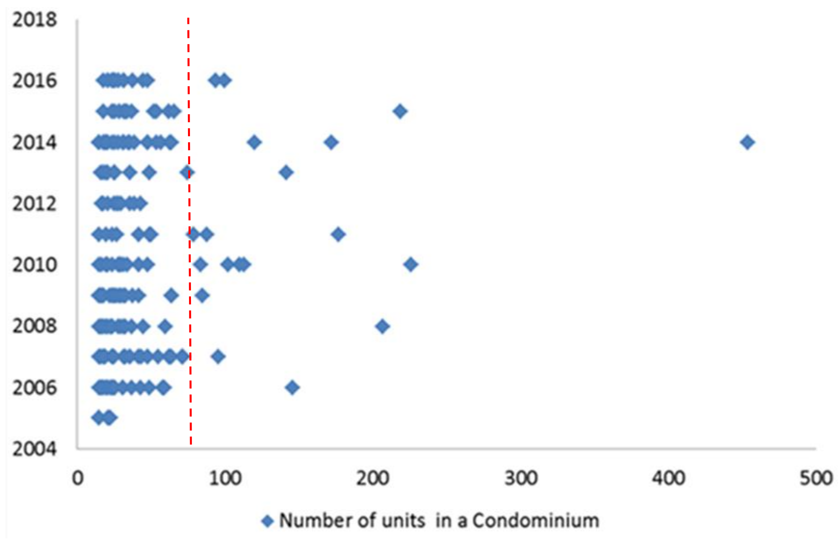

Figure 3.2: Scatter plot of high-rise residential buildings over 15 units in the Colombo metropolitan region and its suburbs

Figure 3.2 above depicts the scatter plot of units in high-rise residential buildings constructed between 2005 and 2016. According to the scatter plot, it is clear that most of the high-rise residential buildings have less than 65 units.

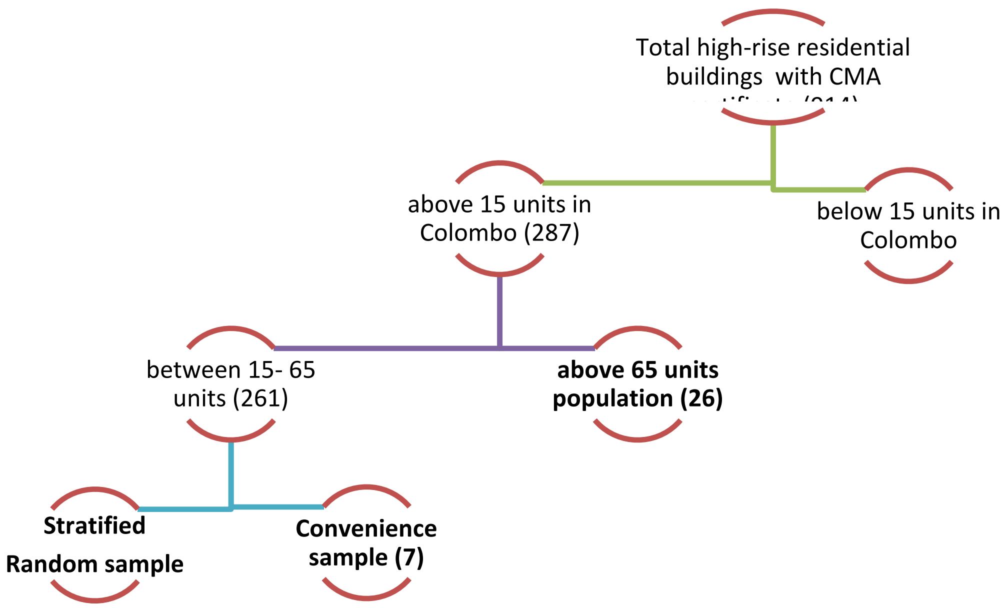

Figure 3.3: Sample selection for the survey of high-rise residential buildings

The sample selection process is indicated in Figure 3.3. Two-hundred and eighty-seven high-rise residential buildings (over 15 units) have received the CMA certificate. Two-hundred and sixty-one of the high-rise residential buildings had between 15 and 65 units, and only 26 had units over 65. Twenty-four high-rise residential buildings with units ranging from 15 to 65 were randomly selected as the sample to represent the population of high-rise residential buildings in the Colombo city and suburbs. Additionally, seven high-rise residential buildings were selected by convenience sampling that had between 15 and 65 units. The total number of high-rise residential buildings (26) above 65 units was included in the sample.

In total fifty-seven high-rise residential buildings were selected for the survey sample. The survey of the sample was conducted from January 2018 to December 2018 by the author and two other research assistants. The level of success in data collection varied from building to building. Architectural drawings of 22 buildings were collected during the survey.

The main focus of the high-rise residential building survey was to identify the building design characteristics of the archetypal high-rise residential building. The building site plans, typical floor plans, section and elevations in the 22 architectural drawings were analysed to inform building characteristics of the high-rise residential buildings in Colombo. Individual building details are given in Appendix E (I) and Appendix E (II).

Figure 3.4 compares the height in floor levels, number of units and the plan forms of the surveyed buildings. The number of units in a building in the sample varies from 16 to 454. The building heights also range from 7 to 38 floors. A distinction between plan forms for buildings over 65 in the sample was observed in Figure 3.4. High-rise residential buildings below 65 units have a compact form, while the buildings with over 65 units have spread out built forms.

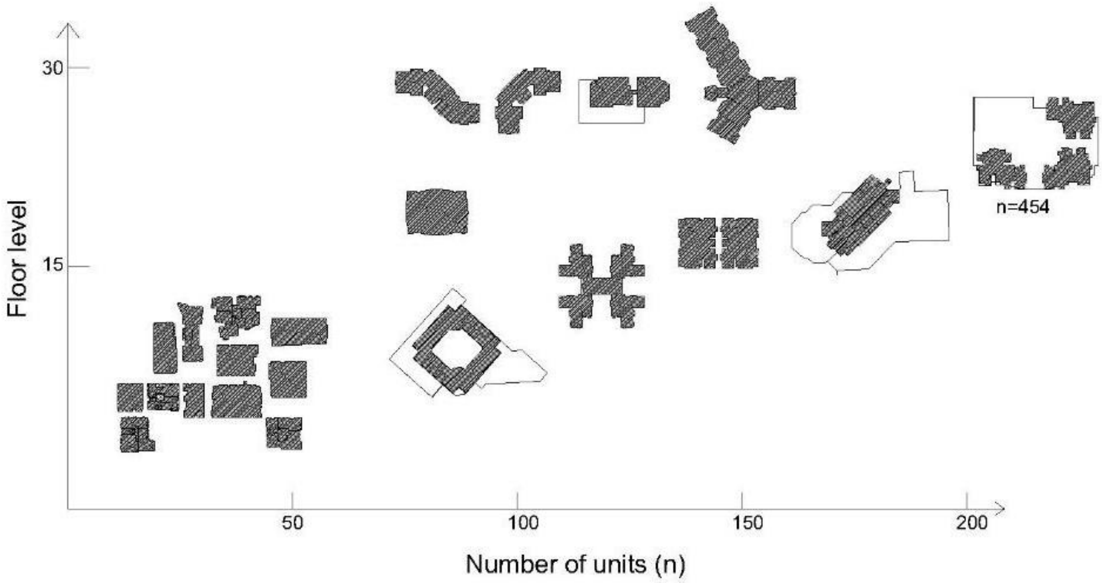

Figure 3.4: Comparison of plan forms in the building sample

The spread-out plan forms are mainly because high-rise residential buildings with over 65 units are located in large sites, where some form of architectural expression is possible. Most high-rise residential buildings in Sri Lanka, which have below 65 units, are located in small sites and have restricted compact forms. Figure 3.4 demonstrates that the sample selected represents a cross-section of characteristics of high-rise residential buildings for determining the archetypal model.

3.2 Characteristics of the archetypal high-rise residential building

The characteristics derived from the building sample are discussed in this section.

Building height- In the literature review, it was noted that the height of a high-rise residential building is subjective to the context. In the Colombo Metropolitan Region, 13 floors or above is considered a high-rise residential building (UDA, 2008). The average number of floors in high-rise residential buildings in the survey was 14.5 floors (Figure 3.5).

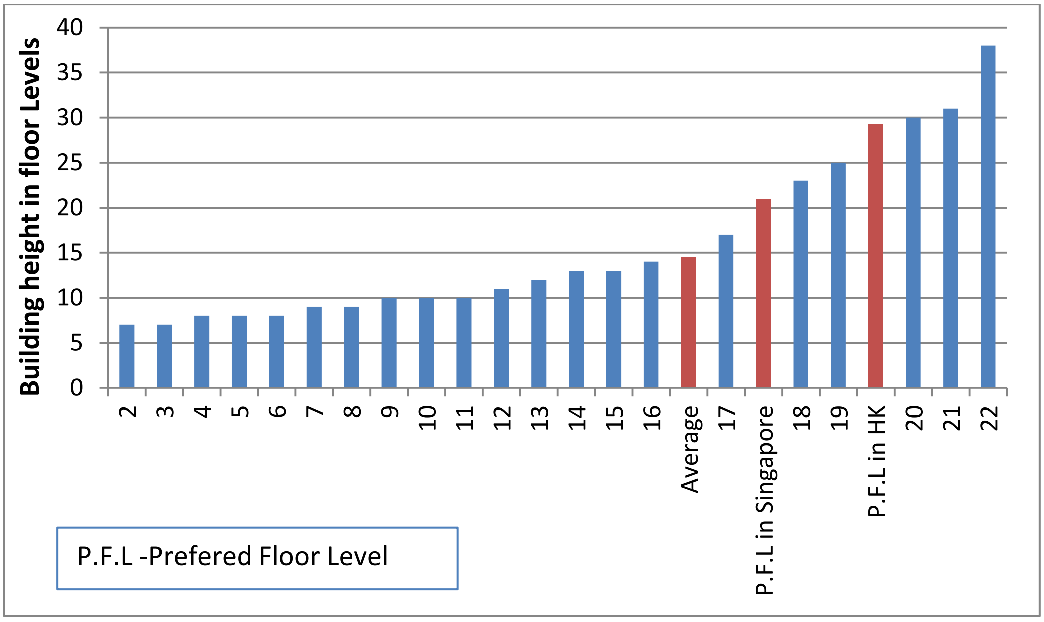

Figure 3.5: Comparison of floor levels of high-rise residential buildings in the sample

The tallest building in the survey had 38 floors. However, 50% of the buildings in the survey have less than 11 floors. As Sri Lanka is still an emerging high-rise residential market, the average building heights in more established cities could indicate future development trends. The mean floor level of the preferred residence is 29.3 in Hong Kong and 20.9 in Singapore (Yuen and Yeh, 2011). Considering the above trends, a range of heights- 11, 21 and 31 floors were established to represent the high-rise residential building height characteristics in Colombo.

The floor height of 3 m was considered for the archetypal building, as it was the mean floor height of the buildings in the sample.

Building Plan- This study focuses on the shading effects due to building height and distance between buildings. Therefore, the building plan is required to be a square plan to compare the results in different cardinal directions. The linear length and width of the tower blocks in the survey are depicted in Figure 3.6. The average length and width calculated was 31 m. Therefore, a compact core-dependent form with a square plan (31 m x 31 m) is used for the simulation models.

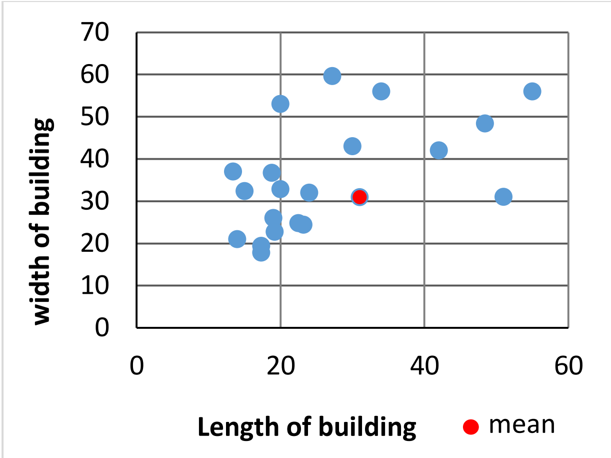

Figure 3.6: Linear width and length of high-rise residential towers in the sample

Window and room dimensions – Living room (LD), bedroom (BR) and window dimensions of the sample were tabulated, of which the relevant box plots are given in Figure 3.7.

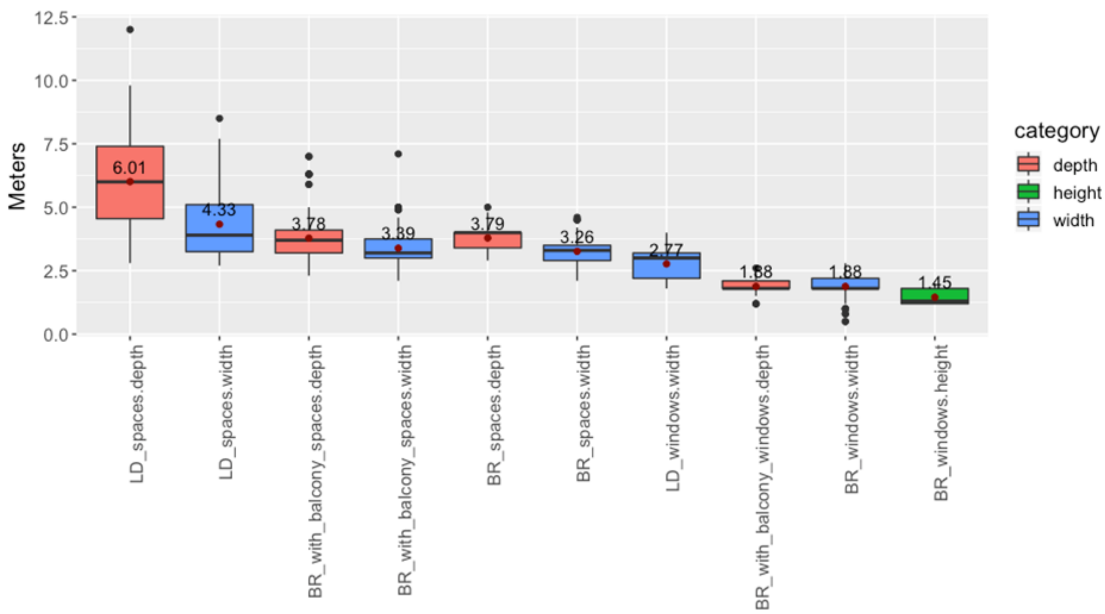

Figure 3.7: Box plots of the living room, bedroom and window dimensions of the high-rise residential buildings in the sample

Except for living rooms, the dimensions of bedrooms and windows have little variation. The average depth and width of the typical living room are 6 m x 4.3 m, bedroom with balcony, 3.8 m x 3.4 m and standard bedroom, 3.8 m x 3.3 m. The average size of a living room window was identified as 2.4 m (h) x 2.8 m (w), bedroom with balcony window is 2.4 m (h) x 1.8 m (w) and a window for the standard bedroom as 1.5 m (h) x 1.8 m (w). The window widths were adjusted to fit common window sizes.

Window to wall ratio (WWR)- The WWR in an elevation, which provides light and ventilation to the living/dining area and bedrooms, is 36% for high-rise residential buildings in the sample. To model the impact of shading in the four cardinal directions, all elevations have a 36% window to wall ratio (Figure 3.8).

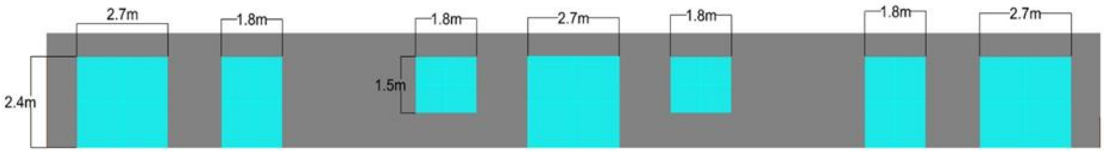

Figure 3.8: Window composition of the typical floor levels in the archetypal high-rise residential building

External shading devices- Most of the high-rise residential buildings in Sri Lanka are characterized by balconies, which could be accessed through the living/dining area or the master bedroom. The simulation model takes into consideration the impact of shading effects on the balconies. Two large balconies (7.8 m x 1m x 0.9 m) and one small balcony (4.3 m x 1m x 0.9 m) are modelled per typical floor.

Cooling system- The survey revealed that 90% of the high-rise residential buildings had bedrooms and living rooms air-conditioned. Therefore, an active system for cooling was considered in the study.

Building Materials- Most of the high-rise residential buildings in the survey sample complied with the materials in Table 3.1 below.

Table 3.1: Materials of the building elements in the sample

Building element	Materials
Structure	Concrete structure
Exterior walls	Cement block wall, 200 mm, outside rendered, inside plastered
Window	Single pane 6 mm clear glass
Window frame	50 mm extruded aluminium profile
Balcony railing	Cement block wall, 150 mm, outside and inside rendered
Roof	Reinforced Concrete flat slab,200 mm, with screed
Floor finish	Tile finish on a concrete slab
Ceiling	Reinforced Concrete slab, 200 mm, screed 63-12 mm painted white
Interior walls	Cement block wall, 150 mm, plastered on both sides
Ground	Compacted earth

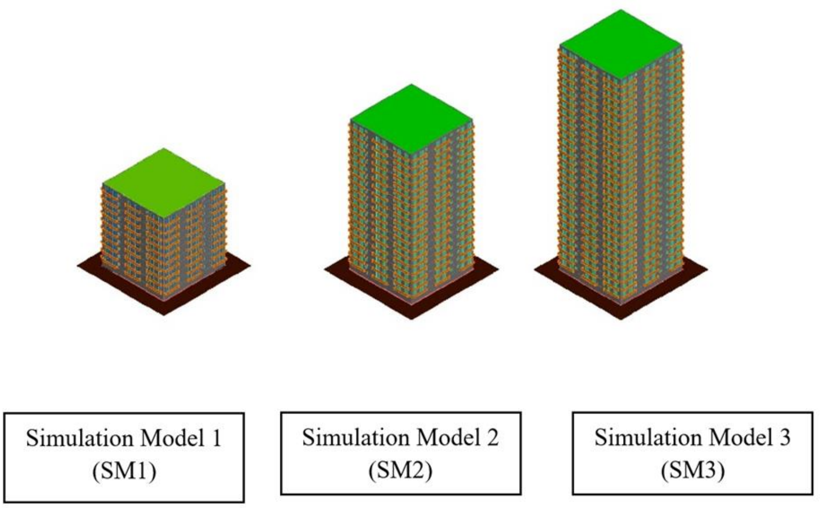

Figure 3.9: Simulation models

Three archetypal high-rise residential buildings of 11, 21, and 31 floors were developed as simulation models to investigate the impact of the high-density urban context on solar access (Figure 3.9).

Phase II

3.3 Developing a parametric urban context for the Simulation models in the tropics

The simulation models were tested in the urban tropical climate of Colombo, Sri Lanka. Therefore, the EPW weather file used is LKA_Colombo-Rathmalana.434670_SWERA.epw for the Colombo district (6.8195° N, 79.8801° E). The characteristics of the tropical climate discussed in the literature review were observed in the data extracted from the EPW file and illustrated in Figure 3. 10 (Global Horizontal Illuminance) and Figure 3.11 (Dry bulb Temperature).

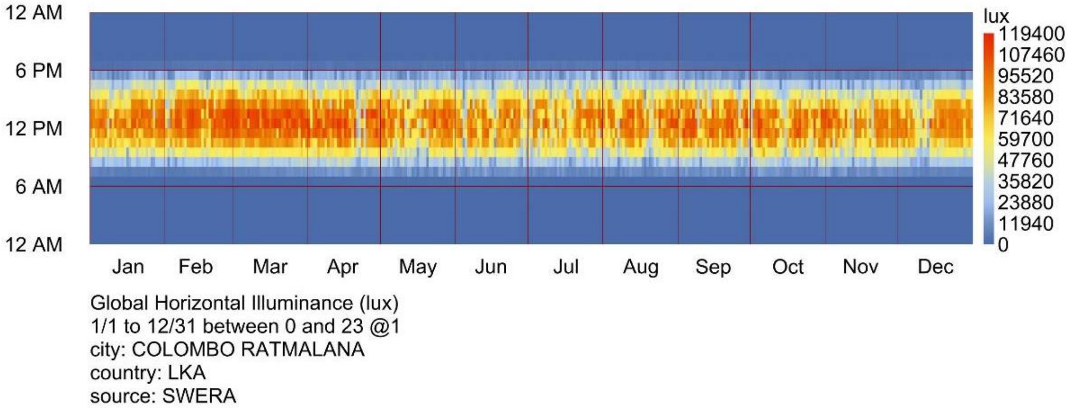

Figure 3.10: Global Horizontal Illuminance (lux) for Colombo visualized in *Grasshopper*

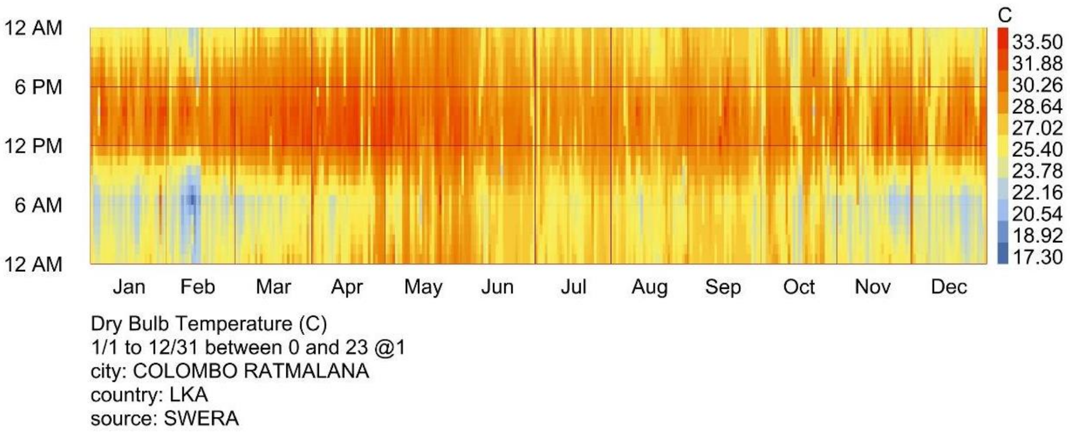

Figure 3.11: Dry-bulb temperature in Colombo visualized in *Grasshopper*

Figure 3.10 indicates very high levels of illuminance during the day-time throughout the year. The intensity of daylight is particularly high during mid-day. Dry-bulb temperature varies between 17 ^{0}C and 33.5 ^{0}C throughout the year as depicted in Figure 3.11. It was also noted that night-time temperatures are not significantly lower than day-time temperatures throughout most of the year.

The building's orientation corresponding to the sun path is a primary consideration in urban design to ensure solar access. Therefore, the impact of the surrounding building layouts and their orientation is vital in the urban microclimate. In terms of the solar potential of the microclimate, the orientation of the building is found to be the most significant parameter in determining the amount of heat gain into the building (Nebia & Aoul, 2017; Samuelson et al., 2016). Therefore, the impact of the urban context on the simulation model is quantified in each cardinal direction for this study.

In order to achieve the research objectives, a parametric urban context was developed to facilitate the multi-objective optimization of solar access for the simulation models. Most high-rise buildings tend to be of the same form and height due to conformity with planning regulations in the urban areas. Hence, for this study, the parametric urban context is simulated as the obstructions of the same height and form in the four cardinal sides of the simulation model (Figure 3.12).

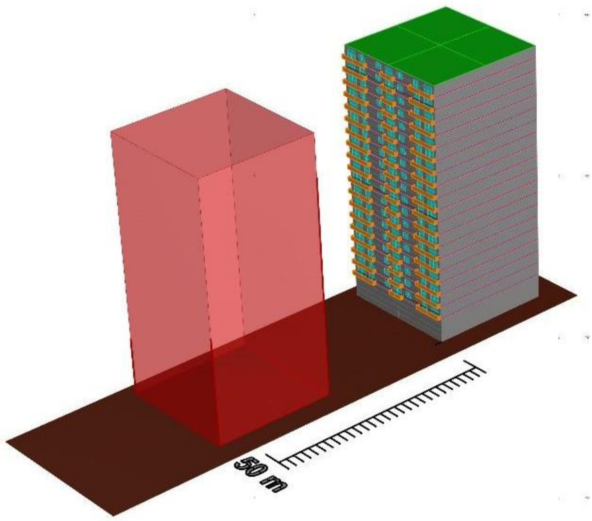

Figure 3.12: Illustration of Simulation model 2 facing the parametric obstruction in the west at 34 m

The distance to the obstruction varies every 2 m, between 2 m and 50 m, by utilizing parametric software. The shading effects of the parametric obstruction on the Simulation model were modelled separately for each cardinal direction, as illustrated in Figure 3.12. Increasing densities resemble when the obstruction is closer to the Simulation model, while decreasing densities resembles when the obstruction moves further away from the simulation model.

3.4 Selection of metrics and simulation tools to quantify the effects of the urban context on solar access

Dual characteristics of solar radiation-light and heat have to be balanced to obtain optimum thermal and visual comfort indoors. Direct exposure to solar radiation in the tropics is not preferred due to heat gain. In case thermal comfort or visual comfort couldn’t be attained by passive means, active means could be employed for creating indoor comfort conditions, as seen in Figure 3.13.

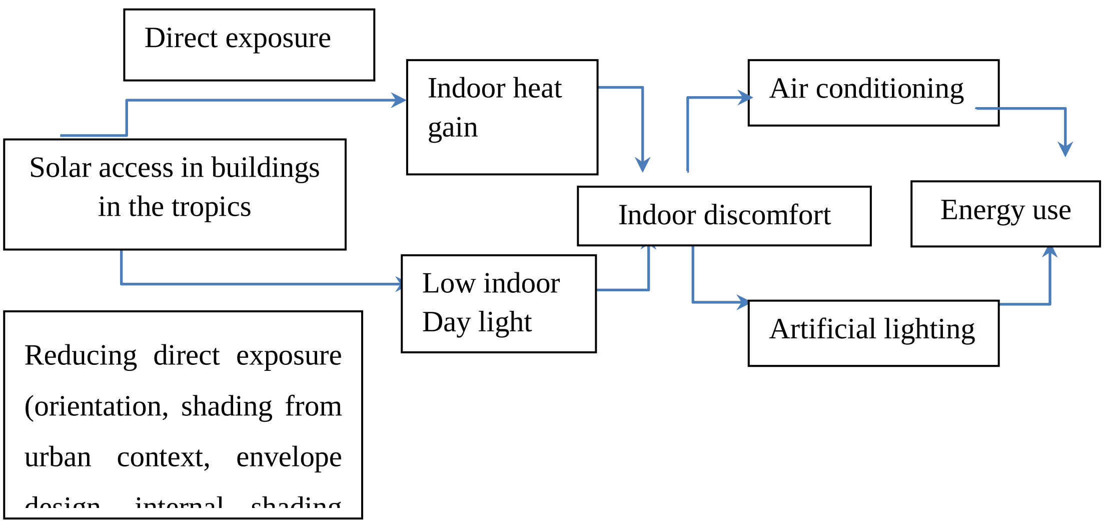

Figure 3.13: Relationship between solar access and energy use in buildings in dense urban tropics

Figure 3.13. established the relationship between solar access and indoor daylight levels, energy use for day-time artificial lighting and energy use for cooling to

mitigate heat gain in dense urban tropics. The metrics for quantifying the above parameters are discussed below.

- Spatial daylight autonomy (sDA)

Several daylight metrics and their limitations were discussed in the literature review. Spatial daylight autonomy (sDA) is a relatively new daylight metric that is based on CBDM. sDA is calculated as the percentage of floor area that receives at least 300 lux for at least 50% of the annual occupied hours (IESNA, 2012). This study utilizes sDA $_{(300lx|50)}$ to estimate external shading effects on indoor daylight levels. The abbreviation sDA from this point, onwards indicates sDA $_{(300lx|50)}$ in this study.

- Annual sunlight exposure (ASE)

Annual sunlight exposure (ASE) is defined as the fraction or percentage of the horizontal work plane that exceeds a specified direct sunlight illuminance level for more than a specified number of hours per year over a specified daily schedule with all operable shading devices retracted (IESNA, 2012). The calculation of ASE is also based on CBDM. ASE is calculated as the percentage of floor area that receives at least 1000 lux for at least 250 occupied hours per year. ASE was calculated for the same daylight grid developed for sDA. From this point onwards, in this study, the abbreviation ASE is used to indicate ASE $_{(1000lx|250)}$.

- Annual energy use for cooling due to external heat gain (kWh/year)

This study focused on the effects of contextual shading on external heat gain due to the solar radiation incident on a high-rise residential building's vertical surface. Energy use could be considered annually without any further distinction into seasonal variations in the tropics. Therefore, the annual energy use for cooling to mitigate external heat gain (kWh/year) indicates cooling energy use of the thermal zone.

- Annual energy use for day-time lighting (kWh/year)

In addition, to cooling energy use, the effects of contextual shading on the day-time lighting energy use of a high-rise residential building is explored. Therefore, the annual day-time lighting energy use (kWh/year) was utilized to indicate artificial lighting energy for the day-time in the daylight model. The annual energy use for day-time lighting was calculated for the same daylight grid developed for sDA.

- Annual total energy use (kWh/year)

The annual total energy use is the sum of annual energy use for cooling due to external heat gain (kWh/year) and annual energy use for day-time lighting (kWh/year).

- Annual cooling energy savings

This study aims to compare the effects of the urban context on energy use for cooling. Therefore, the energy savings from shading from the urban context is presented as a percentage change from the scenario without a context.

Annual cooling energy savings, as a percentage change, was calculated as:

$$\frac{Energy\ use\ for\ cooling\ (x=2-50) - Energy\ use\ for\ cooling\ excluding\ the\ context}{Energy\ use\ for\ cooling\ excluding\ the\ context} \text{ X 100}$$

X= Energy use for cooling at X distance to the obstruction

- Annual total energy savings

This study also compares the effects of the urban context on annual total energy use. Similar to the calculation of annual energy savings for cooling, annual total energy savings, as a percentage change, was calculated as:

$$\frac{Total\ energy\ use\ (x{=}2{-}50) - Total\ energy\ use\ excluding\ the\ context}{Total\ energy\ use\ excluding\ the\ context}\ \text{X}\ 100$$

X = Total energy use for cooling and day-time lighting at X distance to the obstruction

3.4.1 Selection of simulation tools

For this study, several scenarios of the urban context were simulated; therefore, the use of parametric software was quite useful. A parametric simulation tool, which could simulate contextual shading on sDA, ASE, annual energy use for cooling and day-time lighting energy, was selected. Several publications cited in the literature review utilized the *Rhino3D* modelling software with the *Grasshopper* interface to model the urban context (Kosir & Sprah, 2019; Lobaccaro et al., 2017; Natanian et al., 2019; Samuelson et al., 2016). Therefore, *Rhino 3D* modelling software (*Rhinoceros, Version 5*, n.d.) with the *Grasshopper* interface (*Grasshopper for Rhino 5.0*, n.d.) for creating the simulation models and the parametric urban context was selected for this study as well.

To simulate sDA and annual day-time lighting energy use, this study utilized the *Diva4* plug-in. The *Archsim* plugin was used to simulate the annual energy use for cooling. *Archsim* is based on the *EnergyPlus* simulation engine (Samuelson et al., 2016). *RADIANCE* and *Daysim* are responsible for daylighting analysis in *DIVA4* (Jakubiec & Reinhart, 2011).

3.5 Thermal zone model

The thermal zones in SM1, SM2, and SM3 were created by the perimeter/core simulation method (Samuelson et al., 2016). According to the American Society of Heating, Refrigerating and Air (ASHRAE) standards (2007), in multi-family buildings, residential units shall be modelled at least as one thermal block per unit except when those units facing the same orientation, they may be combined into one thermal block. ASHRAE (2007) also required that the perimeter zone be modelled at 5 m depth to simulate energy consumption. However, due to the average living room depth extending to 6 m (Figure 3.7) in the archetypal high-rise residential building, and considering the high levels of solar penetration in tropics, the depth of the perimeter zone was taken as 6 m and the height at 3 m.

The physical characteristics of the thermal zone (Figure 3.14) modelled are given in Table 3.2. Each thermal zone was modelled with all adiabatic surfaces except for the exterior wall, which is exposed to solar radiation. The settings for simulating energy use for cooling and the thermal properties of the construction materials in the thermal model are given in Table 3.3. The settings in SM1, SM2, and SM3 are selected to isolate the effects of solar access on the cooling energy use of the thermal zone. Therefore occupancy, equipment load, window shading and natural ventilation settings were set to 0. The annual cooling load (kWh/per year) was calculated for 24-hour operations for 365 days as heat gain effects could last longer than daylit hours. The thermal zone simulation in *Archsim* only considers shading effects and does not account for building reflections. Three thermal zones were modelled at floor levels given in Table 3.4 for the four cardinal directions.

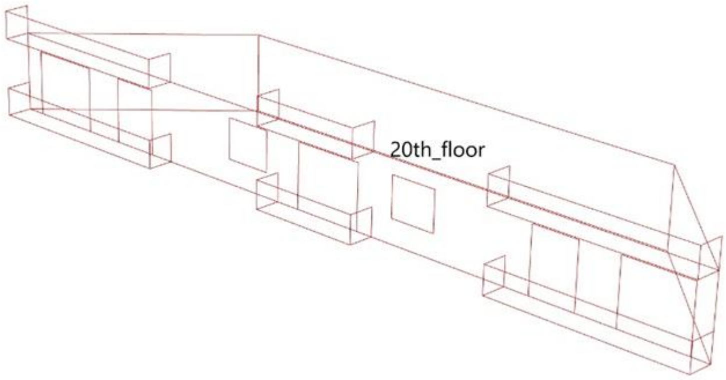

Figure 3.14: Thermal zone model for the 19th floor in SM2

Table 3.2: Thermal zone characteristics

Model component	Measurements
Height	3m
Depth	6m
The total exterior wall exposed to solar radiation in the thermal zone	90.56 m^2
glazed area	33.48 m^2
The total zone area	148 m2
Total zone volume	437 m3

Table 3.3: Thermal model assumptions

Conditioning settings	
Constant set point	26 ^{0}C
Cooling limit	100 W/m^2
Flow limit	100 m^3/s/m^2
Operational Schedule	24hrs for 365 days
Occupancy/equipment	0
Infiltration (ACH)	0
Thermal properties of the model	
Roof	adiabatic
Floor	adiabatic
Internal partition walls	adiabatic
External wall	U value- 2.521 W/m^2-K
Windows	U value- 5.84 W/m^2-K

Table 3.4: Simulated floors

Simulation model	Top floor	Median floor	Bottom floor
SM1	9^{th} floor	5^{th} floor	2^{nd} floor
SM2	19^{th} floor	11^{th} floor	2^{nd} floor
SM3	29^{th} floor	15^{th} floor	2^{nd} floor

The simulation path for the thermal zone is depicted in Figure 3.15. Figure 3.15 illustrates the occupation schedule, the thermal properties of the external wall material, the simulation path for cooling, the animation of the parametric urban context and the recording of the simulation results for each iteration.

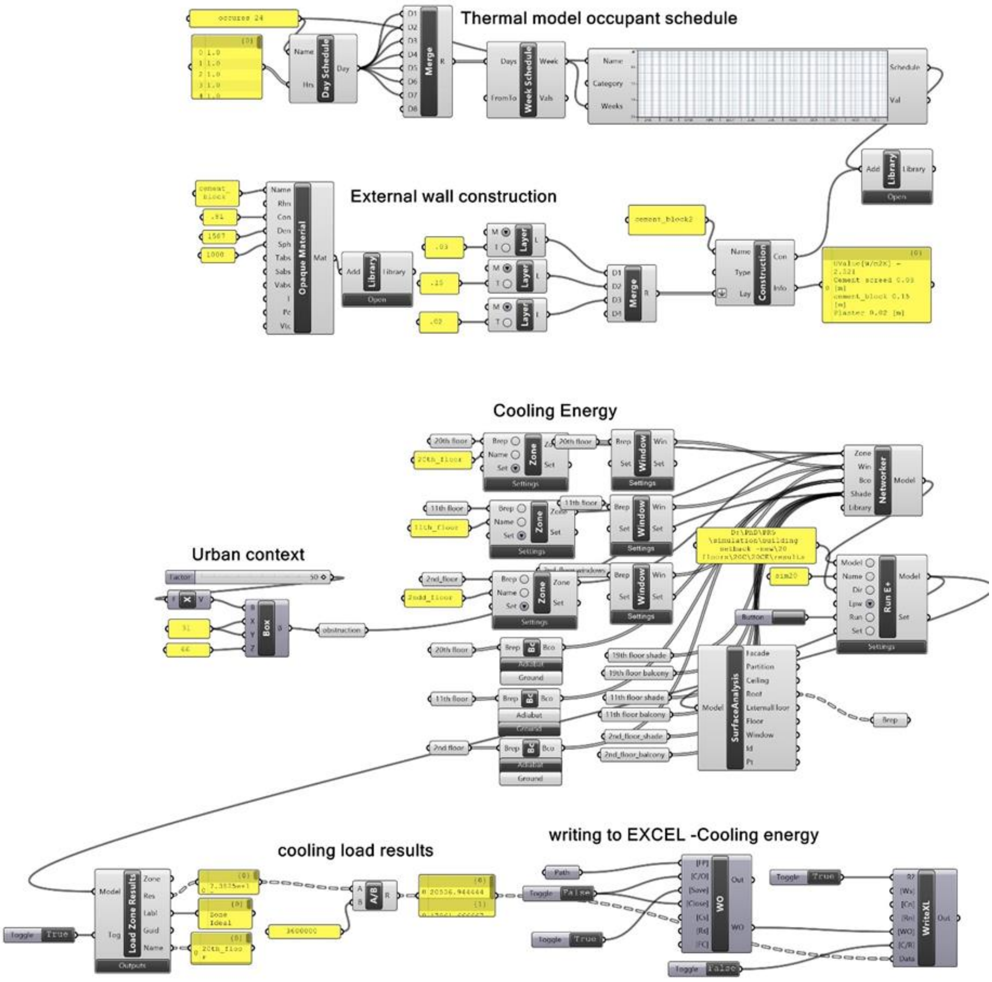

Figure 3.15: Simulation path for the thermal model in SM2 in *Grasshopper*

The parametric urban context animation allows the automatic calculation of cooling energy use at the given distance to the obstruction. At a given distance to the obstruction, the annual cooling energy use of the Simulation model was calculated and exported to an *Excel* sheet. Each annual cooling energy use datum was specified by the thermal zone (floor level), Simulation model (SM1, SM2 and SM3), cardinal direction (east, west, north, south) and distance to the obstruction (2, 4, 6… 50 m). A total of 900 annual cooling energy use data were generated for the 3 Simulation models.

To calculate the energy savings due to contextual shading, the cooling energy use, excluding the urban context, was also simulated using the simulation path in Figure 3.15. The simulated data on annual cooling energy use is available in the Mendeley Repository at https://data.mendeley.com/datasets/r3wpkr2brx/3.

3.6 Daylight and day-time lighting energy model

The daylighting grid was generated based on the periphery/core simulation method utilized for the thermal zone (Figure 3.16). The depth of the grid was taken at 6 m, and the height of the space is 3 m to match the thermal zone model measurements in Table 3.2. The height of the sensor is taken at 0.75 m, and the grid spacing at 0.6 m.

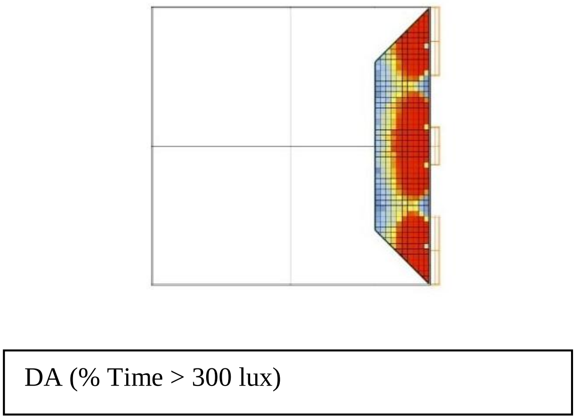

Figure 3.16: *DIVA4* grid for simulating sDA in the 19th floor for SM2 facing the obstruction at 20 m in the east

Radiance parameters can be set at low, medium, high-quality settings in *DIVA4.* The higher quality setting could give more accurate results; however, it would take a longer time. Studies suggest 5 ambient bounces are suited to simulating daylight (Dogan and Park, 2017; Kim, 2013; Lu and Du, 2013; Moazzeni and Ghiabaklou, 2016). Therefore, the medium quality setting was selected for the simulation of daylight illuminance considering speed and accuracy (Table 3.5). *DIVA4* calculations take into account shading as well as building reflections.

Table 3.5: Radiance parameter settings

Parameter	Medium quality
Ambient bounces (ab)	4
Ambient accuracy(aa)	1
Ambient resolution(ar)	256
Ambient divisions(ad)	1024
Ambient super-samples (as)	256

Day-time lighting energy was calculated as annual lighting energy (kWh/per year) for the occupied period per simulated floor. The occupied period was taken from 8.00 a.m. to 5.00 p.m. for 365 days of the year, excluding daylight saving time. The use of internal shading devices was not accounted for in this study, which could complicate the calculations of shading effects on cooling energy use. Table 3.6 depicts the building surface reflectance values for the construction materials.

Table 3.6: Surface reflectance values for materials of the building elements

Building element	Material	Surface reflectance value
Structure	Concrete structure	30
Exterior walls	Cement block wall, 200 mm, outside rendered, inside plastered	30(outside) 70(inside)
Window	Single pane 6 mm clear glass	88
Balcony railing	Cement block wall, 150 mm, outside and inside rendered	30
Floor finish	Tile finish on a concrete slab	40
Ceiling	Reinforced Concrete slab,200 mm, screed 63-12 mm painted white	80
Interior walls	Cement block wall, 150 mm, plastered on both sides	70
Ground	Compacted earth	30

The simulation path for the daylight model is given in Figure 3.17. Figure 3.17 illustrates the sDA, ASE and day-time lighting energy use, the artificial lighting schedule, the occupancy schedule, the animated parametric urban context and the recording of the simulation results for each iteration.

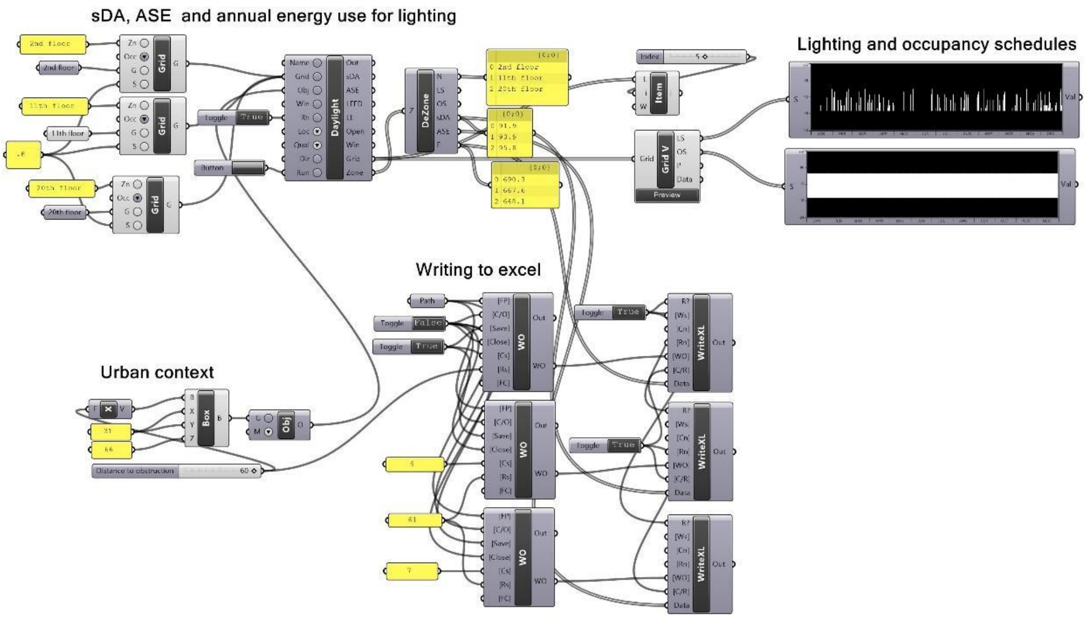

Figure 3.17: Simulation path for the daylight model for SM2 facing east in *Grasshopper*

The parametric urban context animation allows the automatic calculation of sDA, ASE, and annual day-time lighting energy use at the given distance to the obstruction. Each daylight datum was specified by the daylight grid (floor level), Simulation model (SM1, SM2 and SM3), cardinal direction (east, west, north, south) and distance to the obstruction (2, 4, 6… 50 m). A total of 2700 data were generated for the three-day light metrics by the simulation process.

The day-time lighting energy use, excluding the urban context, was also simulated using the simulation path in Figure 3.17 to calculate total energy savings. The simulated data on sDA, ASE and annual day-time lighting energy use is available in the Mendeley Repository https://data.mendeley.com/datasets/r3wpkr2brx/3.

3.7 Optimization process

As discussed in the literature review, the most common method for optimizing the urban context is through the coupling of simulation software and an optimization engine. The Simulation model in this study is complex with detailed elevations, including windows and balconies. Studies considering the effects of the urban context generally consist of block models without a detailed elevation (Lobaccaro et al., 2017; Natanian et al., 2019; J. Zhang et al., 2019). Therefore, due to the complexity of the Simulation model, coupling simulation and optimization would be time-consuming and demand computers with high processing capacity.

Therefore, in this study, the simulation and the optimization process are decoupled. *A-priori* optimization process, which was discussed in the literature review, was utilized where the decision-maker provides preferences before the optimization step during the parameter-setting (David et al., 2015). By using an *a-priori* optimization process, only iterations preferred by the authors that are in-line with the research objectives populate the solution space and carry forward to the optimization step. Therefore, in this study, the number of iterations is limited to 25 for one Simulation model in each cardinal direction. The software and methods leading to the optimization process are depicted in Figure 3.18 below.

Figure 3.18: Steps leading to the optimization process in the study and relevant software

As seen in Figure 3.18, this study does not automate the optimization process to generate the Pareto-front. It utilized a 2D Pareto-front of the sDA and total energy savings, calculated from the simulation results. The Pareto-front is then examined for Pareto-optimal sets of sDA and total energy savings. The method utilized for selecting the Pareto-optimal sets would depend on the trends observed on the Pareto-front. Based on the above optimization process, the thresholds for the definition of optimum solar access for high-rise residential buildings in dense urban tropics are formulated.

3.8 Development and validation of the building setback curves for optimum solar access

The definition of optimum solar access was developed by a multi-objective optimization process of the simulation results discussed in the previous section. As optimum solar access is difficult to calculate at the preliminary design stage, the study results are incorporated into an urban planning tool. A building setback is a simple tool used in urban planning to dictate the open space around the building from the site boundary. The building setback curves were calculated in Chapter 4 by utilizing the threshold values of sDA and total energy use for optimum solar access.

Three high-rise residential buildings in Colombo were utilized for the case studies to test the applicability of the prescribed setback curves. The following criteria were considered when selecting the case studies.

- The Case study should have a square or rectangular floor plan to avoid self-shading effects due to building form.
- Buildings should be within the range of building heights of the Simulation models, from 11 to 31 floors.

Table 3.7 presents the characteristics of the three case studies. All three case studies have a core-dependent compact form that does not account for self-shading. The case studies consist of 10, 17 and 31 floors. The building floor to floor height ranges from 2.85 m to 3.15 m. The building materials of the case studies are also very similar, excluding the variations in the glazing material. The WWR for all three buildings range from 43-36%, and the interior spaces are all air-conditioned.

Table 3.7: Characteristics of the case studies

Building characteristics	Case study 1 (C_1)	Case study 2 (C_2)	Case study 3 (C_3)
			
Number of floors	10	17	31
Floor height	2.85 m	3 m	3.15 m
Floors for parking	2	6	Basement
Units per floor	4	8	4
Exterior walls	Concrete walls and 200mm cement block walls		
Internal walls	Concrete walls and 150mm cement block walls		
Glazing	Single pane clear (glass 6mm)	Double pane (clear glass 6mm)	Green tinted glass (8mm)
Flooring	Laminated timber	Ceramic tile	Ceramic tile
Average WWR	36	40	34
HVAC system	All units are air-conditioned		

3.8.1 Calibration method for case studies

Due to the lack of research in computer modelling of the urban context in the tropics, there is a need to validate the simulation software utilized in this study for applications in the tropics. Therefore, the Simulation models of the three case studies were calibrated.

The parameters of investigation in this study are sDA, annual cooling and day-time lighting energy use. However, field measures of the above parameters are affected by several other variables other than solar access. For example, field data on building energy use includes several aspects such as equipment load, occupant load and schedule, which are not affected by solar access. Therefore, indoor air temperature and daylight illuminance directly affected by solar access were calibrated in the case studies.

Coefficient of Variation of Root Mean Square Error – CV (RMSE) (%) determines the model fit by capturing offset errors between measured and simulated data, without being affected by the cancellation effect (Coakley et al., 2014; Soebarto & Ph, 1997). Several studies (Mustafaraj et al., 2014; Pisello et al., 2014) have utilized the above process to calibrate mean air temperature in building simulation models. Calibration of hourly illuminance using statistical methods is not well established in research. For calibrated simulations, the CV (RMSE) and Normalized Mean Bias Error (NMBE) shall be determined by comparing simulated data ($\hat{s}$) to the field data (m_i), with p = 1. ASHRAE guideline 14 dictates that Simulation models are to be calibrated within CV ($RMSE_{hourly}$) value of $\pm$30% and $NMBE_{hourly}$ $\pm$10% (Ruiz & Bandera, 2017).

$$CV(RMSE_{hourly}) = \frac{\sqrt{\frac{\sum (m_i - \hat{s}_i)^2}{(n-p)}}}{\underline{m}} x\ 100$$

Equation 2: Coefficient of variation of root mean square error (%)

$$NMBE_{\ hourly} = \frac{\sum (m_i - \hat{s}_i)^2}{\underline{m}(n-p)}\ x\ 100$$

Equation 3: Normalized mean bias error (%)

3.8.1.1 Case study 1

Field data on indoor air temperature and indoor hourly illuminance levels were collected using three *Hobo* data loggers (MX-2202) in a bedroom in Case study 1 (Figure 3.19). The locations of the data loggers in the plan are depicted by A, B, and C in Figure 3.20. The bedroom was located on the second floor of the building facing the south. During the data collection period, the windows and doors were closed with curtains open at all times, and there was no occupation. Data were collected from Case study 1 (C_1) during the period from 26.06.2020 to 09.07.2020, at a 10-minute interval. The data logger was located 1.15 m above the ground level.

Figure 3.19: Data collection in a bedroom in Case study 1 utilizing *Hobo* data loggers

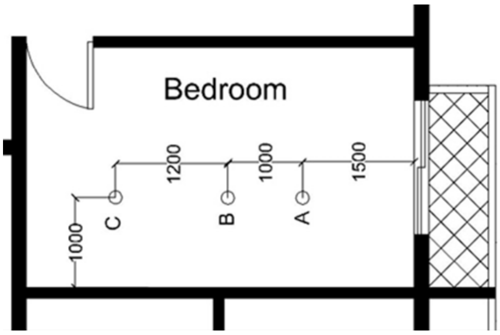

Figure 3.20: Location of data loggers (indicated by A, B, C) 1.15 m above ground in a bedroom in Case study 1

The thermal zone for the bedroom was modelled using the *Archsim* plug-in in *Rhino3D* (Figure 3.21). The material properties in Case study 1 are very much similar to the archetypal high-rise residential building. The settings of the thermal model and space characteristics are given in Table 3.9. The model was simulated without occupation and natural ventilation to match indoor conditions during field data collection. The indoor mean air temperature of the thermal zone was simulated using the workflow stipulated in Figure 3.22.

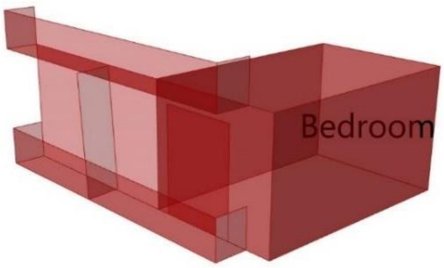

Figure 3.21: Thermal zone for the bedroom in Case study 1 in *Archsim*

Table 3.8: Thermal model settings and space characteristics in Case study 1

Thermal properties of the model	
Typical floors	adiabatic
Internal walls	adiabatic
External walls	U value- 2.521 W/m^2-K
Windows	U value- 5.84 W/m^2-K
Space characteristics	
Height	2.85 m
Floor area	16.8m^2
Window area	4.32m^2

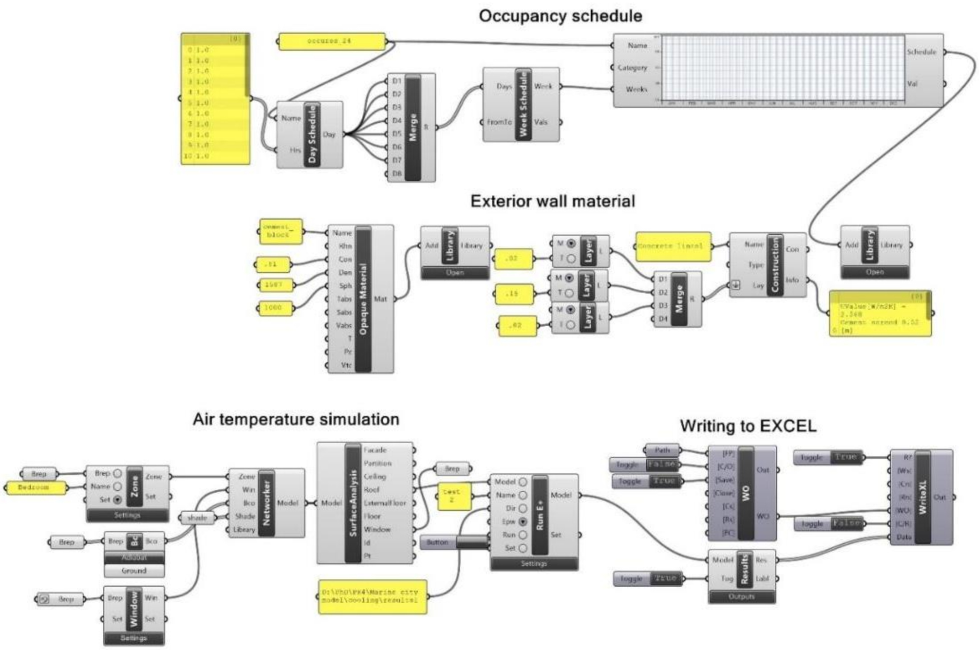

Figure 3.22: Indoor mean air temperature simulation for a bedroom in Case study 1 in *Grasshopper*

The daylight grid for the Simulation model of the bedroom is depicted in Figure 3.23. The same points corresponding to the field data (Figure 3.20) were simulated for hourly illuminance. The daylight model was simulated for the *DIVA4* settings given in Table 3.5 and the reflectance values in Table 3.10.

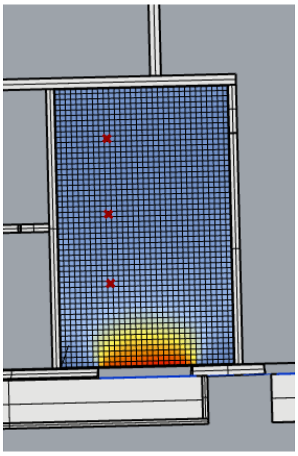

Figure 3.23: Daylight grid for the bedroom in Case study 1 in *DIVA4*

Table 3.9: Surface reflectance values for Case study 1

Building element	**Material**	**Surface reflectance value**
Structure	Concrete structure	30
Exterior walls	Cement block wall, 200 mm, outside rendered, inside plastered	30(outside) 70(inside)
Window	Single pane 6 mm clear glass	88
Balcony railing	Cement blocks, 150 mm, outside and inside rendered	30
Floor finish	Composite wood finish on concrete slab	40
Ceiling	Reinforced Concrete slab,200 mm, screed 63-12 mm painted white	80
Interior walls	Cement block wall, 150 mm, plastered on both sides	70
Interior objects	Furniture	50
Ground	Compacted earth	30

Figure 3.24 depicts the simulation path for hourly illuminance in the daylight grid in Case study 1. Hourly illuminance was calculated for 8760 hours per year. Therefore, the simulation period corresponding to the field data collection was extracted and exported to *Excel* software for calibration.

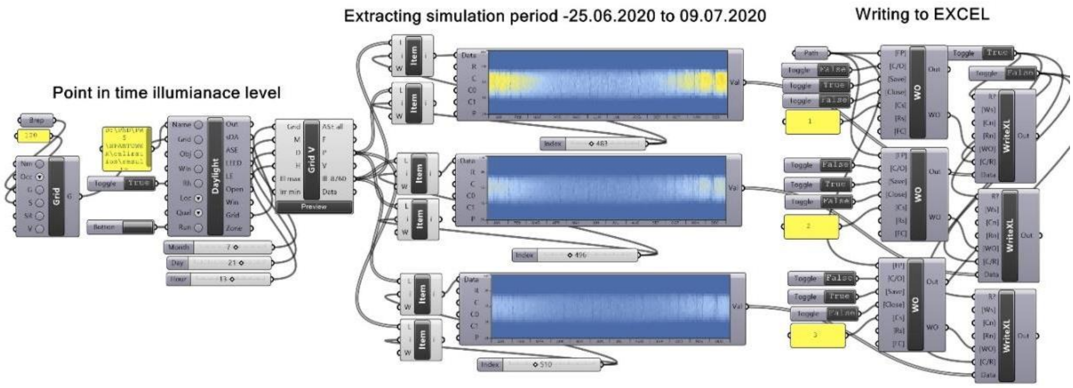

Figure 3.24: Simulation path for point- in time hourly illuminance simulation for a bedroom in Case study 1 in *Grasshopper*

3.8.1.2. Case study 2

Field data on indoor air temperature and indoor illuminance levels for a bedroom in Case study two (C_2) was collected utilizing *Hobo* data loggers from 15.06.2020 to 22.06.2020(Figure 3.25). The bedroom is located on the 11th floor facing the south. Data were collected at 10-minute intervals with three data loggers. The residential units in Case study two were occupied; therefore, the data collection period was limited to one week. The data loggers A, B and C were located 1.15 m above the ground level (Figure 3.26).

Figure 3.25: Data collection in a bedroom in Case study 2 utilizing *Hobo* data loggers

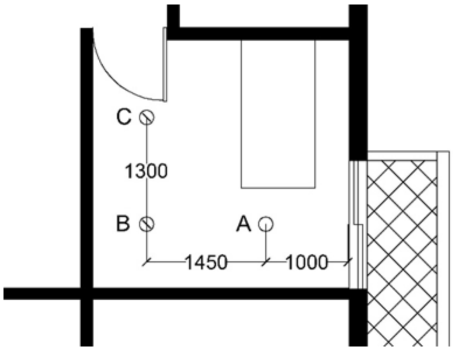

Figure 3.26: Location of data loggers (indicated by A, B, C) 1.15 m above ground in a bedroom in Case study 2

The thermal model for simulation of the mean indoor air temperature for the Case study was developed in *Rhino3D* (Figure 3.27). The thermal model was simulated utilizing the *Archsim* plug-in for the thermal model settings and spatial characteristics given in Table 3.11. The glazing material in C_2 was 6 mm double pane windows which have a lower U value than in the archetypal high-rise residential building. Figure 3.28 depicts the simulation path for C_2.

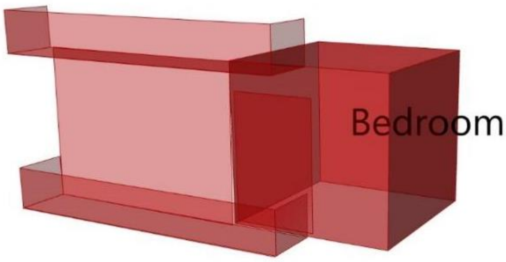

Figure 3.27: Thermal zone for the bedroom in Case study 2 in *Rhino3D*

Table 3.10: Thermal model settings and space characteristics in Case study 2

Thermal properties of the model	
Typical floors	adiabatic
Internal walls	adiabatic
External walls	U value- 2.521 W/m^2-K
Windows	U value- 2.7 W/m^2-K
Space characteristics	
Height	3 m
Floor area	9.7 m^2
Window area	3.7 m^2

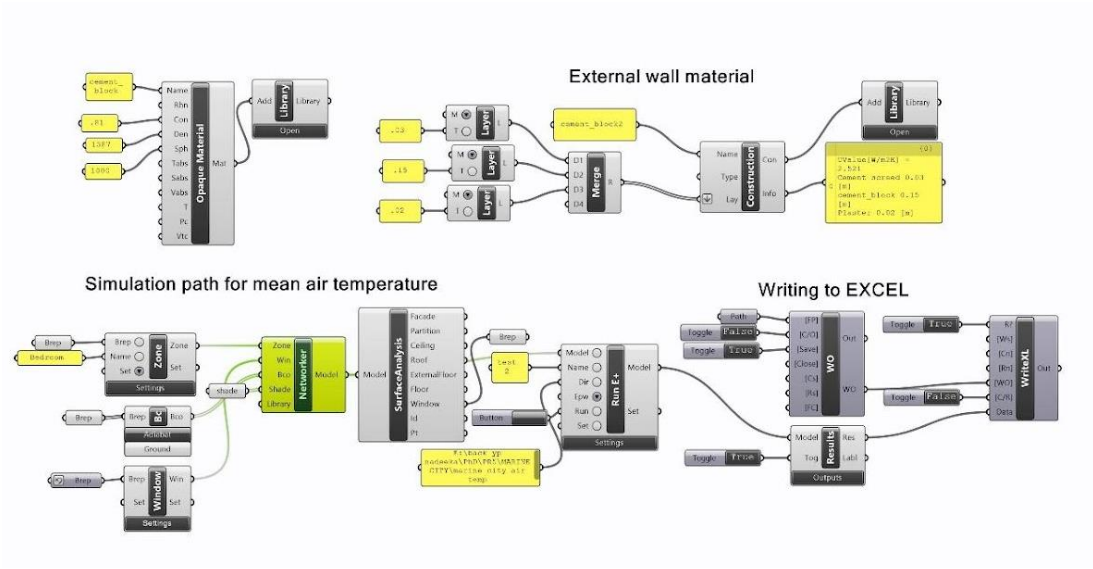

Figure 3.28: Indoor mean air temperature simulation for a bedroom in Case study 2 in *Grasshopper*

The daylight grid for the bedroom simulated in C_2 is depicted in Figure 3.29. The daylight simulation model was developed in *DIVA4* for the given reflectance values in Table 3.12. The simulation path for the point-in-time hourly illuminance levels is depicted in Figure 3.30.

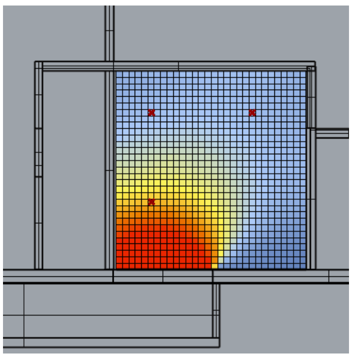

Figure 3.29: Daylight grid for the bedroom in Case study 2 in *DIVA4*

Table 3.11: Surface reflectance values for Case study 2

Building element	Material	Surface reflectance value
Structure	Concrete structure	30
Exterior walls	Cement block wall, 200 mm, outside rendered, inside plastered	30(outside) 70(inside)
Window	Double pane 6 mm clear glass	80
Balcony railing	Cement blocks, 150 mm, outside and inside rendered	30
Floor finish	Tile finish on a concrete slab	40
Ceiling	Reinforced Concrete slab,200 mm, screed 63-12 mm painted white	70
Interior walls	Cement block wall, 150 mm, plastered on both sides	70
Interior objects	Furniture	50
Ground	Compacted earth	30

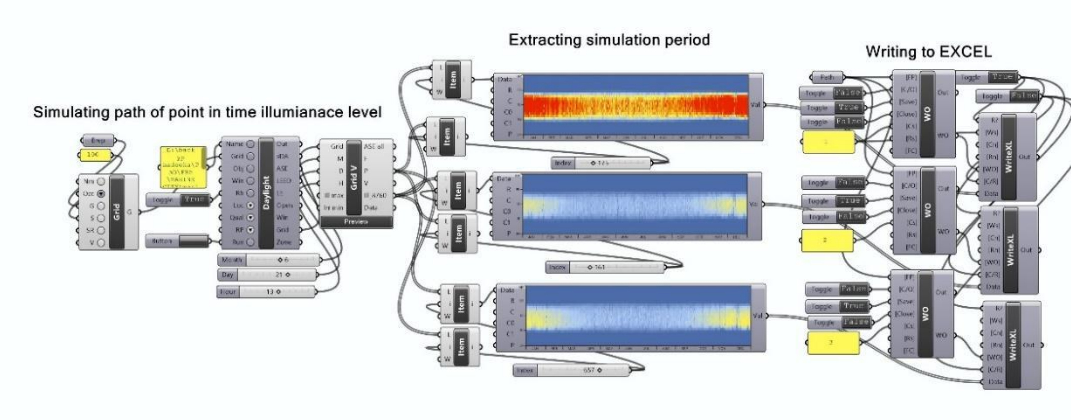

Figure 3.30: Simulation path for point- in time hourly illuminance simulation for a bedroom in Case study 2 in *Grasshopper*

3.8.1.2. Case study 3

The field data for indoor air temperature and daylight illuminance in Case study three (C_3) were collected from 19.02.2020 to 25.02.2020 at 10-minute intervals (Figure 3.31). The bedroom was located on the 17th floor facing the north-west. Data was collected from three data loggers located at A, B and C as depicted in Figure 3.32. The bedrooms in C_3 were in occupied residential units; therefore, the data collection period was limited to one week.

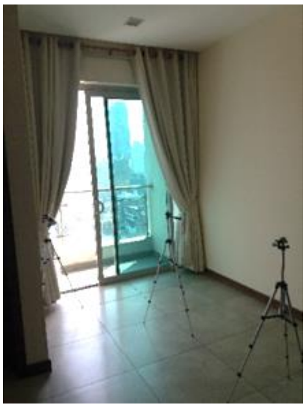

Figure 3.31: Data collection in a bedroom in Case study 3 utilizing *Hobo* data loggers

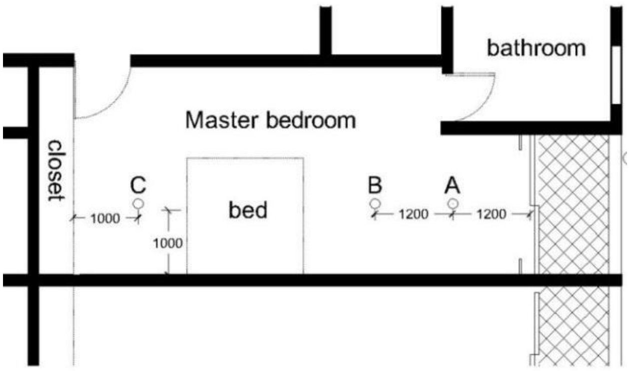

Figure 3.32: Location of data loggers (indicated by A,B,C) 1.15 m above ground in Case study 3

The thermal model was simulated in the *Archsim* plug-in *Rhino3D*. The bedroom modelled in C_3 is depicted in Figure 3.33. The thermal model settings and the spatial characteristics are given in Table 3.13. The windows in C_3 were 8mm in thickness and had a green tint. Therefore, in addition to the external wall construction, the glazing material was also constructed in *Archsim* as indicated in the simulation path in Figure 3.34.

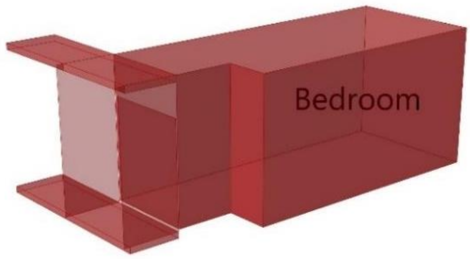

Figure 3.33: Thermal zone for the bedroom in Case study 3 in *Archsim*

Table 3.12: Thermal model settings and space characteristics in Case study 3

Thermal properties of the model	
Typical floors	adiabatic
Internal walls	adiabatic
External walls	U value- 2.521 W/m^2-K
Windows	U value- 5.7 W/m^2-K
Space characteristics	
Height	3 m
Floor area	23 m^2
Window area	5 m^2

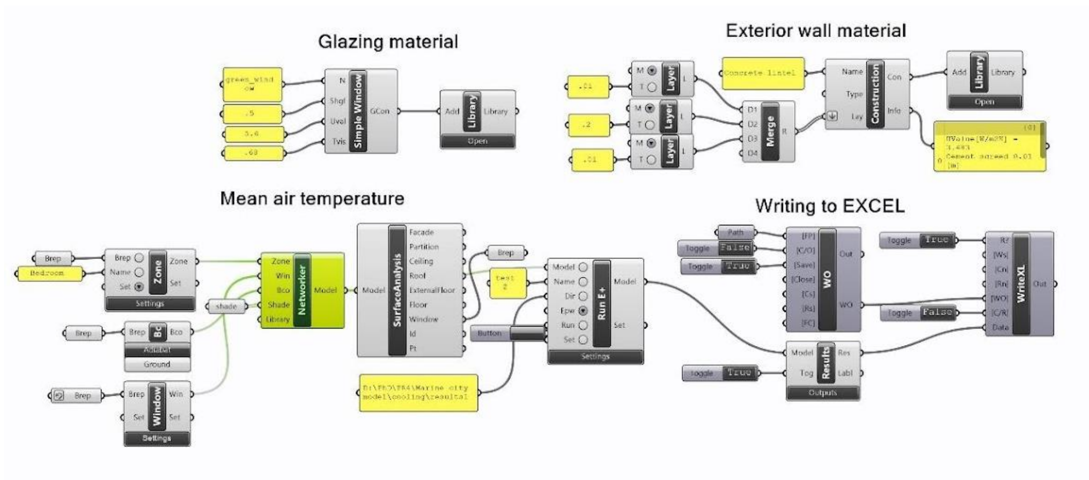

Figure 3.34: Indoor mean air temperature simulation for a bedroom in Case study 3 in *Grasshopper*

The daylight grid in the bedroom for C_3 is depicted in Figure 3.35. The surface reflectance values of materials utilized in the daylight model for C_3 is given in Table 3.14. Due to the green-tint, the surface reflectance value of the glazing is taken as 70 in C_3. The reflectance values of the construction materials common in the case studies were adjusted to represent the effects of discolouration. The simulation path for the daylight model in *DIVA4* plug-in is given in Figure 3.36. The calibration of mean air temperature and the hourly illuminance of case studies are discussed in Section 4.9.

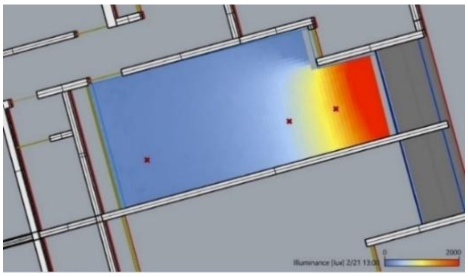

Figure 3.35: Daylight grid for the bedroom in Case study 3 in *DIVA4*

Table 3.13: Surface reflectance values for Case study 3

Building element	**Material**	**Surface reflectance value**
Structure	Concrete structure	30
Exterior walls	Cement block wall, 200 mm, outside rendered, inside plastered	30(outside) 70(inside)
Window	Single pane 8 mm green-tinted glass	70
Balcony railing	Toughened glass 10 mm	-
Floor finish	Tile finish on a concrete slab	40
Ceiling	Reinforced Concrete slab,200 mm, screed 63-12 mm painted white	80
Interior walls	Cement block wall, 150 mm, plastered on both sides	50
Interior objects	Furniture	50
Ground	Compacted earth	30

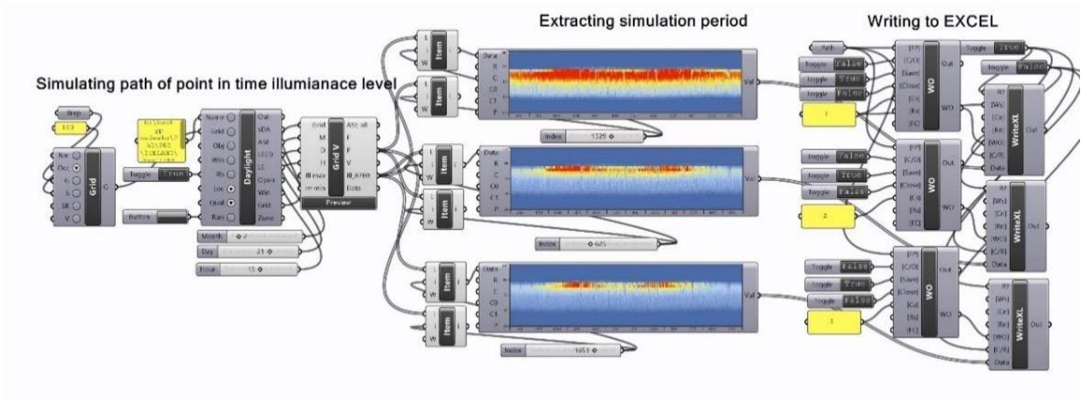

Figure 3.36: Simulation path for point- in time hourly illuminance simulation for Case study 3 in *Grasshopper*

3.8.2 Modelling the impact of contextual shading due to the building setback on daylight and energy use of the case studies

The modelling of the shading effects of the urban contexts on daylight and energy performance of the case studies are discussed in the section. The simulation processes for spatial daylight autonomy, annual day-time lighting energy (LE) and annual cooling energy (CE) for the three case studies are discussed in this section.

Thermal and daylight Simulation models were generated for a typical floor for each Case study. The three case studies were modelled in *AutoCAD* and exported to the *Rhino3D-Grasshopper* interface. The spaces modelled in the typical floor were bedrooms (BR) and living and dining areas (LD) in the residential units (Apt) that had direct solar access. Spaces with solar access from multiple cardinal directions and daylight access from an air-well were not considered in the Simulation model.

At present, most high-rise residential buildings are constructed as standalone structures in Sri Lanka, as discussed in the Introduction. Therefore, two hypothetical urban contexts for investigation of solar access in the case studies were developed as follows:

- The first urban context was developed to represent the current building setback regulations in Sri Lanka. The current building setback regulations are given in Appendix B. The relevant distance to the obstruction corresponding to the Case study building heights are depicted in Table 3.8.

- The second urban context was developed based on the prescribed building setbacks for optimum solar access given in Figure 4.21. The relevant distance to the obstruction for the case studies are depicted in Table 3.8.

Table 3.14: Hypothetical context for case studies

	C_1	C_2	C_3
The hypothetical context for case studies	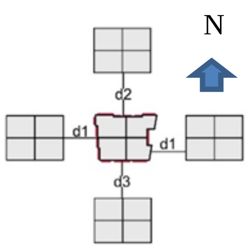	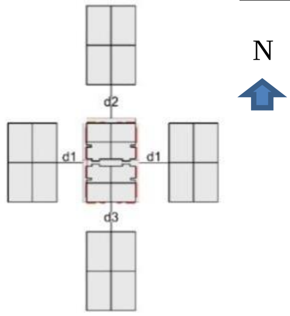	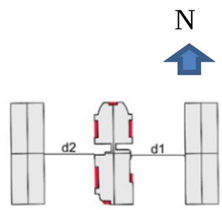 Scenario 1 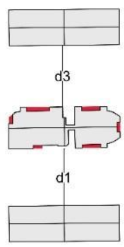 Scenario 2
Current side setback regulations in Sri Lanka	d1 – 6m d2 -6m d3 -6m	d1 -12 m d2 -12 m d3 -12 m	d1 – 12 m d2 -12 m d3 -12 m
Building setback for optimum solar access	d1 – 16.3 m d2 -19.5 m d3 -17.5 m	d1-22 m d2- 24.4 m d3-22.2 m	d1-28 m d2- 27 m d3-30 m

3.8.2.1 Modelling the effects of contextual shading on Case study 1

Case study one is a 10-storey high-rise residential building consisting of 30 units. The ground floor is utilized for parking while from the 2nd floor to the 8th floor has the typical floor plan depicted in Table 3.15. The 9th floor consists of two large units. The building has a central core plan and balconies characteristic of high-rise residential buildings in the tropics. The building materials are listed in Table 3.15. All building materials in Case study one comply with the generic materials identified in the archetypal high-rise residential building.

Table 3.15: Spaces and floor levels modelled in Case study 1

3D model of the building	Spaces (bedrooms and living rooms) modeled for sDA, LE and CE in a typical floor	Floor levels simulated
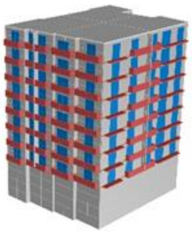	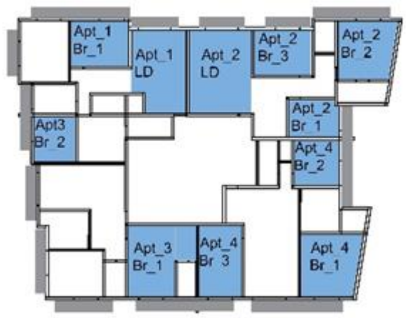	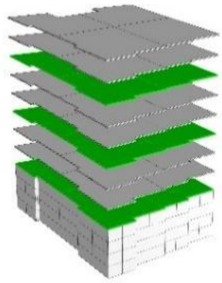 2,5,8 FL

Building materials

Building element	Material	Surface reflectance value	U value (W/m^2-k)
Structure	Concrete structure	30	2.521
Exterior walls	Cement block wall, 200 mm, outside rendered, inside plastered	30(outside) 70(inside)	2.521
Window	Single pane 6mm clear glass	80	5.84
Balcony	150 mm cement blocks	30	Adiabatic
Roof	Reinforced Concrete flat slab, 200 mm, screed 63-12 mm	30	Adiabatic
Floor finish	Tile finish on a concrete slab	40	Adiabatic
Ceiling	Reinforced Concrete slab, 200 mm, screed 63-12 mm painted white	70	Adiabatic
Interior walls	Cement block wall, 150 mm, plastered on both sides	70	2.568
Ground	Compacted earth	30	Adiabatic

The thermal model was developed for the indicated living room and bedroom spaces in Table 3.15 for the 2nd, 5th, 8th floor. Table 3.15 depicts the thermal properties of the construction materials used in the thermal model. The thermal model of a typical floor is illustrated in Figure 3.37. 11 spaces per typical floor were modelled. Interior walls in some spaces were shared. The heat exchanges between these shared walls were also simulated. The cooling load settings are depicted in Table 3.16. The space was simulated for 24 hours for 365 days to attain the annual cooling energy use. The simulation path is given in Figure 3.36. The thermal properties of the external wall and the internal wall were modelled in the simulation path as depicted in Figure 3.37.

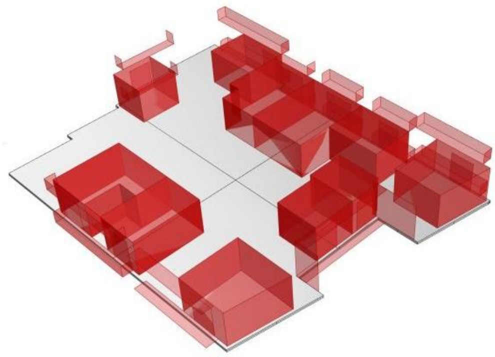

Figure 3.37: Thermal zone for a typical floor in Case study 1 in *Archsim*

Table 3.16: Cooling load settings for case studies

Cooling load settings	
Constant set point	26 ^{0}C
Cooling limit	100 W/m^2
Flow limit	100 m^3/s/m^2
Operational Schedule	24hrs for 365 days
Occupancy/equipment	0
Infiltration (ACH)	0

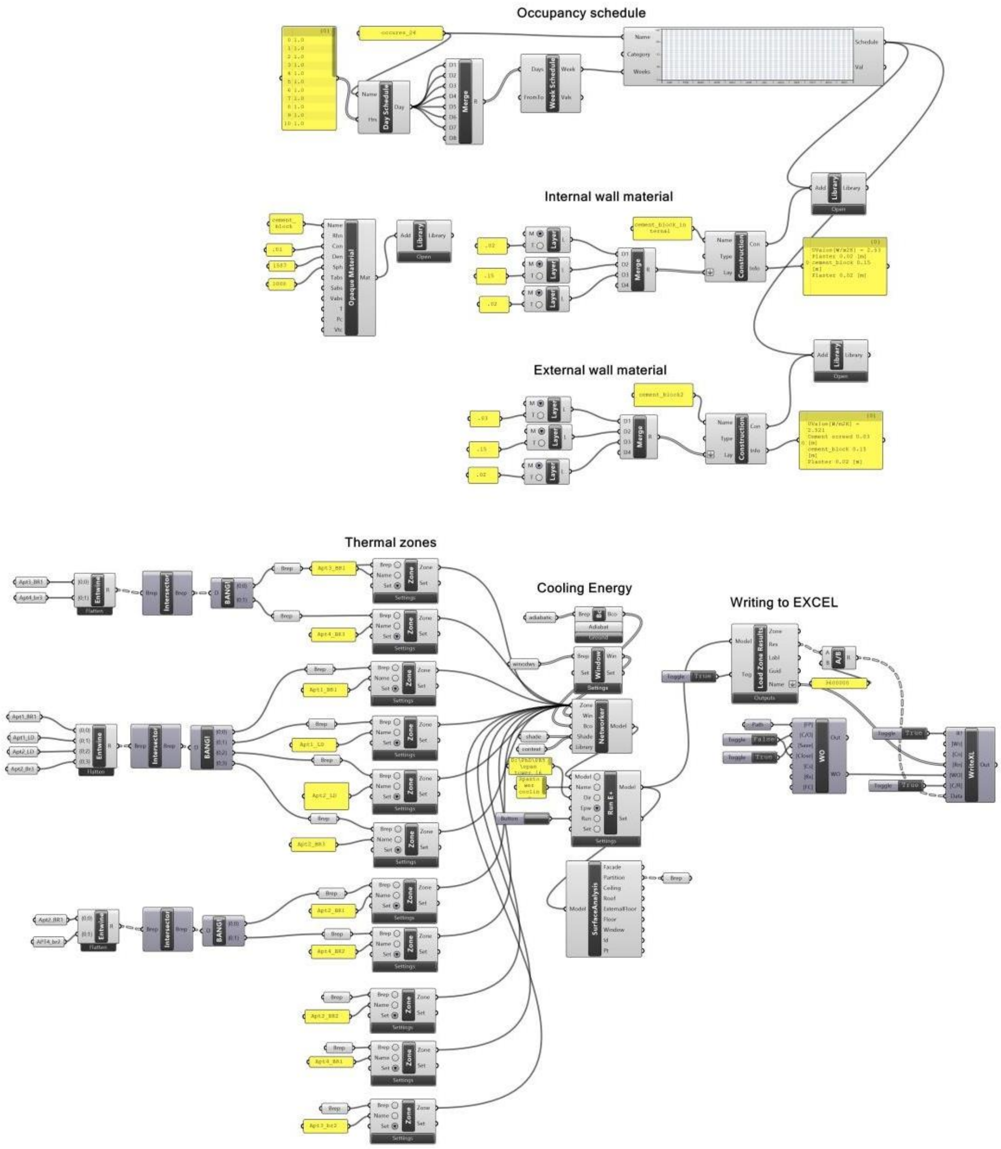

Figure 3.38: Simulation path for annual energy use for cooling in a typical floor of Case study 1 in *Grasshopper*

The daylight grid for the 7th floor in Case study one is depicted in Figure 3.39. The daylight grid was taken 0.75 m above the floor level while grid spacing was taken at 0.6 m. The day-time lighting energy is simulated for occupation between 8.00 a.m. to 5.00 p.m., excluding daylight saving time. The reflectance values for the model were given in Table 3.15. The simulation path for the 11 daylight grids per typical floor is given in Figure 3.40.

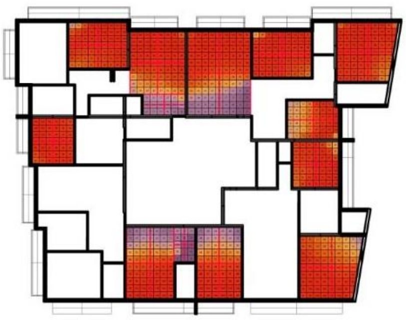

DA (% Time > 300 lux)

Figure 3.39: 7th-floor daylight grid in Case study 2 for the optimized urban context

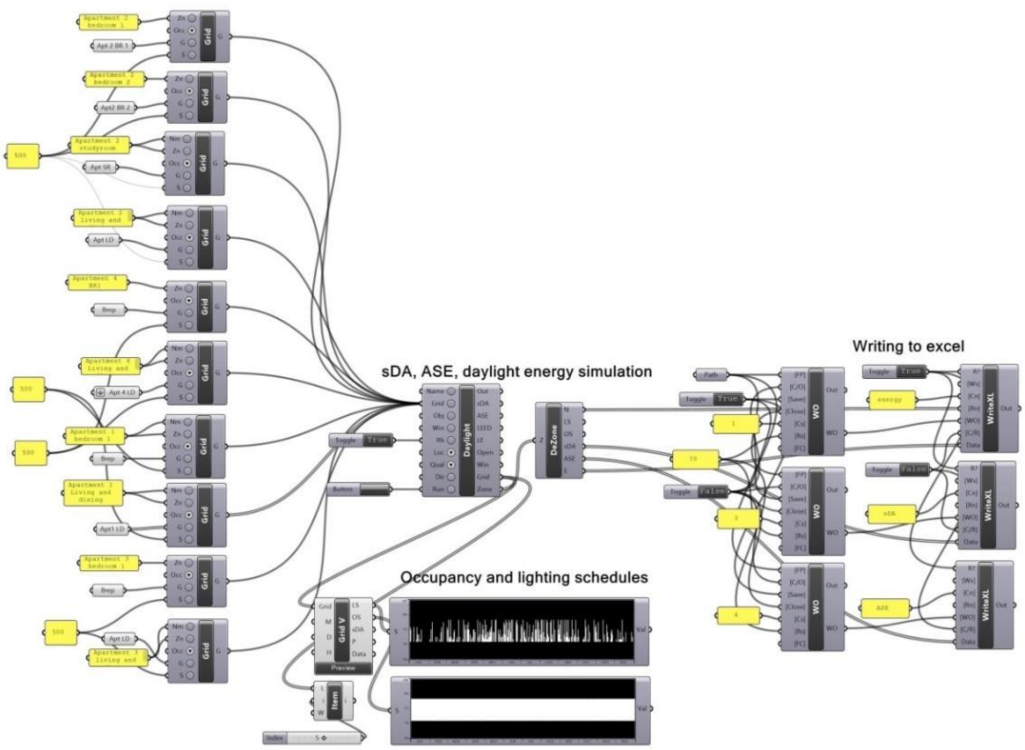

Figure 3.40: Simulation path for sDA and day-time lighting energy in a typical floor of Case study 1 in *Grasshopper*

The thermal and daylight model developed for Case study 1 were simulated separately for the two urban context scenarios described in Table 3.8. The simulated results of the shading effects of the two urban contexts on the spatial daylight autonomy and total energy use in Case study 1 are compared in Section 4.9.3.

3.8.2.2 Modelling the effects of contextual shading on Case study 2

Case study two is a 17-floor residential building with 142 units located in the suburbs of Colombo. The first six floors are utilized as car parks. Therefore, only floors 7 to 15 are considered for simulation. The 16th floor consists of a penthouse in the building.

Table 3.17: Spaces and floor levels modelled in Case study 2

3D model of the building	**Spaces (bedrooms and living rooms) modelled for sDA, LE and CE on a typical floor**	**Floor levels simulated**
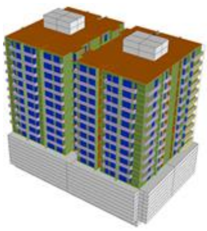	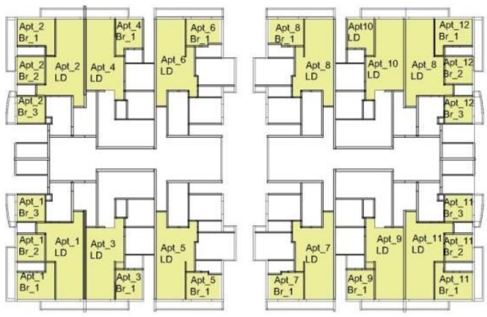	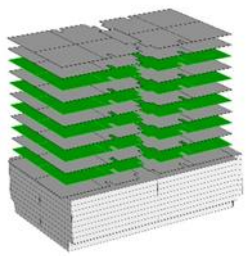 7,9,11,13,15 FL

Building materials

Building element	**Material**	**Surface reflectance value**	**U value (W/m^2-k)**
Structure	Concrete structure	30	2.521
Exterior walls	Cement block wall, 200 mm, outside rendered, inside plastered	30(outside) 70(inside)	2.521
Window	Double pane 6 mm clear glass	80	2.7
Balcony	150 mm cement blocks	30	-
Roof	Reinforced Concrete flat slab,200 mm, screed 63-12 mm	30	Adiabatic
Floor finish	Tile finish on concrete slab	40	Adiabatic
Ceiling	Reinforced Concrete slab,200 mm, screed 63-12 mm painted white	70	-
Interior walls	Cement block wall, 150 mm, plastered on both sides	70	Adiabatic
Ground	Compacted earth	30	-

Thermal zones for 32 living room and bedroom spaces per typical floor were modelled in *Archsim- Rhino3D* as depicted in Figure 3.41. The thermal properties of construction materials used in the Simulation model of C_2 were given in Table 3.17. The window glazing material in the Case study is double-pane 6mm glass which affects the heat gains into the interior spaces. Interior walls in some spaces were shared. The heat exchanges between these shared walls were simulated as well. The thermal properties of the external wall and the internal wall were modelled in the simulation path as depicted in Figure 3.42. The cooling load settings for the three case studies were the same, and they are given in Table 3.16 for Case study 1.

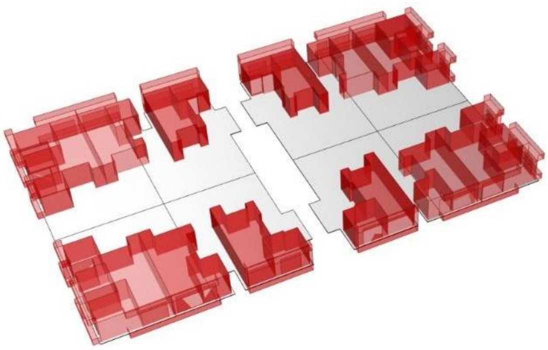

Figure 3.41: Thermal zones for a typical floor in Case study 2 in *Archsim*

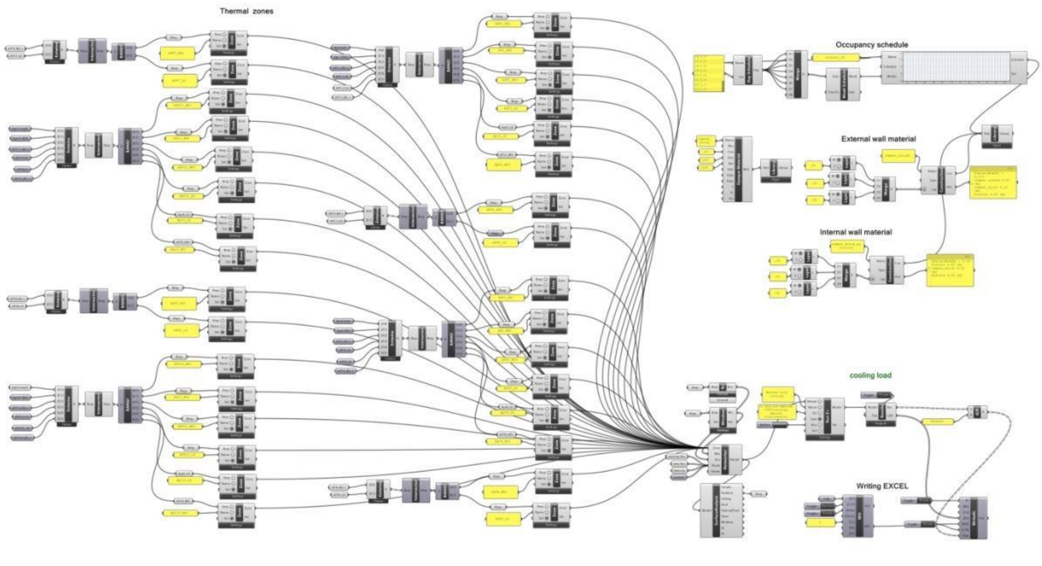

Figure 3.42: Simulation path for annual energy use for cooling in a typical floor of Case study 2 in *Grasshopper*

The daylight grid for C_2 was simulated in *DIVA4* and is depicted in Figure 3.43. The grid is placed 0.75 m above the floor level with 0.6 m spacing of the grid. The day-time lighting energy is simulated for occupation between 8.00 a.m. to 5.00 p.m., excluding daylight saving time. The simulation path for C_2 is given in Figure 3.44. The reflectance values of the materials were given in Table 3.17.

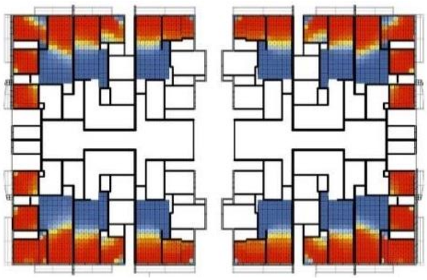

DA (% Time > 300 lux)

Figure 3.43: 10th-floor daylight grid in Case study 2 for the optimized urban context

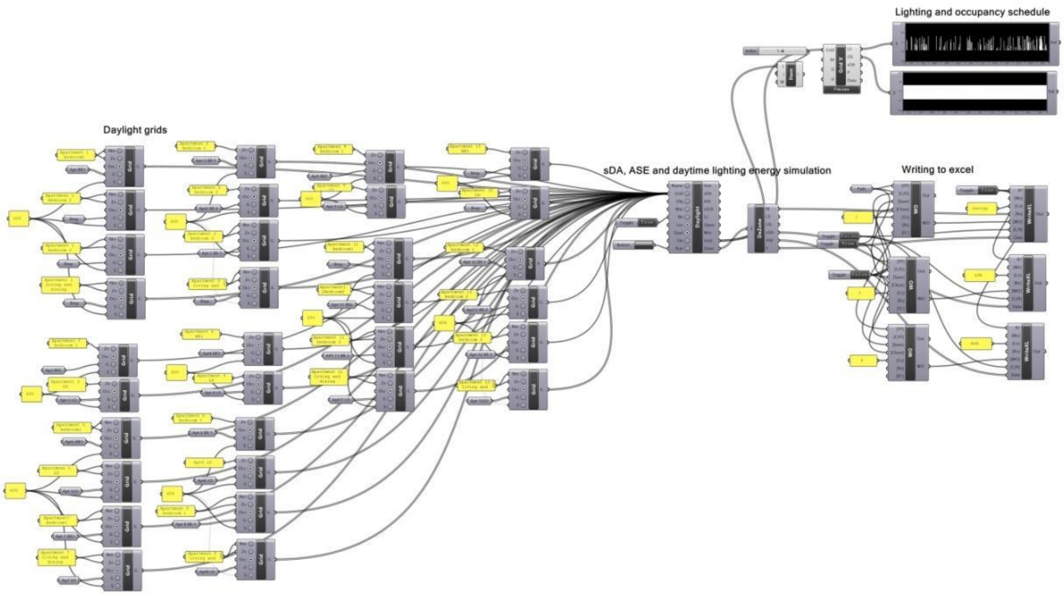

Figure 3.44: Simulation path for sDA and day-time lighting energy in a typical floor of Case study 2 in *Grasshopper*

The thermal and daylight model developed for Case study 2 were simulated separately for the two urban context scenarios described in Table 3.8. The simulated results of the shading effects of the two urban contexts on the spatial daylight autonomy and total energy use in Case study 2 are compared in Section 4.9.4.

3.8.2.3 Modelling the effects of contextual shading on Case study 3

Case study 3 is a 31-storey high-rise residential building consisting of 96 units. The typical floor plans in the 6, 12, 16, 20, 24, and 28 were modelled for thermal and daylight simulation. Ten spaces (4 living rooms and 6 bedrooms) are modelled per typical floor. Table 3.18 lists the building materials.

Table 3.18: Spaces and floor levels modelled in Case study 3

3D model of the building	Spaces (bedrooms and living rooms) modeled for sDA, LE and CE on a typical floor	Floor levels simulated
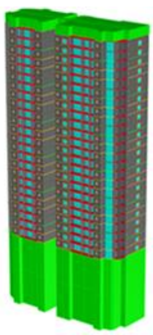	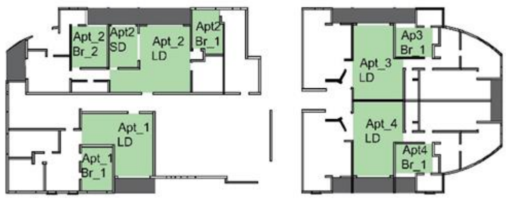	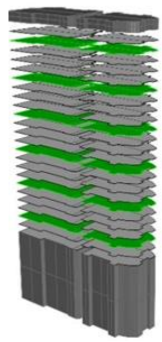 6,12,16,20,24,28 FL

Building materials			
Building element	**Material**	**Surface reflectance value**	**U value (W/m^2-k)**
Structure	Concrete structure	30	2.521
Exterior walls	Cement block wall, 200 mm, outside rendered, inside plastered	30(outside) 70(inside)	2.521
Window	***Single pane 6mm glass**	**88**	**5.84**
Balcony	150 mm cement blocks	30	-
Roof	Reinforced Concrete flat slab,200 mm, screed 63-12 mm	30	Adiabatic
Floor finish	Tile finish on concrete slab	40	Adiabatic
Ceiling	Reinforced Concrete slab,200 mm, screed 63-12 mm painted white	70	-
Interior walls	Cement block wall, 150 mm, plastered on both sides	70	Adiabatic
Ground	Compacted earth	30	-

*The Case study building glazing material is tinted glass with a reflectance value of 70. As the building setback curves were calculated for clear glass, using tinted glass would significantly deviate the results. Therefore, to validate the building setback curves for the given assumptions in this study, 8 mm tinted single-pane glazing of Case study 3 was replaced with 6mm clear single-pane glass in the daylight model.

Ten thermal zones in a typical floor for Case study 3 were modelled as illustrated in Figure 3.45. The thermal properties of the external and internal walls were modelled in the simulation path, as depicted in Figure 3.46. The cooling load settings given in Table 3.16, are common to all three thermal models of the case studies.

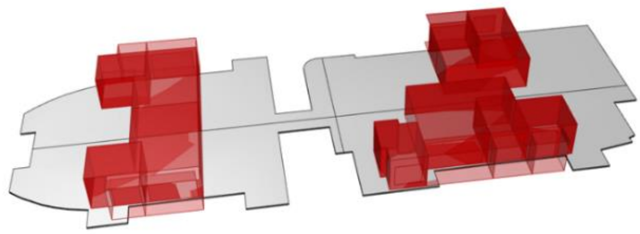

Figure 3.45: Thermal zones in a typical floor in Case study 3

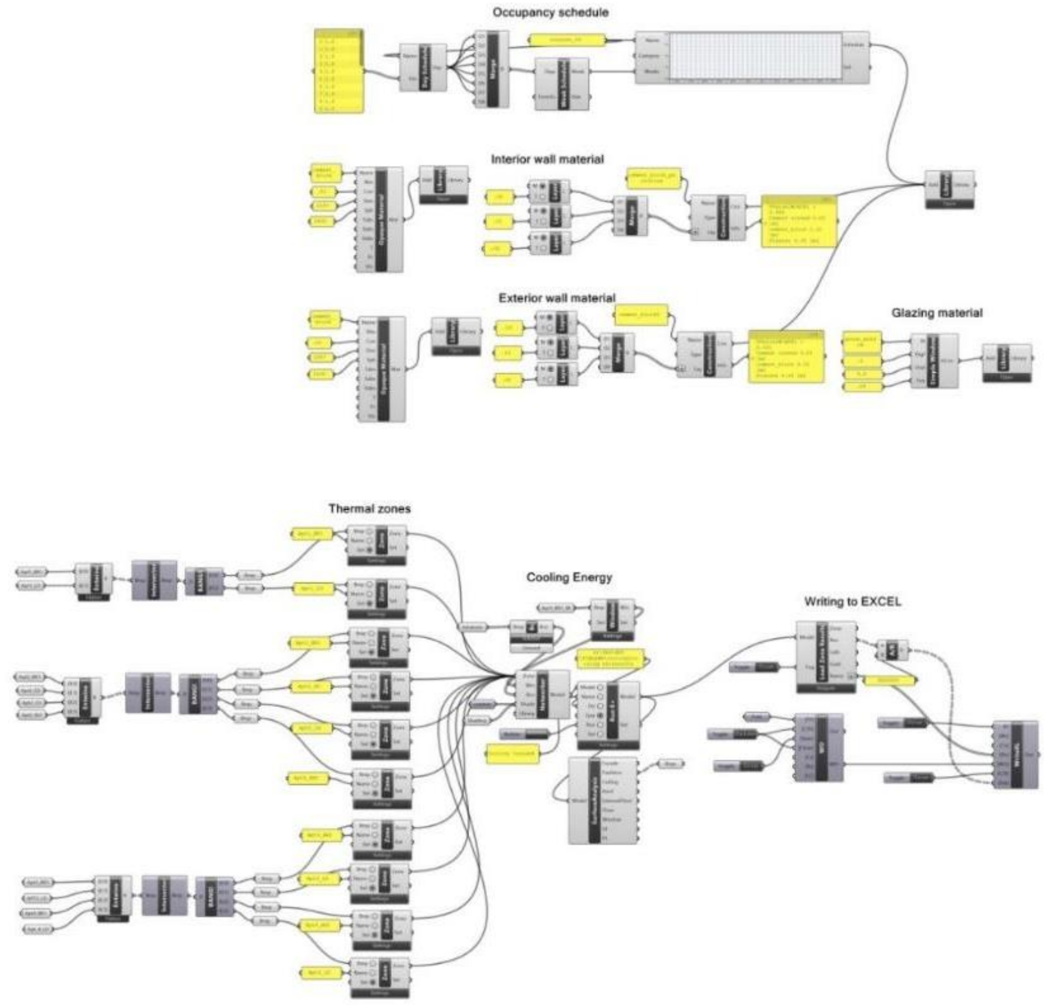

Figure 3.46: Simulation path for annual energy use for cooling in a typical floor in Case study 3 in *Grasshopper*

The daylight grid, depicted in Figure 3.47 for Case study three, was taken 0.75 m above the floor level while the grid spacing was taken at 0.6 m. The day-time lighting energy is simulated for occupation between 8.00 a.m. to 5.00 p.m., excluding daylight saving time. Simulation path for the daylight model for the typical floor is given in Figure 3.48. The reflectance values for the model are given in Table 3.18.

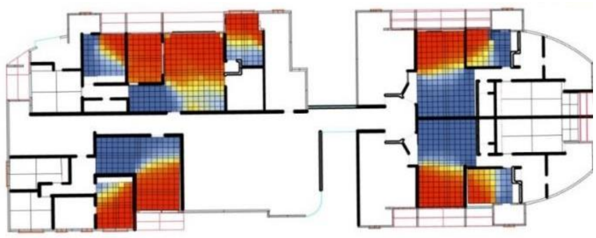

DA (% Time > 300 lux)

Figure 3.47: 6th-floor daylight grid in Case study 3 in the optimized urban context

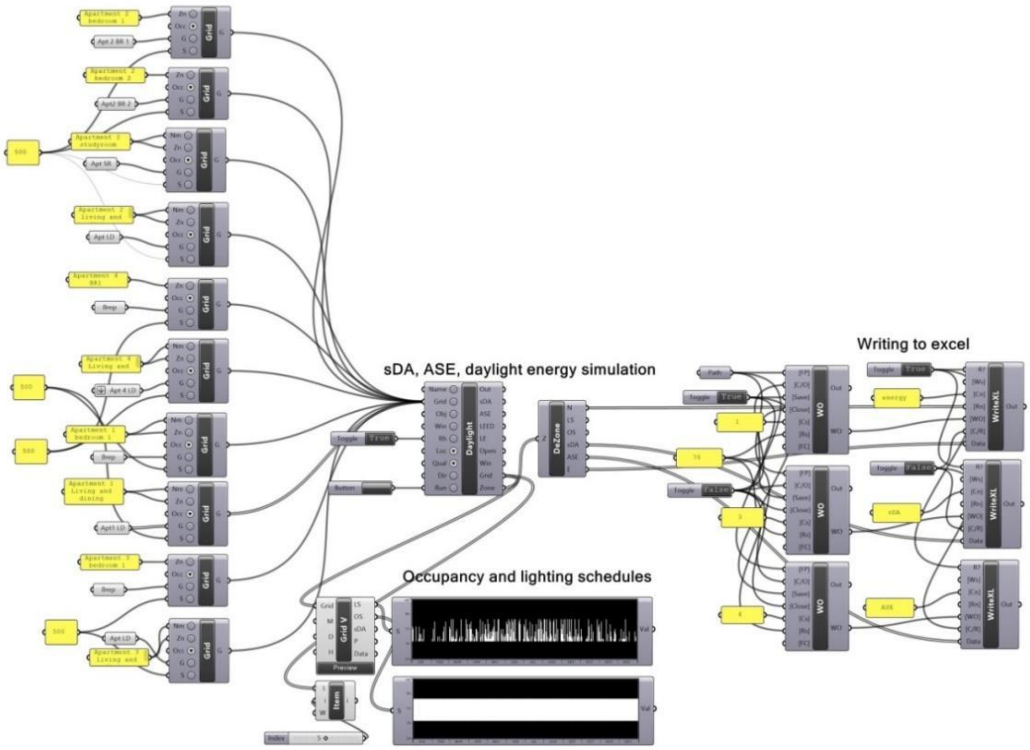

Figure 3.48: Simulation path for sDA and day-time lighting energy in a typical floor of Case study 3 in *Grasshopper*

The thermal and daylight model developed for Case study 3 were simulated separately for the two urban context scenarios described in Table 3.8. The simulated results of the shading effects of the two urban contexts on the spatial daylight autonomy and total energy use in Case study 3 are compared in Section 4.9.4.

Phase III

3.9 Simulating the impact of the urban context on the daylight and energy performance of external shading devices

Simulation model 2 (SM2), which has 21 floors, was used to investigate the effects of the urban context on 27 shading scenarios at three floors levels. The building characteristics of SM2 are the same as described in section 3.2 except for the shading devices and the urban context, which are discussed below.

3.9.1 Characteristics of the external shading scenarios

In most high-rise residential buildings in tropics, the balcony is a common architectural feature that also acts as a shading device for the glazed area below. The balcony is accessed from the living/dining area or the master bedroom. In addition to balconies, vertical panels are also utilized in some buildings. Existing research finds that egg-crates, overhangs and vertical panels effectively reduce heat gain in tropics.

In Phase III, the effectiveness of the most common external shading features of high-rise residential buildings in tropics are explored. Twenty-seven scenarios (C1-27) that consist of combined shading (with balcony and vertical panel), horizontal shading (balcony only) and no shading (no balcony or vertical panel) were modelled in the simulation software. All 27 shading scenarios are tabulated in Table 3.19 and illustrated in Appendix F. The baseline scenario with two large balconies (7.8 m x 1m x 0.9 m) and one small balcony (4.3 m x 1m x 0.9 m) are modelled per typical floor as C14. The no shading scenario was simulated in C1.

Figure 3.49 illustrates the C1- No shading, C14-baseline scenario and C27-Combined shading scenarios investigated in this study.

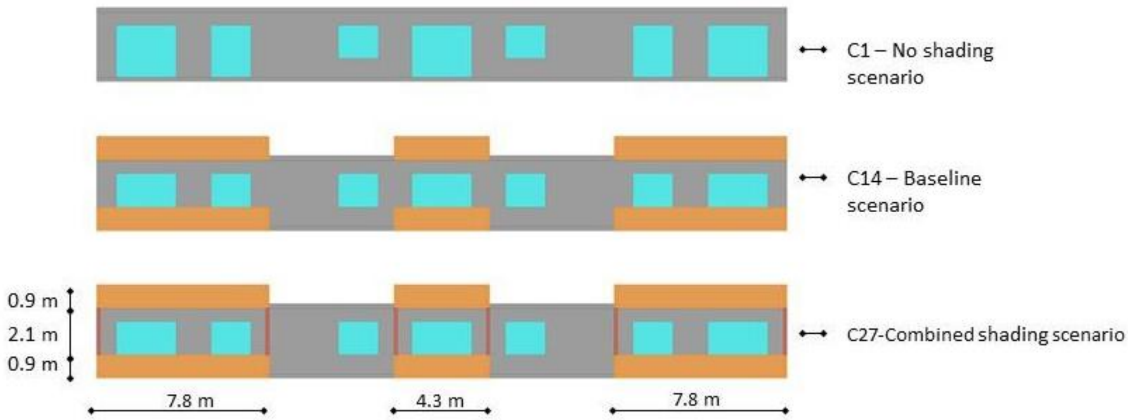

Figure 3.49: Shading scenarios C1, C14 and C27

Table 3.19: External shading scenarios

	Floor level		
	19th floor	**11th floor**	**2nd floor**
C1	None	None	None
C2	None	None	Horizontal shading
C3	None	None	Combined shading
C4	None	Horizontal shading	None
C5	None	Horizontal shading	Horizontal shading
C6	None	Horizontal shading	Combined shading
C7	None	Combined shading	None
C8	None	Combined shading	Horizontal shading
C9	None	Combined shading	Combined shading
C10	Horizontal shading	None	None
C11	Horizontal shading	None	Horizontal shading
C12	Horizontal shading	None	Combined shading
C13	Horizontal shading	Horizontal shading	None
C14	Horizontal shading	Horizontal shading	Horizontal shading

	Floor level		
	19th floor	**11th floor**	**2nd floor**
C15	Horizontal shading	Horizontal shading	Combined shading
C16	Horizontal shading	Combined shading	None
C17	Horizontal shading	Combined shading	Horizontal shading
C18	Horizontal shading	Combined shading	Combined shading
C19	Combined shading	None	None
C20	Combined shading	None	Horizontal shading
C21	Combined shading	None	Combined shading
C22	Combined shading	Horizontal shading	None
C23	Combined shading	Horizontal shading	Horizontal shading
C24	Combined shading	Horizontal shading	Combined shading
C25	Combined shading	Combined shading	None
C26	Combined shading	Combined shading	Horizontal shading
C27	Combined shading	Combined shading	Combined shading

3.9.2 Characteristics of the urban context

In this study, a high-rise, high-density urban context is modelled at the building setback for optimum solar access given in Figure 4.21 to investigate the shading effects on the external shading scenarios indicated above in Section 3.9.1. Based on the building setbacks for a 21-floor building in Figure 4.21, an urban context with obstructions at 24 m in the east and south, 24.3 m in the west and 26 m in the north were modelled as depicted in Figure 3.50 below.

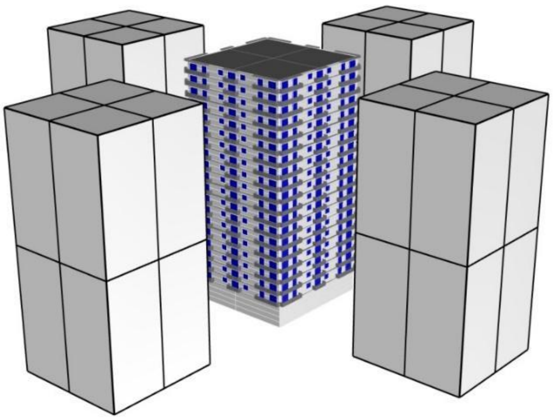

Figure 3.50: Simulation model 2 with a high-rise, high-density context developed for optimum solar access

3.9.3 The thermal and daylight model

The thermal models, excluding shading (C1), baseline scenario (C2) and combined shading (C27) are depicted in Figure 3.51. The thermal zone was defined with the same assumption and settings, as described in Section 3.5 for Simulation model 2. The simulation path to obtain the annual cooling energy use at the 19th, 11th and the 2nd-floor level is depicted in Figure 3.52.

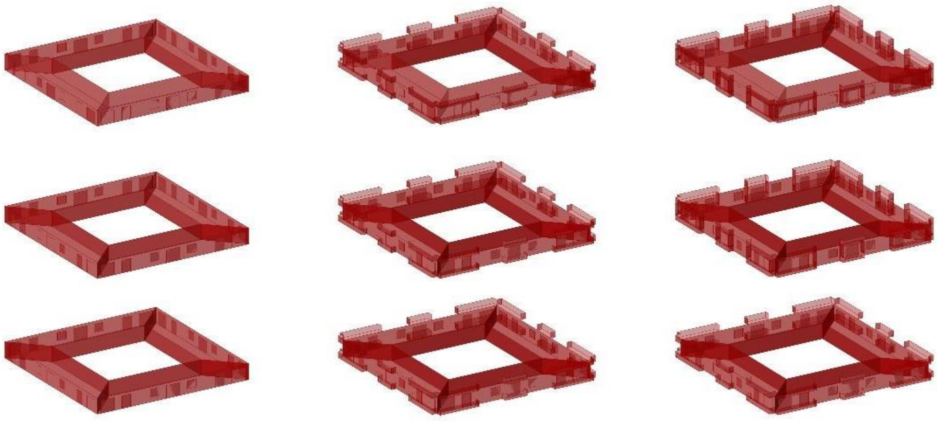

(C1) (C14) (C27)

Figure 3.51: Thermal models for no shading (C1), horizontal shading (C14) and combined shading (C27)

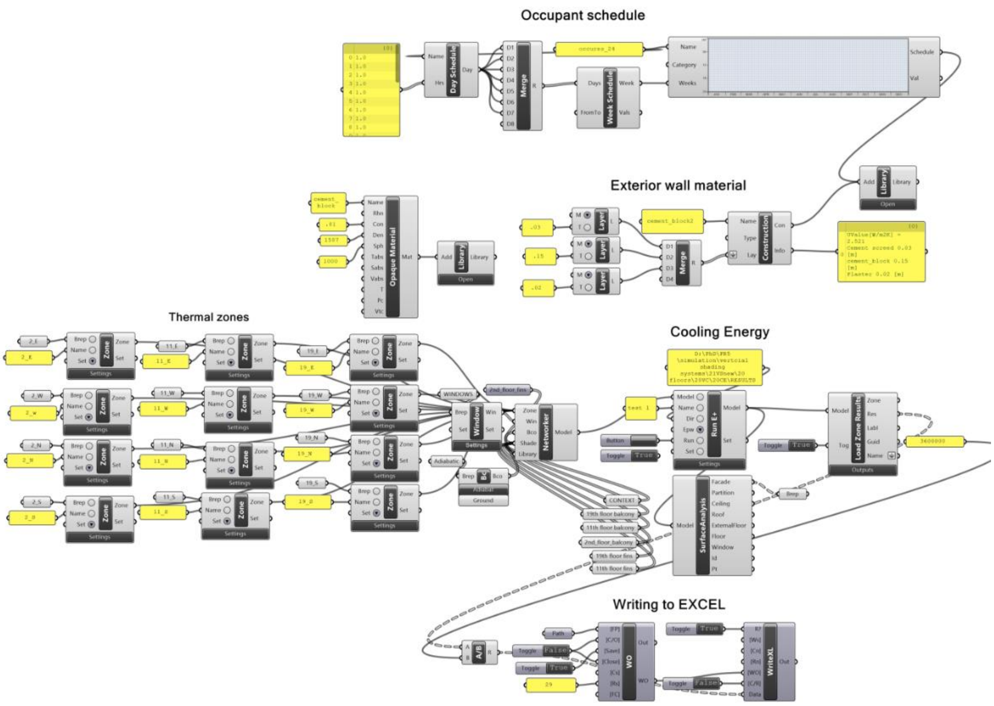

Figure 3.52: Simulation path for cooling energy for Simulation model 2

Spatial daylight autonomy (sDA), annual solar exposure (ASE) and annual day-time lighting energy (LE) for the different shading scenarios were simulated by utilizing a daylight model developed in *DIVA4* in *Rhino3D*. The daylighting grid was defined with the same assumptions and settings, as described in Section 3.6 for Simulation model 2. The simulation path for the daylight model is depicted in Figure 3.53. The simulated data for sDA, ASE, annual day-time lighting energy and annual cooling energy is available in the Mendeley Repository at https://data.mendeley.com/datasets/h8pnz942tv/2.

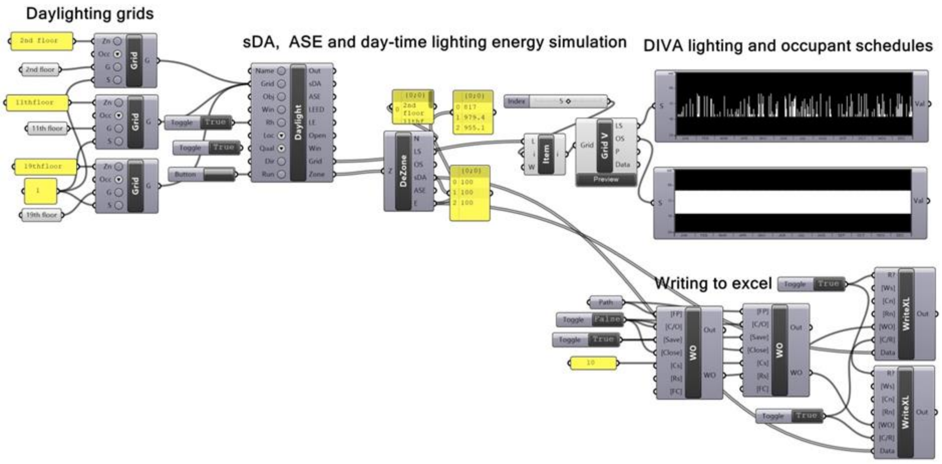

Figure 3.53: Simulation path for the daylight in Simulation model 2

The total annual energy use for cooling and day-time lighting energy was calculated from the simulated results from the thermal and the daylight model.

In order to compare the total annual energy use from the 27 external shading scenarios, the total energy savings (cooling and day time lighting energy use) were calculated as a percentage change as follows:

$$\frac{Total\ energy\ use(c=1-27) - total\ energy\ use\ in\ no\ shading\ scenario\ (C1)}{total\ energy\ use\ in\ no\ shading\ scenario\ (C1)} \quad \text{X } 100$$

C= Shading scenario

The total energy savings and the sDA obtained for the different shading scenarios are analysed to identify the best performance external shading scenario in Section 4.14.

3.10 Modelling the impact of the urban context on the daylight and energy performance of external shading devices in Case study 2

Case study 2 (C_2) was selected to validate the best performing external shading scenario for solar access identified in the Phase III of this study. The typical floor plan, reflectance values and thermal properties of construction materials and reflectance values are the same as depicted in Table 3.16, for Case study 2. The building setbacks for optimum solar access for Case study 2, indicated in Table 3.18 was utilized as the urban context.

Two models, the Baseline model depicted in Figure 3.54 (balconies only from the 6th to 15th floor) and the Best performance scenario model depicted in Figure 3.55 (balconies only from the 7th to 11th floors, fins and balconies from the 12th to 15th floors with) were modelled in *Rhino3D*.

Figure 3.54: Baseline model for C_2

Figure 3.55: Best performance scenario for C_2

The 32 spaces in the typical floor plan were modelled for the 8th,9th,10th,11th,12th,13th,14th and 15th-floor levels in C_2. The annual cooling energy use of the two models followed the simulation path given in Figure 3.40. The sDA, ASE and day-time lighting energy use followed the simulation path in Figure 3.42. The simulation results of the Baseline model and the Best performance scenario model are compared in Section 4.15.

3.11 Summary

Chapter 3 discussed the methodology utilized to achieve the research objectives. The research methodology is conducted in three phases. Phase I of the methodology focused on characterizing the archetypal high-rise residential building in Sri Lanka.

In Phase II the development of the parametric urban context, the selection of the suitable simulation software for the study, the design of the thermal and daylight models and the optimization method for energy savings and daylight were discussed. Further, the calibration method, thermal and daylight models for the three case studies utilized to validate the building setbacks are discussed in Phase II.

Phase III described the methodology for assessing the impact of the urban context on the daylight and energy performance of 27 external shading scenarios in the façade of the Simulation model 2 in an urban context optimized for solar access. The Chapter is concluded by discussing the development of the thermal and daylight models in Case study 2 in an urban context for validating the best performance external shading scenario.

4 Results, analysis and discussion

This Chapter analyses the results of the simulation processes for optimizing solar access for high-rise residential buildings in dense urban tropics as demonstrated in the methodology.

The simulated results of the Phase II of this study are discussed in Sections 1 to 6. The optimization of daylight and energy savings and the formation of the building setbacks for solar access are discussed in Section 7 and 8. The results of the calibration of the case studies and the application of the building setbacks to case studies are discussed in Section 9. In Section 10 the optimum building density for the high-rise residential building typology is formulated.

The simulated results of Phase III of the study are discussed in Sections 11 to 13. Section 14 identified the best performance scenario for daylight and energy in a high-rise residential building façade. The application of the design principles to the case study and further design options for the high-rise residential building façade are discussed in Sections 15 and 16 respectively.

Phase II

4.1 Comparison of the spatial daylight autonomy (sDA) at different floor levels in the Simulation models

The shading effects of the urban context on the spatial daylight autonomy (sDA) at three floor levels of the Simulation models were investigated in this study. Figure 4.1 illustrates the three floors (9^{th} floor, 5^{th} floor and the 2^{nd} floor) simulated for daylight and the parametric obstruction at 50m from the Simulation model 1 (SM1). When the distance to the obstruction is shorter, higher shadings effects are observed and vice versa. The effects of shading from the obstruction (from 2 m to 50 m) on the sDA at different floor levels in SM1 are depicted in Figure 4.2.

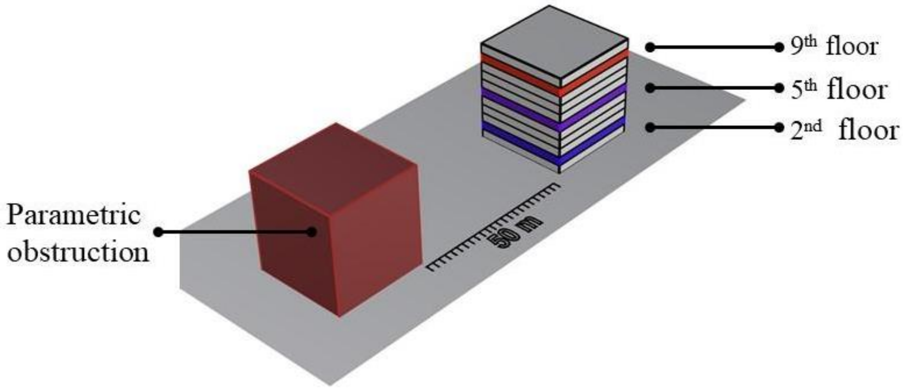

Figure 4.1: Illustration of the Simulation model 1 facing the parametric obstruction in the west at 50m

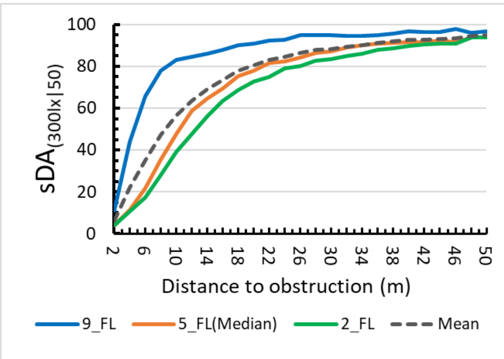

sDA in SM1 facing east

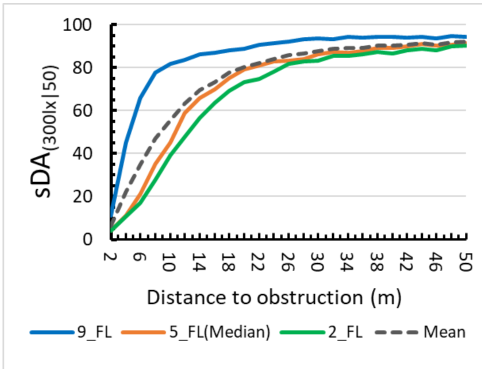

sDA in SM1 facing west

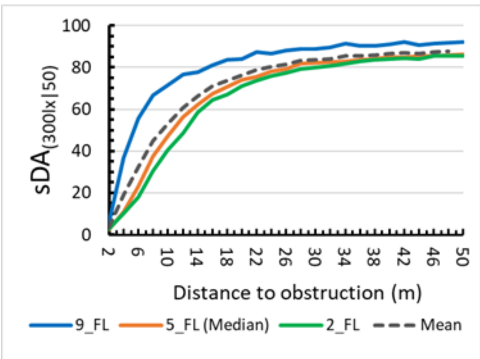

sDA in SM1 facing north

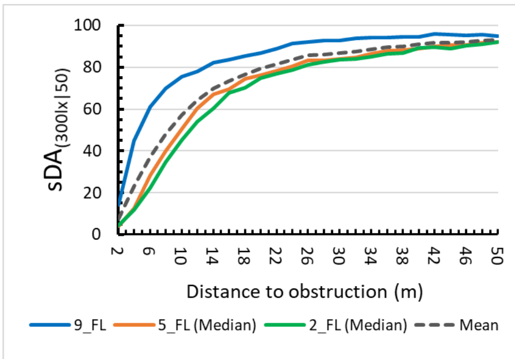

sDA in SM1 facing south

Figure 4.2: The shading impacts of the obstruction on spatial daylight autonomy (sDA) for Simulation model 1 (SM1) in each cardinal direction

The pattern of increase in sDA in relation to the distance to the obstruction was similar for all four cardinal directions in SM1, with slightly less sDA observed in the north. A significant difference in the rate of increase of sDA along with the distance to the obstruction for the 9th floor (9_FL), 5th floor (5_FL) and 2nd floor (2_FL) levels was observed. The increase in sDA is much higher for the 9th floor than the mean, the median floor and the 2nd floor in the east-west than in the north-south direction. Compared to the bottom half of the building, the top half experiences much higher daylight levels in SM1. The impact of the obstruction on sDA for SM2 and SM3 are given in Appendix G. Similar effects of contextual shading on sDA, observed in Figure 4.1 for SM1, were observed in SM2 and SM3 as well.

4.1.1 Estimating the average daylight levels for the Simulation model

The impact of contextual shading on the sDA of the mean, the median floor, the top floor and the bottom floor were discussed in the above section for the three Simulation models. An average value for sDA for each Simulation model needed to be calculated to facilitate the optimization of solar access. The top floor in all Simulation models deviated substantially from the median floor and the arithmetic mean. It was noted that the median floor and the 2nd floor (2_FL) in all the three models had similar sDA percentage. Therefore, the sDA of the median floor level, instead of the arithmetic mean of the three floors, was selected as an indication for average sDA for a Simulation model, based on the following justifications.

- Selecting the median floor level ensures that the top half of the building receives an sDA percentage above the average sDA.
- The 2nd-floor level sDA values are close to the median floor's values, indicating that the values in the bottom half are also close to the indicated average sDA.

4.2 Comparison of annual cooling energy use at different floor levels in the Simulation models

The effects of contextual shading on cooling energy use at three-floor levels in each cardinal direction for Simulation model 1 are illustrated in Figure 4.3.

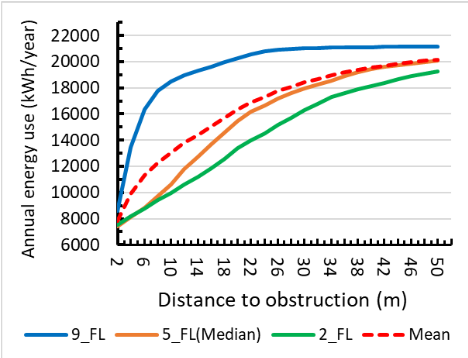

Cooling energy in SM1 facing east

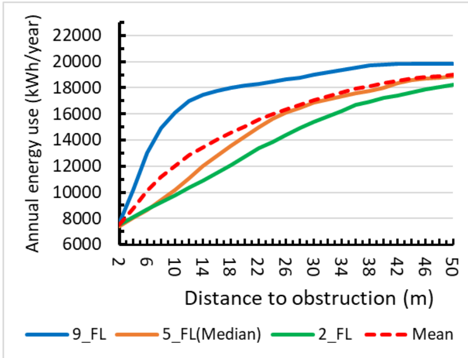

Cooling energy in SM1 facing west

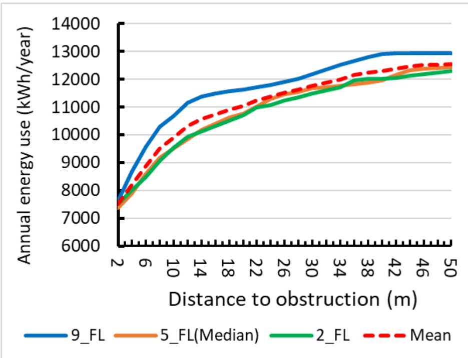

Cooling energy in SM1 facing north

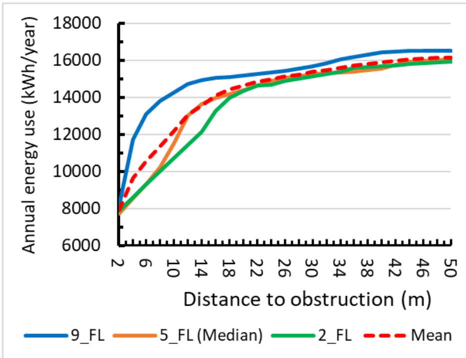

Cooling energy in SM1 facing south

Figure 4.3: The shading impacts of the obstruction on cooling energy use for Simulation model 1 (SM1) in each cardinal direction

The effects of contextual shading on energy use for cooling differed significantly for cardinal directions. The annual cooling energy use ranges from 8000- 21000 kWh/year in the east-west direction, 7000-13000 kWh/year in the north and 8000-17000 kWh/year in the south in response to the shading effects of the obstruction. Therefore, unlike daylight levels with a marginal difference in the north direction, energy use due to contextual shading differs significantly for the cardinal directions.

The increase in cooling energy use is much higher for the 9th floor (9_FL) than the mean in the east-west direction. In the north-south, energy use in all floors remains close to the mean. The effects of shading from the obstruction on SM2 and SM3 are given in Appendix H. The cooling energy use ranges were similar across all three Simulation models, indicating limited effects of building height. This could be due to the fact that the fraction of shading due to the obstruction is similar in all three Simulation models.

4.3 Comparison of total annual energy use at different floors in the Simulation models

The effects of contextual shading on total annual energy use for Simulation model 1 is illustrated in Figure 4.4.

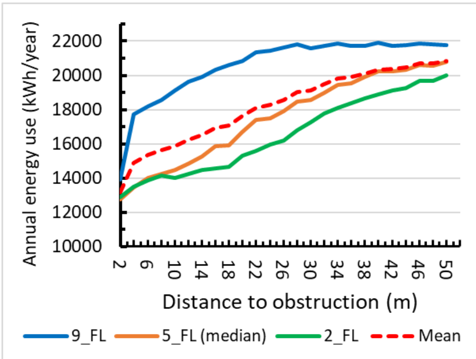

The total energy in SM1 facing east

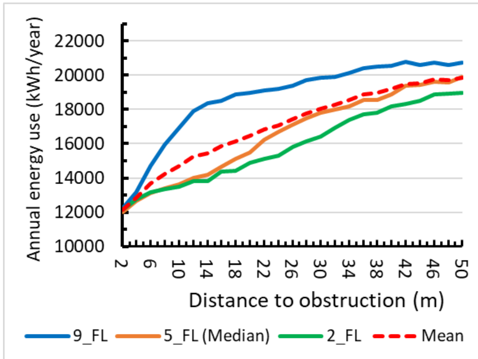

The total energy in SM1 facing west

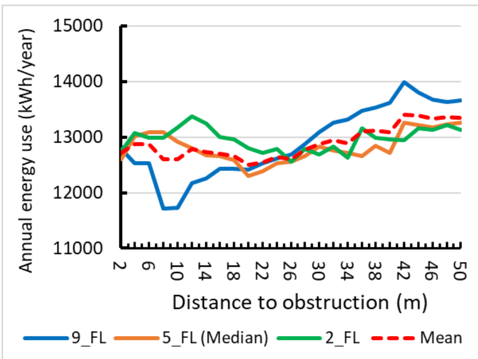

The total energy in SM1 facing north

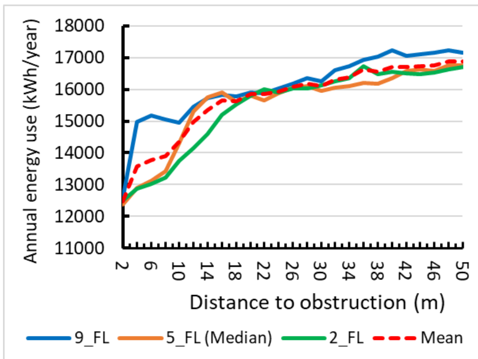

The total energy in SM1 facing south

Figure 4.4: The shading impacts of the obstruction on total energy use for Simulation model 1 (SM1) in each cardinal direction

Total annual energy use is the sum of annual cooling energy use and day-time lighting energy use of the Simulation model. Annual total energy use ranges from 12000-22000 kWh/year in the east-west direction, 11000-14000 kWh/year in the north and 12000-17000 kWh/year in the south in response to contextual shading. The energy ranges indicate a significant increase in total energy use due to day-time lighting energy. A pattern in the increase of total energy use could be observed in the east-west direction. However, the rate of increase is not as smooth as observed in the cooling energy use in Figure 4.3. As observed in the cooling energy use in SM1, the rate of increase in the 9th floor (9_FL) is much higher than the mean, 5th floor (5_FL) and the 2nd floor (2_FL). In the north, the effects of contextual shading on total energy on the 9th floor decreases at 10 m and increases, while the 5th (5_FL) and the 2nd floor (2_FL) do not indicate any effects of contextual shading. In the south, all floor levels show an uneven increase in total energy use.

The corresponding total annual energy use in SM2 and SM3 for the cardinal directions is given in Appendix I. The range in annual total energy use is similar for SM1, SM2 and SM3. Minimal effects of contextual shading on the total energy use pattern were observed in the north in all three Simulation models. In the south, all floor levels and the mean calculated did not deviate much from the median floor for all three models.

4.3.1 Estimating the average total annual energy use for the Simulation model

The impact of contextual shading on annual cooling energy use is illustrated and discussed in section 4.2. However, as this study focused on the optimization of solar access in terms of daylight and energy use, accounting for energy use for cooling only would lead to over-estimated energy benefits. Therefore, the effects of contextual shading on cooling and daytime lighting energy use (total energy use) were utilized to estimate the average energy use in the Simulation models.

It was noted that the patterns observed due to shading effects on cooling energy use are disrupted when considering the total energy use. In the east-west direction, total energy use was higher on the top floor in all Simulation models and deviated substantially from the median floor and the second floor. The median floor and the 2nd floor in all three models had similar energy use at a given distance to the obstruction.

An average value needed to be calculated for annual total energy use for each Simulation model to facilitate the optimization of solar access. The models facing east-west and south indicated consistent effects of shading on cooling and day-time lighting energy use. The north did not show a significant impact of shading on total energy use. Therefore, considering the total energy use in SM1, SM2, and SM3, the median floor was selected to estimate the average total energy use for the Simulation models based on the following justifications.

- The 2nd-floor level total energy use values are close to the values of the median floor, indicating that the values in the bottom half are also close to the indicated average total energy use.

- The average sDA was considered at the median floor. Therefore, to be consistent, the average total energy use was also taken at the median floor.

4.4 Daylight analysis

Figures 4.5 to 4.8 are utilized to compare the impact of contextual shading on the average sDA of the three Simulation models in one graph. A steep increase of the average sDA was noticed in the first 25 m of the obstruction in all directions in all three Simulation models. Within the first 5 m, all three models indicate very low sDA, after which the percentages for SM1 are the highest, followed by SM2 and SM3 in all four directions, indicating that building height affects sDA performance. North incurs comparatively less sDA in comparison to east, west and south directions. Figures 4.5 to 4.8 also show sDA curves tend to flatten after 75. Therefore, increasing sDA beyond 75 does not increase daylight significantly even if the distance between buildings was increased. The effects of an obstruction too close to the building could cause a severe lack of daylight, as seen in the simulation results. Therefore, higher densities in the tropics have a negative effect on daylight availability, despite the high levels of solar insolation in the tropics.

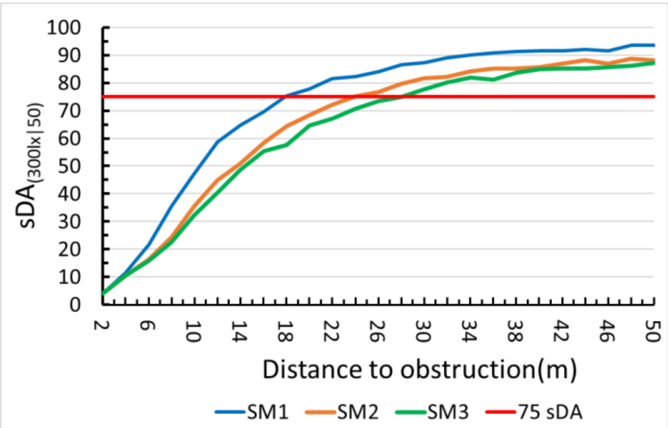

Figure 4.5: Shading effects of the obstruction on average sDA for the three Simulation models in the east

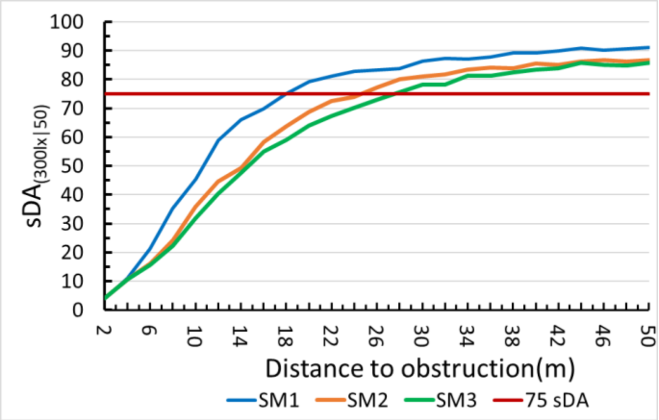

Figure 4.6: Shading effects of the obstruction on average sDA for the three Simulation models in the west

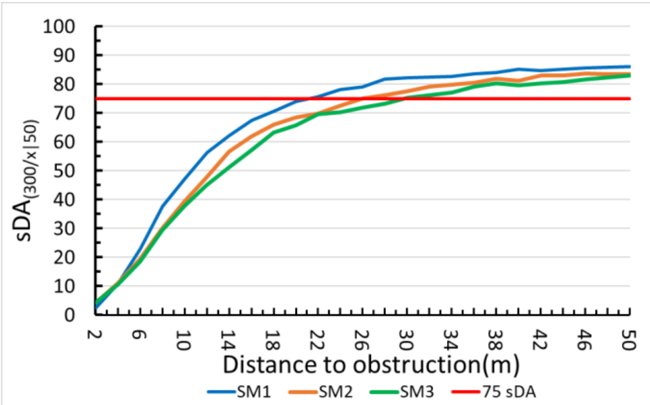

Figure 4.7: Shading effects of the obstruction on average sDA for the three Simulation models in the north

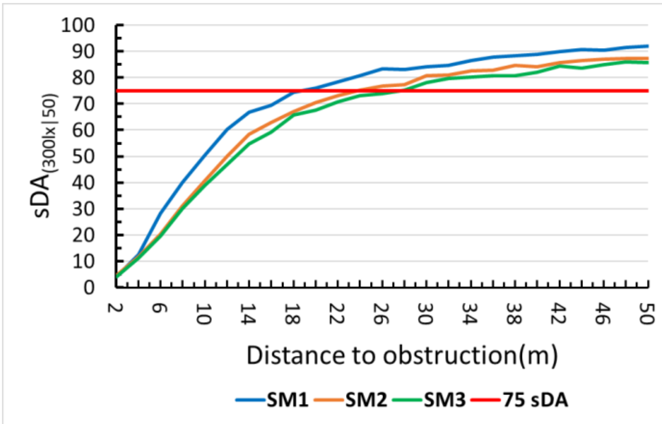

Figure 4.8: Shading effects of the obstruction on average sDA for the three Simulation models in the south

4.5 Annual energy use characteristics

In this section, the average annual cooling energy use (CE) and average annual total energy use (CE+LE) are compared for all three Simulation models. CE is indicated by the dotted line in Figures 4.9, 4.10 and 4.11. All three models exhibit similar patterns of energy increase due to decreasing contextual shading along with the distance to the obstruction.

CE+LE has higher energy levels than CE for all cardinal directions in all Simulation models. The cooling energy use has a steep increase in the first 10m from the obstruction in all directions. However, an increase in CE+LE in the first 10 m is much less than CE due to the addition of day-time lighting energy. In the first 10m, lighting energy accounted for 20-30% of the total energy use and in the next 10-25 meters accounted for 20-10% of the total energy use. The north has significantly less impact of contextual shading on CE due to lack of direct solar radiation exposure. Almost no effects of contextual shading on CE+LE are observed in the north direction for all models. It was noted that the east-west direction benefits greatly from shading from the obstruction, while in the north-south direction, the effects of shading are felt mildly after the first 30m. The lowest CE and CE+LE were observed when the obstructions were closest to the Simulation model.

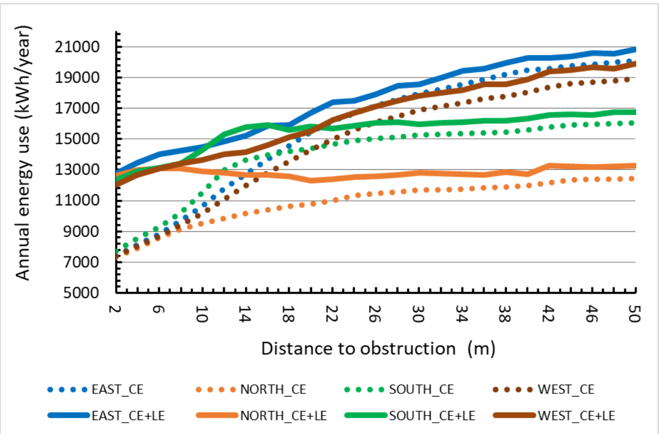

Figure 4.9: Shading effects of the obstruction on cooling energy use (CE) and total energy use (CE+LE) in Simulation model 1

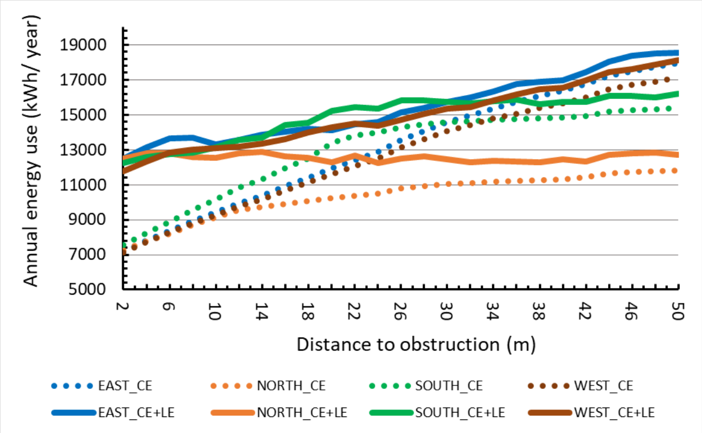

Figure 4.10: Shading effects of the obstruction on cooling energy use (CE) and total energy use (CE+LE) in Simulation model 2

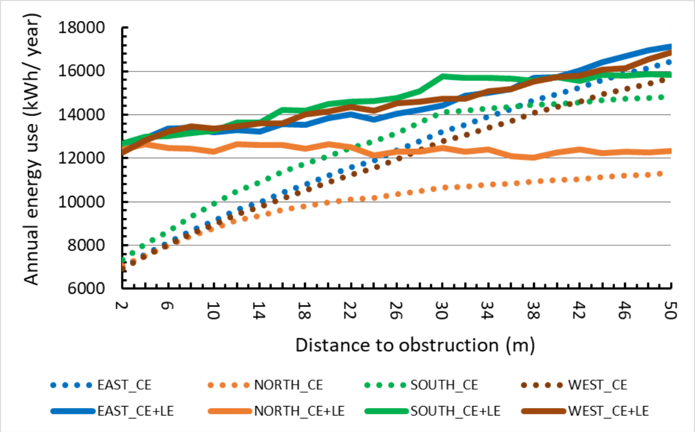

Figure 4.11: Shading effects of the obstruction on cooling energy use (CE) and total energy use (CE+LE) in Simulation model 3

4.6 Annual energy savings analysis

The calculation for annual energy savings percentage was given in Section 3.4. Annual energy savings were calculated as a percentage change in average energy use for the Simulation model at a given distance to the obstruction compared to the "excluded context" scenario. Figures 4.12, 4.13, and 4.14 compare the effects of shading from the obstruction on the cooling energy (CE) savings and total energy (CE +LE) savings.

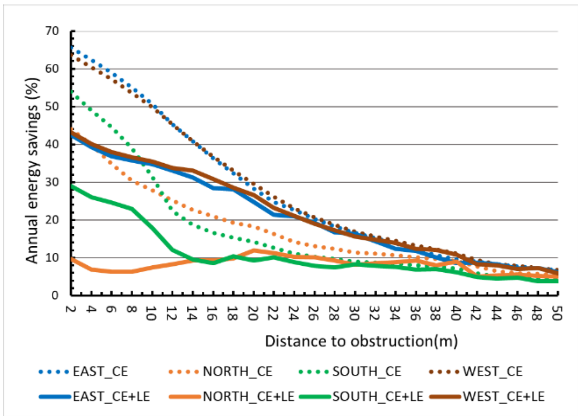

Figure 4.12: - Shading effects of the obstruction on cooling energy (CE) savings and total energy (CE+LE) savings in Simulation model 1

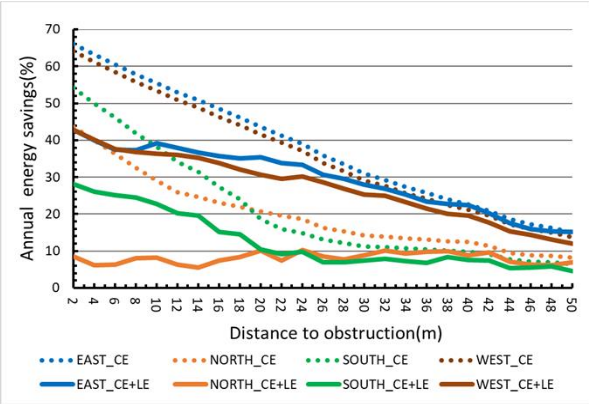

Figure 4.13: Shading effects of the obstruction on cooling energy (CE) savings and total energy (CE+LE) savings in Simulation model 2

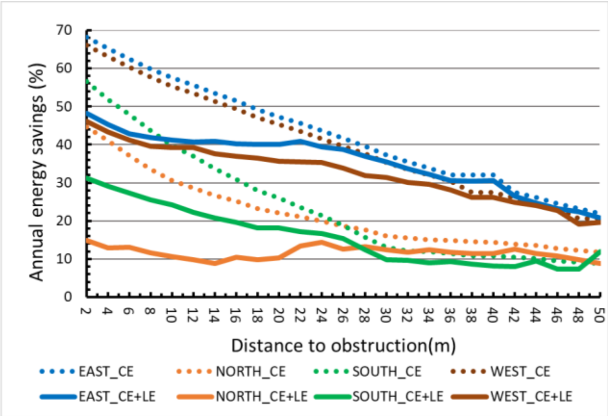

Figure 4.14: Shading effects of the obstruction on cooling energy (CE) savings and total energy (CE+LE) savings in Simulation model 3

For all three models, approximately 60% maximum energy savings for cooling (CE) can be achieved in the east-west direction, compared to approximately 40% of annual total energy savings (CE+LE) when the obstruction is closest to the Simulation model. The cooling energy savings results support the notion that high-density, high-rise housing is preferred compared to low-density, low-rise housing in energy sustainability, discussed in Section 2.3.1. However, Figures 4.12 to 4.14 demonstrated that higher energy savings for cooling without considering day-time lighting energy use lead to overestimated energy savings from high-density developments. Therefore, total annual energy savings (CE+LE) instead of cooling energy savings (CE) should be considered when estimating energy savings from building density. Another aspect observed in the above Figures was that energy savings in the north do not show significant contextual shading effects due to non-exposure to direct solar radiation. Energy savings for cooling (CE) and day-time lighting (CE+LE) in different cardinal directions for all three Simulation models were within the same range.

The analysis of the sDA and energy savings of the simulation models indicate the building heights impact sDA, while the cardinal directions impact energy performance. It was also noted that contextual shading had opposing effects on building daylight and energy performance. Therefore, the highest total energy savings observed in the Simulation models are sub-optimal densities for solar access due to corresponding low sDA. From the above analysis, solar access in the tropics was established as an optimization exercise rather than a maximization exercise for unobstructed solar access.

4.7 Optimization of spatial daylight autonomy (sDA) and energy savings

In this study, the optimization criteria maximize the two parameters, spatial daylight autonomy (sDA) and annual energy savings. However, it was noted that the effects of contextual shading on annual energy savings are weak in the north-south direction in the discussion above. Therefore, only the simulation results in the east-west directions were considered for the optimization process.

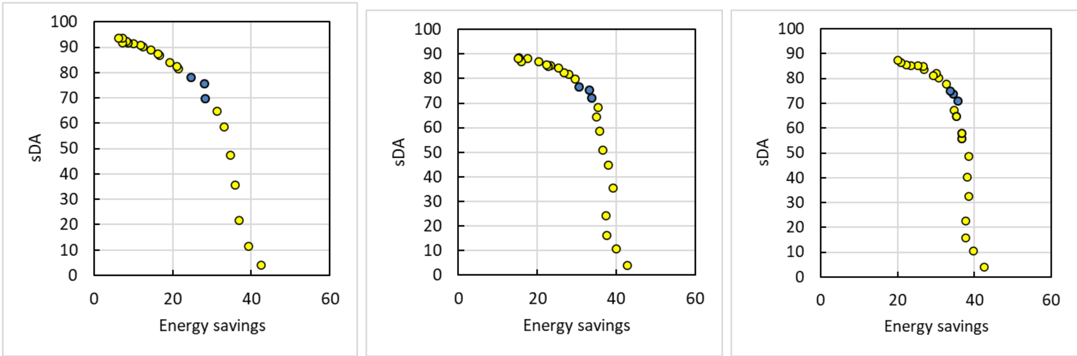

SM1 facing east SM2 facing east SM3 facing east

Figure 4.15: Pareto-front visualization for sDA and energy savings in simulation models facing obstruction in the east

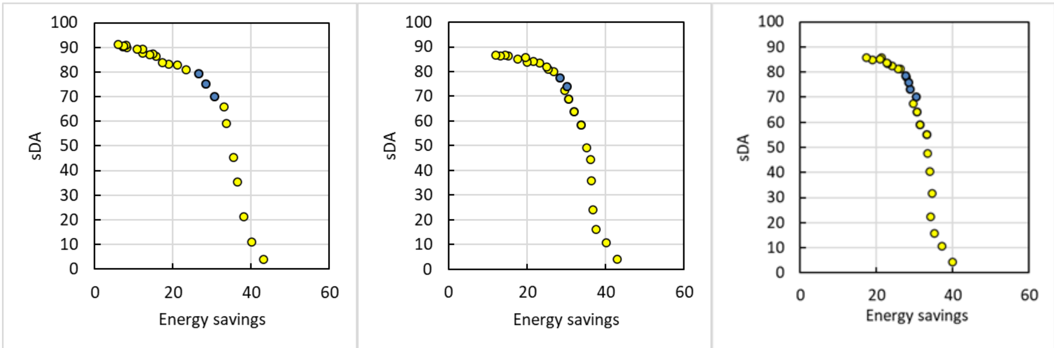

SM1 facing west SM2 facing west SM3 facing west

Figure 4.16: Pareto-front visualization for sDA and energy savings in simulation models facing obstruction in the west

The sDA and annual energy savings facing east and west in the Simulation models are visualized in the scatter-plots in Figures 4.15 and 4.16. As the urban context was constrained to a linear path of 50 m, the data closely followed the Pareto-front. The high intensity of data points close to higher sDA demonstrates weak shading effects. The low intensity of data points at lower sDA is due to higher shading fractions indicating intense shading effects on the two objectives. The Knee of the curve is considered as the best Pareto-optimal set where both sDA and energy savings can no longer be maximized without a significant reduction in the other. This region of the

Knee was visually identified in the scatter plots, where sDA is between 70-80%. These points were indicated in blue on the Pareto-front. The knee points indicated the optimum solar access for all three Simulation models facing east-west directions was close to 75 sDA. Therefore, 75 sDA and corresponding energy savings were considered the threshold for optimum solar access for all three Simulation models facing east and west.

The effects of shading on energy savings are not significant in the north-south to consider multi-objective optimization. However, the strong effects of shading on daylight were observed in the north-south in Figure 4.5 to 4.8. Therefore, even though the north-south directions do not affect energy use, the impact of contextual shading on sDA cannot be disregarded. It was also noted in Figures 4.5 to 4.8, the increase in sDA flattens after 75 for all cardinal directions. Therefore, 75 sDA was considered the optimum sDA for north-south as well as east-west. The corresponding energy savings for 75 sDA for the three Simulation models are depicted in Figure 4.17.

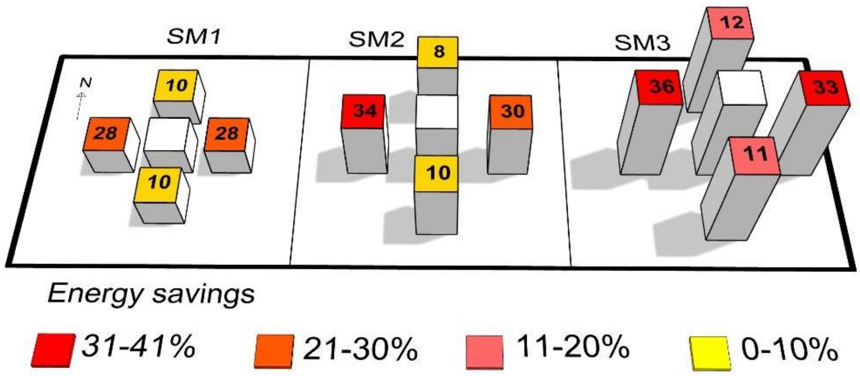

Figure 4.17: Energy savings corresponding to 75 sDA for the three Simulation models in an urban context developed for optimum solar access

Based on the above optimization, the thresholds for optimum solar access could be taken at 75 sDA and corresponding energy savings for all three Simulation models.

Optimum solar access is defined as a perimeter zone in a high-rise residential building that achieves 75 sDA $_{(300lx|50)}$ with corresponding annual energy savings of 28%-36% in the east-west and 8%-12% savings in the north-south direction.

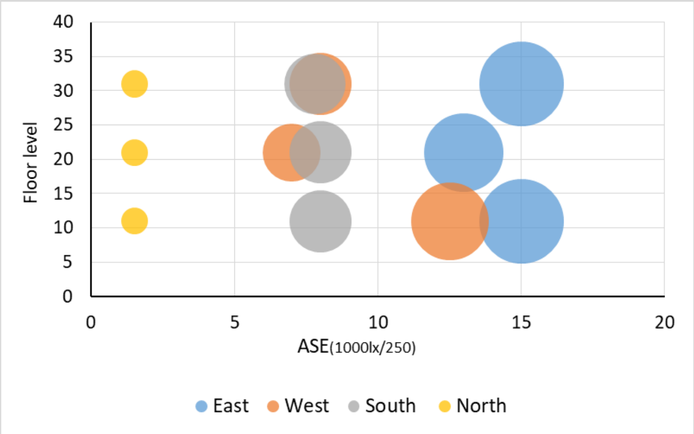

Figure 4.18: Comparison of ASE in Simulation models corresponding to 75 sDA

The corresponding annual solar exposure (ASE) for 75 sDA is depicted in Figure 4.18. ASE of over 10% is found in east-west directions. The European standard EN 17037 requires at least 1.5 hours of direct sunlight exposure per day. High levels of solar exposure for short periods, especially in the morning, would be welcome, given the health benefits. If direct solar exposure is unwelcome, it could be overcome with internal shading even though lack of daylight cannot be improved quickly (Dogan and Park, 2017). Therefore, the corresponding ASE obtained for 75 sDA was considered acceptable limits in this study.

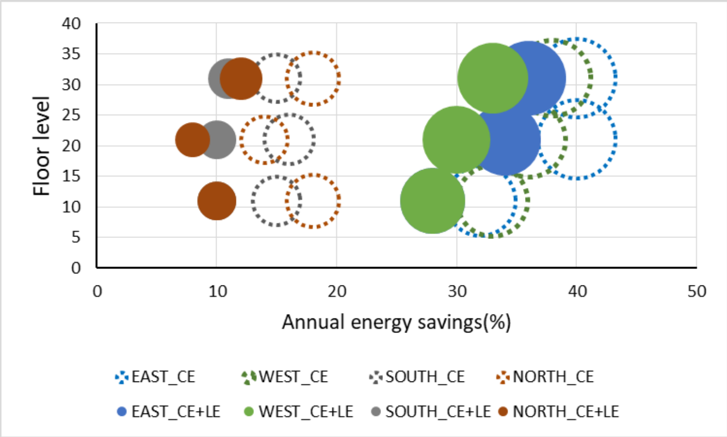

Figure 4.19: Comparison of annual energy savings for cooling and total energy savings corresponding to 75 sDA

The annual energy savings analysis discussed in Section 4.6 indicated that considering only cooling energy savings (CE) overestimated energy savings of high densities. The corresponding cooling energy savings (CE) for 75 sDA indicated in Figure 4.19 was 4%-8% higher than the total energy savings (CE+LE). According to the Figure above, the building height had only a marginal impact on energy-saving potential.

4.8 Prescribing building setback curves for optimum solar access

The distance to the obstruction for optimum solar access for SM1, SM2 and SM3 are illustrated in Figure 4.20. At the given distance, an indoor daylight level of 75 $sDA_{(300lx|50)}$ is achieved in the perimeter zone in all three simulation models with corresponding annual energy savings of 28%-36% in the east-west and 8%-12% savings in the north-south direction.

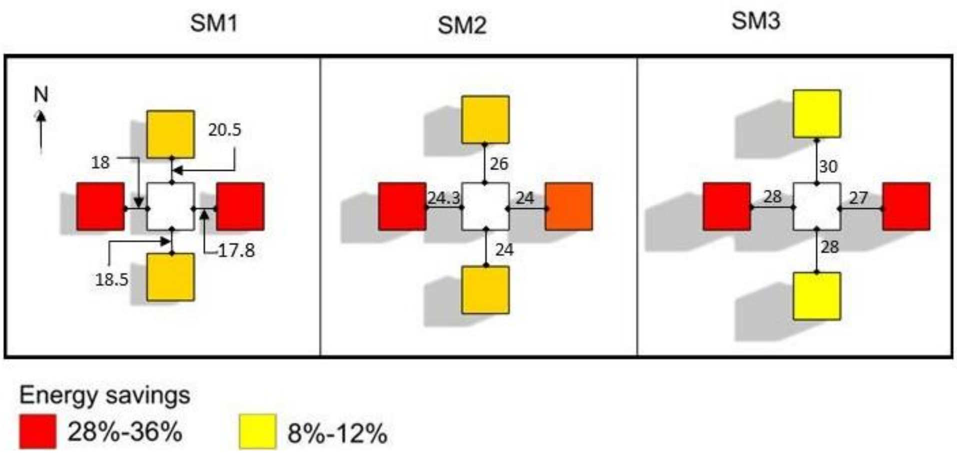

Figure 4.20: Distance to the obstruction (m) for optimum solar access for the three Simulation models

The building setback is calculated at half of the distance to the obstruction for each Simulation model. The building setback curves for optimum solar access were developed by estimating an exponential curve between the building setbacks for SM1, SM2, and SM3.

The prescribed setback curves in Figure 4.21 are satisfied for an archetypal high-rise residential building within the following assumptions.

- Obstructions are of the same height and form
- The form does not account for shelf shading.
- Calculated for optimum solar access

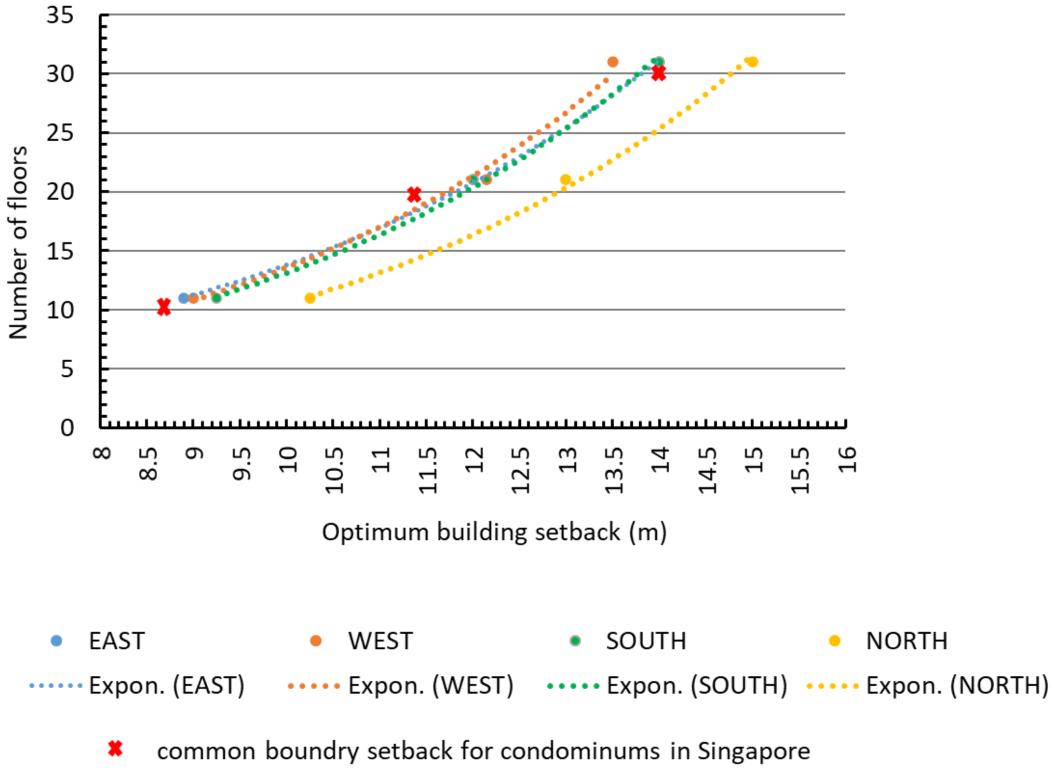

Figure 4.21: Building setback for optimum solar access

The prescribed setback curves depicted in the above Figure far exceeds the current open-space around buildings in planning regulations in Sri Lanka (Appendix B), which requires only a 3 m setback from the boundary for a 10-floor building, and a 6 m setback for a building with over 15 floors. The current building setback has resulted in inadequate daylight in interiors of high-rise residential buildings in Colombo (Rajapaksha & Jayaweera, 2018). As the lack of building setback is apparent in Sri Lanka, the proposed setback was compared with the common boundary setbacks for condominiums in Singapore, given in Appendix C (URA, 2019). The Singaporean regulation fits closely to the setback curves proposed in this study, as indicated in Figure 4.21.

4.9 Validation of the building setback curves for optimum solar access with case studies

Three high-rise residential buildings in Colombo were utilized to test the applicability of the prescribed setback curves. Table 3.7 in Section 3.8 presents the characteristics of the three case studies. The analysis of the calibration and simulation results of the case studies are discussed in this Section.

4.9.1 Calibration of the indoor mean air temperature of the case studies

The mean indoor air temperature was obtained by averaging the 3 data loggers' data in each Case study. The field data and the simulated data are compared in Figures 4.22, 4.23 and 4.24 for Case study 1, 2 and 3, respectively. The mean indoor air temperature ranges between 29 ^{0}C and 31.5 ^{0}C for C_1, between 29.5 ^{0}C and 31.5 ^{0}C for C_2 and between 26.5 ^{0}C and 29.5 ^{0}C for C_3. Therefore, according to the Figures, the day and night-time temperature variations are very low in the tropics as expected.

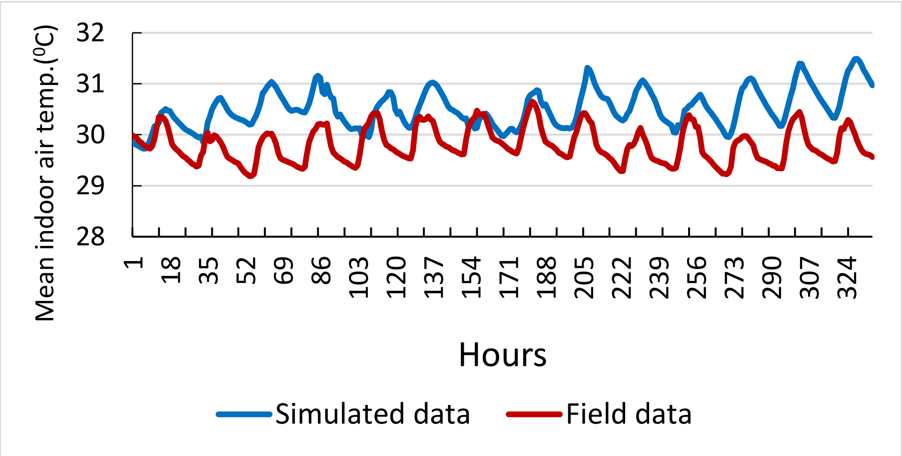

Figure 4.22: Comparison of mean air temperature in Case study 1

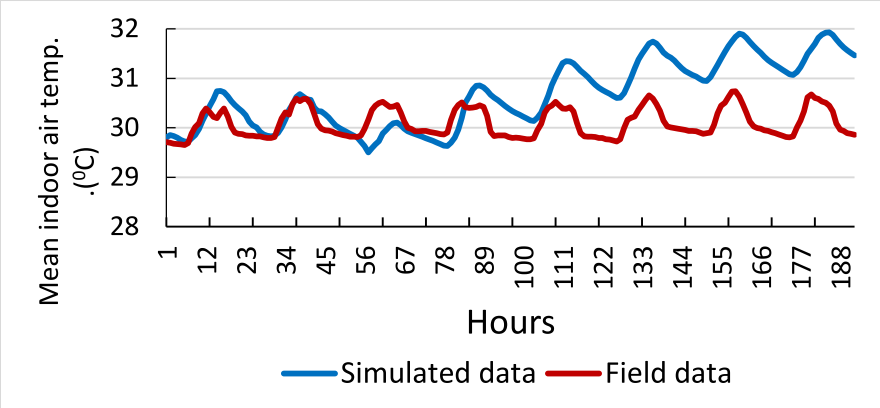

Figure 4.23: Comparison of mean air temperature in Case study 2

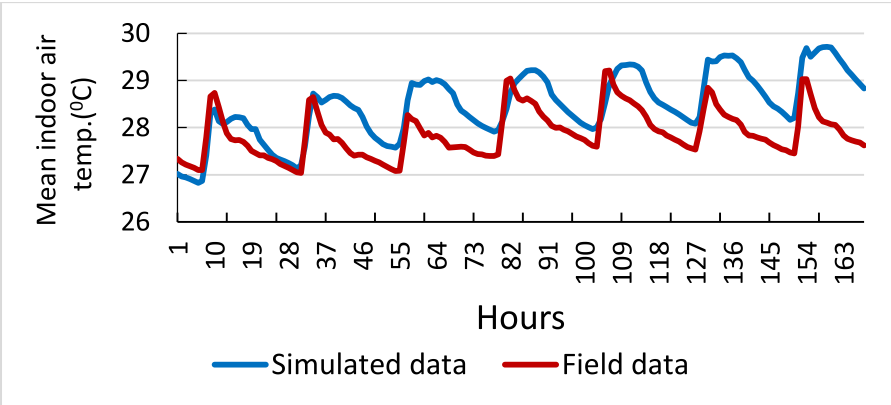

Figure 4.24: Comparison of mean air temperature in Case study 3

The Simulation models were calibrated within the ASHRAE 14 guidelines, as presented in Table 4.1.

Table 4.1: Measures of uncertainty in mean air temperature in case studies

	Standard deviation in field data	**NMBE $_{hourly}$**	**CV (RMSE $_{hourly}$)**
C _1	0.33	2%	2%
C _2	0.28	1.8%	2.8%
C _3	0.50	2%	2%

All three Simulation models fall within the maximum threshold for Normalized mean biased error (NMBE $_{hourly}$) and Coefficient of variation of root mean square error (CV (RMSE $_{hourly}$)). Robust calibration of the thermal models of the case studies could be attributed to the very low standard deviation in hourly air temperature in the tropics, as indicated in Table 4.1.

4.9.2 Calibration of indoor hourly illuminance of the case studies

The same points corresponding to the location of the *Hobo* data loggers in Figures 3.18, 3.24 and 3.30 were simulated for hourly illuminance using *DIVA4* plugin for the three case studies as discussed in Section 3.8.1. However, due to high levels of direct solar radiation indoors, a characteristic of the tropical climate, the data loggers closest to the window recorded spikes in illuminance, making it difficult to calibrate. Therefore, only the data logger located furthest away from the window was used for the calibration process. As far as the ASHRAE standards for calibration were considered, only C_1 satisfied the CV ($RMSE_{hourly}$), whereas all three models were within the stipulated NMBE threshold, as indicated in Table 4.2. The high standard deviation of hourly illuminance indicated in Table 4.2, throughout the day makes it difficult to calibrate daylight within +30% of the CV ($RMSE_{hourly}$).

Table 4.2: Measures of uncertainty in hourly illuminance in the case studies

	Standard deviation in field data	**$NMBE_{hourly}$**	**CV ($RMSE_{hourly}$)**
C _1	89.75	1.8%	28%
C _2	117.15	6%	46%
C _3	118.44	-4%	43%

To further investigate daylight calibration issues, Figures 4.25, 4.26 and 4.27 compared the simulated and field data of illuminance for the three case studies.

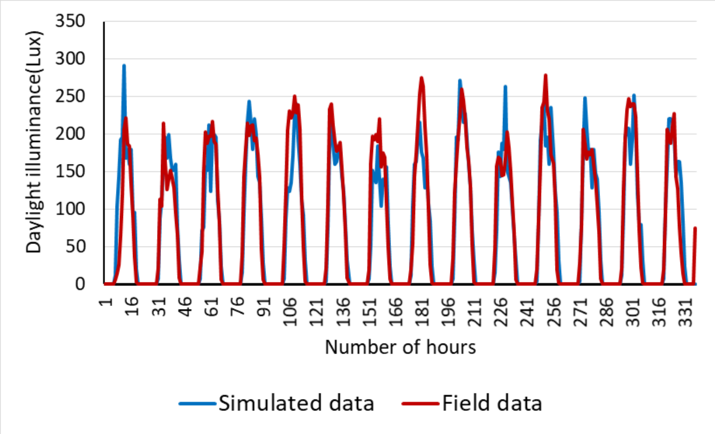

Figure 4.25: Comparison of illuminance data in Case study 1

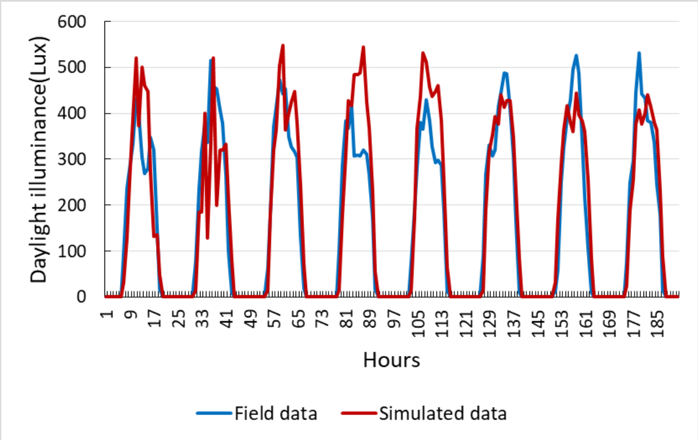

Figure 4.26: Comparison of illuminance data in Case study 2

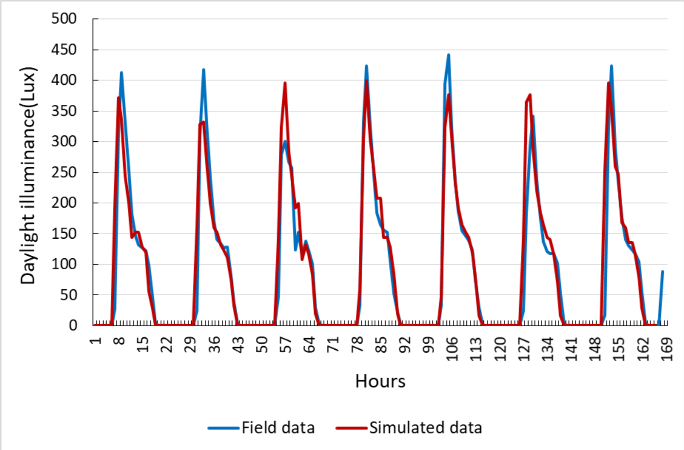

Figure 4.27: Comparison of luminance data in Case study 3

Lower field illuminance levels overlap with simulated data. While the errors are mostly recorded during mid-day. This could be attributed to direct solar radiation entering the bedroom during mid-day. As the errors are primarily due to direct solar radiation effects and not due to errors in calculating diffused solar radiation, the daylight models of C_2 and C_3 could be used for estimating sDA and day-time lighting in this study.

4.9.3 Analysis of the effects of contextual shading on Case study 1

Figure 4.28 compares the floor areas and window areas of the simulated spaces in Case study 1 (C_1). The floor areas range from 10-30 sq. m. The window sizes (around 5 sq. m.) do not increase with the floor area. Therefore, the solar access for the larger bedrooms and living rooms is expected to be less than the smaller bedrooms due to the low ratio of the window to the floor area of the room.

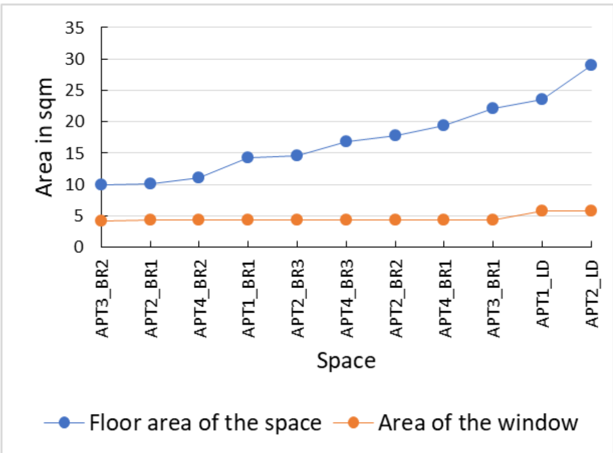

Figure 4.28: Floor area and window area of spaces simulated in Case study 1

Table 4.3 compares the sDA and annual total energy savings of C_1 with an urban context to represent the current building setback regulations in Sri Lanka. It can be observed from Table 4.3 that 45% of the spaces simulated had less than 25 sDA. High sDA levels were observed in Apt4_BR1 and Apt2_BR2; this was mainly because they are located in the corner of the building exposed to minimal shading effects. Energy savings decrease as the floor levels increase in the east-west direction as expected. However, in the north-south, a decrease in energy savings (compared to the 8th floor) was observed in the living spaces. The decrease in energy savings at lower floor levels could be due to the higher day-time lighting energy requirement in the living rooms. If contextual shading decreases daylight levels to as low as 25 sDA at lower floor levels, it decreases the total energy savings. It was noted that in spaces with a large floor area (e.g. living rooms), total energy savings from shading is negatively impacted due to the increase in artificial lighting energy.

Table 4.3: Spatial daylight autonomy (sDA) and energy savings in Case study 1 in an urban context based on the current building setback regulation

Window direction	Space	Case study 1		
		3rd_FL	5th_FL	8th_FL
East	Apt2_BR1			
East	Apt4_BR2			
West	Apt3_BR2			
North	Apt1_BR1			
North	Apt2_BR2			
North	Apt2_BR3			
North	Apt1_LD			
North	Apt2_LD			
South	Apt3_BR1			
South	Apt4_BR3			
South	Apt4_BR1			

Energy savings		
		55%
		1%
sDA level		
		>=75
75>		>=55
55>		>=25
25>		

Table 4.4 compares the sDA and total annual energy savings of C_1 with the urban context based on prescribed building setbacks for optimum solar access. 100% of the spaces on the three levels satisfied 55 sDA. It was also noted that smaller floor areas had higher sDA levels due to high solar access levels. Higher energy savings are observed in the lower floors compared to the 8th floor for all spaces. The east-west direction indicates higher energy savings than the north-south direction. Since the building setbacks maintain optimum solar access, daylight levels are maintained at 55 sDA for all spaces at the three-floor levels. As the artificial lighting energy is not

high during the day-time, the energy savings at lower floor levels are higher at lower floor levels than the top floor as expected.

Table 4.4: Spatial daylight autonomy (sDA) and energy savings in Case study 1 in an urban context for optimum solar access

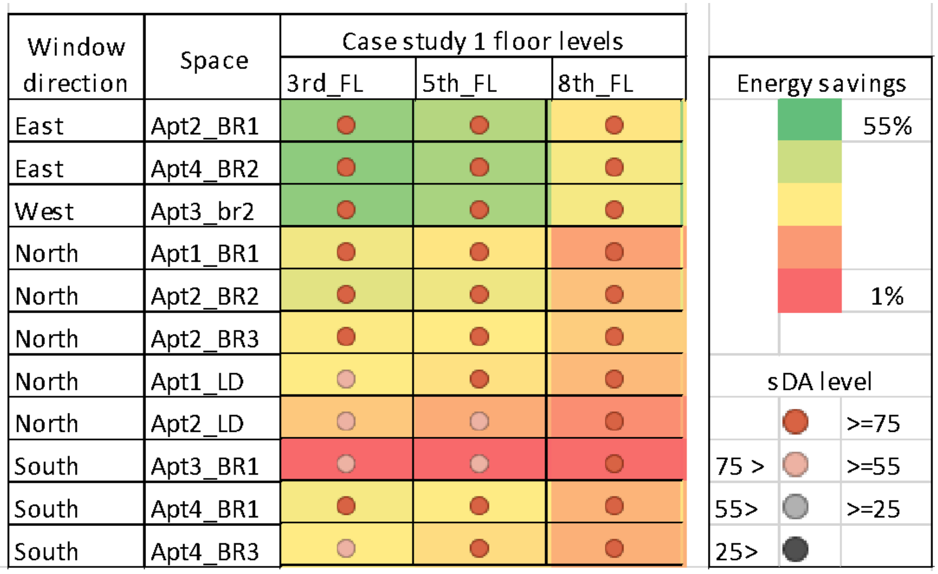

Table 4.5: Effects of contextual shading on spatial daylight autonomy (sDA) and energy savings in Case study 1

Urban context	**Percentage of spaces with:**		**The average energy savings percentage**			
	sDA >=55	**sDA >=75**	**East facade**	**West facade**	**North facade**	**South facade**
Current setback regulations	30%	24%	40	38.6	10	14
Setback for optimum solar access	100%	81%	28.6	30	9.5	9.1

Table 4.5 compares the impact of the current regulations and the setback for optimum solar access on daylight and energy savings. Only 30% of all spaces had over 55 sDA for the urban context developed according to current planning regulations in Sri Lanka. Corresponding energy savings of 38%-40% were observed in the east-west, while 10%-14% were observed in the north-south direction.

The urban context developed according to the building setback for optimum solar access ensured over 55 sDA for 100% of the spaces and over 75 sDA for 81% of the spaces in C_1. At the given setback, C_1 also maintains energy savings of 28%-30% in the east-west and 9% in the north-south direction.

Though the current planning scenario results in higher total energy savings, it significantly reduced daylight in interior spaces. However, applying the prescribed building setbacks for optimum solar access in C_1 maintained adequate daylight levels while meeting the total energy savings thresholds for optimum solar access.

4.9.4 Analysis of the effects of contextual shading on Case study 2

Figure 4.29 depicts the floor area and window sizes of 12 living rooms and 20 bedrooms simulated per typical floor in Case study 2 (C_2). The floor area of the living rooms is 250% larger than the bedrooms. However, the window sizes increase for living rooms compared to bedrooms only by 120%. Therefore, reduced solar access is expected for living rooms than bedrooms due to the low ratio of the window to the floor area of the room.

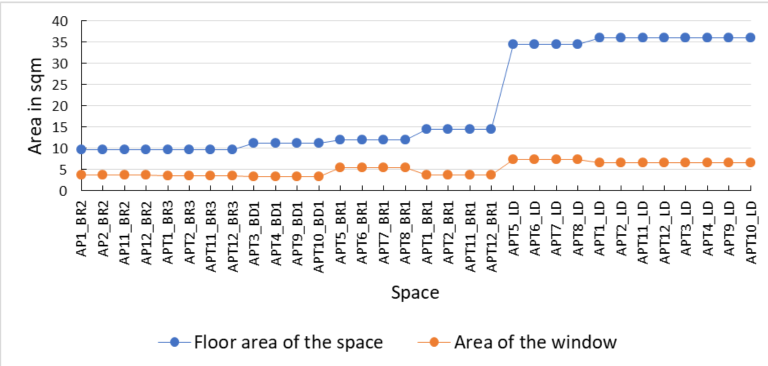

Figure 4.29: Floor area and window area of spaces simulated in Case study 2

In Table 4.6, sDA and energy savings of 100 bedrooms spaces and 60 living room spaces in four cardinal directions are compared for the current setback regulations (6 m building setback). 20% of the spaces had an sDA of less than 25. The majority of the spaces with low daylight levels are living rooms with room depths exceeding 6m. It is noted that bedrooms in the north-east and south-east directions have higher sDA levels due to lack of shading in the building corners, east of the building. In the east-west direction, most bedrooms indicate higher energy savings and low daylight levels. Bedrooms incur more energy savings than living rooms due to lower day-time lighting requirements. In all spaces, energy savings in the lower levels are higher than in the upper floors, as expected.

Table 4.6: Spatial daylight autonomy (sDA) and energy savings in Case study 2 in an urban context based on the current building setback regulation

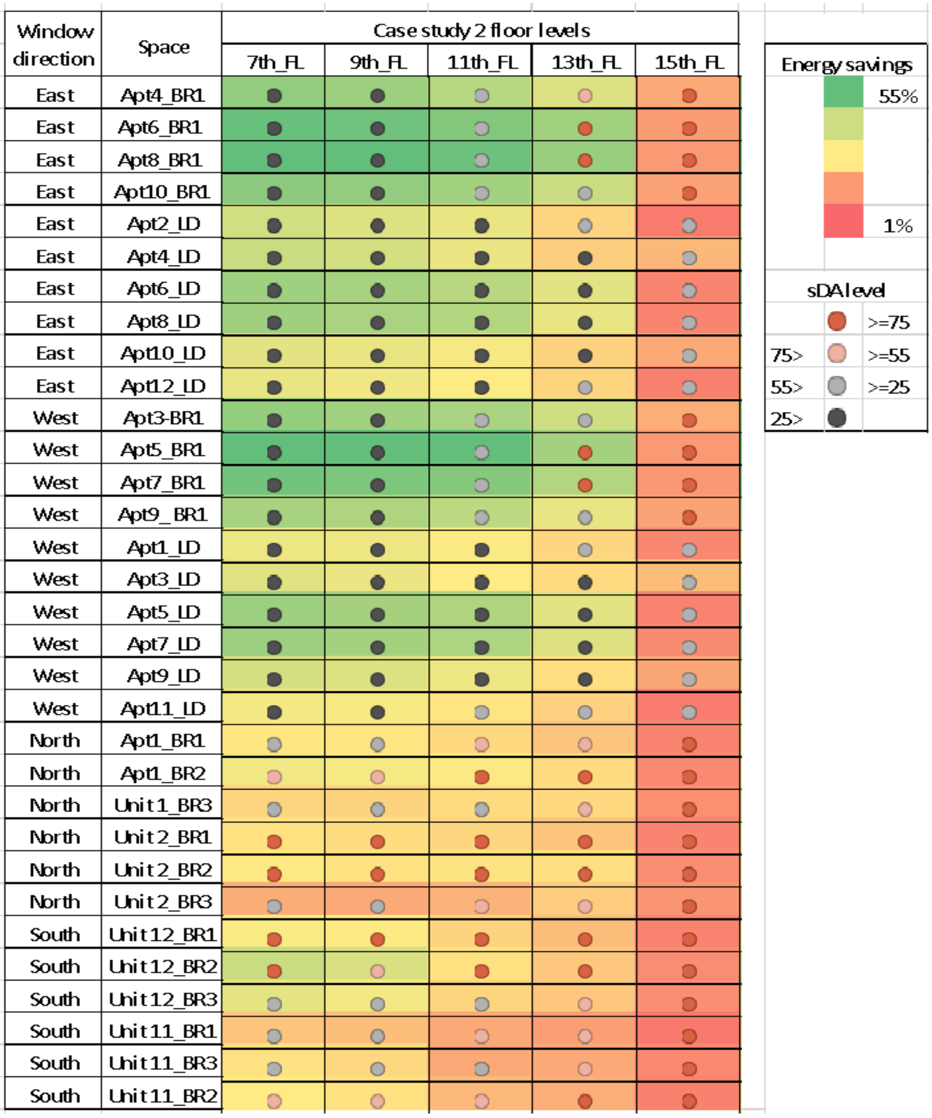

Table 4.7 indicates the sDA and energy savings in C_2 for the setbacks given for optimum solar access. All bedrooms in C_2 had sDA between 63.3-100%, which suggest that the building setback for optimum solar access provided adequate

daylight for bedrooms in all cardinal directions. Due to the depth of the living rooms exceeding 6 m, the daylight levels in living rooms are below 55 sDA. Therefore, the room depth of 6 m could be taken as the maximum depth for daylight in high-rise residential buildings. Beyond 6 m, spaces should depend on artificial lighting during the day-time, even at building setbacks at optimum solar access. Energy savings from contextual shading are higher in lower floors in the east-west direction. The highest total energy savings were observed on the 7th floor (east-west-38.2%, north-south-17.8%) and the lowest on the 15th floor (east-west-9%, north-south-6%) in C_2.

Table 4.7: Spatial daylight autonomy (sDA) and energy savings in Case study 2 in an urban context for optimum solar access

Window direction	Space	Case study 2 floor levels				
		7th_FL	9th_FL	11th_FL	13th_FL	15th_FL
East	Apt 4_BR1					
East	Apt 6_BR1					
East	Apt 8_BR1					
East	Apt10_BR1					
East	Apt 2_LD					
East	Apt 4_LD					
East	Apt 6_LD					
East	Apt 8_LD					
East	Apt 10_LD					
East	Apt 12_LD					
West	Apt 3-BR1					
West	Apt 5_BR1					
West	Apt 7_BR1					
West	Apt 9_ BR1					
West	Apt 1_LD					
West	Apt 3_LD					
West	Apt 5_LD					
West	Apt 7_LD					
West	Apt 9_LD					
West	Apt 11_LD					
North	Apt 1_BR1					
North	Apt 1_BR2					
North	Apt 1_BR3					
North	Apt 2_BR1					
North	Apt 2_BR2					
North	Apt 2_BR3					
South	Apt 12_BR1					
South	Apt 12_BR2					
South	Apt 12_BR3					
South	Apt 11_BR1					
South	Apt 11_BR3					
South	Unit 11_BR2					

Energy savings		
		55%
		1%
sDA level		
		>=75
75>		>=55
55>		>=25
25>		

Table 4.8: Effects of contextual shading on spatial daylight autonomy (sDA) and energy savings in Case study 2

Urban context	**Percentage of spaces with:**		**The average energy savings percentage**			
	sDA >=55	sDA >=75	East facade	West facade	North facade	South facade
Current setback regulations	38%	27%	33	33	21	19
Building setback for optimum solar access	64%	59%	26.3	25.6	15.1	12.7

Table 4.8 compares the current regulation and the proposed building setbacks for optimum solar access in C_2. The current regulation led to 38% of the spaces with more than 55 sDA with corresponding energy savings of 33% in the east-west and 19%-21% energy savings in the north-south.

The proposed building setbacks resulted in 64% of spaces with over 55 sDA with corresponding energy savings of 25%-26% in the east-west and 12%-15% in the north-south direction. A significant improvement in sDA could be observed with the proposed building setback over the current regulations while maintaining annual energy savings close to the optimum solar access thresholds.

4.9.5 Analysis of the effects of contextual shading on Case study 3

The floor area of the bedrooms and their window areas are depicted for Case study 3 (C_3) in Figure 4.30. The living rooms have more than double the floor area than the bedrooms, while the window sizes show only a marginal increase. Therefore, in Case study 3, solar access in the living rooms was less than in the bedrooms.

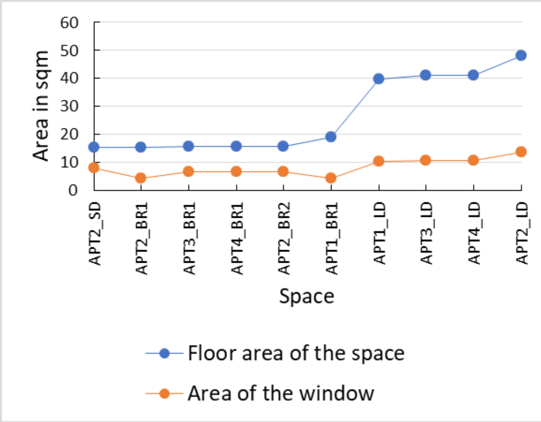

Figure 4.30: Floor area and window area of spaces simulated in Case study 3

Table 4.9 shows the sDA and energy savings of the simulated spaces in four cardinal directions for the current regulations (6 m building setback). According to Table 4.9, 76% of the spaces in Case study 3 have less than 25 sDA, of which most are located below the 16th floor. The severe lack of daylight could be attributed to the building height and the high floor area in spaces compared to C_1 and C_2. This Case study is the tallest of the buildings. Therefore, it indicated how increasing heights of residential buildings in a dense urban context impact indoor daylight level. According to daylight results in this Case study of the current regulations, the building residents of residential towers of over 30 floors would have to rely heavily on energy for day-time lighting. Energy savings are higher in the east-west direction than in the north-south, as expected. Energy savings in C_3 do not show a significant pattern as the floor levels increase, as was observed in C_1 and C_2. This could be attributed to an increase in artificial lighting energy during the day-time. Therefore, the high-density urban context decreased energy savings in Case study 3.

Table 4.9: Spatial daylight autonomy (sDA) and energy savings in C_2 in an urban context based on the current building setback regulation

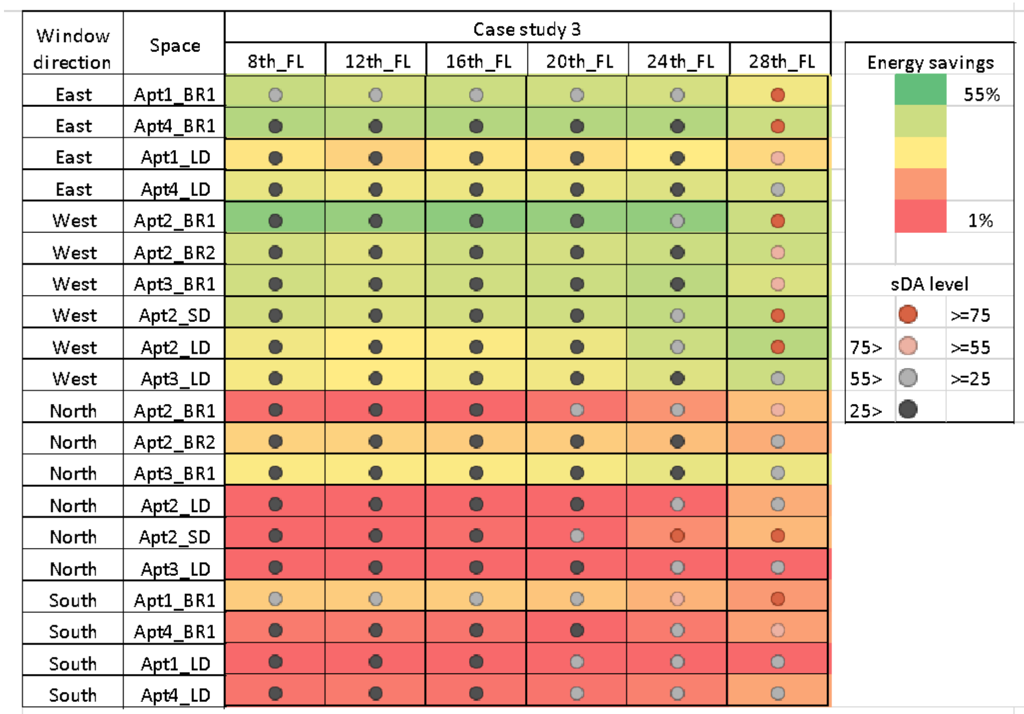

Table 4.10 indicates the effects of optimum solar access in Case study 3. Fifty-three per cent of the spaces in C_3 met over 55 sDA. In addition to contextual shading, aspects such as the size of the opening and the depth of the space affect the sDA (similar to the observations in C_1 and C_2 where sDA is lower in living rooms than in bedrooms).

Higher energy savings, indicated in green in Table 4.10, were observed in the east-west direction than in the north-south as expected. In C_3, a steady decrease in energy savings parallel to floor level increase was not observed. Annual energy savings for the 8th floor through to the 20th floor was between 22%-23% for east-west and 10%-11% for north-south in C_3, indicating only a marginal increase. The effects of energy savings from the urban context were less than observed in the other two case studies. This indicates that as buildings become taller, higher densities do not result in higher energy savings in the tropics.

Table 4.10: Spatial daylight autonomy (sDA) and energy savings in Case study 3 in an urban context for optimum solar access

Window direction	Space	Case study 3 floor levels					
		8th_FL	12th_FL	16th_FL	20th_FL	24th_FL	28th_FL
East	Apt1_BR1	>=75	>=75	>=75	>=75	>=75	>=75
East	Apt4_BR1	55> >=25	55> >=25	75> >=55	75> >=55	>=75	>=75
East	Apt1_LD	55> >=25	55> >=25	55> >=25	55> >=25	75> >=55	75> >=55
East	Apt4_LD	55> >=25	55> >=25	55> >=25	55> >=25	55> >=25	>=75
West	Apt2_BR1	55> >=25	55> >=25	55> >=25	75> >=55	>=75	>=75
West	Apt2_BR2	55> >=25	55> >=25	55> >=25	55> >=25	75> >=55	>=75
West	Apt3_BR1	55> >=25	55> >=25	55> >=25	75> >=55	75> >=55	>=75
West	Apt2_SD	>=75	>=75	>=75	>=75	>=75	>=75
West	Apt2_LD	55> >=25	55> >=25	75> >=55	>=75	>=75	>=75
West	Apt3_LD	55> >=25	55> >=25	55> >=25	55> >=25	55> >=25	>=75
North	Apt2_BR1	55> >=25	55> >=25	55> >=25	75> >=55	>=75	>=75
North	Apt2_BR2	55> >=25	55> >=25	55> >=25	55> >=25	75> >=55	>=75
North	Apt3_BR1	55> >=25	55> >=25	55> >=25	75> >=55	75> >=55	>=75
North	Apt2_SD	>=75	>=75	>=75	>=75	>=75	>=75
North	Apt2_LD	55> >=25	55> >=25	75> >=55	>=75	>=75	>=75
North	Apt3_LD	55> >=25	55> >=25	55> >=25	55> >=25	55> >=25	>=75
South	Apt1_BR1	>=75	>=75	>=75	>=75	>=75	>=75
South	Apt4_BR1	55> >=25	55> >=25	75> >=55	75> >=55	>=75	>=75
South	Apt1_LD	55> >=25	55> >=25	55> >=25	55> >=25	75> >=55	75> >=55
South	Apt4_LD	55> >=25	55> >=25	55> >=25	55> >=25	55> >=25	>=75

Energy savings	
55%	
1%	
sDA level	
>=75	
75>	>=55
55>	>=25
25>	

Table 4.11 compares the sDA and energy savings of the current and the optimum solar access scenarios for the urban context in Case study 3. As discussed above, deficient sDA levels were observed due to the current setback regulations in C_3. Only 12% of spaces could satisfy 55 sDA levels while energy savings of 29%-32% were observed in the east-west and 4% in the north-south directions. However, in the optimum solar access scenario, 53% of the space had over 55 sDA, annual energy savings of 30%-31% was observed in the east-west and 8%-12% in the north-south direction. Therefore, it is clear that the prescribed building setback ensures 55 sDA for over 50% of the spaces and has better energy savings than the current scenario.

Table 4.11: Effects of contextual shading on spatial daylight autonomy (sDA) and energy savings in Case study 3

Urban context	Percentage of spaces with:		The average energy savings percentage			
	sDA >=55	sDA >=75	East facade	West facade	North facade	South facade
Current setback regulations	12%	7%	29	32	4	4
Building setback for optimum solar access	53%	38%	30.2	31.3	12.3	8.9

The above analyses of the case studies indicate that the building setback is crucial in ensuring adequate solar access. In addition to the building setback, window size and room depth are also essential tools in providing solar access. Figure 4.31 depicts the window to floor area ratios of the simulated spaces for all three case studies. In the building regulations in Sri Lanka, the window to floor area ratio of 1/7 or 0.14 is the minimum window opening size. The minimum threshold is indicated in red in Figure 4.31. It was observed that all the windows comply with the mandatory regulation. Even though the window openings are maximized and far exceeds the requirement, many spaces had less than 55 sDA when the urban context complied with the current regulations. Therefore, it is clear that dictating the window to floor area ratio would not ensure solar access to the interior spaces in the tropics.

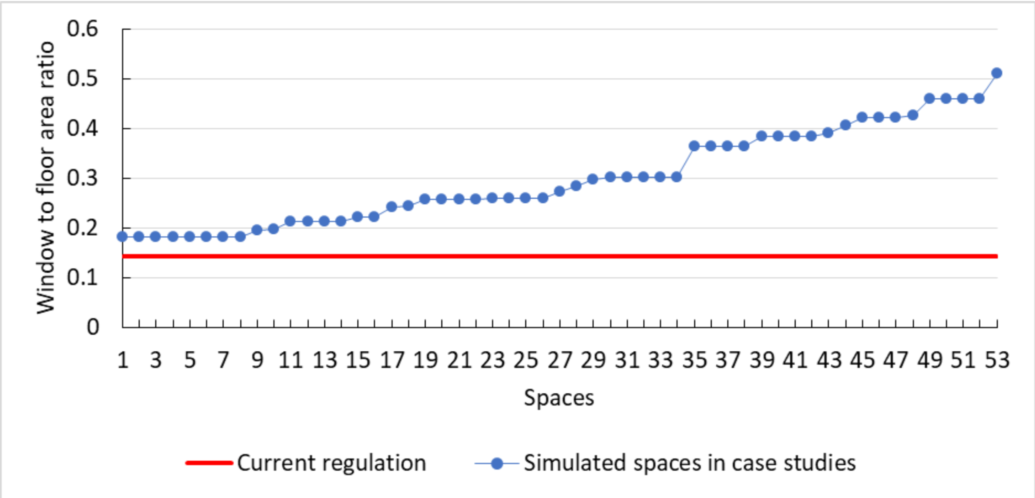

Figure 4.31: Window to floor area ratios of the simulated spaces in the case studies

A lack of standards for CBDM based daylight metrics for tropics and residential buildings were discussed in the literature review. The 75 sDA threshold for optimum solar access derived in this study is for the perimeter zone in a high-rise residential building. Therefore, it could not compare the daylight levels in the living room and bedroom spaces in a residential unit. LEED requires $sDA_{(300lx/50)}$ to achieve at least 55% (2pts) or 75% (3pts) of occupied spaces for new construction, core and shell, schools, retail, data centres, warehouses & distribution centres and hospitality (LEED, n.d.). Though the LEED standard has its limitations of not specifying residential buildings, it provides guidelines for acceptable daylight levels for occupied interior spaces based on sDA. Considering the above guideline, achieving 55% $sDA_{(300lx|50)}$ for over 50% of the spaces was considered the acceptable percentage for a high-rise residential building in the tropics.

Table 4.12 compares the summarized sDA and energy savings of the case studies for optimum solar access. More than 50% of the spaces (living rooms and bedrooms) in C_1, C_2 and C_3 have 55 sDA. C_1, C_2 and C_3 indicate average energy savings of 26-31% in east-west and 12-15% in the north-south directions, which is consistent with the energy savings predicted for the optimum building setbacks.

Table 4.12: Comparison of case studies for optimum solar access

	Percentage of spaces with:		**The average annual energy savings percentage**			
	55<= sDA	**sDA >=75**	**East facade**	**West facade**	**North facade**	**South facade**
Case study 1	100%	81%	28.6	30	9.5	9.1
Case study 2	64%	59%	26.3	25.6	15.1	12.7
Case study 3	53%	38%	30.2	31.3	12.3	8.9

According to the above analysis of the three case studies, the prescribed setback curves in Figure 4.21 could predict the annual energy savings for optimum solar access and ensure 55% $sDA_{(300lx|50)}$ for 50% of the residential spaces modelled in

C_1, C_2 and C_3. Therefore, the prescribed building setback curves for optimizing solar access are recommended for buildings between 10 and 31 floors.

4.10 Optimum building density for the high-rise residential building typology in the tropics

Sections 4.1 to 4.9 led to the development and validation of building setback curves for optimum solar access. The above sections have, therefore, answered research questions one and two. In this section, the third research question, the optimum building density for the high-rise residential building typology, is explored. The effects of building density on solar access, daylight, and energy efficiency were discussed in the literature review. Ensuring solar access in high-rise residential buildings is a key concern in dense urban tropics. The effects of building density on solar access in high-rise residential buildings are discussed in this Section.

Figure 4.32 compares maximum, optimum, and minimum building densities and corresponding solar access levels for the Simulation models (SM1, SM2, and SM3).

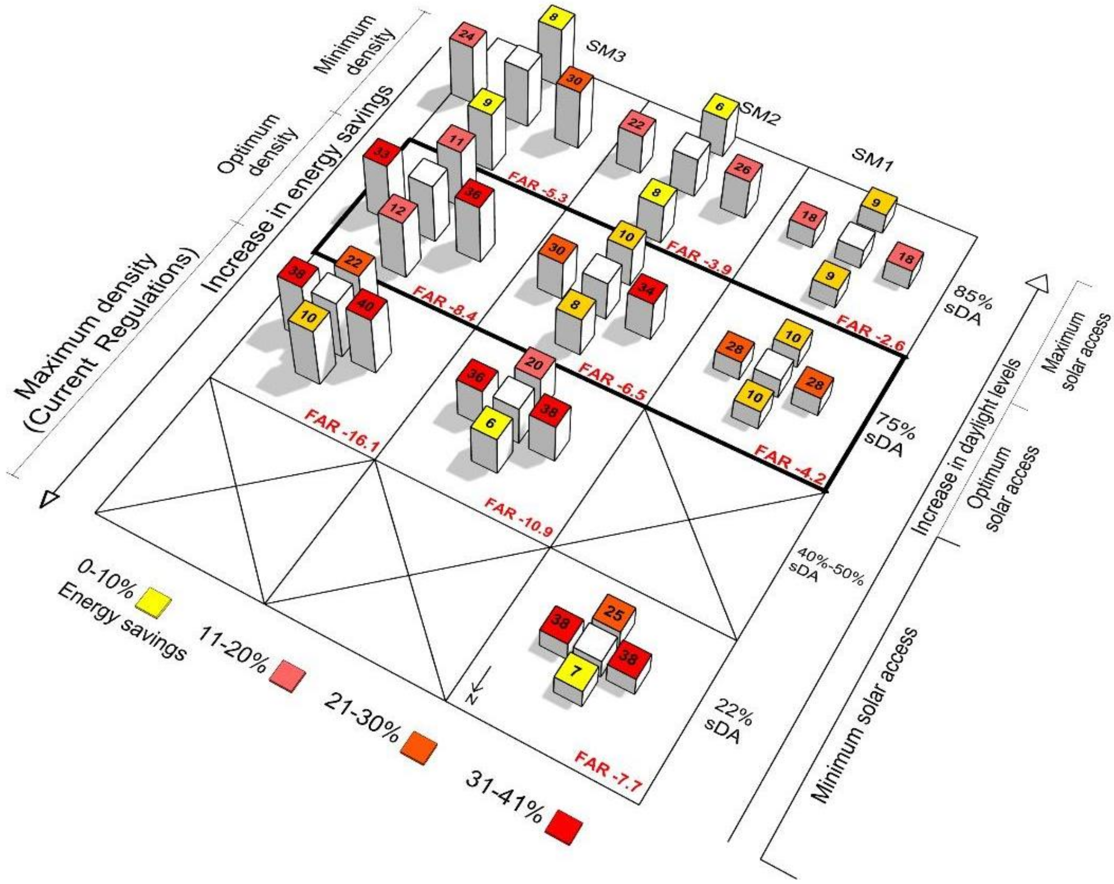

Figure 4.32: Comparison of minimum, optimum and maximum density and solar access

The maximum building density was calculated from the building setback based on current building regulations for 11, 21 and 31-floor buildings. The setback regulation for an 11-floor building is 3 m, while the setback for a 21 and 31-floor building is 6 m (Appendix B). The floor area ratio (FAR) calculated for maximum building density for SM1, SM2 and SM3 are 7.7, 10.9, and 16.1, respectively. For SM1, sDA of 22% with corresponding energy savings of 38% in the east-west direction, while 7% in the north and 25% in the south are observed in the maximum density scenario. For SM2 and SM3, sDA of 40%-50% is obtained at the current setback regulations, while energy savings of 38% -40% in the east-west direction, 6% -10% in the north, and 20%-22% in the south are observed. It was noted that low daylight and solar access levels correspond to very high building densities.

The optimum building density indicated in Figure 4.32 was based on the building setback curves for optimum solar access in Figure 4.21. The FAR calculated for optimum building density for SM1, SM2, and SM3 are 4.2, 6.5, and 8.4, respectively. For all three models at optimum building density, sDA levels of 75% and corresponding energy savings of 28%-36% in the east-west direction, while energy savings of 8%-12% in the north-south was observed.

The minimum building density indicated in Figure 4.32 is based on the maximum daylight level of 85 sDA. The setbacks for maximum daylight levels are based on the building density corresponding to 85 sDA. The total energy savings corresponding to 85 sDA were obtained from Figure 4.12 to 4.14. The FAR calculated for minimum building density for SM1, SM2, and SM3 are 2.6, 3.9, and 5.3, respectively. For all three models, sDA levels of 85% and corresponding energy savings of 18%-26% in the east-west direction and 6%-9% in the north-south were observed. Minimum densities allow maximum solar access; however, it decreases energy savings in all cardinal directions. In addition, for an increase of 10% in sDA (from 75% to 85%), the FAR is reduced by 30%. Therefore, minimum building densities result in inefficient land use and a reduction in energy savings from contextual shading.

According to the literature review, a key component of the Radiant city concept and the more recent successful high-rise residential developments is increasing building density to free more green space. However, due to misguided notions of building density, unsustainably high densities are being promoted in high-rise residential developments in Sri Lanka. Therefore, an optimum building density based on ensuring solar access should be incorporated in the typology of the high-rise residential building to avoid unsustainable densities in the future. This study proposes the optimum building density depicted in Figure 4.33 for the high-rise residential building typology in dense urban tropics.

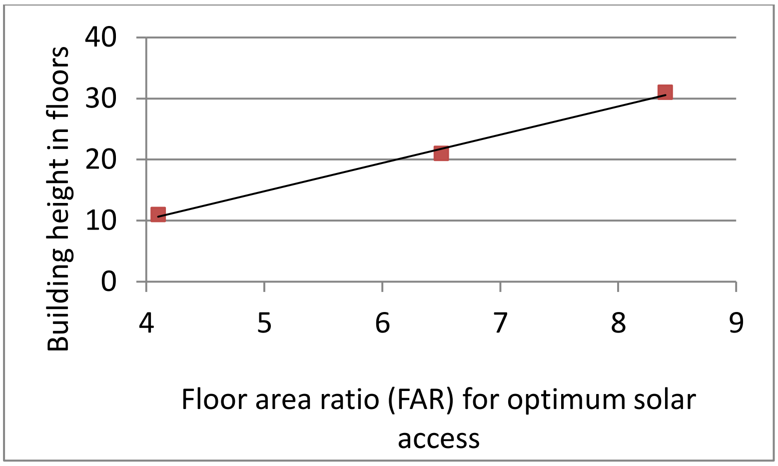

Figure 4.33: Floor area ratio for optimum solar access

Figure 4.33 above depicts the FAR for optimum solar access based on the analysis depicted in Figure 4.32. A linear trend line for optimum building density could be obtained based on the FAR values of the three Simulation models.

The need to utilize more than one building density parameter to describe the physical characteristics of a residential building typology was discussed in the literature review. Therefore, to ensure optimum solar access, the optimum building density obtained from Figure 4.33 should be accompanied by the building setback curves indicated in Figure 4.21.

Phase III

4.11 The impact of the urban context on the daylight and energy performance of external shading devices

The impact of the distance between two buildings and the building height on solar access in high-rise residential buildings in urban tropics were investigated in Phase II of this study. In Phase III, contextual shading on solar access of the vertical façade of a high-rise residential building was investigated. The design of the daylight and thermal models to simulate 27 external shading scenarios in Simulation model 2 was discussed in Section 3.9. In this Section, the results of the Simulation process are discussed.

4.11.1 Impact of contextual shading on different floor levels in Simulation model 2 (SM2)

As discussed in Section 3.9, this study utilized the Simulation model 2(SM2) to evaluate the impact of the urban context optimized for solar access on daylight and energy performance of external shading devices. Figure 4.34 compares the effects of the optimized urban context on the sDA and annual energy savings on SM2.

The sDA for the 2nd, 11th and 19th floors is 71.7, 75, and 92, respectively. The 2nd-floor sDA was slightly below the threshold for optimum solar access at 75 sDA. The annual total energy use on the 19th floor is 6000kWh, higher than the building energy use on the 11th floor. Therefore, it is clear that optimizing the building setback for the 11th floor did not achieve the optimum sDA and energy savings for all floors, but only on average for the building. However, this shortcoming could be overcome by further improving the daylight and energy performance of the vertical building façade.

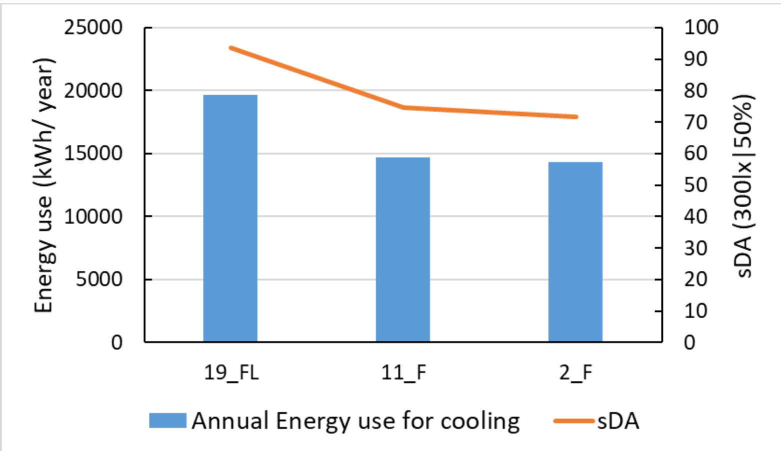

Figure 4.34: Impact of the optimized urban context on the spatial daylight autonomy and annual energy savings at different floor levels in Simulation model 2

4.11.2 Comparison of energy savings from balconies at different floor levels

Figure 4.35 compares the energy savings from balconies for the 19th, 11th and 2nd floor within the optimized urban context for solar access in SM2.

The total energy savings from balconies as a percentage change was calculated for one floor level as follows:

$$\frac{Total\ energy\ use\ with\ balcony - Total\ energy\ use\ excluding\ balcony}{Total\ energy\ use\ excluding\ balcony} \text{ X } 100$$

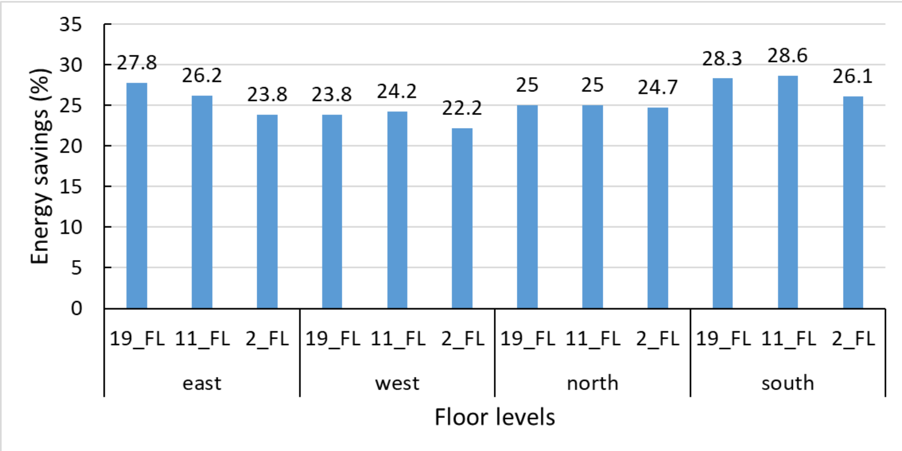

Figure 4.35: Energy savings due to balconies in Simulation model 2

Energy savings increased between 23%-28% due to the inclusion of a balcony on each floor. Due to the contextual shading, slightly lower energy savings were observed on the second floor. The application of balconies was slightly more effective in the south than in other directions. According to Figure 4.35, over 20% of energy savings was achieved by applying the standard balcony in high-rise residential buildings in the tropics.

4.12 Daylight analysis of external shading scenarios

The impact of the optimized urban context on 27 external shading scenarios is discussed in this section. Figures 4.36 to 4.38 compare the external shading scenarios (1-27) on sDA for each cardinal direction. sDA vary between 60% and 95% for each shading scenario. On the second floor, the highest sDA was observed in the north-south, while on the 19th floor, the highest sDA was observed in an east-west direction. This indicated that contextual shading decreased sDA in the east-west direction in comparison to the north-south. Therefore, in high-density urban contexts, the east and west could result in lower sDA than the north-south direction.

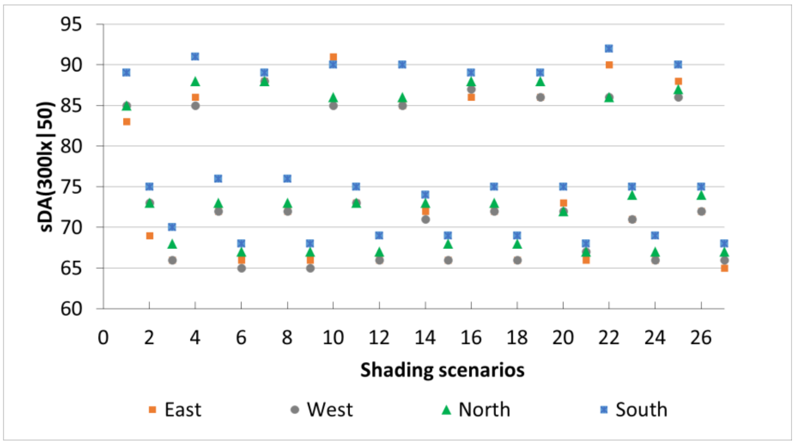

Figure 4.36: Comparison of spatial daylight autonomy of different shading scenarios on the 2nd floor

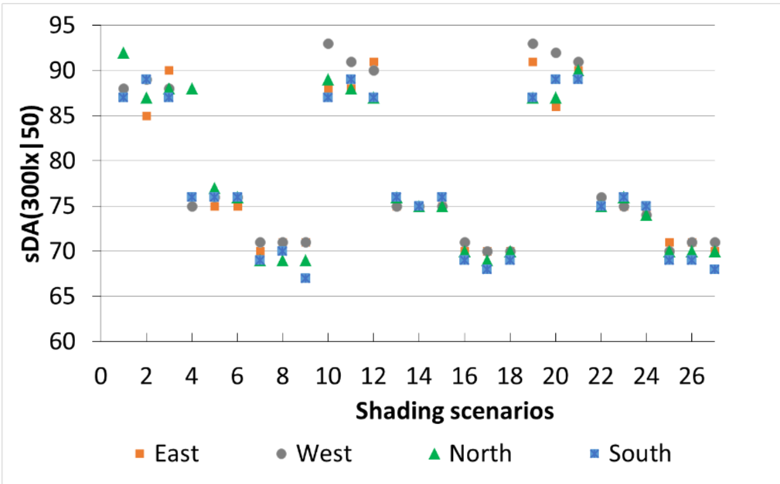

Figure 4.37: Comparison of spatial daylight autonomy of different shading scenarios on the 11th floor

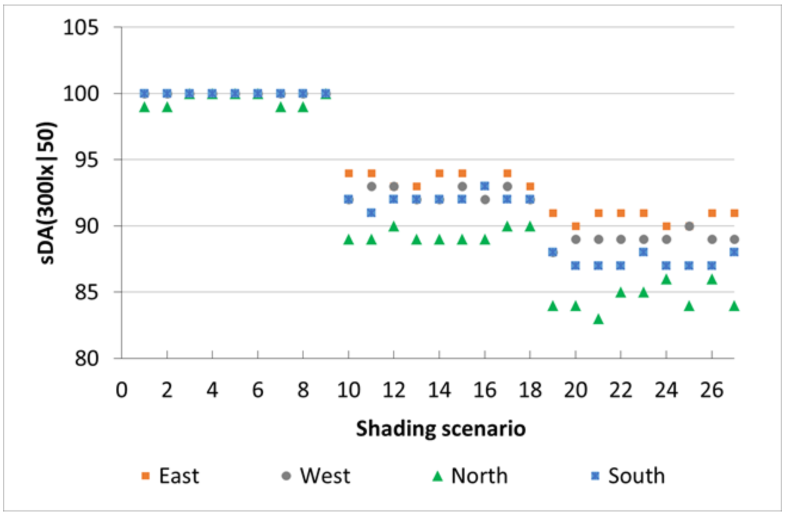

Figure 4.38: Comparison of spatial daylight autonomy of shading scenarios in the 19th floor

The threshold values for sDA and energy savings needed to be established to identify the best performance shading scenario. According to the optimum solar access definition for urban tropics, 75 sDA is the required threshold. Therefore, 75 sDA for the perimeter zone of SM2 was taken as the threshold value for daylight to be satisfied by the best performance external shading scenarios.

4.13 Energy analysis of external shading scenarios

Figure 4.39 depicts the average annual energy savings of the shading scenarios (C1-27) for each cardinal direction. According to the Figure, the highest energy savings from external shading devices were observed in the south, followed by north, west and east. The literature review identified that energy savings from external shading are higher in the east-west direction. However, Figure 4.39 shows that when considering urban context and day-time lighting energy use, the north-south direction leads to higher energy savings. The maximum energy savings were observed at 25% for C27 for the façade facing south. However, considering the 75 sDA requirement, a lower value of 15% annual average energy savings was selected as the threshold value for energy savings to identify the best performance scenario.

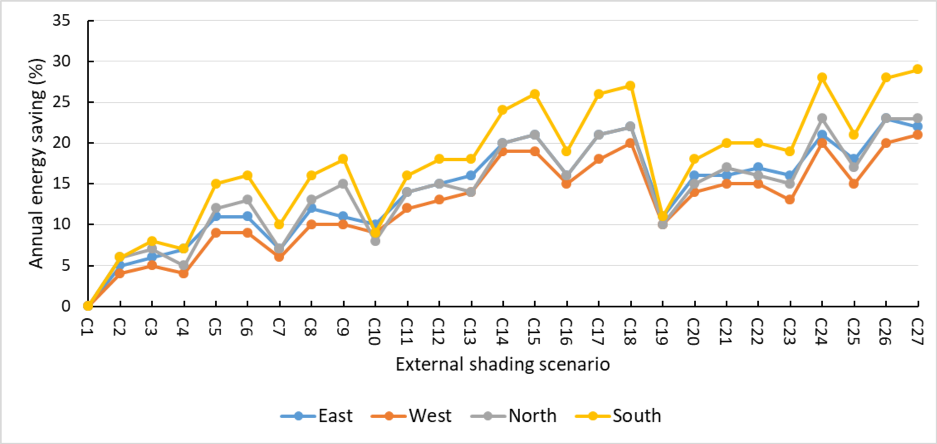

Figure 4.39: Comparison of energy savings of shading scenarios for cardinal directions

4.14 Identifying the best performance external shading scenario

The shading scenarios, which satisfied 75 sDA for all three floors simulated in the model and satisfied the 15% annual average energy savings threshold, were considered as meeting the best performance criteria. Tables 4.13 to 4.16 compare the average energy savings for cooling and daytime lighting against sDA of the Simulation model. sDA above 75% are indicated in red, while the annual energy savings above 15% are green. To select the best performance scenario, the minimum threshold set for energy savings and daylight should be satisfied. In Table 4.13, where the façade faces an obstruction in the east, two scenarios, C13 and C22, satisfy the threshold values for sDA and energy savings. However, C22 has higher energy savings of 17%. The baseline scenario (C14) has higher energy savings; however, it did not meet 75 sDA at the lowest floor level. Table 4.14 indicates the shading effects on the west-facing facade. C22 again satisfied both the sDA requirement for all floors and energy savings at 15%.

Table 4.13:Façade facing obstruction in east

Scenario	Annual energy savings	sDA (300lx|50) percetnage per floor		
		2_FL	11_FL	19_FL
C1	0	83	87	100
C2	5	69	85	100
C3	6	66	90	100
C4	7	86	76	100
C5	11	72	75	100
C6	11	66	75	100
C7	7	88	70	100
C8	12	72	71	100
C9	11	66	71	100
C10	10	91	88	94
C11	14	73	88	94
C12	15	66	91	93
C13	16	85	75	93
C14	20	72	75	94
C15	21	66	75	94
C16	16	86	70	93
C17	21	72	70	94
C18	22	66	70	93
C19	11	86	91	91
C20	16	73	86	90
C21	16	66	90	91
C22	17	90	75	91
C23	16	71	75	91
C24	21	66	74	90
C25	18	88	71	90
C26	23	72	71	91
C27	22	65	70	91
	>75% sDA(300lx150)		>15% annual energy savings	

Table 4.14: Façade facing obstruction in west

Scenario	Annual energy savings	sDA (300lx|50) percetnage per floor		
		2_FL	11_FL	19_FL
C1	0	85	88	100
C2	4	73	89	100
C3	5	66	88	100
C4	4	85	75	100
C5	9	72	76	100
C6	9	65	76	100
C7	6	88	71	100
C8	10	72	71	100
C9	10	65	71	100
C10	9	85	93	92
C11	12	73	91	93
C12	13	66	90	93
C13	14	85	75	92
C14	19	71	75	92
C15	19	66	75	93
C16	15	87	71	92
C17	18	72	70	93
C18	20	66	70	92
C19	10	86	93	88
C20	14	72	92	89
C21	15	67	91	89
C22	15	86	76	89
C23	13	71	75	89
C24	20	66	74	89
C25	15	86	70	90
C26	20	72	71	89
C27	21	66	71	89
	>75% sDA(300lx l50)		>15% annual energy savings	

In the north-facing façade (Figure 4.15), only C22 satisfied both criteria. In the south façade, C5, C20, C22 and C23 all meet the minimum criteria for the best performance external shading scenario (Figure 4.16). However, the highest energy savings were reported in C22. Therefore, C22 is considered the best performance external shading scenario for all cardinal directions.

Table 4.15: Façade facing obstruction in north

Scenario	Annual energy savings	sDA (300lx|50) percetnage per floor		
		2_FL	11_FL	19_FL
C1	0	85	92	99
C2	6	73	87	99
C3	7	68	88	100
C4	5	68	88	100
C5	12	73	77	100
C6	13	67	76	100
C7	7	88	69	99
C8	13	73	69	99
C9	15	67	69	100
C10	8	86	89	89
C11	14	73	88	89
C12	15	67	87	90
C13	14	93	76	89
C14	20	73	75	89
C15	21	68	75	89
C16	16	88	70	89
C17	21	73	69	90
C18	22	68	70	90
C19	10	88	87	84
C20	15	72	87	84
C21	17	67	90	83
C22	16	86	75	85
C23	15	74	76	85
C24	23	67	74	86
C25	17	87	70	84
C26	23	74	70	86
C27	23	67	70	84

	> 75% sDA(300lx I50)		> 15% annual energy savings

Table 4.16: Façade facing obstruction in south

Scenario	Annual energy savings	sDA (300lx|50) percetnage per floor		
		2_FL	11_FL	19_FL
C1	0	89	87	100
C2	6	75	89	100
C3	8	70	87	100
C4	7	91	76	100
C5	15	76	76	100
C6	16	68	76	100
C7	10	89	69	100
C8	16	76	70	100
C9	18	68	67	100
C10	9	90	87	92
C11	16	75	89	91
C12	18	69	87	92
C13	18	92	76	92
C14	24	74	75	92
C15	26	69	76	92
C16	19	89	69	93
C17	26	75	68	92
C18	27	69	69	92
C19	11	89	87	88
C20	18	75	89	87
C21	20	68	89	87
C22	20	92	75	87
C23	19	75	76	88
C24	28	69	75	87
C25	21	90	69	87
C26	28	75	69	87
C27	29	68	68	88

	> 75% sDA(300lx I50)		> 15% annual energy savings

Annual solar exposure (ASE) levels corresponding to shading scenarios are given in Table 4.17. In C22, which is considered the best performance scenario, the ASE ranges from 16% to 30% in the east, 10% to 19% in the west, 1% to 2% in the north and 6% to 17% in the south. High ASE levels in the east are experienced for a few hours in the morning in the tropics. High levels of direct solar exposure for short periods, especially in the morning, is welcome, given the health benefits. In addition, internal shading could avoid unwanted direct solar exposure for short periods. Therefore, high ASE was not considered a disadvantage for residential buildings.

Table 4.17: Annual Solar Exposure (ASE) levels for external shading scenarios

Scenario	East			North			South			West		
	2_FL	11_FL	19_FL	2_FL	11_FL	19_FL	2_FL	11_FL	19_FL	2_FL	11_FL	19_FL
C1	14.2	14.8	32.4	7.6	7.6	7.6	17.6	17.9	17.9	10.4	10.7	21.4
C2	11	14.8	32.4	2.7	7.6	7.6	7.8	17.9	17.9	6.3	10.7	21.4
C3	13	16.5	32.4	1.8	7.6	7.6	6.2	17.9	17.9	6.3	10.7	21.4
C4	16	13.5	32.4	1.8	7.6	7.6	17.6	8	17.9	10.4	6.7	21.4
C5	13	13.5	32.4	2.7	2.7	7.6	7.8	8	17.9	6.3	6.7	21.4
C6	13	13.5	32.4	1.8	2.7	7.6	6.2	8	17.9	6.3	6.7	21.4
C7	16	13.5	32.4	7.6	1.8	7.6	17.6	6.4	17.9	10.4	6.7	21.4
C8	13	13.5	32.4	2.7	1.8	7.6	7.8	6.4	17.9	6.3	6.7	21.4
C9	13	13.5	32.4	1.8	1.8	7.6	6.2	6.4	17.9	6.3	6.7	21.4
C10	16	16.5	30.8	7.6	7.6	2.7	17.6	17.9	8	10.4	10.7	19.4
C11	13	16.5	30.8	2.7	7.6	2.7	7.8	17.9	8	6.3	10.7	19.4
C12	13	16.5	30.8	1.8	7.6	2.7	6.2	17.9	8	6.3	10.7	19.4
C13	16	13.5	30.8	7.6	2.7	2.7	17.6	8	8	10.4	6.7	19.4
C14	13	13.5	30.8	2.7	2.7	2.7	7.8	8	8	6.3	6.7	19.4
C15	13	13.5	30.8	1.8	2.7	2.7	6.2	8	8	6.3	6.7	19.4
C16	16	13.5	30.8	7.6	1.8	2.7	17.6	6.4	8	10.4	6.7	19.4
C17	13	13.5	30.8	2.7	1.8	2.7	7.8	6.4	8	6.3	6.7	19.4
C18	13	13.5	30.8	1.8	1.8	2.7	6.2	6.4	8	6.3	6.7	19.4
C19	16	16.5	30.8	7.6	7.6	1.8	17.6	17.9	6.4	10.4	10.7	19.4
C20	16	16.5	30.8	2.7	7.6	1.8	7.8	17.9	6.4	6.3	10.7	19.4
C21	13	16.5	30.8	1.8	7.6	1.8	6.2	17.9	6.4	6.3	10.7	19.4
C22	16	13.5	30.8	7.6	2.7	1.8	17.6	8	6.4	10.4	6.7	19.4
C23	13	13.5	30.8	2.7	2.7	1.8	7.8	8	6.4	6.3	6.7	19.4
C24	13	13.5	30.8	1.8	2.7	1.8	6.2	8	6.4	6.3	6.7	19.4
C25	16	13.5	30.8	7.6	1.8	1.8	17.6	6.4	6.4	10.4	6.7	19.4
C26	13	13.5	30.8	2.7	1.8	1.8	7.8	6.4	6.4	7.8	6.4	6.4
C27	13	13.5	30.8	1.8	1.8	1.8	6.2	6.4	6.4	6.2	6.4	6.4

(shaded) ASE>10%

The best performance external shading scenario was identified in the study as Scenario 22, where the 19th floor had combined shading, the median floor had only balconies, and the 2nd floor had no shading devices. The following design principles based on the best performance scenario were formed from the analysis in Phase III. The design principles are applied to SM2 and illustrated in Figure 4.40.

- When considering the entire façade, the windows in the bottom one-third of the building's floors should be without or minimal shading techniques.
- The windows in the middle one-third of the building should have only horizontal shading (e.g., balconies).
- The top one third should have combined fins and balconies for external shading of windows.

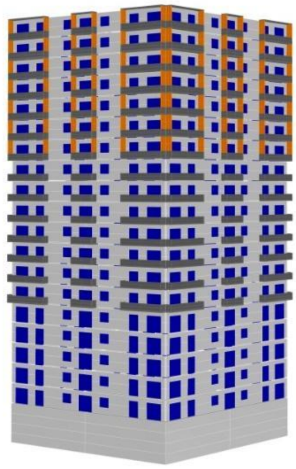

Figure 4.40: Application of the design principles in Simulation model 2

4.15 Application of design principles to the Case study 2

The aim of applying the research findings to a Case study was to consider design options for a real-world building in a dense urban context. Case study 2 was utilized for the application of design principles. The urban context was developed using the building setback curves for optimum solar access in Figure 4.21, as discussed in Section 3.12. Tables 4.18 and 4.19 demonstrate the sDA and energy savings of the Baseline and the Best performance scenario model, respectively. The *DIVA4* daylight grids for the Best performance scenario are given in Appendix J. The baseline and best performance scenarios satisfied 62% of spaces with 55 sDA, while 58% of spaces met 75 sDA. An increase in sDA is observed at higher floor levels due to higher contextual shading fraction than at the lower floors in both scenarios. sDA is below 55% for all living rooms than the bedrooms, where 93% have above 55 sDA. Lack of daylight in living rooms could be attributed to the increase in room depth of living rooms. Energy savings are higher on the lower floors compared to the higher floors in both scenarios. Combined shading from the 12th to 16th floors (best performance scenario) increased energy savings for an average floor by 1.7% in the east, 2% in the west, 6% in the north and 7% compared to the Baseline scenario for the respective floors.

Table 4.18: Energy savings and spatial daylight autonomy in Case study 2 for the Baseline scenario

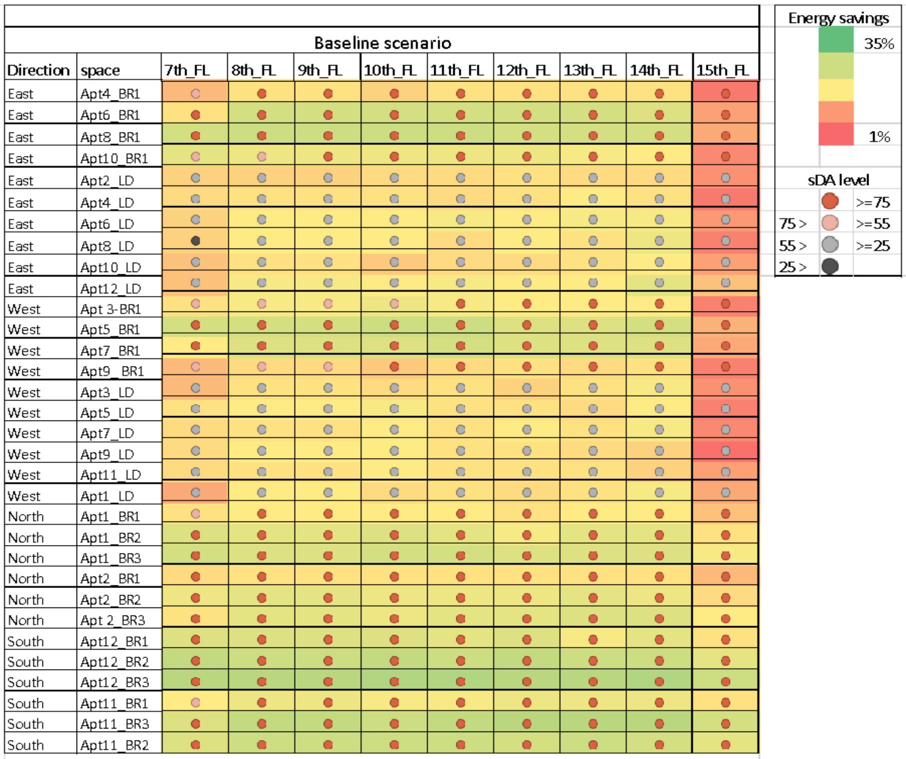

Table 4.19: Energy savings and spatial daylight autonomy in Case study 2 for Best performance scenario

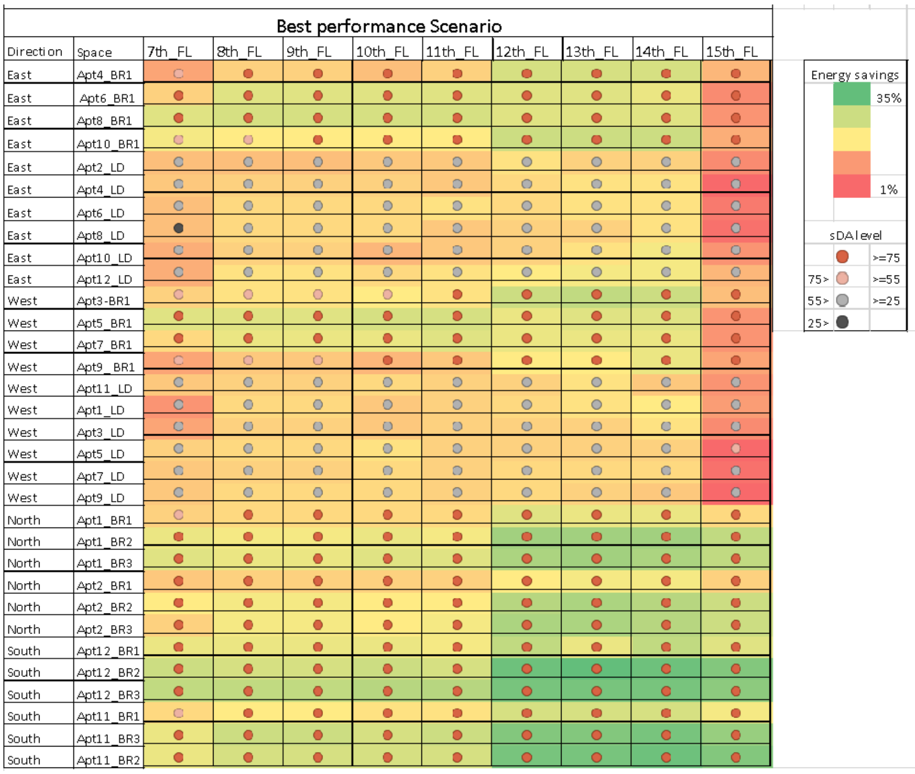

Table 4.20 compares the summarized simulated results of sDA and annual energy savings for the baseline and best performance scenario in Case study 2. The sDA percentage did not change for the baseline and best performance scenario. As the bottom floors were car parks, the benefits of the non-shading for lower floors on increasing daylight levels was not investigated in this Case study. The benefits of having combined shading for energy savings in the top floors were observed in this study, even though the effects were marginal. One percent of the increase in energy savings could be observed in the east-west and 3% increase in the north-south direction in the Best performance scenario compared to the Baseline scenario. The marginal increase in energy savings percentage could be due to the structural elements (ducts, structural walls, columns) in C_2 that act like fins providing shading to the glazed area, which were included in the baseline scenario.

Table 4.20: Comparison of the Baseline and Best performance scenario on spatial daylight autonomy (sDA) and energy savings in Case study 2

	Percentage of spaces with:		**The average annual energy savings percentage**			
	sDA >=55	**sDA >=75**	**East facade**	**West facade**	**North facade**	**South facade**
Baseline scenario	62	58	16.1	15.7	18.3	22.0
Best performance scenario	62	58	17	16.5	21.2	25.1

4.16 Design options based on the best performance shading scenario

The use of static external shading devices as architectural elements was discussed in Section 2.7. Two design options for the vertical façade utilizing the design principles identified in Section 4.14 are discussed in this section.

Figure 4.41 depicts the external shading scenario for Design option 1. A continuous vertical shading device for increasing the shading on the windows without obstruction to the view in the top floors was utilized for Design option 1 (D_1). The use of non-combustible material is vital when considering a continuous façade on a vertical plane of a building. Balconies only shade the middle floor levels, while the bottom floors have no shading devices.

In Figure 4.41, due to the non-existence of a dense urban context, the east façade of the building is exposed to direct sunlight. Figure 4.42 depicts the shading effects of the urban context on the vertical façade. The urban context developed is based on the building setback for optimum solar access given in Figure 4.21. The reference data and time for shadow casting is 20th of March 2020, 9.00 a.m. and 3.00 p.m. (close to the vernal Equinox).

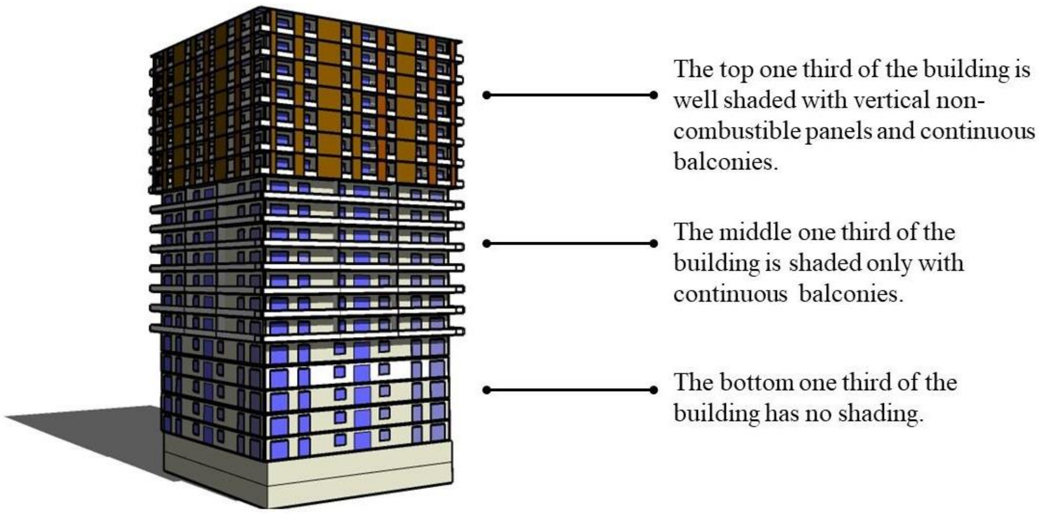

Figure 4.41: External shading devices in Design option 1 without the urban context

In Figure 4.42, floors up to the 14th floor (the bottom one third) are shaded by the urban context at the reference date and time. According to Figure 4.42, it was noted that the vertical and horizontal devices shade the glazed areas from direct solar exposure at the given times of shadow casting in the east and west facade. The middle and bottom floors are well shaded by the urban context. Hence, they do not need to have vertical shading devices to avoid heat gain through the glazed surfaces most of the day.

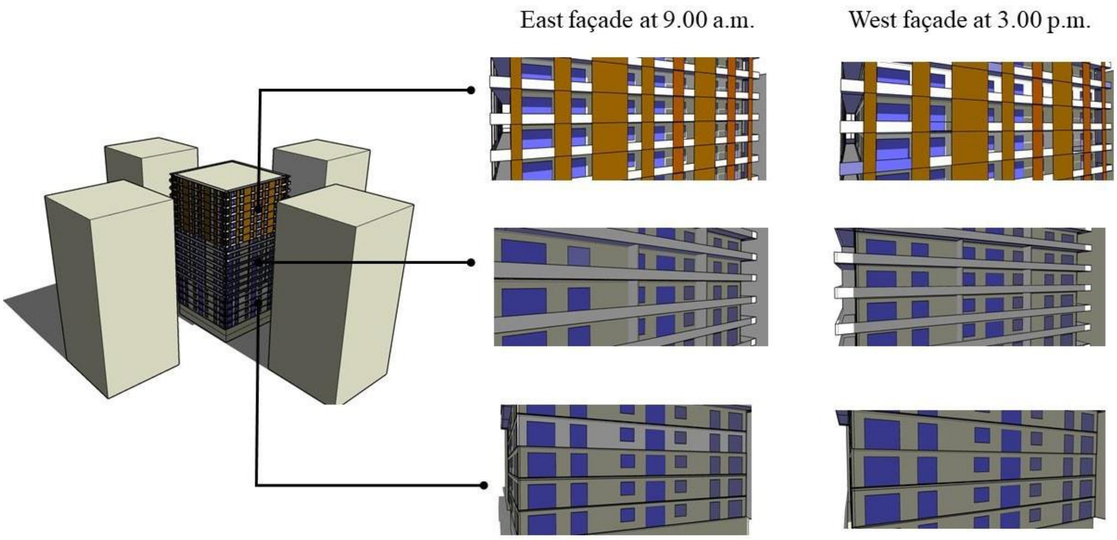

Figure 4.42: Effects of shading of the urban context on external shading devices in Design option 1

Figure 4.43 depicts the external shading scenario for Design option 2. Vertical fins, pergolas and balconies in the top floors which also form an irregular pattern on the building façade in Design option 2 (D_2). Balconies and pergolas shade the middle floors while the bottom one-third have an overhang over the window, as depicted in Figure 4.43.

Figure 4.44 compares the effects of shading from the urban context on D_2. The reference data and time for shadow casting is 20th of March 2020, 9.00 a.m. and 3.00 p.m. (close to the vernal Equinox). Similar to D_1, it was found that increased shading in the top floors are effective in shading the glazed areas, while a reduction in external shading devices in the bottom floors is needed to ensure daylight.

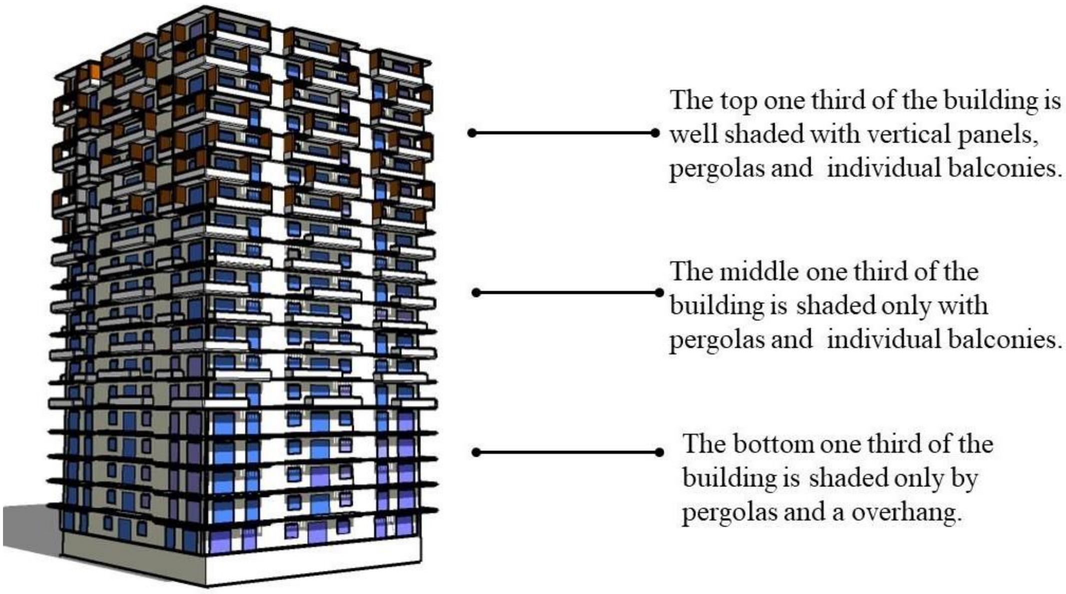

Figure 4.43: External shading devices in Design option 2 without the urban context

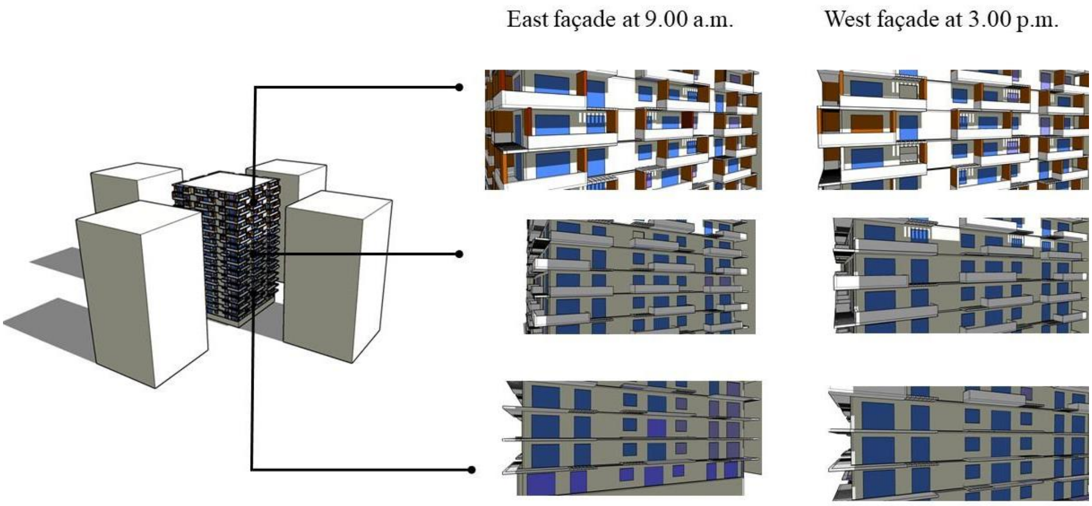

Figure 4.44: Effects of shading of the urban context on external shading devices in Design option 2

4.17 Summary

Chapter 4 consisted of analysing and discussing the simulation results of the archetypal models and the calibrated case studies. Section 4.1 to 4.10 analysed the Phase II simulation results of the research study. In Section 4.1 to 4.3, the basis for the average sDA and annual energy use of the Simulation models were explained. Section 4.4 and 4.6 analysed the daylight and energy savings results. Section 4.7 optimized the sDA and energy savings to define optimum solar access for the Simulation models. In Section 4.8 and 4.9, the building setbacks for optimum solar access were developed and validated with three calibrated case studies. The building density for optimum solar access in terms of FAR was identified in Section 4.10. The simulation results of the 27 external shading scenarios in SM2 were analysed in Phase III. The best performance scenario was identified in Section 4.14. The implications of the performance scenario applied to Case study 2 were discussed in Section 4.15, and further design options were explored in Section 4. 16.

5 Conclusion

Solar access is a topic predominantly investigated in the urban contexts at higher latitudes and to a much lesser extent in the tropics. Current regulations for high-rise residential buildings in Sri Lanka, a country located in the tropics, do not adequately ensure solar access for the residents. Therefore, the shading effect of the urban context on solar access in high-rise residential buildings in the tropics was investigated in this study. Four research objectives were formulated in this study to investigate the definition, typology, planning and architectural issues of solar access in high-rise residential buildings in dense urban tropics. The study was conducted and analysed in three phases as discussed below.

Phase I

5.1 Characteristics of the archetypal high-rise residential building in Sri Lanka

In the first phase of this study, a survey of high-rise residential buildings in Colombo, Sri Lanka, was conducted to develop the characteristics of an archetypal high-rise residential building. A sample of high-rise residential buildings was selected to represent a cross-section of characteristics in terms of building heights, number of units and plan forms. The height of the archetypal high-rise residential building in Sri Lanka ranges between 11 and 31 floors. The core-dependent building floor plan had an average linear length and width of 31 m x 31 m. The window to wall ratio in an archetypal high-rise residential building was 36%, indicating that the openings are maximized for solar access and view. The window composition was designed based on the window sizes calculated from the living rooms and bedrooms in the sample. The common materials of construction were also identified in the study and incorporated into the archetypal building. Balconies characterized the vertical façade of the archetypal high-rise residential building in the tropics. Mechanical ventilation was the most common form of achieving indoor thermal comfort in the buildings. Three Simulation models (SM1, SM2, and SM3) were developed based on the archetypal high-rise residential building characteristics identified in Phase I of the study.

Phase II

5.2 The impact of the urban context on solar access in high-rise residential buildings in dense urban tropics

Three of the four research questions formulated in this research study were answered in phase II.

The most challenging task in this study was modelling solar shading effects due to various high densities in the urban context in the Simulation models. This challenge was overcome by creating an urban context with a parametric obstruction of varying distances from 2 to 50 m in *Rhino3D* using *Grasshopper* interphase. The study successfully used parametric modelling to generate 100 urban contexts for each Simulation model to facilitate an optimization process for solar access.

The effect of the urban context on annual cooling energy in terms of mitigating external heat gain was quantified utilizing the Archsim plugin in *Rhino3D*. A perimeter/core model was selected to simulate the effects of heat gain into the building. A distance of 6 m from the façade was considered the perimeter zone depth based on the average living room depth in the archetypal models. The annual day-time lighting energy and spatial daylight autonomy (sDA) was quantified utilizing *DIVA4* plugin in *Rhino3D* for the daylight grid of 6 m depth above 0.75 m above ground level. A multi-objective optimization process was utilized to optimize sDA and total energy savings. Based on the Pareto-optimal sets identified in the Pareto-front, the threshold value for sDA and energy savings were calculated.

The first research objective was achieved by defining the optimum solar access in urban tropics. The optimum solar access for a high-rise residential building in the tropics was defined in this study for a perimeter zone in a high-rise residential building that achieves 75 sDA $_{(300lx|50)}$ with corresponding annual energy savings of 28-36% in the east-west and 8-12% savings in the north-south direction.

The second research objective incorporated sDA and energy savings to the building setback, making it a meaningful planning tool. As optimum solar access is difficult to calculate at the early design stage, the optimum solar access thresholds were interpreted using a building design tool. The building setback is the most effective planning tool to ensure solar access into the building. Though the building setback has existed in planning regulations, it did not indicate the corresponding daylight levels and energy savings. The prescribed building setback developed in this study ensures optimum solar access for the high-rise residential building.

The prescribed building setback curves were applied to three calibrated case studies for validation. Calibration of the case studies is an essential step in this research study. There were relatively few studies conducted in the tropics in terms of solar access utilizing computer software. Therefore, the validation of computer software for the tropics through calibration was explored in this study. According to the ASHRAE guidelines, the indoor air temperature calibration was found to be robust in the tropics. However, the daylight models in Case study two and Case study three did not meet the CV (RMSE $_{hourly}$) criterion for calibration. As the errors are primarily due to direct solar radiation effects and not due to errors in calculating diffused solar radiation, the daylight models were used for estimating sDA and day-time lighting in this study.

All case studies with the building setback for optimum solar access demonstrated 50% of interior spaces (living rooms and bedrooms) with 55 sDA $_{(300lx/50)}$ and annual energy savings of 26-31% in east-west and 8-15% north-south direction. Therefore, the prescribed setback curves for optimum solar access could be applied to high-rise residential buildings between 10-31 floors in the tropics. This study provided a scientific approach to modify the building setback tool to steer high-rise residential developments towards better solar access.

The third research objective estimated the optimum building density for solar access in the high-rise residential building typology. At present, solar access has been disregarded in the planning regulations in Sri Lanka mainly due and misguided notions of maximizing density for profits. The FAR based on the current building regulation for building setback, the FAR based on the building setback for optimum solar access and the FAR based on the building setback for maximum solar access for SM1, SM2 and SM3 were compared. The study found that the current regulations incur high building densities resulting in minimum solar access. The proposed optimum FAR for high-rise residential buildings in this study optimize daylight, energy savings and land-use efficiency. The FAR calculated for optimum building density for SM1, SM2, and SM3 are 4.2, 6.5, and 8.4, respectively.

At the conclusion of phase II, the study redefined solar access for the tropics, prescribed building setbacks for optimum solar access and informed optimum building density for the high-rise residential building typology.

Phase III

5.3 The impact of the urban context on the performance of external shading devices

Two building design elements affecting solar access into the building interiors were investigated in this study. The first building design element was the urban context, investigated in phase II. The second is the design elements in the building façade.

External shading devices are standard architectural features controlling solar access into the high-rise residential building. The effectiveness of external shading devices in energy-saving and daylight was investigated within the urban context in Phase III.

An archetypal high-rise residential building of 21 floors (SM2) was used to simulate the impact of the urban context on external shading scenarios. Twenty-seven shading scenarios (C1-27) consisting of combined shading (with balcony and vertical panel), horizontal shading (balcony only) and no shading (excluding balcony or vertical panel) were modelled for the 2nd, 11th and 19th floor. Using 3D modelling software *Rhino3D*, parametric interface *Grasshopper* and plugins, *DIVA4* and

Archsim, the performance of the external shading scenarios in terms of daylight and energy savings were simulated. The urban context was generated based on the building setback curves developed for optimum solar access.

The fourth research objective identified the best performance external shading scenario to enhance the daylight and energy performance of a high-rise residential building façade in an urban context. Shading scenarios that satisfied 75 sDA for all three floors simulated in the model and satisfied 15% annual energy savings threshold were considered the best performance external shading criteria. The maximum energy savings were observed at 25% for C27 (all floors with combined shading) for the façade facing south. However, C27 did not satisfy the 75 sDA requirement for the 11th and 2nd floor. The baseline scenario (balcony only on all floors -C14) had energy savings of 19-24%; however, it did not meet the 75 sDA criterion for the 2nd floor level. The results indicated that shading scenario - C22 (no shading on the 2nd floor, balcony on the 11th floor, combined shading on the 19th floor) satisfied the sDA requirement for all floors with energy savings percentages of 16,17,20 and 21 for east, west, north and south directions respectively. Therefore, C22 is considered the best performance external shading scenario.

When considering the entire façade of the building, the bottom one-third floors should not have shading techniques. In the same façade, the middle one third should have only horizontal shading. The top one-third should have combined shading with fins and balconies to achieve the best performance external shading scenario for a high-rise residential building in urban tropics. The literature review stated that energy savings from external shading are higher in the east-west direction. However, when considering urban context and day-time lighting energy use, north-south directions lead to higher energy savings than east-west. The study found that shading is most effective in the south orientation in the tropics.

A high-rise residential building with 17 floors and 142 residential units located in the Colombo Metropolitan Region was utilized as a calibrated Case study to apply the design principles identified in Phase III of the study. The hypothetical urban context for the case study was generated using the building setback curves for optimum solar access. Two models, the Baseline (balconies only from the 6th to 15th floor) and Best performance scenario model (balconies only from 7th to 11th floors and fins and balconies from 12th to 15th floors) were simulated to compare daylight and energy savings. The baseline and best performance scenario models provided 62% of spaces with 55 sDA, while 58% of spaces satisfied 75 sDA. The benefits of having combined shading for energy savings in the top floors were observed in this study, even though the effects were marginal. 1% increase in energy savings could be observed in the east-west, and a 3% increase in the north-south direction in the best performance scenario compared to the Baseline scenario. The marginal energy savings could be attributed due to the structural elements (ducts, structural walls, columns) in the Case study that act like fins providing shading to the glazed area. Phase III analysis is concluded with the introduction of two design options to enhance the daylight and energy performance of the vertical façade in Simulation model 2.

5.4 Limitations of the study

A few limitations were identified in this study while conducting the research. The study did not account for effects of solar radiation at the ground level due to increasing densities in the urban context. As the study took into account the heat gains due to solar access in levels above the 2nd floor of the buildings, the effects of solar radiation at the ground level were expected to have limited effects on heat gain in the simulated floors at the upper levels.

In addition, the study took the building heights to be the same in a given planning zone in Colombo and its suburbs, in order to model the hypothetical urban context. This would affect the application of the proposed building setback for optimum solar access to standalone high-rise residential buildings constructed in small plots. Therefore, the proposed building setback in this study would be more practically applied for high-rise residential buildings in neighbourhoods and estates designated for high-rise developments.

5.5 Broader implications and further research

Three broader implications of this research were noted. First, three interrelated aspects- urban planning regulations, building typology, and the building design of the vertical façade should be considered for optimum solar access, as illustrated in Figure 5.1. Therefore, without addressing the three aspects holistically, problems in solar access in the urban tropics could not be effectively resolved.

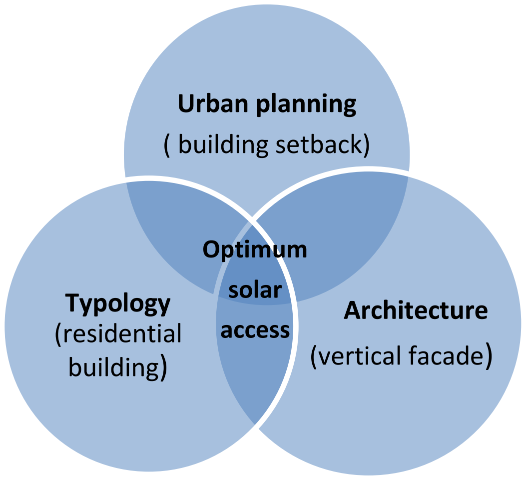

Figure 5.1: Holistic approach to optimizing solar access in dense urban tropics

Second, planning and building regulations are an integral part of sustainable development in cities. However, the stakeholders in the construction industry are reluctant to accept their impact on human-wellbeing, as most regulations are not backed by scientific evidence. Therefore, there is a need to bridge the gap in research by modifying existing planning and building regulations based on a scientific approach.

Third, the outcomes of this study resolved the research gaps in solar access in high-rise residential buildings in the urban tropics. Thus, establishing a much-needed platform to develop a conversation on solar rights in dense urban tropics.

This research was limited to the study of high-rise residential buildings in the tropical urban city of Colombo, Sri Lanka. Further research could be conducted to investigate the optimum solar access and building setback curves to commercial buildings located in the urban tropics. The study focused on two aspects of building design, the building microclimate and the building envelope. The impact of shading from the urban context on the building form merits further investigation.

In addition, more research is needed to inform the calibration processes for the validation of simulation software for application in the tropics. The results of the simulations conducted in this study are available in the *Mendeley* data repository for further analysis by other researchers.

- https://data.mendeley.com/datasets/r3wpkr2brx/3
- https://data.mendeley.com/datasets/h8pnz942tv/2

References

Aflaki, A., Mahyuddin, N., Manteghi, G., & Baharum, M. (2014). Building Height Effects on Indoor Air Temperature and Velocity in High Rise Residential Buildings in Tropical Climate. OIDA International Journal of Sustainable Development, 07(07), 39–48.

Alexander, Ernest R.; Reed, K. David; and Murphy P.(1998).Density Measures and Their Relation to Urban Form. Center for Architecture and Urban Planning Research Books.

Al-tamimi, N., Fairuz, S., & Fadzil, S. (2011). The potential of shading devices for temperature reduction in high-rise residential buildings in the tropics. Proceedia Engineering, 21, 273–282. https://doi.org/10.1016/j.proeng.2011.11.2015

Al-tamimi, N., Fairuz, S., & Fadzil, S. (2012). Energy-efficient envelope design for high-rise residential buildings in Malaysia. Architectural Science Review, 55(May 2012), 119–127. https://doi.org/10.1080/00038628.2012.667938

Apartment Ownership (Amendment) Act (No. 39 of 2003)

ARCADIS. (2018). Sustainable cities Index: 2018. Retrieved from https://www.arcadis.com/media/1/D/5/%7B1D5AE7E2-A348-4B6E-B1D7-6D94FA7D7567%7DSustainable_Cities_Index_2018_Arcadis.pdf

Archdaily (2020). https://www.archdaily.com/

Arifin, N. A., & Denan, Z. (2015). An Analysis of Indoor Air Temperature and Relative Humidity in Office Room with Various External Shading Devices in Malaysia. Procedia - Social and Behavioral Sciences, 179, 290–296. https://doi.org/10.1016/j.sbspro.2015.02.432

Ariyawansa, R.G, & Udayanthika, A. G. P. I. (2012). Living in high-rise: An analysis of demand for condominium properties in Colombo, International Journal of Sociology and Anthropology Vol. 4(1), pp. 31-37

Ascione, F., Bianco, N., De Masi, R. F., Mauro, G. M., & Vanoli, G. P. (2015). Design of the building envelope: A novel multi-objective approach for the optimization of energy performance and thermal comfort. Sustainability (Switzerland), 7(8), 10809–10836. https://doi.org/10.3390/su70810809

ASHRAE/IESNA. (2007). ASHRAE 90.1-2007 Standard-energy Standard for Buildings except Low-rise Residential Buildings, Appendix G.

Asyary, A., & Veruswati, M. (2020). Sunlight exposure increased Covid-19 recovery rates : A study in the central pandemic area of Indonesia. Science of the Total Environment, 729, 139016. https://doi.org/10.1016/j.scitotenv.2020.139016

Attia, S., Evrard, A., & Gratia, E. (2012). Development of benchmark models for the Egyptian residential buildings sector. Applied Energy, 94(2012), 270–284. https://doi.org/10.1016/j.apenergy.2012.01.065

Berghauser Pont M & Haupt P. (2007) The relation between urban form and density, Urban Morphology (2007), International Seminar on Urban Form

Berghauser Pont M & Haupt P. (2010) Spacematrix: Space, density and urban form. Rotterdam: Nai Publishers

Bâldea M. and Dumitrescu C. (2013). High-Density Forms in Contemporary Architecture. Acta Technica Napocensis: Civil Engineering & Architecture Vol. 56, No. 2

Branke, J., Deb, K., Dierolf, H., & Osswald, M. (2004). Finding knees in multi-objective optimization. Lecture Notes in Computer Science, 3242, 722–731. https://doi.org/10.1007/978-3-540-30217-9_73

Brownlee, A., & Wright, J. (2012). Solution analysis in multi-objective optimization. First Building Simulation and Optimization Conference, September, 317–324. https://dspace.lboro.ac.uk/2134/10275

Capeluto, I. G., & Shaviv, E. (2001). Modeling the Design of Urban Fabric With Solar Rights Considerations. Solar Energy, 70(October), 275–280.

Ceylon Electricity Board. (2014). Statistical digest

Ceylon Electricity Board (2015). Statistical digest

Ceylon Electricity Board. (2017). Transmission and Generation Planning Branch Transmission, LONG TERM GENERATION EXPANSION PLAN 2018-2037 (draft)

Cheung, C. K., Fuller, R. J., & Luther, M. B. (2005). Energy-efficient envelope design for high-rise apartments. 37(March 2004), 37–48. https://doi.org/10.1016/j.enbuild.2004.05.002

Cheung, C. T., Mui, K. W., & Wong, L. T. (2015). A hybrid simulation approach to predict cooling energy demand for public housing in Hong Kong. Building Simulation, 8(6), 603–611. https://doi.org/10.1007/s12273-015-0233-8

Chi, D. A., Moreno, D., & Navarro, J. (2017). Design optimisation of perforated solar façades in order to balance daylighting with thermal performance. Building and Environment, 125, 383–400. https://doi.org/10.1016/J.BUILDENV.2017.09.007

Cho, J., Yoo, C., & Kim, Y. (2014). Viability of exterior shading devices for high-rise residential buildings : Case study for cooling energy saving and economic feasibility analysis. Energy & Buildings, 82, 771–785. https://doi.org/10.1016/j.enbuild.2014.07.092

Choi, S. J., Lee, D. S., & Jo, J. H. (2017). Lighting and cooling energy assessment of multi-purpose control strategies for external movable shading devices by using shaded fraction. Energy and Buildings, 150, 328–338. https://doi.org/10.1016/j.enbuild.2017.06.030

Chua, K. J., & Chou, S. K. (2010). Evaluating the performance of shading devices and glazing types to promote energy efficiency of residential buildings. Building Simulation, 3, pages181–194.

Chung, W., Hui, Y. V., & Lam, Y. M. (2006). Benchmarking the energy efficiency of commercial buildings. Applied Energy, 83(1), 1–14. https://doi.org/10.1016/j.apenergy.2004.11.003

Coakley, D., Raftery, P., & Keane, M. (2014). A review of methods to match building energy simulation models to measured data. Renewable and Sustainable Energy Reviews, 37, 123–141. https://doi.org/10.1016/j.rser.2014.05.007

Cohen, R., & Bordass, W. (2006). Fixed and customized benchmarks for building energy performance certificates based on operational ratings. European Energy Performance of Buildings Directive at EPIC 2006 AIVC Conference, 3–8. http://eplabel.org/links/EPLabel_EPIC_paper_final_03Jul06_corr.pdf

Compagnon, R. (2004). Solar and daylight availability in the urban fabric. Energy and Buildings, 36(4), 321–328. https://doi.org/10.1016/j.enbuild.2004.01.009

Council on Tall Buildings and Urban Habitat (CTBUH). (n.d). Search skyscraper centre. https://www.skyscrapercenter.com

Council on Tall Buildings and Urban Habitat (CTBUH). (2015). Best tall buildings. Images publishing, Australia.

Council on Tall Buildings and Urban Habitat (CTBUH). (n.d.) Height criteria. Retrieved December 12, 2019, from https://www.ctbuh.org/resource/height

Curtis, William J.R. (1986). Le Corbusier : ideas and forms, Oxford Phaidon Press

Curtis, William J.R., (1982). Modern architecture since 1900, Oxford Phaidon Press

David, M., Sigrid, K., Frayret, J. M., Gilles, P., & Nicolas, G. (2015). A review and taxonomy of interactive optimization methods in operations research. ACM Transactions on Interactive Intelligent Systems, 5(3). https://doi.org/10.1145/2808234

Dawodu, A., & Cheshmehzangi, A. (2017). Impact of Floor Area Ratio (FAR) on Energy Consumption at Meso Scale in China : Case Study of Ningbo. Energy Procedia, 105(i), 3449–3455. https://doi.org/10.1016/j.egypro.2017.03.789

De Luca, F., & Dogan, T. (2019). A novel solar envelope method based on solar ordinances for urban planning. Building Simulation, 12(5), 817–834. https://doi.org/10.1007/s12273-019-0561-1

Department of Census and Statistics. (2012). Census of Population and Housing 2012 – Final Report. Retrieved from http://www.statistics.gov.lk/PopHouSat/CPH2011/Pages/Activities/Reports/FinalReport/FinalReport.pdf

Department of Census and Statistics. (2015). Statistical newsletter. Retrieved from http://www.statistics.gov.lk/Newsletters/DCSB-PUB-2015-01.pdf

Department of Land Use Policy Planning, National Land Use Policy of Sri Lanka. Retrieved fromhttp://www.luppd.gov.lk/web/images/content_image/downloads/pdf/national_land_use_policy.pdf

DOE. (n.d.). EnergyPlus Documentation. https://energyplus.net/sites/default/files/pdfs_v8.3.0/EngineeringReference.pdf

Dredge D. & Coiacetto E. (2011). Strata Title: Towards a Research Agenda for Informed Planning Practice, Planning Practice & Research, 26:4, 417-433, DOI:10.1080/02697459.2011.582383

Durvasula, S., Kok, C., Sambrook, P. N., Cumming, R. G., Lord, S. R., March, L. M., Mason, R. S., Seibel, M. J., Simpson, J. M., & Cameron, I. D. (2010). Sunlight and health: Attitudes of older people living in intermediate care facilities in southern Australia. Archives of Gerontology and Geriatrics, 51(3), e94–e99. https://doi.org/10.1016/J.ARCHGER.2010.01.008

Durvasula, S., Sambrook, P. N., & Cameron, I. D. (2012). Factors influencing adherence with therapeutic sunlight exposure in older people in intermediate care facilities. Archives of Gerontology and Geriatrics, 54(2), e234–e241. https://doi.org/10.1016/J.ARCHGER.2011.08.009

Edwards L. and Torcellini P. (2002). A Literature Review of the Effects of Natural Light on Building Occupants retrieved from http://www.osti.gov/bridge

Emmanuel, R. (2005). An Urban Approach To Climate Sensitive Design Strategies for the Tropics. Taylor & Francis. London

Ewing R.H. (2008). Characteristics, Causes, and Effects of Sprawl: A Literature Review. In: Marzluff J.M. et al. (eds.) Urban Ecology. Springer, Boston, MA

EN 17037. (2018) Daylight in buildings. (European Union)

Pererz-Lombard, L., Ortis, J., Gonzalez, R., & Maestre, I. (2009). A review of benchmarking, rating and labelling concepts within the framework of building energy certification schemes. Energy and Buildings, 41, 272–279. https://doi.org/10.1016/j.enbuild.2008.10.004

Evans G.W., Wells N.M. and Moch A. (2003). Housing and mental health: a review of the evidence and a methodological and conceptual critique. J Soc. Issues 59:475–500.

Ewing R.H. (2008). Characteristics, Causes, and Effects of Sprawl: A Literature Review. In: Marzluff J.M. et al. (eds.) Urban Ecology. Springer, Boston, MA

Ewing, R. (2010). The Impact of Urban Form on U.S. Residential Energy Use. Housing Policy Debate, 19(April 2013), 37–41. https://doi.org/10.1080/10511482.2008.9521624

Fanning D.M., (1967). Families in flats. British Medical Journal. 18; 4(5576): 382–386. Retrieved from https://www.ncbi.nlm.nih.gov/pmc/articles/PMC1748722/

Forsyth, A. (2003). Measuring Density: Working Definitions for Residential Density and Building Intensity. Design Center for American Urban Landscape, 8(8), 2–8.

Freewan, A. A. Y. (2014). Impact of external shading devices on thermal and daylighting performance of offices in hot climate regions. Solar Energy, 102, 14–30. https://doi.org/10.1016/J.SOLENER.2014.01.009

Fumo, N., Mago, P., & Luck, R. (2010). Methodology to estimate building energy consumption using EnergyPlus Benchmark Models. Energy and Buildings, 42(12), 2331–2337. https://doi.org/10.1016/j.enbuild.2010.07.027

Futrell, B. J., Ozelkan, E. C., & Brentrup, D. (2015). Optimizing complex building design for annual daylighting performance and evaluation of optimization algorithms. Energy and Buildings, 92, 234–245. https://doi.org/10.1016/j.enbuild.2015.01.017

Gao, X., & Malkawi, A. (2014). A new methodology for building energy performance benchmarking: An approach based on intelligent clustering algorithm. Energy and Buildings, 84, 607–616. https://doi.org/10.1016/j.enbuild.2014.08.030

Gauzin-Muller, D.(2002). Sustainable architecture and urbanism: concepts, technologies, examples, Basel Birkhauser

Gifford R. (2007). The Consequences of Living in High-Rise Buildings, Architectural Science Review, 50, 2007 -1, 2-17

Giridharan, R., Lau, S. S. Y., & Ganesan, S. (2005). Nocturnal heat island effect in urban residential developments of Hong Kong. Energy and Buildings, 37(9), 964–971. http://doi.org/10.1016/j.enbuild.2004.12.005

Givoni, B. (1998). Climate considerations in building and urban design. Building, 241–300. http://books.google.com/books?id=MGkArZ_berAC&pgis=1

Google Inc. (n.d.) Google maps. https://www.google.com/streetview/

Gossard, D., Lartigue, B., & Thellier, F. (2013). Multi-objective optimization of a building envelope for thermal performance using genetic algorithms and artificial neural network. Energy and Buildings, 67, 253–260. https://doi.org/10.1016/j.enbuild.2013.08.026

Grasshopper for Rhino 5.0. (n.d.). https://www.grasshopper3d.com

Grout, D. Z. (1980). Access to Sunlight: New Mexico's Solar Rights Act. 10.N.M.L.Rev.169(Winter 1980).

Gunaratna, K. L. (2006). Spatial concerns in development: a Sri Lankan perspective, New Delhi Atlantic 2006

Hamzah, B., & Lau, S. S. Y. (2016). The development of visible sky area as an alternative daylight assessment method for high-rise buildings in high-density urban environments.

Architectural Science Review, 59(3), 178–189. https://doi.org/10.1080/00038628.2014.963021

Han, Y., Taylor, J. E., & Pisello, A. L. (2017). Exploring mutual shading and mutual reflection inter-building effects on building energy performance. Applied Energy, 185, 1556–1564.

Hawkes, D., (1996). The Environmental tradition: studies in the architecture of environment, London E & FN Spon

Hawkes, D., (2008). The Environmental imagination: technics and poetics of the architectural environment, Oxon Taylor and Francis

Hawkes, D., McDonald, J., & Steemers, K.,(2002).The Selective environment, London Spon Press

Hraška, J. (2020). Approaches, Methods and Tools of Rights of Access to Sunlight around the World. Slovak Journal of Civil Engineering, 27(4), 45–52. https://doi.org/10.2478/sjce-2019-0031

Huang, L., & Zhao, S. (2017). Perforated thermal mass shading: An approach to winter solar shading and energy, shading and daylighting performance. Energies, 10(12). https://doi.org/10.3390/en10121955

Hyde, R. (2000). Climate Responsive Design. London; New York: E & FN Spon.

IPCC. (2014). Summary for Policymakers. In Climate Change 2014: Synthesis Report. Contribution of Working Groups I, II and III to the Fifth Assessment Report of the Intergovernmental Panel on Climate Change. https://doi.org/10.1017/CBO9781107415324

Jabareen, Y. R. (2006). Sustainable Urban Forms. Journal of Planning Education and Research, 26(3), 38–52. https://doi.org/10.1177/0739456X05285119

Jakubiec, J. A., & Reinhart, C. F. (2011). DIVA 2.0: Integrating daylight and thermal simulations using rhinoceros 3D, DAYSIM and EnergyPlus. Proceedings of Building Simulation 2011: 12th Conference of International Building Performance Simulation Association, 2202–2209.

Johnston N.R and Reid, S.,(2013) Multi-owned developments: a life cycle review of a developing research area, Property Management, Vol. 31 Issue: 5, pp.366-388, https://doi.org/10.1108/PM-01-2013-0003

Jones Lang La Salle. (2011). Real Estate in Sri Lanka Prospects and Potential Translating Economic Growth into Real Developments in Colombo

Kaplan, J.(2007). Sustainable design in High rise residential, CTUBH Journal Summer 2007

Khin, A., Lau, K., Salleh, E., Lim, C. H., & Sulaiman, M. Y. (2016). Potential of shading devices and glazing configurations on cooling energy savings for high-rise office buildings in hot-humid climates: The case of Malaysia. International Journal of Sustainable Built Environment, 5(2), 387–399. https://doi.org/10.1016/j.ijsbe.2016.04.004

Khoshnevisan, S., Gong, W., Wang, L., & Juang, C. H. (2014). Robust design in geotechnical engineering – an update. Georisk, 8(4), 217–234. https://doi.org/10.1080/17499518.2014.980274

Kim, J. (2013). Adaptive façade design for the daylighting performance in an office building: The investigation of an opening design strategy with cellular automata. International Journal of Low-Carbon Technologies, 10(3), 313–320. https://doi.org/10.1093/ijlct/ctt015

Kim, J. T., & Kim, G. (2010). Advanced External Shading Device to Maximize Visual and View Performance. Indoor and Built Environment, 19(1), 65–72. https://doi.org/https://doi.org/10.1177/1420326X09358001

Knowles, R. L. (2003). The solar envelope: its meaning for energy and buildings. Energy and Buildings, 35(35), 15–25. https://doi.org/10.1192/bjp.111.479.1009-a

Ko, Y. (2013). Urban form and residential energy use: A review of design principles and empirical findings. Journal of Planning Literature, 28(4), 327–351. https://doi.org/10.1177/0885412213491499

Koenigsberger, O. H., T. G. Ingersoll, A. Mayhew, S., Szokolay V.S. (1973). Manual of Tropical Housing and Building Design. London: Longman.

Kosir, M., & Sprah, N. (2019). Daylight Provision Requirements According to EN 17037 as a Restriction for Sustainable Urban Planning of Residential Developments. Sustainability, 12(1), 1–22. https://doi.org/10.3390/su12010315

Kwofie, T. E., Fugar, F., Adinyira, E., & Ahadzie, D. K. (2014). Identification and Classification of the Unique Features of Mass Housing Projects. Journal of Construction Engineering, 2014. http://dx.doi.org/10.1155/2014/927652

Lai, C. M., & Wang, Y. H. (2011). Energy-saving potential of building envelope designs in residential houses in Taiwan. Energies, 4(11), 2061–2076. https://doi.org/10.3390/en4112061

Lam, J. C. (2000). Shading effects due to nearby buildings and energy implications. Energy Conversion and Management, 41(7), 647–659. https://doi.org/10.1016/S0196-8904(99)00138-7

Lansiaux, É., Pébaÿ, P. P., Picard, J., & Forget, J. (2020). Spatial and Spatio-temporal Epidemiology Covid-19 and vit-d : Disease mortality negatively correlates with sunlight exposure. 0. https://doi.org/10.1016/j.sste.2020.100362

Lau, K. L., Ng, E., & He, Z. J. (2011). Residents' preference of solar access in high-density sub-tropical cities. Solar Energy, 85(9), 1878–1890. https://doi.org/10.1016/j.solener.2011.04.026

Laukkarinen, A., Kero, P., & Vinha, J. (2018). Condensation at the exterior surface of windows. Journal of Building Engineering, 19, 592–601. https://doi.org/10.1016/J.JOBE.2018.06.014

Lavin, C., & Fiorito, F. (2017). Optimization of an External Perforated Screen for Improved Daylighting and Thermal Performance of an Office Space. Procedia Engineering, 180, 571–581. https://doi.org/10.1016/j.proeng.2017.04.216

LEED BD+C: Healthcare | v4 - LEED v4 Daylight. (n.d.). Leadership in Energy and Environmental Design (LEED).

Li, C., Song, Y., & Kaza, N. (2018). Urban form and household electricity consumption: A multilevel study. Energy and Buildings, 158, 181–193. https://doi.org/10.1016/j.enbuild.2017.10.007

Li, D. H. W., Wong, S. L., Tsang, C. L., & Cheung, G. H. W. (2006). A study of the daylighting performance and energy use in heavily obstructed residential buildings via computer simulation techniques. Energy and Buildings, 38(11), 1343–1348. https://doi.org/10.1016/j.enbuild.2006.04.001

Lim, T., Yim, W.S., Kim, D.D., 2020. Evaluation of daylight and cooling performance of shading devices in residential buildings in South Korea. Energies 13. https://doi.org/10.3390/en13184749

Lima, I., Scalco, V., & Lamberts, R. (2019). Estimating the impact of urban densification on high-rise office building cooling loads in a hot and humid climate. In Energy and Buildings (Vol. 182, pp. 30–44). https://doi.org/10.1016/j.enbuild.2018.10.019

Lin, H., Xiao, Y., & Musso, F. (2018). Shading Effect and Heat Reflection Performance of Green Façade in Hot Humid Climate Area: Measurements of a Residential Project in Guangzhou, China. IOP Conference Series: Earth and Environmental Science, 146, 012006. https://doi.org/10.1088/1755-1315/146/1/012006

Lobaccaro, G., Carlucci, S., Croce, S., Paparella, R., & Finocchiaro, L. (2017). Boosting solar accessibility and potential of urban districts in the Nordic climate: A case study in Trondheim. Solar Energy, 149, 347–369. https://doi.org/10.1016/J.SOLENER.2017.04.015

Lu, L., Anderson-Cook, C. M., & Robinson, T. J. (2011). Optimization of designed experiments based on multiple criteria utilizing a pareto frontier. Technometrics, 53(4), 353–365. https://doi.org/10.1198/TECH.2011.10087

Lu, M., & Du, J. (2013). Assessing the daylight and sunlight availability in high- density residential areas : a case in North-east China. Architectural Science Review, November 2014, 37–41. https://doi.org/10.1080/00038628.2012.729311

Machairas, V., Tsangrassoulis, A., & Axarli, K. (2014). Algorithms for optimization of building design : A review. Renewable and Sustainable Energy Reviews, 31, 101–112.

Méndez Echenagucia, T., Capozzoli, A., Cascone, Y., & Sassone, M. (2015). The early design stage of a building envelope: Multi-objective search through heating, cooling and lighting energy performance analysis. Applied Energy, 154, 577–591. https://doi.org/10.1016/j.apenergy.2015.04.090

Ministry of Housing and Construction. (2017). National Housing Policy -Revision of 2017. Retrieved from https://drive.google.com/file/d/0B6o-6gqv4JNBRGFfRE1IWXRvXzQ/view

Ministry of Megapolis and Western Development, Master plan 2030. Retrieved from https://megapolis.gov.lk/downloads/ on 01.12.2017

Mustafaraj, G., Marini, D., Costa, A., & Keane, M. (2014). Model calibration for building energy efficiency simulation. 130, 72–85. https://doi.org/10.1016/j.apenergy.2014.05.019

Natanian, J., Aleksandrowicz, O., & Auer, T. (2019). A parametric approach to optimizing urban form, energy balance and environmental quality: The case of Mediterranean districts. Applied Energy, 254(June), 113637. https://doi.org/10.1016/j.apenergy.2019.113637

National Environment Agency (NEA). (2017). Household energy consumption study, 2017. https://www.e2singapore.gov.sg/overview/households/saving-energy-at-home/households-studies

Nebia, B., & Aoul, K. T. (2017). Overheating and daylighting; assessment tool in early design of London’s high-rise residential buildings. Sustainability (Switzerland), 9(9). https://doi.org/10.3390/su9091544

Nejat, P., Jomehzadeh, F., Mahdi, M., & Gohari, M. (2015). A global review of energy consumption, CO 2 emissions and policy in the residential sector (with an overview of the top ten CO 2 emitting countries). Renewable and Sustainable Energy Reviews, 43, 843–862. https://doi.org/10.1016/j.rser.2014.11.066

Newman, P., & Kenworthy, J. (2006). Urban Design to Reduce Automobile Dependence. Opolis: An International Journal of Suburban and Metropolitan Studies, 2(1).

Ng, E. (2003). Studies on Daylight Design and Regulation of High-density Residential Housing in Hong Kong. Lighting Research & Technology, 35(2), 127–139.

Nguyen, A. T., Reiter, S., & Rigo, P. (2014). A review on simulation-based optimization methods applied to building performance analysis. Applied Energy, 113, 1043–1058. https://doi.org/10.1016/j.apenergy.2013.08.061

Nikolaou, T., Kolokotsa, D., & Stavrakakis, G. (2011). Advances in Building Energy Research Review on methodologies for energy benchmarking , rating and classification of buildings Review on methodologies for energy benchmarking , rating and classification of buildings. Advances in Building Energy Research, 5(1), 53–70. https://doi.org/10.1080/17512549.2011.582340

Norman, J., MacLean, H. L., & Kennedy, C. A. (2006). Comparing High and Low Residential Density: Life-Cycle Analysis of Energy Use and Greenhouse Gas Emissions.

Journal of Urban Planning and Development, 132(1), 10–21. https://doi.org/10.1061/(ASCE)0733-9488(2006)132:1(10)

O'Brien, W. T., Kennedy, C. A., Athienitis, A. K., & Kesik, T. J. (2010). The relationship between net energy use and the urban density of solar buildings. Environment and Planning B: Planning and Design, 37(6), 1002–1021. https://doi.org/10.1068/b36030

Offiong, A., & Ukpoho, A. U. (2004). External window shading treatment effects on internal environmental temperature of buildings. Renewable Energy, 29(14), 2153–2165. https://doi.org/10.1016/j.renene.2003.11.015

Patterson, M. G. (1996). What is energy efficiency? Concepts, indicators and methodological issues. Energy Policy, 24(5), 377–390. https://doi.org/10.1016/0301-4215(96)00017-1

Pérez-Lombard, L., Ortiz, J., González, R., & Maestre, I. R. (2009). A review of benchmarking, rating and labelling concepts within the framework of building energy certification schemes. In Energy and Buildings (Vol. 41, Issue 3, pp. 272–278). https://doi.org/10.1016/j.enbuild.2008.10.004

Pisello, A. L., Castaldo, V. L., Taylor, J. E., & Cotana, F. (2014). Expanding Inter-Building Effect modeling to examine primary energy for lighting. Energy and Buildings, 76, 513–523. https://doi.org/10.1016/j.enbuild.2014.02.081

Pisello, A. L., Taylor, J. E., Xu, X., & Cotana, F. (2012). Inter-building effect: Simulating the impact of a network of buildings on the accuracy of building energy performance predictions. Building and Environment, 58, 37–45. https://doi.org/10.1016/J.BUILDENV.2012.06.017

Quan, S. J., Economou, A., Grasl, T., & Yang, P. P. J. (2014). Computing energy performance of building density, shape and typology in urban context. Energy Procedia, 61, 1602–1605. https://doi.org/10.1016/j.egypro.2014.12.181

Quan, S. J., Wu, J., Wang, Y., Shi, Z., Yang, T., & Yang, P. P. J. (2016). Urban form and building energy performance in Shanghai neighborhoods. Energy Procedia, 88, 126–132. https://doi.org/10.1016/j.egypro.2016.06.035

Rajapaksha, U., & Jayaweera, N. (2018). Condominium development in Sri Lanka: Current status and recommendations. University of Moratuwa, Sri Lanka.

Rajasekar, E., & Ramachandraiah, A. (2011). A study on thermal parameters in residential buildings associated with hot humid environments. Architectural Science Review, 54(1), 23–38. https://doi.org/10.3763/asre.2009.0082

Ramos, G., & Ghisi, E. (2010). Analysis of daylight calculated using the EnergyPlus programme. Renewable and Sustainable Energy Reviews, 14(7), 1948–1958. https://doi.org/10.1016/J.RSER.2010.03.040

Rapport, A. (1969), House, Form and Culture, New Jersey Prentice Hall

Ratcliffe, M., & Day, T. (2004). Improving Office Staff Productivity while Reducing Carbon Dioxide Emissions. Cibse, 1–10. www.cibse.org/pdfs/8aratcliffe.pdf

Ratti, C., Baker, N., & Steemers, K. (2015). Energy consumption and urban texture. Energy and Buildings, 37(7), 762–776. https://doi.org/10.1016/j.enbuild.2004.10.010

Razzaque, M. S. (2018). Sunlight exposure: Do health benefits outweigh harm? The Journal of Steroid Biochemistry and Molecular Biology, 175, 44–48. https://doi.org/10.1016/J.JSBMB.2016.09.004

RECS. (2009). Survey Data Consumption and Expenditures, accessible from: http://www.eia.gov/consumption/residential/data/2009/index.cfm? view¼consumption

Reinhart, C. F., Dogan, T., Jakubiec, J. A., Rakha, T., & Sang, A. (2013). UMI - An urban simulation environment for building energy use, daylighting and walkability. Proceedings of BS 2013: 13th Conference of the International Building Performance Simulation Association, July 2014, 476–483.

Resch, E., André, R., Kvamsdal, T., & Lohne, J. (2016). Impact of urban density and building height on energy use in cities. Energy Procedia, 96(1876), 800–814. https://doi.org/10.1016/j.egypro.2016.09.142

Rhinoceros, version 5. (n.d.). https://www.rhino3d.com/

Rode, P., Keim, C., Robazza, G., Viejo, P., & Schofield, J. (2014). Cities and energy: Urban morphology and residential heat-energy demand. Environment and Planning B: Planning and Design, 41(1), 138–162. https://doi.org/10.1068/b39065

Rosen G, & Walks A.(2013).Castles in Toronto’s sky: condo-ism and urban transformation, Journal of Urban Affairs, Volume 37, Issue 3, 289–310

Rossi, A. (1931). The Architecture of the city, MIT Press, Cambridge, UK

Roy, R., Hinduja, S., & Teti, R. (2008). Recent advances in engineering design optimisation: Challenges and future trends. CIRP Annals - Manufacturing Technology, 57(2), 697–715. https://doi.org/10.1016/j.cirp.2008.09.007

Ruiz, G. R., & Bandera, C. F. (2017). Validation of calibrated energy models: Common errors. Energies, 10(10). https://doi.org/10.3390/en10101587

Sakamoto, R. R. (2019). Sunlight in Vitamin D Deficiency: Clinical Implications. The Journal for Nurse Practitioners, 15(4), 282–285. https://doi.org/10.1016/J.NURPRA.2019.01.014

Samuelson, H., Claussnitzer, S., Goyal, A., Chen, Y., & Romo-castillo, A. (2016). Parametric energy simulation in early design : High-rise residential buildings in urban contexts. Building and Environment, 101, 19–31. https://doi.org/10.1016/j.buildenv.2016.02.018

Santamouris, M., Cartalis, C., Synnefa, A., & Kolokotsa, D. (2015). On the impact of urban heat island and global warming on the power demand and electricity consumption of buildings - A review. Energy and Buildings, 98, 119–124. https://doi.org/10.1016/j.enbuild.2014.09.052

Santamouris, M. (Ed.) (2001). Energy and climate in the urban built environment. James and James London.

Santos, I. G. dos, Auer, T., & Souza, R. V. G. de. (2017). Optimized indoor daylight for tropical dense urban environments. Ambiente Construído, 17(3), 87–102. https://doi.org/10.1590/s1678-86212017000300164

Senaratne, S., Zainudeen, N.,& Weddikkara,C.,(2006). Factors Affecting Condominium: Development In Sri Lanka, Built-Environment-Sri Lanka - Vol. 07, Issue 01

Seong, Y. B., Lim, J. H., Yeo, M. S., Goh, I. Du, & Kim, K. W. (2006). HELIOS: Solar rights analysis system for apartment buildings. Solar Energy, 80(6), 723–741. https://doi.org/10.1016/j.solener.2005.11.008

Shabunko, V., Lim, C. M., Brahim, S., & Mathew, S. (2014). Developing building benchmarking for Brunei Darussalam. Energy and Buildings, 85, 79–85. https://doi.org/10.1016/j.enbuild.2014.08.047

Shahdan, M. S., Ahmad, S. S., & Hussin, M. A. (2018). External shading devices for energy efficient building. IOP Conference Series: Earth and Environmental Science, 117(1). https://doi.org/10.1088/1755-1315/117/1/012034

Shaviv, E., & Yezioro, A. (1997). Analyzing mutual shading among buildings. Solar Energy, 59(1–3), 83–88. https://doi.org/10.1016/S0038-092X(96)00103-X

Sherif, A., Sabry, H., & Rakha, T. (2012). External perforated Solar Screens for daylighting in residential desert buildings: Identification of minimum perforation percentages. Solar Energy, 86(6), 1929–1940. https://doi.org/10.1016/J.SOLENER.2012.02.029

Shi, X. (2011). Design optimization of insulation usage and space conditioning load using energy simulation and genetic algorithm. Energy, 36(3), 1659–1667. https://doi.org/10.1016/j.energy.2010.12.064

Shi, Z., Fonseca, J. A., & Schlueter, A. (2017). A review of simulation-based urban form generation and optimization for energy-driven urban design. Building and Environment, 121, 119–129. https://doi.org/10.1016/j.buildenv.2017.05.006

Soebarto, V. I., & Ph, D. (1997). Calibration of Hourly Energy Simulations Using HourlyMonitored Data and Monthly Utility Recordsfor Two Case Study Buildings. Http://Www.Ibpsa.Org/Proceedings/BS1997/BS97_P017.Pdf, March. http://www.ibpsa.org/proceedings/BS1997/BS97_P017.pdf

Steemers, K. (2003). Energy and the city: density, buildings and transport. Energy and Buildings, 35(1), 3–14. https://doi.org/10.1016/S0378-7788(02)00075-0

Tereci, A., Ozkan, S. T. E., & Eicker, U. (2013). Energy benchmarking for residential buildings. Energy and Buildings, 60, 92–99. https://doi.org/10.1016/j.enbuild.2012.12.004

Tian, Z., Zhang, X., Jin, X., Zhou, X., Si, B., & Shi, X. (2018). Towards adoption of building energy simulation and optimization for passive building design: A survey and a review. Energy and Buildings, 158(November), 1306–1316. https://doi.org/10.1016/j.enbuild.2017.11.022

Toutou, A., Fikry, M., & Mohamed, W. (2018). The parametric based optimization framework daylighting and energy performance in residential buildings in hot arid zone. Alexandria Engineering Journal, 57(4), 3595–3608. https://doi.org/10.1016/j.aej.2018.04.006

Urban Development Authority. (1999). City of Colombo Development Plan-1999

Urban Development Authority. (2005). Building and planning regulations made easy.

Urban Development Authority. (2008). City of Colombo Development Plan (Amendment)-2008

Urban Development Authority. (2008). Development plan for the Dehiwela-Mount Lavinia Municipal Council area

Urban Development Authority. (2015). Planning and building regulations (General)

Urban Development Authority. Planning and Building regualtions-2008-2020

Urban Redevelopment Authority of Singapore. (2019). The handbook Development control parameters for residential development. Retrieved from https://www.ura.gov.sg/uol/publications/technical/dc-handbooks.

Urban, F. (2011). Tower and Slab: Histories of Global Mass Housing. Routledge.

Valladares-Rendón, L. G., Schmid, G., & Lo, S. L. (2017). Review on energy savings by solar control techniques and optimal building orientation for the strategic placement of façade shading systems. Energy and Buildings, 140(71), 458–479. https://doi.org/10.1016/j.enbuild.2016.12.073

Van der Rhee, H. J., de Vries, E., & Coebergh, J. W. (2016). Regular sun exposure benefits health. Medical Hypotheses, 97, 34–37. https://doi.org/10.1016/J.MEHY.2016.10.011

Vermeulen, T., Knopf-Lenoir, C., Villon, P., & Beckers, B. (2015). Urban layout optimization framework to maximize direct solar irradiation. Computers, Environment and Urban Systems, 51, 1–12. https://doi.org/10.1016/j.compenvurbsys.2015.01.001

Versage, R., Melo, A. P., & Lamberts, R. (2010). Impact of Different Daylighting Simulation Results on the Prediction of Total Energy Consumption. SimBuild 2010, 1–7.

Western Region and Megapolis Planning Authority of Sri Lanka(WRMP), Megapolis Regulations and Guidelines - Planning, Zoning, Environmental and Building Draft retrieved from https://megapolis.gov.lk/downloads/. Accessed on 27/10/2017.

Williams, K., Burton, E. and Jenks, M. eds. (2000.) Achieving sustainable urban form, London E & FN Spon

Wong, N. H., & Li, S. (2007). A study of the effectiveness of passive climate control in naturally ventilated residential buildings in Singapore. Building and Environment, 42(3), 1395–1405. https://doi.org/10.1016/j.buildenv.2005.11.032

Wong, Nyuk Hien, & Istiadji, A. D. (2004). Effect of external shading devices on daylighting penetration in residential buildings. Lighting Research and Technology, 36(4), 317–333. https://doi.org/10.1191/1365782804li126oa

World Bank. (2016). Leveraging Urbanization in South Asia. http://library1.nida.ac.th/termpaper6/sd/2554/19755.pdf

Wu, H., Wang, D., Liu, Y., & Wang, Y. (2017). Study on the effect of building envelope on cooling load and life-cycle cost in low latitude and hot-humid climate. Procedia Engineering, 205, 975–982. https://doi.org/10.1016/j.proeng.2017.10.153

Wüstenrot Foundation. (n.d.). Brutalism. http://www.brutalismus.com/e/?/concept/

Xie, J.C., Xue, P., Mak, C.M., Liu, J.P., 2017. Balancing energy and daylighting performances for envelope design: A new index and proposition of a case study in Hong Kong. Appl. Energy 205, 13–22 https://doi.org/10.1016/j.apenergy.2017.07.115

Xue, P., Mak, C. M., & Cheung, H. D. (2014). The effects of daylighting and human behavior on luminous comfort in residential buildings: A questionnaire survey. Building and Environment, 81(November), 51–59. https://doi.org/10.1016/j.buildenv.2014.06.011

Yang, F. (2016). High-Rise Urban Form and Environmental Performance - An Overview on Integrated Approaches to Urban Design. International Journal of High-Rise Buildings, 5(2), 87–9

Yeang K. (1994). Bioclimatic skyscrapers, London Artemis

Yi, Y. K., & Kim, H. (2015). Agent-based geometry optimization with Genetic Algorithm (GA) for tall apartment's solar right. Solar Energy, 113, 236–250. https://doi.org/10.1016/j.solener.2014.11.007

Yıldız, Y. & Arsan, Z.D.(2011).Identification of the building parameters that influence heating and cooling energy loads for apartment buildings in hot-humid climates, Energy, Volume 36, Issue 7,Pages 4287-4296,ISSN 0360-5442, https://doi.org/10.1016/j.energy.2011.04.013.

Yoon, Y. B., Manandhar, R., & Lee, K. H. (2014). Comparative study of two daylighting analysis methods with regard to window orientation and interior wall reflectance. Energies, 7(9), 5825–5846. https://doi.org/10.3390/en7095825

Yuen, B, Yeh, A. and Appold, S.J. (2006). High-rise Living in Singapore Public Housing, Urban Studies, 4

Yuen, B., and Yeh, A. (2011). High-Rise Living in Asian Cities, Springer

Zhang, A., Bokel, R., van den Dobbelsteen, A., Sun, Y., Huang, Q., & Zhang, Q. (2017). Optimization of thermal and daylight performance of school buildings based on a multi-objective genetic algorithm in the cold climate of China. Energy and Buildings, 139, 371–384. https://doi.org/10.1016/j.enbuild.2017.01.048

Zhang, J., Xu, L., Shabunko, V., Tay, S. E. R., Sun, H., Lau, S. S. Y., & Reindl, T. (2019). Impact of urban block typology on building solar potential and energy use efficiency in tropical high-density city. Applied Energy, 240, 513–533. https://doi.org/10.1016/j.apenergy.2019.02.033

Appendix A- The zoning plan-2020 of the Colombo Metropolitan region

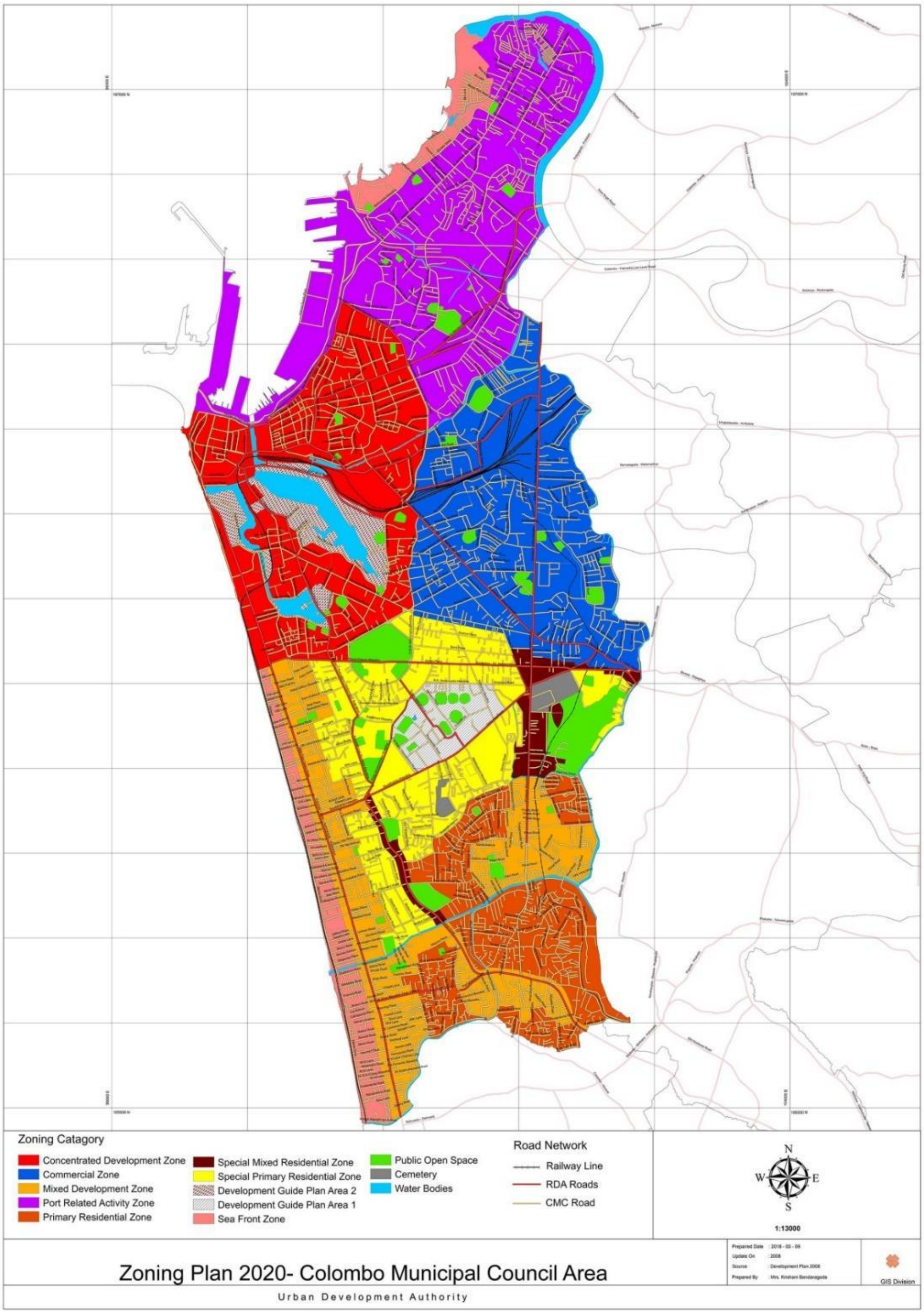

Source: https://www.uda.gov.lk/

Appendix B- Building setback regulations in Sri Lanka

Building	Maximum number of floors including ground floor	Colombo Metropolitan Region			Dehiwela-Mt.Lavina Municipal area			
		Min. rear space (m)	Min. one side space (m)	Min. space on each side (m)	Min. rear space (m)	Min. on sides (m)		Setback in side
						one side	other side	
Low rise	Ground floor	2.3	-	-	2.3	-	-	1
	2	2.3	-	-	3	-	-	1
	3	3	-	-	3.5	-	-	1
	4	3	-	-	4	-	-	1.5
Intermediate	5	3	2	-	4	-	-	1.5
	6	4	2	-	4	-	-	2
	7	4	3	-	4.5	2	-	2
	8	4	3	-	5	2	2	3
Middle rise	9	5	-	2	5.5	3	3	3
	10	5	-	3	6	4	3	3
	11	5	-	3	6	5	3	4
	12	5	-	3	7	6	3	5
High rise	13	6	-	4	10	6	6	5.5
	14	6	-	4	10	6	6	5.5
	15-20	6	-	6	10	6	6	5.5
	21 and above	6	-	6	10	6	6	5.5

Sources:

Urban Development Authority. (2008). City of Colombo Development Plan (Amendment)-2008

Urban Development Authority. Planning and Building regualtions-2008-2020

Appendix C- Building setback regulations in Singapore for condominiums

Storey Height	Common Boundary Setback for Condominiums		Storey Height	Common Boundary Setback for Condominiums
1	3.0 m		19	11.1 m
2			20	11.3 m
3	3.4 m		21	11.6 m
4	3.8 m		22	11.8 m
5	4.7 m		23	12.1 m
6	5.5 m		24	12.4 m
7	6.4 m		25	12.7 m
8	7.2 m		26	12.9 m
9	8.0 m		27	13.2 m
10	8.7 m		28	13.4 m
11	9.0 m		29	13.7 m
12	9.2 m		30	14.0 m
13	9.5 m		31	14.2 m
14	9.8 m		32	14.5 m
15	10.1 m		33	14.7 m
16	10.3 m		34	15.0 m
17	10.6 m		35	15.2 m
18	10.8 m		36 and above	15.5 m

Note: A 2 m-wide (minimum) planting strip is to be provided along all common boundaries of the development site.

Source:

Urban Redevelopment Authority of Singapore. (2019). The handbook Development control parameters for residential development. Retrieved from https://www.ura.gov.sg/uol/publications/technical/dc-handbooks.

Appendix D- Comparison of urban density parameters, solar access indicators, climate of study and building typology

Urban density measures	solar access indicators				Climate conditions				Building type		
	Solar irradiation/ hours/volume	**Energy use for daylight**	**Energy for cooling/heating**	**Indoor Daylight levels/hours**	**Continental climate**	**Temperate /Mediterranean climate**	**Tropical climate *(sub-tropical)**	**Dry climate**	**Commercial**	**Residential**	**Building not classified/urban context**
FAR	(Dawodu & Cheshmehzangi, 2017)	(Samuelson et al., 2016)	(Ratcliffe & Day, 2004)(Quan et al., 2014) (Quan et al., 2016) (Natanian et al., 2019)	(Kosir & Sprah, 2019) (Natanian et al., 2019) (Saratsis et al., 2017)	(Kosir & Sprah, 2019) (Saratsis et al., 2017)	(Dawodu & Cheshmehzangi, 2017) (Natanian et al., 2019)	* (Quan et al., 2016)		(Natanian et al., 2019)	(Quan et al., 2016) (Natanian et al., 2019) (Kosir & Sprah, 2019) (Dawodu & Cheshmehzangi, 2017)	(Saratsis et al., 2017)
Plot ratio	(Epstein & Moran, 2006) (Compagnon, 2004)(Lobaccaro et al., 2017)		(Quan et al., 2014)(Steemers, 2003)(Lobaccaro et al., 2017)			(Quan et al., 2014) (Compagnon, 2004)					(Compagnon, 2004)
Setback/ Distance between buildings	(Alzoubi & Alshboul, 2010) (Capeluto & Shaviv, 2001b)		(Natanian et al., 2019)	(Natanian et al., 2019)		(Capeluto & Shaviv, 2001b)		(Alzoubi & Alshboul, 2010)		(Alzoubi & Alshboul, 2010)	(Capeluto & Shaviv, 2001b)

Urban density	solar access indicators				Climate conditions				Building type		
	Solar irradiation/ hours/volume	**Energy use for daylight**	**Energy for cooling/heating**	**Indoor Daylight levels/hours**	**Continental climate**	**Temperate /Mediterranean climate**	**Tropical climate *(sub-tropical)**	**Dry climate**	**Commercial**	**Residential**	**Building not classified/urban context**
Height	(Vermeulen et al., 2015) (Capeluto & Shaviv, 2001b) (De Luca & Dogan, 2019)		(Resch et al., 2016)		(Vermeulen et al., 2015) (De Luca & Dogan, 2019)	(Resch et al., 2016) (De Luca & Dogan, 2019)				(Resch et al., 2016)	(Vermeulen et al., 2015) (De Luca & Dogan, 2019)
Solar azimuth	(Seong et al., 2006)		(H. J. Kim, 2016)	(H. J. Kim, 2016)	(Seong et al., 2006)	(H. J. Kim, 2016)				(H. J. Kim, 2016) (Seong et al., 2006)	
Urban Canyon/ Aspect ratio	(Strømann-Andersen & Sattrup, 2011) (Cárdenas-Jirón et al., 2014) (Lobaccaro et al., 2017)	(Strømann-Andersen & Sattrup, 2011)	(Strømann-Andersen & Sattrup, 2011) (Lobaccaro et al., 2017)	(Strømann-Andersen & Sattrup, 2011) (Fernández Expositó et al., 2015) (Santos et al., 2017)	(Strømann-Andersen & Sattrup, 2011) (Cárdenas-Jirón et al., 2014)	(Fernández Expositó et al., 2015)	(Santos et al., 2017)		(Strømann-Andersen & Sattrup, 2011)	(Strømann-Andersen & Sattrup, 2011) (Lobaccaro et al., 2017)	(Cárdenas-Jirón et al., 2014) (Fernández Expositó et al., 2015) (Santos et al., 2017)

Urban density measures	solar access indicators				Climate conditions				Building type		
	Solar irradiation/ hours/volume	Energy use for daylight	Energy for cooling/heating	Indoor Daylight levels/hours	Continental climate	Temperate /Mediterranean climate	Tropical climate *(sub-tropical)	Dry climate	Commercial	Residential	Building not classified/urban context
Angle of obstruction/ Obstruction sky view		(D. H.W. Li et al., 2006)2006)	(Steemers, 2003) (Ratti et al., 2015)(Danny H.W. Li & Wong, 2007)	(D. H.W. Li et al., 2006) Li and Wong, 2007)		(Steemers, 2003) (Ratti et al., 2015)	*(D. H.W. Li et al., 2006) *Li and Wong, 2007)		(Steemers, 2003) (Ratti et al., 2015) Li and Wong, 2007)	(Steemers, 2003) (D. H.W. Li et al., 2006)	
Visible sky area				(Hamzah & Lau, 2016)			*(Hamzah & Lau, 2016)			(Hamzah & Lau, 2016)	
Inter building effects (IBE)		(Pisello et al., 2014)	Pisello et al., 2012) (Han et al., 2017)	(Han et al., 2017)	(Pisello et al., 2012)	(Han et al., 2017) (Pisello et al., 2014)	(Pisello et al., 2012)		(Han et al., 2017) (Pisello et al., 2014)	(Pisello et al., 2012)	
Block typology/pre-defined context	(J. Zhang et al., 2019) (M. Lu & Du, 2013b)	Samuelson et al., 2016)	(O'Brien et al., 2010)(Samuelson et al., 2016) (Lima et al., 2019)	(M. Lu & Du, 2013b)	(O'Brien et al., 2010) (M. Lu & Du, 2013b)	Samuelson et al., 2016)	(J. Zhang et al., 2019) (Lima et al., 2019)		(Lima et al., 2019)	(J. Zhang et al., 2019),Samuelson et al.,2016) (O'Brien et al., 2010)(M. Lu & Du, 2013b)	

Appendix E (I) - Details of the high-rise residential buildings (between 15 and 65 units) in the sample survey

Building	units (*per tower)	Number of floors	Site extent (sq.m) (*part of a housing estate)	FAR	Plot Ratio	Linear width (m)	Linear length (m)	WWR (per typical floor)	Building setback (m)			
									front	side 1	side 2	rear
S1	16	7	558.97	6.3	0.66	23.2	24.4	0.3	-	-	-	-
S2	16	7	2033.8	4.03	0.45	17.3	17.8	-	-	-	-	-
S3	18	8	458.3	8.2	0.82	17.3	19.4	0.35	1	Blind wall	Blind wall	4.5
S4	20	6	754.6	4.4	0.73	13.4	37	-	2.3		2	4.3
S5	26	10	689	7.3	0.74	15	32.4	0.38	3.8	Blind wall	3	4
S6	28	8	232.5	5.8	0.81	14	21	-	1.6	-	-	3.2
S7	32	9	605	7.6	0.81	19.2	22.7	0.38	1.5	1.5	Blind wall	4.1
S8	32	10	725.4	7.1	0.74	19	26	0.35		-	2.3	3.3
S9	36	10	823	7.3	0.73	24	32	0.3	2.1	-	varies	3.7
S10	42	9	831.6	6.7	0.81	18.8	36.7	-	2.5	Blind wall	Blind wall	4.2
S11	48	8	1121.8	6.4	0.59	22.5	24.8	0.38	1.5	Blind wall	2	4.5

Appendix E (II-)Details of the high-rise residential buildings (over 65 units) in the sample survey

Building	units (*per tower)	Number of floors	Site extent (sq.m) (*part of a housing estate)	FAR	Plot Ratio	Linear width (m)	Linear length (m)	WWR (per typical floor)	Building setback (m)			
									front	side 1	side 2	rear
S12	66	11	1043.7	7.1	0.69	20	32.8	0.38	3.7	-	2	6.4
S13	88	14	1922	8.2	0.97	30	43	0.42	3.3	4.7	6.6	5
S14	94	12	*9397	-	--	55	56	-	-	-	-	-
S15	110	31	3424	8.3	0.48	20	53	0.34	8	9.5	11.2	8.4
S16	112	23	*66759	-	-	43	43	-	-	-	-	-
S17	113	25	*66759	-	-	34	56	0.3	-	-	-	-
S18	140	13	7664	3.2	0.5	48.4	48.4	-	-	-	-	-
S19	142	18	4046.86	6.1	0.44	51	31	0.4	3	12.3	4.4	7.7
S20	142	13	7953	3	0.3	-	-	-	-	-		-
S21	*151	38	7000	9.2	0.62	-	-	-	9	8.5	4	8.7
S22	197	30	7153	6.2	0.2	27.2	59.6	0.4	-	-	-	-

Appendix F- External shading scenarios

HS-Horizontal shading

CS-Combined shading

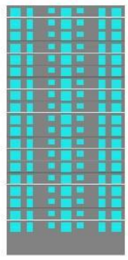 C1			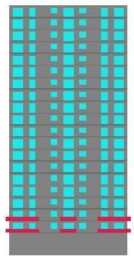 C2			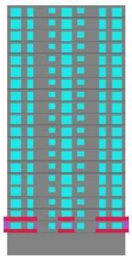 C3		
20_FL	11_FL	2_FL	20_FL	11_FL	2_FL	20_FL	11_FL	2_FL
None	None	None	None	None	HS	None	None	CS
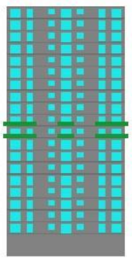 C4			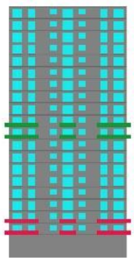 C5			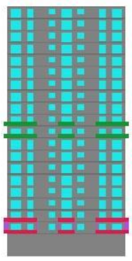 C6		
20_FL	11_FL	2_FL	20_FL	11_FL	2_FL	20_FL	11_FL	2_FL
None	HS	None	None	HS	HS	None	HS	CS
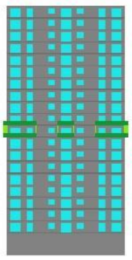 C7			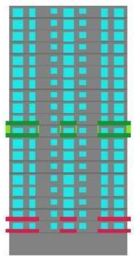 C8			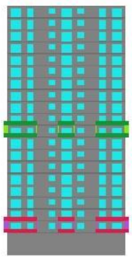 C9		
20_FL	11_FL	2_FL	20_FL	11_FL	2_FL	20_FL	11_FL	2_FL
None	CS	None	None	CS	HS	None	CS	CS

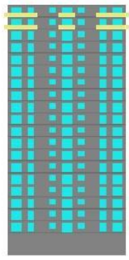 C10			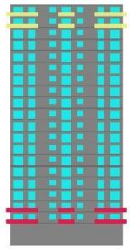 C11			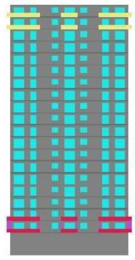 C12		
20_FL	11_FL	2_FL	20_FL	11_FL	2_FL	20_FL	11_FL	2_FL
HS	None	None	HS	None	HS	HS	None	CS
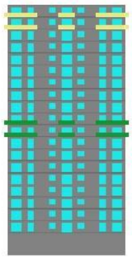 C13			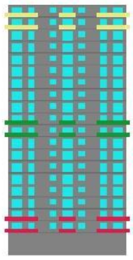 C14 (Baseline)			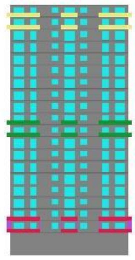 C15		
20_FL	11_FL	2_FL	20_FL	11_FL	2_FL	20_FL	11_FL	2_FL
HS	HS	None	HS	HS	HS	HS	HS	CS
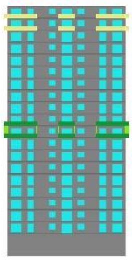 C16			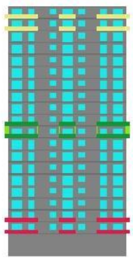 C17			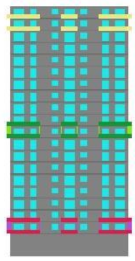 C18		
20_FL	11_FL	2_FL	20_FL	11_FL	2_FL	20_FL	11_FL	2_FL
HS	CS	None	HS	CS	HS	HS	CS	CS

<table>
<tr><td colspan="3">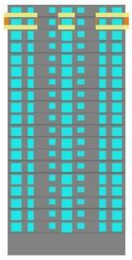
C19</td><td colspan="3">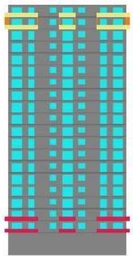
C20</td><td colspan="3">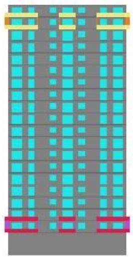
C21</td></tr>
<tr><td>20_FL</td><td>11_FL</td><td>2_FL</td><td>20_FL</td><td>11_FL</td><td>2_FL</td><td>20_FL</td><td>11_FL</td><td>2_FL</td></tr>
<tr><td>CS</td><td>None</td><td>None</td><td>CS</td><td>None</td><td>HS</td><td>CS</td><td>None</td><td>CS</td></tr>
<tr><td colspan="3">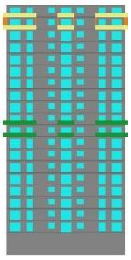
C22</td><td colspan="3">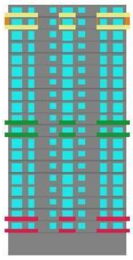
C23</td><td colspan="3">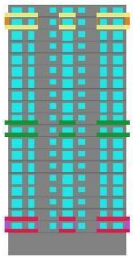
C24</td></tr>
<tr><td>20_FL</td><td>11_FL</td><td>2_FL</td><td>20_FL</td><td>11_FL</td><td>2_FL</td><td>20_FL</td><td>11_FL</td><td>2_FL</td></tr>
<tr><td>CS</td><td>HS</td><td>None</td><td>CS</td><td>HS</td><td>HS</td><td>CS</td><td>HS</td><td>CS</td></tr>
<tr><td colspan="3">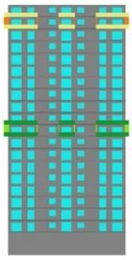
C25</td><td colspan="3">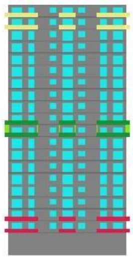
C26</td><td colspan="3">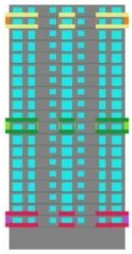
C27</td></tr>
<tr><td>20_FL</td><td>11_FL</td><td>2_FL</td><td>20_FL</td><td>11_FL</td><td>2_FL</td><td>20_FL</td><td>11_FL</td><td>2_FL</td></tr>
<tr><td>CS</td><td>CS</td><td>None</td><td>CS</td><td>CS</td><td>HS</td><td>CS</td><td>CS</td><td>CS</td></tr>
</table>

Appendix G- Effects of the urban context on spatial daylight Autonomy (sDA) in SM2 and SM3

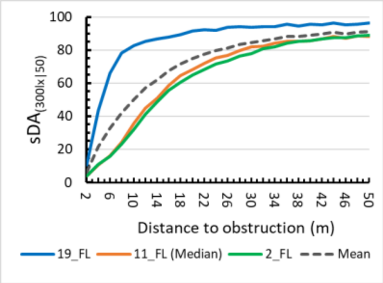

sDA in SM2 facing east

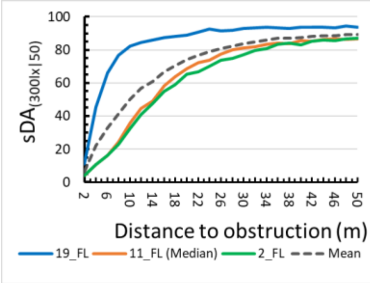

sDA in SM2 facing west

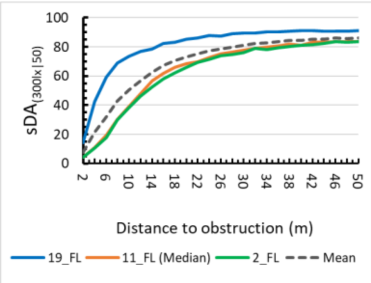

sDA in SM2 facing north

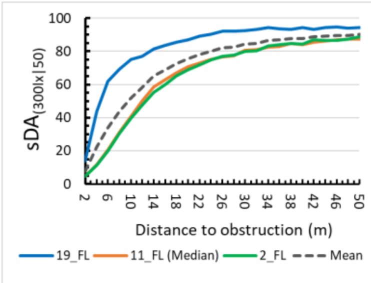

sDA in SM1 facing south

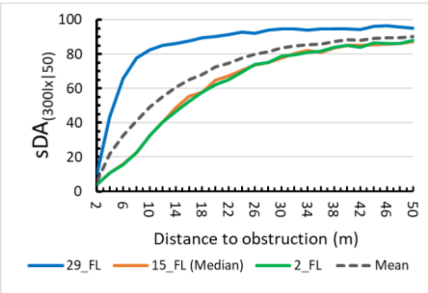

sDA in SM3 facing east

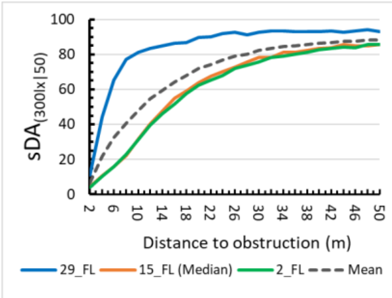

sDA in SM3 facing west

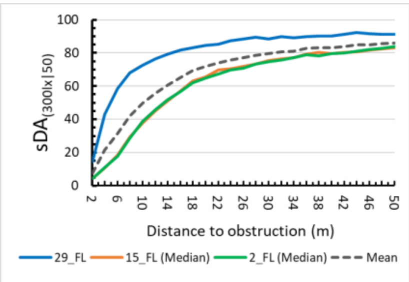

sDA in SM3 facing north

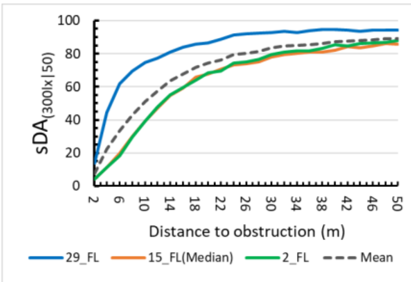

sDA in SM3 facing south

Appendix H- Effects of the urban context on cooling energy use in SM2 and SM3

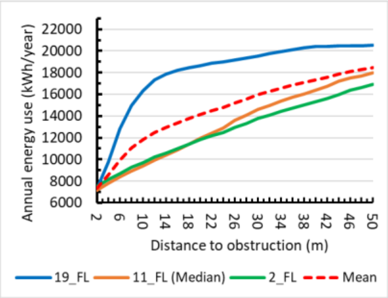

Cooling energy in SM2 facing east

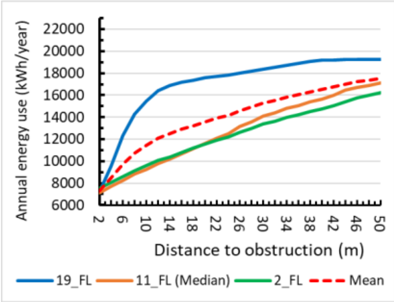

Cooling energy in SM2 facing west

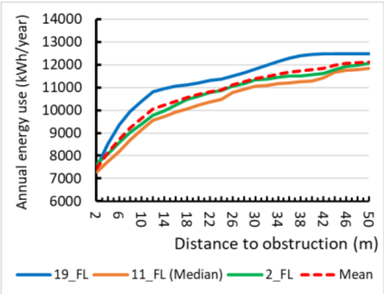

Cooling energy in SM2 facing north

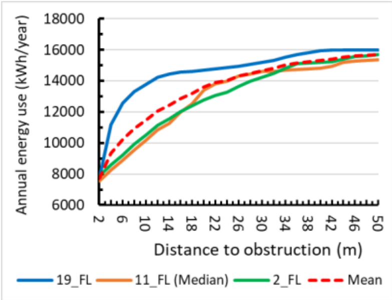

Cooling energy in SM2 facing south

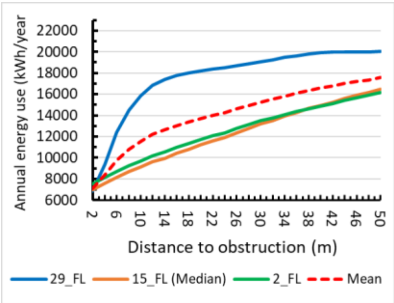

Cooling energy in SM3 facing east

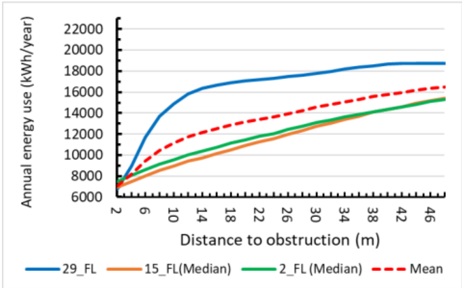

Cooling energy in SM3 facing west

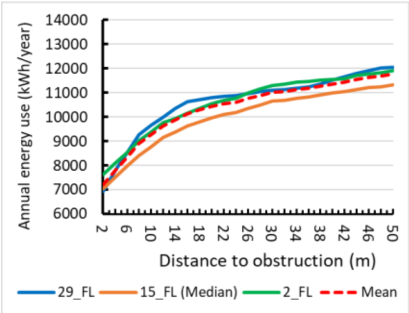

Cooling energy in SM3 facing north

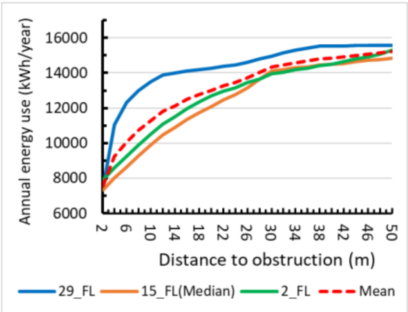

Cooling energy in SM3 facing south

Appendix I- Effects of the urban context on total annual energy use in SM2 and SM3

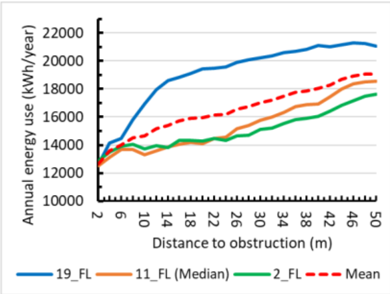

Total energy in SM2 facing east

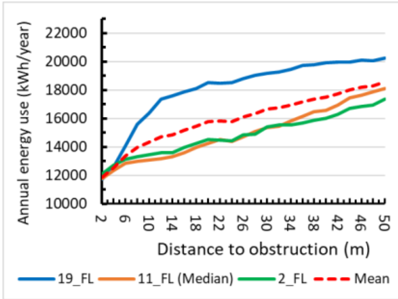

Total energy in SM2 facing west

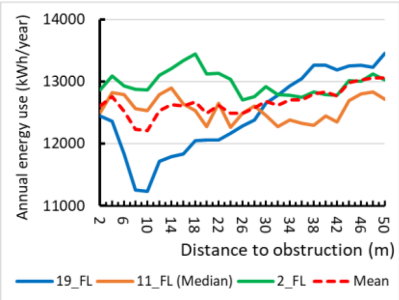

Total energy in SM2 facing north

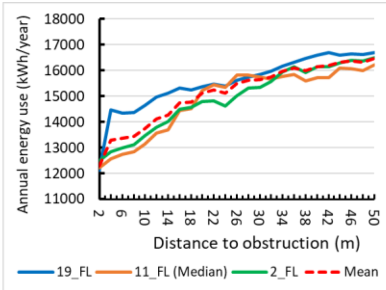

Total energy in SM2 facing south

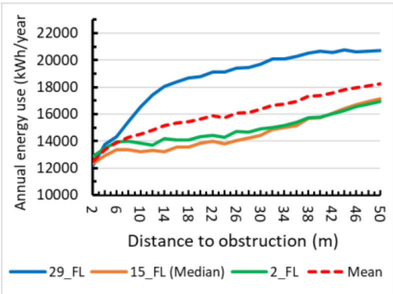

Total energy in SM3 facing east

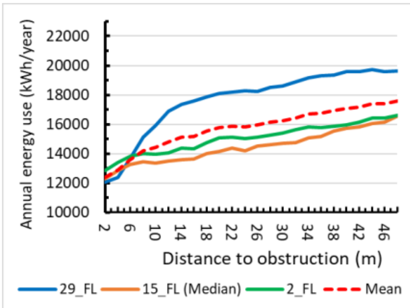

Total energy in SM3 facing west

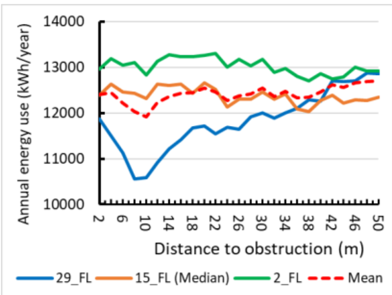

Total energy in SM3 facing north

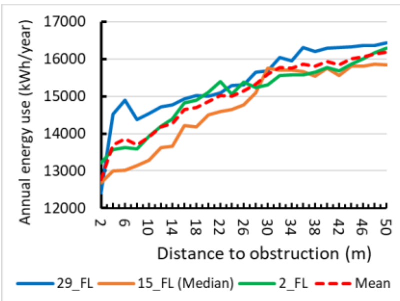

Total energy in SM3 facing south

Appendix J– Simulation results of the daylight grid for the best performance scenario in Case study two

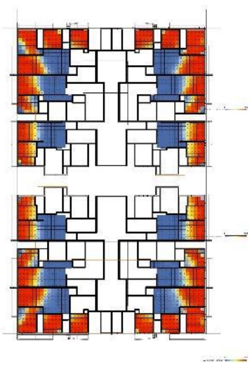 7th floor with balcony	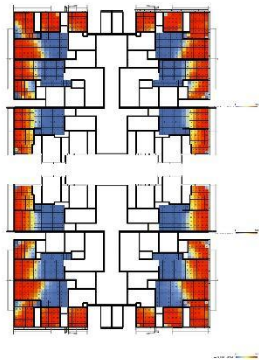 8th floor with balcony	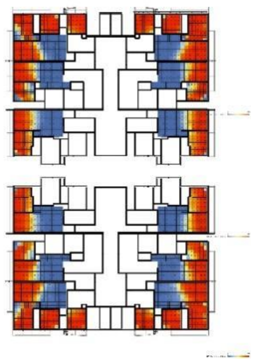 9th floor with balcony
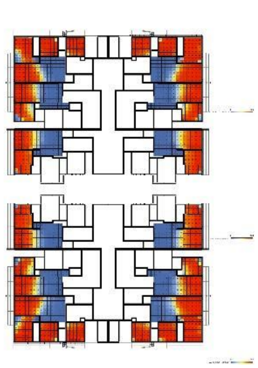 10th floor with balcony	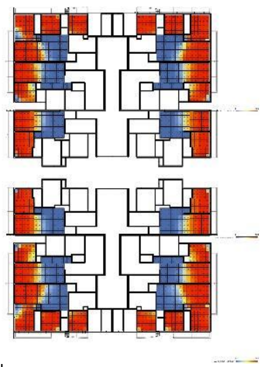 11th floor with balcony	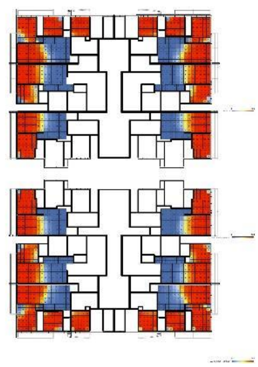 12th floor with balcony and fins
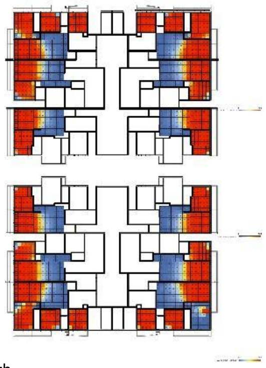 13th floor with balcony and fins	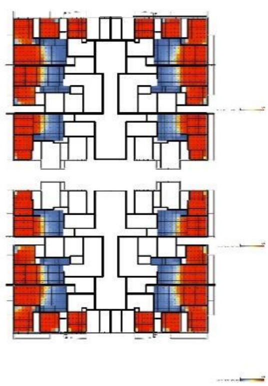 14th floor with balcony and fins	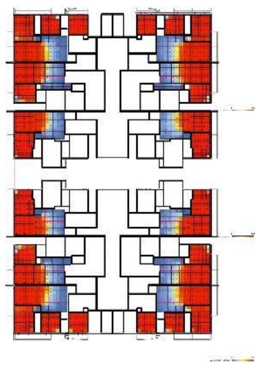 15th floor with balcony and fins

DA (% Time > 300 lux)